Austrian Journal of Technical and Natural Sciences

2025, No 3–4

PREMIER Publishing

Vienna
2025

Austrian Journal of Technical and Natural Sciences

Scientific journal

№ 3–4 2025

ISSN 2310-5607

Proofreading Kristin Theissen

Cover design Andreas Vogel

Additional design Stephan Friedman

Editorial office Premier Publishing s.r.o.

Praha 8 – Karlín, Lyčkovo nám. 508/7, PSČ 18600

E-mail: pub@ppublishing.org

Homepage: ppublishing.org

Austrian Journal of Technical and Natural Sciences is an international, English language, peer-reviewed journal. The journal is published in electronic form.

The decisive criterion for accepting a manuscript for publication is scientific quality. All research articles published in this journal have undergone a rigorous peer review. Based on initial screening by the editors, each paper is anonymized and reviewed by at least two anonymous referees. Recommending the articles for publishing, the reviewers confirm that in their opinion the submitted article contains important or new scientific results.

Premier Publishing is not responsible for the stylistic content of the article. The responsibility for the stylistic content lies on an author of an article.

Instructions for authors

Full instructions for manuscript preparation and submission can be found through the Premier Publishing home page at: http://ppublishing.org.

Material disclaimer

The opinions expressed in the conference proceedings do not necessarily reflect those of the Premier Publishing, the editor, the editorial board, or the organization to which the authors are affiliated.

Premier Publishing is not responsible for the stylistic content of the article. The responsibility for the stylistic content lies on an author of an article.

Included to the open access repositories:

Scientific Journal Impact Factor

TOGETHER WE REACH THE GOAL

SJIF 2024 = 6.62 (Scientific Journal Impact Factor Value for 2024).

Crossref OAK.UZ eLIBRARY.RU

Included to the Uzbekistan OAK journals bulletin.

The Austrian Journal of Technical and Natural Sciences, No 3–4
ISSN 2310-5607

PREMIER Publishing
ppublishing.org

Section 1. Architecture

DOI:10.29013/AJT-25-3.4-3-8

FIRE PREVENTION AND FIGHTING FOR HIGHER EDUCATION INSTITUTIONS IN VIETNAM

Dang Tuan Tu [1]

[1] Fire Prevention and Fighting University, Vietnam

Cite: *Dang Tuan Tu. (2025). Fire Prevention and Fighting for Higher Education Institutions in Vietnam. Austrian Journal of Technical and Natural Sciences 2025, No. 3–4.* https://doi.org/10.29013/AJT-25-3.4-3-8

Abstract

Fire prevention and fighting work for higher education institutions in Vietnam is of great significance in realizing the educational and training goals in the digital age. The article focuses on analyzing the results achieved in fire prevention and fighting work, pointing out the limitations, shortcomings and causes, on that basis, orienting the issues that need further research.
Keywords: *Higher education institutions; fire prevention and fighting; Vietnam*

1. Problem

According to statistics by the end of 2024, there are 247 higher education institutions in Vietnam, including those at the ministerial, provincial and private levels. Due to the professional characteristics of teaching, learning and scientific research, higher education institutions are a type of facility consisting of many different construction items, and during operation, many flammable substances are used. In addition, higher education institutions are always crowded, often with high density of people, with a system of laboratories and service facilities that pose many risks of fire. When a fire occurs, it can cause serious damage to people, property and affect social order and safety. Therefore, ensuring fire safety at higher education institutions is very necessary. However, according to statistics from the Fire and Rescue Police Department of the Ministry of Public Security of Vietnam, from 2014 to the end of 2024, there were 116 fires in higher education institutions in Vietnam. One of the effective solutions and measures is to do a good job of fire prevention and fighting, contributing to ensuring security and safety for sustainable development in education and training, and international integration.

2. Research results

2.1. Research results and achievements

The Vietnam Fire and Rescue Police Force has closely followed the direction of the Government and the Ministry of Public Security; at the same time, it has proactively advised Party committees and local authorities, and

sectors to deploy many measures and solutions to help effectively implement state management of fire and rescue for higher education institutions, thereby promptly resolving emerging problems in state management of fire and rescue. In localities, the Fire and Rescue Police Force has proactively advised provincial authorities to issue many directive documents, develop plans to implement fire and rescue for higher education institutions; coordinate with ministries and sectors to effectively implement state management of fire and rescue for higher education institutions in construction investment and during operation, contributing to limiting the number of incidents and damage caused by fires at higher education institutions. In particular, there have been initial strategic directives and plans on fire prevention and fighting for higher education institutions in the area. The work of promulgating, guiding and organizing the implementation of documents on state management of fire prevention and fighting in higher education institutions has had many positive changes, achieving positive results.

The Fire and Rescue Police Force from the central to local levels have focused on strengthening and implementing well the work of disseminating knowledge of fire prevention and fighting laws for higher education institutions, providing guidance on basic knowledge of fire prevention and fighting with many forms of propaganda that are relatively rich, diverse and staged, thus attracting the attention of all levels, sectors and a large number of people to participate in response, specifically: organizing training courses, seminars, conferences, competitions, integrating the program through the political activities at the beginning of the course of students, signing commitments to implement regulations on ensuring fire prevention and fighting safety for higher education institutions. Design review work from 2014 to present has continued to be strengthened and promoted, strictly implementing regulations on administrative procedure reform according to the "one-stop-shop" mechanism in construction investment work, publicly posting regulations on content, components of design documents, response time; organizing the reception and quick processing of review documents, creating convenience for agencies, businesses and people in reviewing and accepting fire prevention and fighting.

Fire and Rescue Police forces of units and localities have proactively guided the construction and practice of Fire fighting plan for higher education institutions, bringing about many positive results in this work. At the same time, the Fire and Rescue Police force has consulted with local authorities, coordinated with heads of higher education institutions to organize Fire fighting plan practice to ensure combat plans for each hypothetical fire and explosion situation, avoiding the practice of Fire fighting plan practice in a formal manner.

The Fire and Rescue Police force has actively and proactively carried out fire prevention and rescue safety inspections for higher education institutions, and at the same time conducted inspections for higher education institutions under construction. The issuance of decisions on administrative sanctions for violations in the field of fire and rescue for higher education institutions by the Fire and Rescue Police force basically follows the correct order, procedures and authority. At the Ministry of Public Security, the Fire and Rescue Police Department has actively coordinated with ministries and departments to issue legal documents, standards and technical regulations on fire prevention and fighting for higher education institutions. At the same time, the Fire and Rescue Police force in many localities has proactively coordinated with other forces inside and outside the People's Public Security to effectively carry out state management of fire prevention and fighting for higher education institutions. On the other hand, it has also coordinated in advising leaders at all levels to issue documents and coordination regulations to facilitate coordination with forces inside and outside the People's Public Security.

2.2. Research results on limitations and shortcomings

The quality of consulting and proposing work is not really high, especially in proposing the development of documents to implement policies, laws on state management of fire prevention and fighting for higher education institutions, which is not timely, and has not concretized the policies and guidelines of the Party and the State in state management

of fire prevention and fighting for higher education institutions, especially in conjunction with sustainable development of the education and training sector. Consulting on the promulgation of a system of legal documents, standards and regulations is not timely, suitable for the actual conditions of construction and development for higher education institutions, some legal documents issued are not really suitable, leading to difficulties in application; a separate system of standards and regulations on fire prevention and fighting for higher education institutions has not been developed. The work of propagating and disseminating knowledge and laws on fire prevention and fighting for higher education institutions has not been carried out regularly, not extensively, and not linked to educational and training activities at higher education institutions, leading to limited awareness of fire prevention and fighting work among staff, teachers and students at higher education institutions; greatly affecting the work of ensuring fire prevention and fighting safety for people at higher education institutions. The content of the propaganda work is still general for all types of facilities under management, and has not highlighted the characteristics of higher education institutions, including the role and responsibility of the head of the higher education institution and of each staff, teacher and student in fire prevention and fighting work for higher education institutions, especially the issue of escape at higher education institutions and the issue of ensuring safety during the learning and experimental process; The forms of propaganda are not rich and diverse, and there is not much application of information technology in propaganda activities for higher education institutions.

The system of legal documents, standards, and technical regulations as a legal basis for appraisal and acceptance is not yet complete and suitable for the conditions and construction situation of projects, designs, and acceptance of university education facilities; the process of receiving and handling administrative procedures in the appraisal and acceptance of university education facilities is not yet unified and synchronized, leading to many difficulties for investors and enterprises in complying with regulations on appraisal and acceptance; the capacity of officers in charge of appraisal and acceptance is still limited, leading to many limitations in the guidance, inspection, and comparison of appraisal and design work; the means serving the appraisal work are not really guaranteed, especially the means serving the appraisal work through online public services. In the process of fire prevention and fighting acceptance for works in higher education institutions, there are still many limitations and shortcomings, such as: lack of equipment for testing fire prevention and fighting systems that have been equipped at higher education institutions such as ventilation systems, pressure boosting systems, water pressure from fire hydrants, etc., so reliability and accuracy are not yet guaranteed according to regulations. Fire prevention and fighting inspection for higher education institutions is still a formality, inspection for the sake of completion, and a specific and complete inspection plan has not been developed for fire prevention and fighting inspection of higher education institutions; inspectors still manage too many facilities, leading to a situation of chasing targets without fully inspecting according to the process, leading to the omission of violations; there is still a mindset of deference in deciding to punish violations of fire prevention and fighting safety regulations. The professional qualifications of inspectors are still limited. The number of fire safety inspectors with intermediate qualifications and training from outside the fire safety industry accounts for a high proportion. Therefore, during the inspection process, inspectors cannot detect all violations of fire safety regulations at the facility, especially the implementation of fire safety standards and technical regulations... On the other hand, the means and equipment serving the fire safety inspection work of the Fire Police and Rescue Force have not received due attention.

Compliance with fire safety conditions for higher education institutions is still limited, specifically as follows: Renovation and change of use of items of the construction without a certificate of fire safety design approval; escape solutions do not comply with regulations; no periodic inspection and maintenance of fire safety equipment systems; no organization of fire safety training and operations; no

practice of situations in Fire fighting plan; no smoke protection solutions for corridors, stairwells, etc. In the construction of Fire fighting plan of the institution, the content and requirements are still sketchy and do not reflect the nature and characteristics of fire and explosion hazards at higher education institutions; have not anticipated fire and explosion situations that may occur in accordance with the actual situation of the higher education institution; have not calculated the forces and means needed to participate in fire fighting; the assignment of specific tasks to the grassroots fire safety force is not clear. The implementation of the plan practice is still formal and perfunctory, the forces participating in the plan practice are still superficial, there is still a lack of attention and care during the practice of the plan at the university, even in some places the fire prevention forces at these universities are still confused when asked about the fire prevention systems, traffic, water sources serving fire prevention work during the practice of the plan, as well as the use of fire prevention equipment, some people do not know how to use it. The Fire fighting plan practice is only theoretical, without studying and training in real hypothetical situations according to the approved plans.

The coordination of the issuance of legal documents, the system of standards, regulations and the implementation of directive documents of competent authorities in general state management and state management of fire prevention and fighting for higher education institutions has not been maintained regularly and promptly, mainly the issuance of documents chaired by the Ministry of Public Security has not been coordinated continuously. The coordination between the Fire and Rescue Police force for administrative management of social order, and the Department of Education and Training has been given attention but has not been regular and has not achieved high results as expected.

2.3. Research results on the causes of limitations and shortcomings

(1) Regarding objective causes

Along with the economic development of the country is the rapid increase in construction works in higher education institutions while the state management of fire prevention and fighting for higher education institutions has not changed to keep up with this development. On the other hand, some higher education institutions built before 2001 (before the Law on Fire Prevention and Fighting) have not had their fire prevention and fighting designs approved, so they do not ensure fire prevention and fighting safety. There is no definitive solution to solve this problem for these higher education institutions; at the same time, the arrangement and installation of fire prevention and fighting equipment for these higher education institutions are still limited, not ensuring effective fire fighting when a fire occurs. The planning area, construction architecture and design of higher education institutions have not met the needs of education and training, so there is a situation of changing functions, adding, using a building with many different functions, such as: classrooms, laboratories, libraries... leading to failure to ensure fire prevention and fighting safety for higher education institutions.

Investment funds for fire prevention and fighting work at higher education institutions have not met the requirements for equipment, installation of on-site fire prevention and fighting equipment and tools, construction and practice of Fire fighting plan; The policy for grassroots fire prevention and fighting forces is not suitable, leading to the situation where grassroots fire prevention and fighting forces do not work effectively, enthusiastically, and actively, and still work in a perfunctory, perfunctory manner, with a low sense of responsibility.

(2) Regarding subjective causes

The system of legal documents on fire prevention and fighting issued is not synchronous, not complete and not strict. The system of regulations and standards on fire prevention and fighting techniques for houses and constructions issued is not timely or is lacking and not suitable for the actual situation and has been for too long and is not suitable for the current actual conditions.

The Fire and Rescue Police force in the state management of fire prevention and fighting for higher education institutions in many localities has not been proactive in basic investigation, survey, grasping the situation, advising and proposing to levels, sectors and local authorities to issue guiding documents, leading and directing the

resolution of difficulties and problems in the process of implementing state management of fire prevention and fighting for higher education institutions, the concretization of legal regulations on fire prevention and fighting for higher education institutions is still slow.

Propaganda, dissemination and education of fire prevention and fighting laws for higher education institutions: The staff performing the duties of the Fire and Rescue Police Force is still lacking in number, especially the number of staff specializing in fire prevention and fighting propaganda, the assignment of local staff and facility management exceeds the regulations, so it is impossible to perform well the task of organizing propaganda, dissemination and education of fire prevention and fighting laws and knowledge to each individual related to the higher education institution.

The work of reviewing and approving designs and accepting fire prevention and fighting laws for higher education institutions: The order and procedures for reviewing and approving designs and accepting fire prevention and fighting laws are not really smooth and quick, creating conditions for businesses in the implementation process; the qualifications of staff reviewing and approving designs and accepting fire prevention and fighting laws for higher education institutions are still limited; Coordination in the process of design approval and acceptance of fire prevention and fighting for higher education institutions is not really effective in many cases...

Inspection and handling of violations of fire prevention and fighting regulations for higher education institutions: Fire safety inspectors for higher education institutions have not been regularly trained, leading to limited inspection qualifications and capacity...

Work on developing fire fighting plans and organizing fire fighting practice for higher education institutions: Special plans for higher education institutions have not been developed; The construction of the plan's content is often sketchy and does not fully reflect the nature and characteristics of fire and explosion hazards in higher education institutions. The study and assignment of practice tasks for the plan are not specific, etc. The awareness of a significant number of investors and management units of higher education institutions regarding fire prevention and fighting in higher education institutions is still incorrect. They do not see the importance of fire prevention and fighting in higher education institutions, leading to a situation where some higher education institutions have been invested in and put into operation for many years, while the fire prevention and fighting equipment system has not met the requirements of current regulations and standards on fire prevention and fighting. Some investors deliberately do not comply with the requirements for review and acceptance (putting some projects that have not been reviewed and accepted into operation; converting and changing functions but not conducting review and acceptance). The awareness of cadres, lecturers, employees and students in fire prevention and fighting work for higher education institutions is still limited, with the idea that fire prevention and fighting work belongs to the authorities, to the Fire and Rescue Police Force, leading to a situation where they do not grasp the provisions of the law on fire prevention and fighting, and do not fully perform their responsibilities in fire prevention and fighting work for higher education institutions. People's Committees at all levels, together with units of the People's Committee, have not really paid attention to the state management of fire prevention and fighting for higher education institutions, leading to the infrequent issuance of documents and instructions on state management of fire prevention and fighting for higher education institutions, and the situation of assigning the state management of fire prevention and fighting for higher education institutions to the Fire and Rescue Police Force.

2.4. Some directions that need to be further studied to contribute to ensuring fire prevention and fighting for higher education institutions

(1) Continue to study ways to organize propaganda, dissemination, education of knowledge and laws on fire prevention, fighting, rescue and salvage; guide the development of a mass movement to participate in fire prevention, fighting, rescue and salvage;

(2) Study the work of design appraisal and inspection of fire prevention and fighting acceptance for works in higher education institutions;

(3) Strengthen the inspection and strict and thorough handling of violations of regulations on fire prevention and fighting for higher education institutions;

(4) Continue to study the process of organizing the establishment, consolidation, maintenance of the operation of the grassroots fire prevention and fighting force and improve the quality of professional training for the grassroots fire prevention and fighting force for higher education institutions;

(5) Research on the development and practice of fire prevention and fighting plans and fire fighting organization as well as research on the coordination relationship in state management of fire prevention and fighting for higher education institutions...

3. Conclusion

The article presented the research results, including pointing out the achieved results, limitations, shortcomings and causes of limitations and shortcomings in fire prevention and fighting work for higher education institutions in Vietnam; identified issues that need further research to improve the effectiveness of fire prevention and fighting work for higher education institutions in Vietnam, contributing to ensuring security, safety, and ensuring sustainable development of the education and training sector in Vietnam today.

References:

Nguyen Ngoc Anh (2019). “Overview of the legal system in the field of Fire and Rescue and Directions for Supplementation and Improvement”, Proceedings of the Scientific Conference on Law on Fire Prevention, Fire Fighting and Rescue in Practice and Application, Fire Prevention and Fighting University, Hanoi.

Dao Huu Dan, Vu Van Binh, Hoang Ngoc Hai. (2021). Theoretical and practical issues on state management of Fire P and Rescue in the current period, Monograph for PhD training, CAND Publishing House, Hanoi.

National Assembly. (2024). Law on Fire and Rescue, 2024. Hanoi.

submitted 14.04.2025;
accepted for publication 24.04.2025;
published 29.05.2025

Contact: tudt@daihocpccc.edu.vn

The Austrian Journal of Technical and Natural Sciences, No 3–4
ISSN 2310-5607

PREMIER Publishing
ppublishing.org

Section 2. Chemistry

DOI:10.29013/AJT-25-3.4-9-14

OXIDATION KINETICS, THERMAL PROPERTIES, AND FUNCTIONAL ACTIVITY OF CARBOXYMETHYL INULIN

Ashurov Mirshod [1], ***Khusenov Arslonnazar*** [1],
Rakhmanberdiev Gappar [1], ***Abdullayev Otabek*** [2]

[1] Shakhrisabz branch of Tashkent Institute of Chemical Technology

[2] University of Economics and Education

Cite: *Ashurov M., Khusenov A., Rakhmanberdiev G., Abdullayev O. (2025). Oxidation Kinetics, Thermal Properties, and Functional Activity Of Carboxymethyl Inulin. Austrian Journal of Technical and Natural Sciences 2025, No 3–4.* https://doi.org/10.29013/AJT-25-3.4-9-14

Abstract

This study investigates the properties of dialdehyde carboxymethyl inulin samples obtained as a result of the periodate oxidation reaction of carboxymethyl inulin. The dependence of the oxidation process on time, the effect of the degree of substitution, and the selectivity of the reaction were analyzed. Thermal analysis was conducted to examine the thermal stability of inulin and its modified derivatives, identifying the influence of structure and functional groups on degradation.
Keywords: *carboxymethyl inulin, periodate oxidation, dialdehyde polysaccharide, thermal analysis*

Introduction

In recent years, extensive research has been conducted on the development of next-generation materials based on natural polymers in the fields of chemistry, chemical technology, medicine, and pharmaceuticals. Dialdehyde polysaccharides hold a special place in this area, as they are primarily obtained through the oxidation of natural polysaccharides such as cellulose, starch, chitosan, and others. These dialdehyde polysaccharides contain aldehyde groups, which provide high reactivity and modifiability. Due to their antibacterial properties, regenerative activity, and lack of toxicity, they are becoming increasingly important in polymer chemistry, medical applications, and industrial material production.

Dialdehyde polysaccharides are mainly synthesized through the selective oxidation of vicinal diol groups using sodium periodate ($NaIO_4$) or potassium periodate (KIO_4). The reaction depends on the structure of the polysaccharide, the concentration of the oxidizing agent, pH level, temperature, and time. For instance, dialdehyde cellulose can be obtained by oxidizing microcrystalline cellulose with 0.1–0.5 M $NaIO_4$ for 4 to

24 hours (Chang-Qing Ruan, Xiaoou Kang, Kaifang Zeng, 2022; Simona Káčerová, Monika Muchová, Hana Doudová, Lukáš Münster, Barbora Hanulíková, Kristýna Valášková, Věra Kašpárková, Ivo Kuřitka, Petr Humpolíček, Zdenka Víchová, Ondřej Vašíček, Jan Vícha Chitosan 2023; Wenjie Wang, Wen-Can Huang, Jie Zheng, Changhu Xue, Xiangzhao Mao, 2023). Similarly, dialdehyde starch is synthesized through periodate oxidation at 20–30 °C, depending on the type of starch used as the raw material (Wei Ding, Yanbei Wu, 2020; Wegrzynowska-Drzymalska K., Grebicka P., Mlynarczyk D. T., Chelminiak-Dudkiewicz D., Kaczmarek H., Goslinski T., Ziegler-Borowska M., 2020). Additionally, in dialdehyde chitosan, carbonyl groups are formed due to the cleavage of the C_2–C_3 bonds (Sherif M. A.S. Keshk, Ahmed M. Ramadan, Abdullah G. Al-Sehemi, Ahmad Irfan, Samir Bondock, 2017; Gao C., Wang S., Liu B., Yao S., Dai Y., Zhou L., Qin C., Fatehi P., 2021).

The oxidation of all polysaccharides generally leads to the opening of the polysaccharide ring, resulting in the formation of two aldehyde groups per repeating unit. This modification creates a basis for subsequent immobilization and conjugation reactions. The dialdehydation process significantly affects the molecular structure and physicochemical properties of polysaccharides. Aldehyde groups are mainly positioned at the C_2 and C_3 sites, making them highly reactive centers. The structural properties of the synthesized products, such as solubility, viscosity, and bioactivity, depend on the level of aldehyde formation, which directly contributes to the formation of stronger, covalently bonded structures between polymer chains (Tiina Nypelö, Barbara Berke, Stefan Spirk, Juho Antti Sirviö. 2020; Carolina O. Pandeirada, Max Achterweust, Hans-Gerd Janssen, Yvonne Westphal, Henk A., 2022; Xia Sun, Feng Jiang, 2024).

Dialdehyde polysaccharides are biologically active, easily modifiable, environmentally friendly, and offer broad potential applications in medicine. Their ability to form bonds with other active compounds through aldehyde groups plays a crucial role in the development of innovative materials across various fields.

Objective of the study

The aim of this research is to study the structural and functional transformations of carboxymethyl inulin under periodate oxidation conditions and to evaluate the reactivity of the resulting dialdehyde carboxymethyl inulin, particularly its reactions with primary amine compounds.

Materials and methods

The study utilized inulin, sodium carboxymethyl inulin (Na-CMI) with various degrees of substitution, as well as chemically pure and analytically pure reagents for experiments.

Synthesis of Polyaldehyde Derivatives of Carboxymethyl Inulin. A sample of carboxymethyl inulin (3 g) was measured and placed into a 500 ml heat-resistant dark glass vessel. Then, 100 ml of water was added, and the mixture was stirred on a magnetic stirrer. After dissolving the sample, 150 ml of freshly prepared acetate buffer solution with pH = = 5 was added. After thorough mixing, a 0.2 N $NaIO_4$ solution was added in a carboxymethyl inulin: $NaIO_4$ = 1:1 molar ratio. The oxidation of carboxymethyl inulin proceeded at t = 20–25 °C for 1–6 hours. To terminate the reaction, 50 ml of ethylene glycol was added. After completion of the reaction, the resulting mixture was dialyzed in distilled water until complete removal of IO_4^- and IO_3^- ions (monitored using silver nitrate solution). The quantitative content of aldehyde groups in the final product, dried by lyophilization, was analyzed by iodometric titration.

Determination of Thermal Stability of Polysaccharide Samples Using TG DSC Method. Thermo-analytical studies of the samples were carried out using a STA-409 PG TG-DSC analyzer manufactured by NETZSCH, equipped with a K-type (Low RG Silver) thermocouple and aluminum crucibles. For experiments, samples weighing 5–6 mg were used. All measurements were performed in an inert nitrogen atmosphere with a flow rate of 50 ml/min. The heating rate during measurements was 10 K/min, and the temperature range was +20...+600 °C. The measurement system was calibrated using standard substances – indium, bismuth, tin, zinc, and cesium chloride.

Result and discussions

In the periodate oxidation process of polysaccharides, maintaining the selectivity of the reaction is crucial. This is because the presence of periodate ions in the reaction medium can further oxidize the formed -CHO groups to -COOH groups. As a result, the number of aldehyde groups in the synthesized dialdehyde polysaccharides decreases significantly.

The periodate oxidation reaction of carboxymethyl inulin samples at pH=5.0 was carried out according to the following scheme:

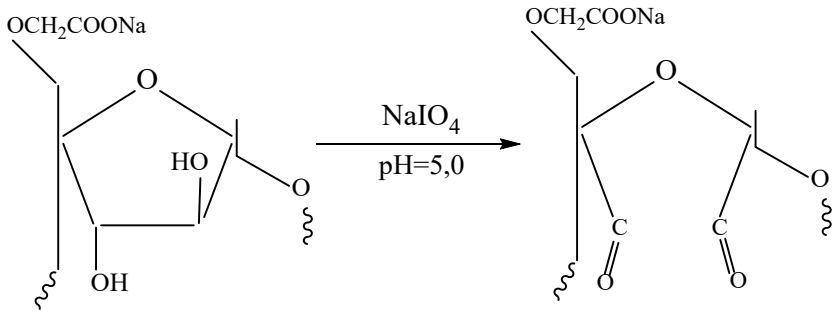

The effect of time on the oxidation degree of Na-CMI samples with different degrees of substitution was studied. The experimental results are presented in Figure 1.

Figure 1. *Effect of time on periodate oxidation of Na-CMI samples with substitution degrees of 85 mol% (1) and 34 mol% (2)*

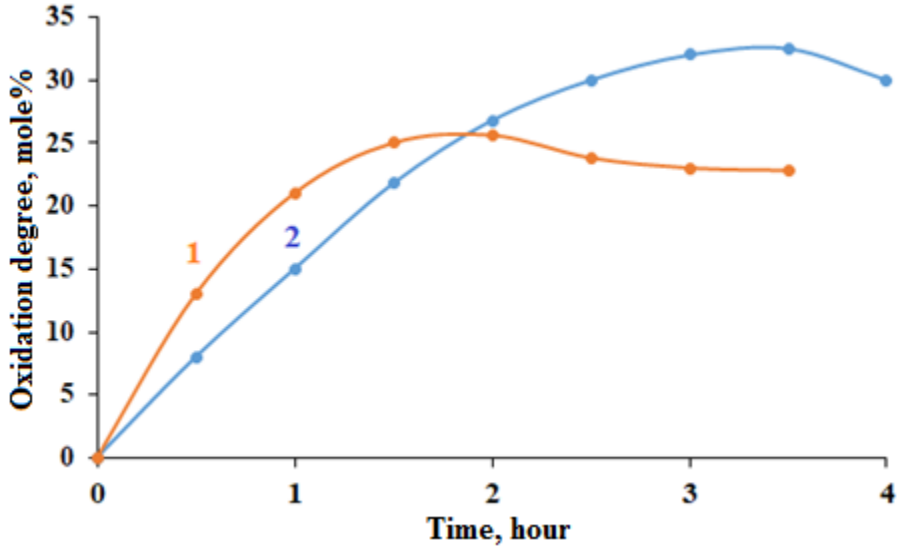

As seen from Figure 1, the oxidation degree of the Na-CMI sample with a substitution degree of 85 mol% increases from 13 mol% to 21 mol% in the first 0.5–1 hour. Extending the oxidation reaction beyond 2 hours leads to a decrease in the number of aldehyde groups from 26 mol% to 23 mol%. This is due to the oxidation of the formed aldehyde groups to -COOH by the IO_4^- ions present in the reaction medium.

A sample of sodium carboxymethyl inulin (Na-CMI) with a substitution degree of 34 mol% exhibited oxidation degrees of only 8 and 14 mol% during the initial 0.5–1 hour. This slow reaction rate is attributed to the low content of hydrophilic $-CH_2-COO^-$ groups in the inulin macromolecule. However, extending the oxidation reaction to 3 hours resulted in a dialdehyde carboxymethyl inulin (DACMI) sample with an oxidation degree of 33 mol%. Oxidation of Na-CMI over 3.5 to 4 hours led to a gradual decrease in aldehyde groups.

Thermal analysis, a method for studying how substances change under the influence of temperature, was employed to investigate the thermal properties of inulin and its modified derivatives such as Na-CMI and DACMI. The objectives were to determine the thermal stability of these polysaccharides, assess the impact of substitution or oxidation degrees on their thermal properties, and evaluate their resistance for various processing

applications. The thermal characteristics of inulin, carboxymethyl inulin, and DACMI samples with varying degrees of oxidation are presented in Figure 2.

Figure 2. *Thermal analysis of 1-Inulin; 2-Na-CMI (substitution degree 34 mol%); 3-DACMI (oxidation degree 14 mol%); 4-DACMI (oxidation degree 33 mol%)*

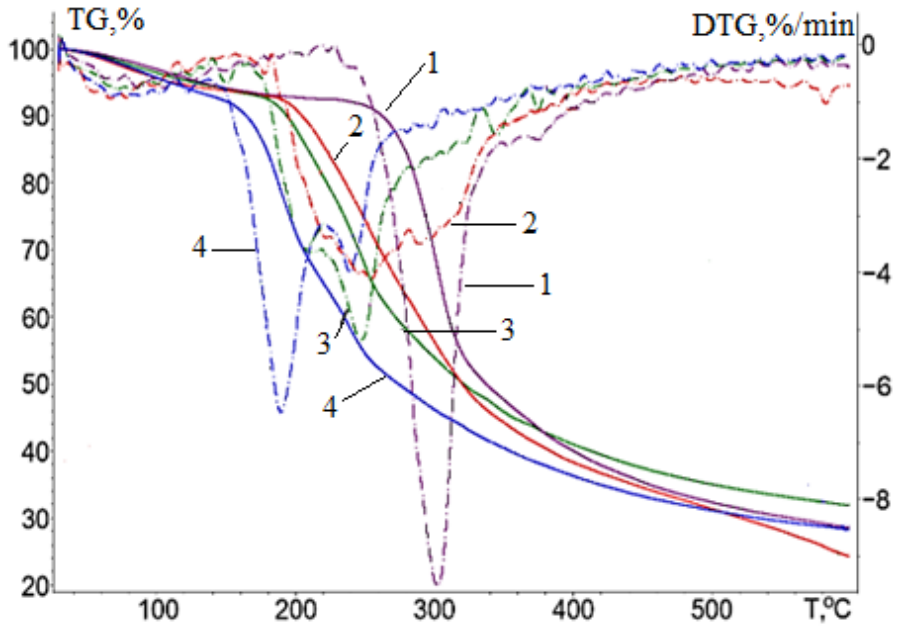

As shown in Figure 2, introducing -CH2-COO⁻ or -CHO groups into the inulin macromolecule alters the polysaccharide's temperature stability and its degradation mechanism. Thermal analysis results indicate that all samples undergo degradation in three stages:

- The first stage occurs between 68–165 °C, where adsorbed moisture begins to evaporate;
- In the second stage, between 165–390 °C, the polysaccharide chain starts to degrade;
- In the third stage, at 390–600 °C, the process concludes with carbonization.

Notably, in the second stage, all samples exhibit a weight loss of approximately 48%. Differential thermogravimetric (DTG) curves reveal that the degradation of carboxymethyl inulin and DACMI samples occurs in two parts (at 190–218 °C and 230–256 °C), whereas the thermal degradation of the inulin macromolecule proceeds at around 300 °C. Additionally, the carbonization temperature of inulin derivatives is lower compared to that of inulin itself.

To confirm the presence of aldehyde groups in the Na-CMI macromolecule and determine their reactivity, we conducted a reaction with hydroxylamine, a nucleophilic reagent with high reactivity commonly used in the quantitative analysis of aldehyde groups. The reaction between DACMI and hydroxylamine was carried out according to the following scheme:

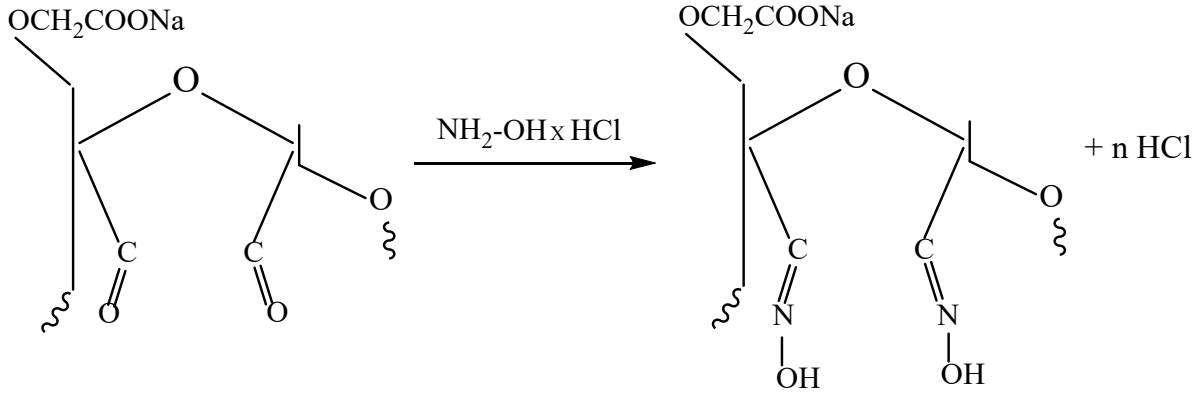

Table 1 presents the composition of compounds synthesized from DACMI samples with varying oxidation degrees and hydroxylamine. The data indicate that as the oxidation degree of DACMI samples increases, the nitrogen content in the reaction products also rises. This finding demonstrates the feasibility of chemically attaching various primary amines to the DACMI macromolecular chain, suggesting the potential application of inulin ethers as polymer matrices.

Table 1. *Composition of compounds synthesized from DACMI and hydroxylamine (DACMI: NH_2 -OH = 1:2.5; t = 20–25 °C; τ = 1 hour)*

№	DACMI oxidation degree, mole %	Nitrogen content,%	Substitution degree, mole%
1.	14	1,1	12
2.	21	1,8	19
3.	26	2,1	25
4.	30	2,5	29
5.	33	2,8	33

The data presented in Table 1 indicates a consistent increase in nitrogen content corresponding to the rise in oxidation levels. This suggests that as the number of aldehyde groups formed through oxidation in the DAKMI molecule increases, they react with hydroxylamine to form oxime bonds. The nitrogen content serves as a direct indicator of the amount of hydroxylamine participating in this reaction.

Additionally, the formation of more functional groups leads to higher reactivity with hydroxylamine. This reactivity is directly linked to the number of reactive sites within the DACMI structure. Notably, despite the reaction between DACMI and NH_2OH being conducted at 20–25 °C for only 1 hour, the sample with an oxidation degree of 33 mole% demonstrates high efficiency.

Conclusion

The conducted research has, for the first time, identified that the rate of oxidation reaction and the quantity of aldehyde groups in carboxymethylinulin samples are influenced by the substitution degree of the synthesized polysaccharide ester and the reaction time. An increase in the oxidation degree enhances the reactivity of the DACMI molecule with hydroxylamine, providing the ability to control structural changes and functional properties of derivatives synthesized based on DACMI.

References:

Chang-Qing Ruan, Xiaoou Kang, Kaifang Zeng. Preparation of water-soluble dialdehyde cellulose enhanced chitosan coating and its application on the preservation of mandarin fruit // International Journal of Biological Macromolecules. 2022. – V. 203. URL: https://doi.org/10.1016/j.ijbiomac.2022.01.010.

Simona Káčerová, Monika Muchová, Hana Doudová, Lukáš Münster, Barbora Hanulíková, Kristýna Valášková, Věra Kašpárková, Ivo Kuřitka, Petr Humpolíček, Zdenka Víchová, Ondřej Vašíček, Jan Vícha Chitosan/dialdehyde cellulose hydrogels with covalently anchored polypyrrole: Novel conductive, antibacterial, antioxidant, immunomodulatory, and anti-inflammatory materials // Carbohydrate Polymers. 2024. – V. 327. URL: https://doi.org/10.1016/j.carbpol.2023.121640.

Wenjie Wang, Wen-Can Huang, Jie Zheng, Changhu Xue, Xiangzhao Mao. Preparation and comparison of dialdehyde derivatives of polysaccharides as cross-linking agents // International Journal of Biological Macromolecules. 2023. – V. 236. URL: https://doi.org/10.1016/j.ijbiomac.2023.123913.

Wei Ding, Yanbei Wu. Sustainable dialdehyde polysaccharides as versatile building blocks for fabricating functional materials: An overview // Carbohydrate Polymers 2020. – V. 248. URL: https://doi.org/10.1016/j.carbpol.2020.116801.

Wegrzynowska-Drzymalska K., Grebicka P., Mlynarczyk D. T., Chelminiak-Dudkiewicz D., Kaczmarek H., Goslinski T., Ziegler-Borowska M. Crosslinking of Chitosan with Dialdehyde Chitosan as a New Approach for Biomedical Applications // Materials (Basel). 2020. – V.13(15). Doi: 10.3390/ma13153413.

Sherif M. A.S. Keshk, Ahmed M. Ramadan, Abdullah G. Al-Sehemi, Ahmad Irfan, Samir Bondock. An unexpected reactivity during periodate oxidation of chitosan and the affinity of its 2, 3-di-aldehyde toward sulfa drugs // Carbohydrate Polymers. 2017. – V. 175. URL: https://doi.org/10.1016/j.carbpol.2017.08.027.

Gao C., Wang S., Liu B., Yao S., Dai Y., Zhou L., Qin C., Fatehi P. Sustainable Chitosan-Dialdehyde Cellulose Nanocrystal Film // Materials (Basel). 2021. – V. 14(19). Doi: 10.3390/ma14195851.

Tiina Nypelö, Barbara Berke, Stefan Spirk, Juho Antti Sirviö. Review: Periodate oxidation of wood polysaccharides-Modulation of hierarchies // Carbohydrate Polymers. 2021. – V. 252. Periodate oxidation of wood polysaccharides-Modulation of hierarchies https://doi.org/10.1016/j.carbpol.2020.117105.

Carolina O. Pandeirada, Max Achterweust, Hans-Gerd Janssen, Yvonne Westphal, Henk A. Schols. Periodate oxidation of plant polysaccharides provides polysaccharide-specific oligosaccharides // Carbohydrate Polymers. 2022. – V. 291. URL: https://doi.org/10.1016/j.carbpol.2022.119540.

Xia Sun, Feng Jiang. Periodate oxidation-mediated nanocelluloses: Preparation, functionalization, structural design, and applications // Carbohydrate Polymers. 2024. – V. 341. URL: https://doi.org/10.1016/j.carbpol.2024.122305.

submitted 25.03.2025;
accepted for publication 08.04.2025;
published 29.05.2025

Contact: jamoliddinaa23@gmail.com

The Austrian Journal of Technical and Natural Sciences, No 3–4
ISSN 2310-5607

PREMIER Publishing
ppublishing.org

DOI:10.29013/AJT-25-3.4-15-20

ANALYSIS OF SULFOCATIONITE BASED ON PYROLYSIS OIL FOR WASTEWATER TREATMENT

Ergasheva Yulduzoy [1], ***Beknazarov Hasan*** [1], ***Yigitaliyev Sardorbek*** [1]

[1] Department of General Medicine, Faculty of Treatment, Angren University

Cite: *Ergasheva Y., Beknazarov H., Yigitaliyev S. (2025). Analysis of Sulfocationite Based on Pyrolysis Oil for Wastewater Treatment. Austrian Journal of Technical and Natural Sciences 2025, No 3–4.* https://doi.org/10.29013/AJT-25-3.4-15-20

Abstract

This study describes the results of investigating the products of the sulfonation reaction between pyrolysis oil and sulfuric acid at various temperatures and time intervals. The highest sulfur content in sulfonated cation exchangers was observed at sulfonation temperatures of 100 and 120 °C for the pyrolysis oil with a reaction time of 2 hours. The resulting product is widely used as a dispersant for coatings and paints, a plasticizer for cement, and for other purposes. It is a synthetic polymer consisting of a network of interconnected sulfonic acid functional groups, which makes it highly charged and highly selective.

Keywords: *Pyrolysis oil, sulfonation, structural group analysis, sulfonic cation exchangers, water softening, polycondensation, ion-exchange resin, acidity*

The production of sulfonic cation exchangers through sulfonation of industrially manufactured polymers and oligomers, as well as their application, is widespread. However, considering that this type of macromolecular compound has certain limitations, numerous scientific studies confirm that superior results are achieved when using ion exchangers (anion or cation exchangers) obtained by preliminary modification with various organic compounds followed by sulfonation for diverse purposes. Ion exchangers contain multiple functional groups, including hydroxyl, primary, secondary, tertiary amino groups, carboxyl, and other groups. As polyfunctional compounds, their applications are diverse. Currently, the chemical industry is transitioning from raw materials to finished products through the production of semi-finished products, including those using organic synthesis and nanotechnology, while effectively utilizing local raw materials. At the same time, one of the urgent tasks is the gradual reduction of raw material exports (natural gas, industrial salts, etc.) and the organization of their processing within the republic. For this purpose, a cation exchanger was synthesized using secondary products by processing the by-product “pyrolysis oil” from the Ustyurt Gas Chemical Complex, owned by Uz-KorGaz Chemical LLC.

In general, sulphocation exchangers are universal and highly selective ion exchangers. These compounds are recognized as one of the vital substances for life processes and are used in various industrial processes (Pat.2241665.

RF. 2004). In the process of obtaining sulfonic cation exchangers from heavy oil residues, the waste generated during oil refining was treated with solid sulfuric acid under constant stirring conditions. The ionic modifier, which is the target product, is washed with water, purified from unreacted sulfuric acid, and dried to a neutral medium (pH=7), then brought to a constant mass. This method allows for obtaining a sulfocationite based on heavy oil residues in a short time at room temperature. It was established that the main characteristics of the sulfocationite obtained by this method are superior. The production of this ion exchanger can be considered environmentally safe, as oil refining waste was used as the raw material for its production (Pat. 2623574C1. RF. 2016). In accordance with classical theory, the patterns of absorption and swelling of new ion exchangers were studied. The obtained results enable the creation of ion exchangers with optimal properties for the purification of industrial wastewater (Rakhimova L. S., Abdutalipova N. M., Nazirova R. A., Tursunov T. T., Berdieva M. I., Mutalov Sh.A., 2014). The use of polymeric ion-exchange oligomer-ionites has been known for many years. The application of oligomeric-type catalysts is due to the wide selection of oligomeric matrices and the possibility of incorporating cationic and anionic catalytic centers within them. One of the main advantages of using ion-exchange oligomers is the ease of separating them from the reaction mixture. This facilitates the isolation and washing of catalysts, prevents the formation of stable emulsions, and avoids the accumulation of large volumes of wastewater. The absence of wastewater simplifies the technological scheme of production processes. Another advantage of ionites is their ability to be stably reused multiple times and applied for long periods in continuous processes (Yaroslavtsev A. B., Nikenenko V. V., Zabolotskiy V. I., 2003). β-Naphthalenesulfonic acid was obtained from industrial naphthalene through high-temperature sulfonation, after which a small amount of α-naphthalenesulfonic acid isomer was isolated by hydrolysis. The condensation reaction between β-naphthalenesulfonic acid and formaldehyde was conducted in an acidic medium. The condensate of naphthalenesulfonic acid and formaldehyde was then produced by neutralization with an alkali (Wang, T. H., 2004). Highly mineralized water is also characterized by a lower capacity to retain heavy metal ions and hardness ions compared to organic and inorganic ions (Vaaramaa, K., 2003). The application of the acidic form of weakly acidic cation exchangers in water pre-treatment provides effective decarbonization, despite the low efficiency of water softening (Makarenko, I., 2012). The application of weakly acidic cation exchangers in their acid form under conditions of low alkalinity and high water mineralization cannot provide effective water softening (Makarenko, I., 2014). Overall, despite the widespread use of ion exchange in water purification, the application of this method for stabilizing saline natural waters and wastewater is ineffective (Alexandratos, S. D., 2009). One of the drawbacks of using weakly acidic cation exchangers for water softening is their extremely low regeneration efficiency. However, it is precisely for this reason that their use is advisable for softening saline waters with high sodium ion content (Gomelja, N., 2004).

Methodology

For the synthesis of sulphocationic exchange resin, the following processes are carried out: Pyrolysis oil is sulfonated with concentrated sulfuric acid (molar ratio 1:1.5) at 160–165 °C for 3–4 hours, resulting in a dark black sulfomass; the sulfomass, placed in a pressure vessel, is diluted with distilled water and subjected to polycondensation with 38% formaldehyde (initial molar ratio of naphthalene to formaldehyde 1:2) at 110–120 °C and a pressure of 2–4 MPa; the water-insoluble solid polycondensate is mechanically ground and heated at 90–95 °C for 12 hours to complete polycondensation.

Synthesis of naphthalene sulfonic acid. Pyrolysis oil is sulfonated with concentrated H2SO4 to produce β-naphthalene sulfonic acid. The pyrolysis oil is mixed with sulfuric acid at 70 °C and boiled for 1 hour. According to equation 1, to achieve complete conversion, the reaction water formed during the sulfonation process is distilled off using an azeotropic method. During the reaction, along with β-naphthalene sulfonic acid, naphthalene disulfonic acids or dinaphthyl sulfones with a double naphthalene ring may also be formed.

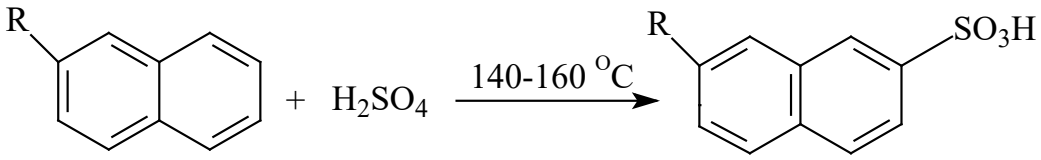

Naphtali β-naphthalenesulfonic acid

The graph illustrating the influence of various factors on the yield of sulfocation exchanger derived from pyrolysis oil, specifically time and molar ratios of the starting materials, is presented below in Figure 1.

Figure 1. *Time-dependent yield of sulfocationite derived from pyrolysis oil*

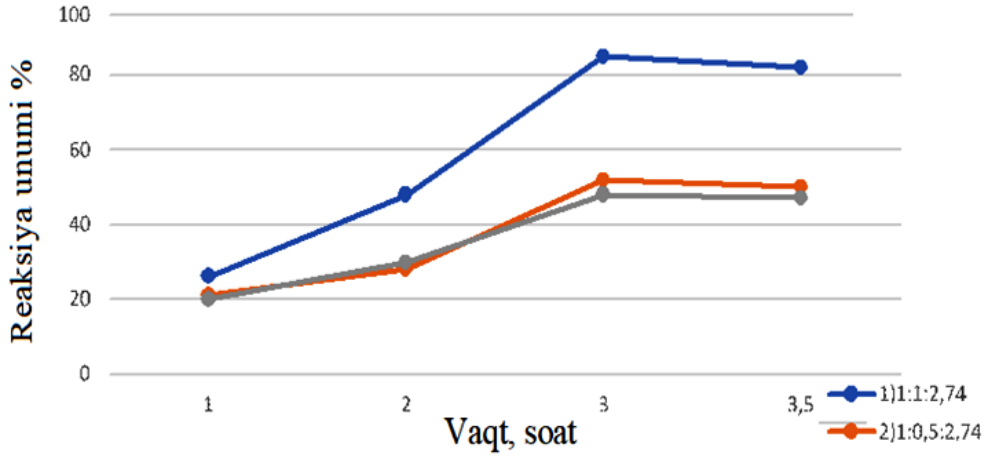

Molar ratio of pyrolysis oil and sulfuric acid: 1–(1:1,5); 2–(1:0.5);

The relationship between the yield of sulphocatonite obtained from pyrolysis oil and time is presented in Figure 1. As shown in Figure 1, the highest efficiency compared to other variants is achieved with a pyrolysis oil to sulfuric acid ratio of 1:1.5. The synthesis process lasts for 3 hours. In an experiment conducted over 3.5 hours, the yield of sulphocatonite gradually decreases. This can be explained by the fact that the substances used as raw materials exist in various states of aggregation for 3 hours or more.

Figure 2. *Relationship between the yield of sulphocationite produced from pyrolysis oil and the molar ratio of pyrolysis oil to sulfuric acid*

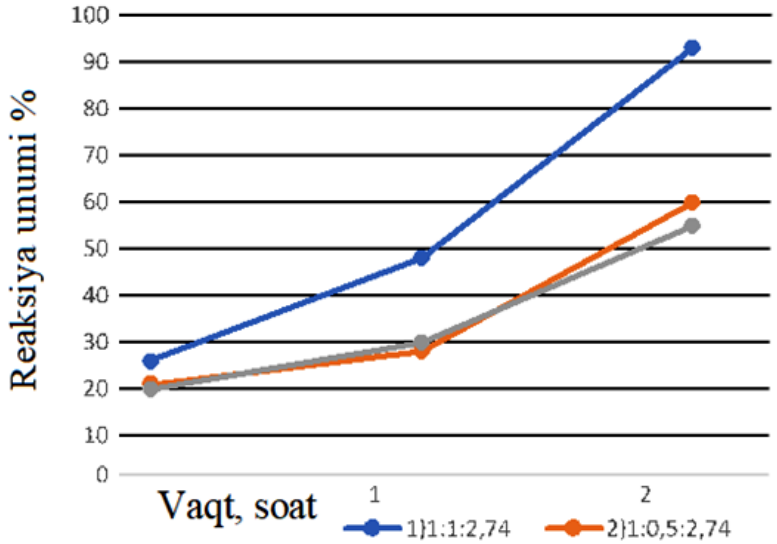

Pyrolysis oil, molar ratio of sulfuric acid 1-(1:1,5); 2-(1:0,5);

The presence of interacting substances in two different states of aggregation reduces the effectiveness of their interaction. The dependence of the synthesized sulphocatonite yield on temperature can be seen in Figure 2.

As shown in Figure 2, the optimal component ratio for sulfocatonite production is 1:1.5, with the profitability of sulfocatonite reaching 79.8%. The highest dry residue is obtained at a ratio of initial products of 1:0.5; however, the plasticizing effect of the resulting sulfocatonites is low in this case. Based on these findings, the optimal temperature of 160 °C was chosen for sulfocatonite production. Reaction time also plays a significant role in the production of sulfocatonites. To determine the optimal reaction yield temperature, all three ratios of initial products were tested. The figure below illustrates the dependence of sulfocatonite yield on reaction time at a temperature of 160 °C. As evident from the figure, when the reaction is carried out for 180 minutes under optimal conditions, the sulfocatonite yield is 79.8%. Under these conditions, prolonging the reaction further leads to a decrease in product yield. As shown in the figure, when the reaction is conducted for 180 minutes under optimal conditions, the yield of sulfocatonite is 79.8%.

Results and analysis. Our research investigated the effects of temperature, time, and molar ratios of substances on the product yield in the production of a sulfocation exchanger using pyrolysis oil and sulfuric acid. The obtained results are presented in Table 1 below.

Table 1. *Influence of molar ratios of substances and reaction time on product yield*

№	Molar ratios	Time, hour	Yield, %	№	Molar ratios	Time, hour	Yield, %
1.	1:0,5		26,2	11	1:0,5		49,4
2.	1:0,8		37,3	12	1:0,8		65,8
3.	1:1,2	1	47,4	13	1:1,2	**3**	72,5
4.	1:1,3		54,3	14	1:1,3		78,7
5.	1:1,5		56,5	**15**	1:1,5		**79.8**

Table 1 reflects the influence of various factors on the yield of sulfokationite: time and the molar ratios of the initial substances. As can be seen from Figure 2, the highest yield compared to other variants is achieved when the ratio of pyrolysis oil to sulfuric acid is 1:1.5, however, the resulting product contains derivatives of di-naphthylsulfones. Therefore, when studying the plasticizing effect of mono-, di-, and other derivatives, the derivatives of polyhydric alcohols are of particular importance. From the obtained results, it can be seen that at a mol ratio of pyrolysis oil, sulfuric acid, and formaldehyde of 1:1.5 and a process duration of 3 hours, the yield of sulfokation exchanger was the highest. The study was conducted using a MIRA 2 LMU scanning electron microscope equipped with an INCA Energy 350 energy-dispersive microanalytical system.

Figure 3. *Electron-microscopic analyses of sulfokationite*

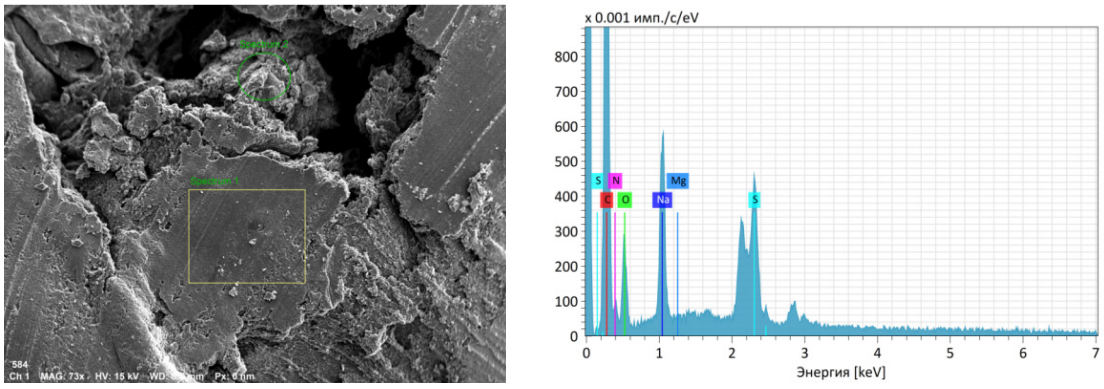

The microscope's resolution is 1 nm, and the sensitivity of the INCA Energy detector is 133 eV/10 mm^2, allowing for the analysis of elements from beryllium to plutonium. Analyses using the scanning electron microscope are carried out under high vacuum conditions. Using the same device, a microanalysis of chemical elements was performed, and areas were studied with an accelerating voltage of 20 keV and a beam current of 1 nA. In this work, images from the electron scanner were obtained at an accelerating voltage of 30 keV with a magnification of 50 times. The results of the elemental analysis and the scanning electron microscope data are presented in Figure 3.

Table 2. *Table of results from SEM analysis of sulfonated cation exchange resin*

Elements	Atomic number	The mass is normal %	Abs program [%]
C	6	64.13	1.88
O	8	15.64	0.56
N	7	9.66	0.58
Na	11	6.45	0.32
S	16	3.94	0.14
Mg	12	0.18	0.03
		100	

An electron microscopic image of the superplasticizer SP-Na revealed that the mass fraction of the functional group in the elemental composition consists of: 15.64% oxygen, 64.13% carbon, 9.66% nitrogen, 20.6% sodium metal, and 3.94% sulfur.

Conclusion

Pyrolysis oil reacts with concentrated sulfuric acid to form naphthalenesulfonic acid at high temperatures. Polysulfonation products and sulfonates may also form, which affects the purity of the target product. When condensing with formaldehyde after sulfonation, the acidity of the system significantly influences the degree of condensation. At low sulfuric acid concentrations, the sulfonation reaction does not yield good results. High acidity can easily trigger explosive polymerization, leading to high viscosity and reduced water solubility. It is theorized that the sulfonation process proceeds more effectively if the amount of sulfuric acid during sulfonation exceeds the amount of pyrolysis oil.

References

Pat.2241665. RF. 2004.

Pat. 2623574C1. RF. 2016.

Rakhimova L. S., Abdutalipova N. M., Nazirova R. A., Tursunov T. T., Berdieva M. I., Mutalov Sh. A. Synthesis and property of new polycondensation type of ion exchanging polimer. The advanced science journal. 2014. – Vol. 7. – P. 91–96.

Yaroslavtsev A. B., Nikenenko V. V., Zabolotskiy V. I. Ion transport in membrane and ion exchange materials. Journal Advances in Chemistry, 2003. – Vol. 75. – P. 438–470. (in Russian).

Wang, T. H. (2004). Synthesis of naphthalene sulfonic acid formaldehyde condensate and its application in ammonium nitrate modification. Nanjing University of Science and Technology.

Vaaramaa, K. Removal of metals and anions from drinking water by ion exchange [Text] / K. Vaaramaa, J. Lehto // Desalination. 2003. – Vol. 155. – Issue 2. – P. 157–170. Doi: 10.1016/s0011-9164(03)00293-5

Makarenko, I. Use cation exchenger Dowex Mac-3 in asidic form at stabilization processing of water [Text] / I. Makarenko, O. Glushko, V. Risuhin, V. Malin // Eastern-European Journal of Enterprise Technologies. 2012. – Vol. 3. – Issue 6 (57). – P. 16–20. – Available at: http://journals.uran.ua/eejet/article/view/4034/3699

Makarenko, I. Stabilizing treatment of seawater during it desalination by reverse osmosis [Text] / I. Makarenko // Ecology and Industry. 2014. – Issue 4. – P. 60–65.
Alexandratos, S. D. Ion-exchange resins: a retrospective from industrial and engineering chemistry research [Text] / S. D. Alexandratos // Industrial & Engineering Chemistry Research. 2009. – Vol. 48, Issue 1. – P. 388–398. Doi: 10.1021/ie801242v
Gomelja, N. Water conditioning for resource saving systems of water consumption [Text] / N. Gomelja, T. Shablij, Ju. Nosacheva // Eco-technologies and Resource Saving. 2004. – Issue 4. – P. 55–58.

submitted 14.04.2025;
accepted for publication 28.04.2025;
published 29.05.2025

Contact: hasanbeknazarov130@gmail.com

The Austrian Journal of Technical and Natural Sciences, No 3–4
ISSN 2310-5607

PREMIER Publishing
ppublishing.org

DOI:10.29013/AJT-25-3.4-21-27

INVESTIGATION OF THE INHIBITORY AND COLLOID-CHEMICAL PROPERTIES OF GXMA (GUANIDINE CHLORIDE METHYLACRYLATE) SYNTHESIZED ON THE BASIS OF GUANIDINE

G'afurova Gulnoz Alixanovna [1], ***Olimov Bobir Bahodirovich*** [1]
Bukhara State Technical University 1, Bukhara, Uzbekistan

Cite: *G'afurova G.A., Olimov B.B. (2025). Investigation of the Inhibitory and Colloid-Chemical Properties of Gxma (Guanidine Chloride Methylacrylate) Synthesized on the Basis of Guanidine. Austrian Journal of Technical and Natural Sciences 2025, No 3–4.* https://doi.org/10.29013/AJT-25-3.4-21-27

Abstract

In this study, guanidine chloride methylacrylate (GXMA), a newly synthesized compound based on guanidine, was investigated as an effective corrosion inhibitor for steel in a 15% hydrochloric acid (HCl) solution. Steel grade St-20 was selected for the experiments, and the inhibitory effect of GXMA at various concentrations (100–300 mg/L) was evaluated using the gravimetric method. The tests were conducted over a period of 300 hours within a temperature range of 343–363 K. The experimental results demonstrated that GXMA significantly reduced corrosion rates. Notably, at a concentration of 300 mg/L, GXMA provided a protection efficiency of 93.3% for St-20 steel. The corrosion rate inhibition coefficient was found to be up to 15 times higher compared to the control. Based on weight loss measurements of steel coupons, the effectiveness of GXMA was found to fully comply with the requirements of GOST (RH)39.0–051:2007. To gain deeper insights into the adsorption mechanisms, graphical analyses were conducted using the Langmuir, Temkin, Frumkin, and Flory-Huggins adsorption isotherms. The obtained R^2 coefficients confirmed that the adsorption of GXMA closely follows the Langmuir model, indicating monomolecular and physico-chemical adsorption on the metal surface. Thermodynamic analyses were carried out based on the Arrhenius equation, and the observed increase in activation energy (Ea), along with a negative entropy change, indicated the predominance of GXMA adsorption processes on the metal surface. The findings revealed that GXMA exhibits maximum inhibitory performance within the concentration range of 250––300 mg/L. This study suggests that GXMA is a promising corrosion inhibitor for protecting metal structures operating in acidic environments, particularly in the oil and gas industry. The results confirm GXMA's potential as a highly efficient, economically viable, and environmentally friendly corrosion inhibitor.

Keywords: *corrosion, inhibitor, guanidine chloride methylacrylate (GXMA), HCl solution, steel coupons, gravimetric method, adsorption isotherm, Langmuir model, activation energy, thermodynamic analysis, physico-chemical adsorption, monomolecular layer, acidic environment, metal protection, oil and gas industry*

1. Introduction

The corrosion of metallic structures operating in acidic environments presents significant technical and economic challenges. Therefore, the use of effective chemical inhibitors is crucial for mitigating corrosion-related damage. In particular, when steel materials used in the oil and gas industry are exposed to strong acidic solutions, there is a pressing need for specialized chemical compounds to extend their service life (Narzullaev A. Kh., Beknazarov Kh. S., Dzhalilov A. T., 2019).

In recent years, guanidine derivatives have gained special attention among organic corrosion inhibitors. This study investigates the corrosion-inhibiting effectiveness of guanidine chloride methylacrylate (GXMA), synthesized from guanidine thiocyanate, formaldehyde, and acrylic acid using locally available raw materials, through the gravimetric method (Beknazarov Kh. S., Dzhalilov A. T., 2015). While guanidine chromate and its derivatives with mineral acids have previously been applied as corrosion inhibitors, the behavior of GXMA in acidic environments remains insufficiently studied. The aim of this research is to evaluate the anticorrosion performance of GXMA and to elucidate its adsorption characteristics (Yaro A. S., Abdul Masih N. Sh., Khadom A. A., 2000; Oguzie E. E., 2006).

During the corrosion process, the adsorption of inhibitors onto the metal surface plays a vital role. To understand these adsorption behaviors, mathematical models are employed. Adsorption isotherms represent mathematical relationships that describe the equilibrium distribution of substances on the surface of the adsorbent. Among these, the Langmuir, Temkin, and Frumkin isotherms are widely used. In particular, the Langmuir isotherm, which assumes monolayer adsorption where each adsorption site binds to only one molecule, is frequently applied (Odiongenyi A. O., Odoemelam S. A. and Eddy N. O., 2009; Olimov B. B., Yoldosheva N. J.). This study explores how these isotherms help explain the interaction of GXMA with the metal surface and assesses their compatibility with experimental results.

2. Materials and Methods

An experimental investigation was conducted to evaluate the corrosion-inhibiting properties of the synthesized GXMA compound. Various concentrations of guanidine chloride methylacrylate were prepared using hydrochloric acid (HCl) solution. Steel samples of grade St-20 were used in the experiments. The steel coupons were polished using SiC abrasive papers, degreased in 96.6% ethanol, and then dried with acetone (Panoev E. R., Dustov H. B., Akhmedov V. N., 2021; Bobir O., Mashhura S., Islom B., 2022).

The cleaned steel coupons were tied with thread and immersed in 100 mL of test solutions maintained at temperatures ranging from 343 to 363 K. A total of six metal coupons were prepared for each test series. One coupon was immersed in a 15% HCl solution without the inhibitor, serving as the control, while the remaining five were placed in 15% HCl solutions containing GXMA at concentrations of 100, 150, 200, 250, and 300 mg/L, respectively.

Table 1. *Dependence of corrosion-inhibiting characteristics of GXMA on its concentration. The experiment was conducted on St-20 steel*

Sample	S, 10^{-4} m^2	τ, hour	mass m_0, g	mass m, g	Δm	Consentration of inhibitor, mg/ml	Rate of corrosion, g/hour·m^2	Z, %	γ
1.	21	300	23,52	22,7	0,813	–	1,29	–	–
2.	21	300	23,68	23,48	0,193	100	0,306	76,2	4,21
3.	21	300	23,76	23,6	0,158	150	0,25	80,6	5,16
4.	21	300	23,61	23,51	0,096	200	0,153	88,1	8,43
5.	21	300	23,65	23,57	0,082	250	0,131	89,8	9,84
6.	21	300	23,77	23,72	0,054	300	0,086	93,3	15

To analyze weight loss due to corrosion, the coupons were kept in the solutions for a duration of 300 hours. At the end of the exposure period, the following post-treatment steps were performed:

— Coupons were cleaned with a soft brush;
— Rinsed with distilled water;
— Washed with acetone;
— Dried until a constant mass was achieved.

The difference between the initial and final mass of each coupon was calculated using the gravimetric method. The results of the gravimetric analysis are presented in Table 1.

3. Results and Discussion (Part)

The effects on the surface of steel samples (coupons) subjected to corrosion were examined over a 300-hour period in both a 15% HCl solution containing guanidine chloride methylacrylate (GXMA) and in an uninhibited 15% HCl solution. In the inhibitor-containing solution, almost no visible changes were observed on the metal surface. In contrast, clear signs of corrosion were evident on the surface of the sample exposed to the uninhibited acidic solution.

According to the results presented in Table 1 and in compliance with clause 5.3 of document NGH (RH)39.0–051:2007, the protective efficiency determined by the gravimetric method on steel samples should not be less than 90% at concentrations not exceeding 500 mg/L for general corrosion resistance.

The determination of the corrosion inhibitor's mechanism of action requires analyzing the energy state of the thermodynamic system. Accordingly, it is necessary to evaluate the system's thermodynamic energy during corrosion in both inhibited and uninhibited conditions at different concentrations. To analyze energy changes, calculations were conducted based on the Arrhenius equation:

$$CR = A \cdot \exp\left(\frac{-E_a}{RT}\right)$$

Where:

E – is the activation energy (kJ/mol),

R – is the universal gas constant, 8.314 J/mol·K,

T – is the temperature in Kelvin,

$A \cdot \exp$ – is the pre-exponential factor.

The application of a corrosion inhibitor in the solution leads to observable changes in activation energy (E_a). When the inhibitor is added, the activation energy of the corrosion process increases, and this increase becomes more pronounced with higher inhibitor concentrations. A higher value of activation energy indicates the predominance of physical adsorption, whereas unchanged or lower values of E suggest chemical adsorption. A significant increase in the activation energy compared to the uninhibited system confirms that the inhibitor is adsorbing onto the steel surface. In the absence of an inhibitor, the activation energy of the corrosion process is determined based on the concentration of iron ions released into the solution in their active state.

4. Results and Discussion

The newly synthesized inhibitor demonstrated a protection efficiency of 93.3%, as determined by the gravimetric method, which meets the requirements of established standards. In this study, the corrosion inhibitor was synthesized using locally available raw materials. The inhibitory properties of the synthesized compound were tested under laboratory conditions in an artificially created aggressive environment. Gravimetric analysis revealed that at a concentration of 300 mg/L, the GXMA inhibitor provided a 93.3% protection efficiency for St-20 steel, with a 15-fold reduction in the corrosion rate compared to the uninhibited solution. The investigation was carried out across a range of inhibitor concentrations from 100 mg/L to 500 mg/L. However, it was found that the optimal inhibitory effect was achieved at 300 mg/L. The Langmuir adsorption isotherm is a specific mathematical model related to adsorption phenomena. It is primarily used to describe the equilibrium state of adsorption and helps in understanding the nature of the bonding between the adsorbate and the surface. According to Equation (1), the model assumes that adsorption occurs on a homogeneous surface with a fixed number of identical sites, where each site can hold only one adsorbate molecule, and there is no interaction between adsorbed molecules. This equation describes monolayer adsorption, implying that the adsorption

process occurs in a single molecular layer (monomolecular adsorption). One of the key assumptions of the Langmuir model is that each adsorption site binds to only one molecule, the adsorbate molecules do not interact with one another, and they are uniformly distributed over the adsorbent surface.

$$\frac{C}{\theta} = \frac{1}{K} + C \quad (1)$$

$$long\left(\frac{C}{\theta}\right) = long\,C - long\,K \quad (2)$$

To evaluate the compatibility of the experimental results with theoretical models, the data were tested using various adsorption isotherm equations. At temperatures of 343 K, 353 K, and 363 K, the relationship between log(C/θ) and log(C) was analyzed. As shown in Figure 1, the resulting plots exhibited a linear correlation, indicating that the adsorption process conforms well to the assumptions of the isotherm models at the given temperatures.

Figure 1. *Langmuir adsorption isotherm plots of GXMA inhibitor on steel surface at: (a) 343 K, (b) 353 K, and (c) 363 K*

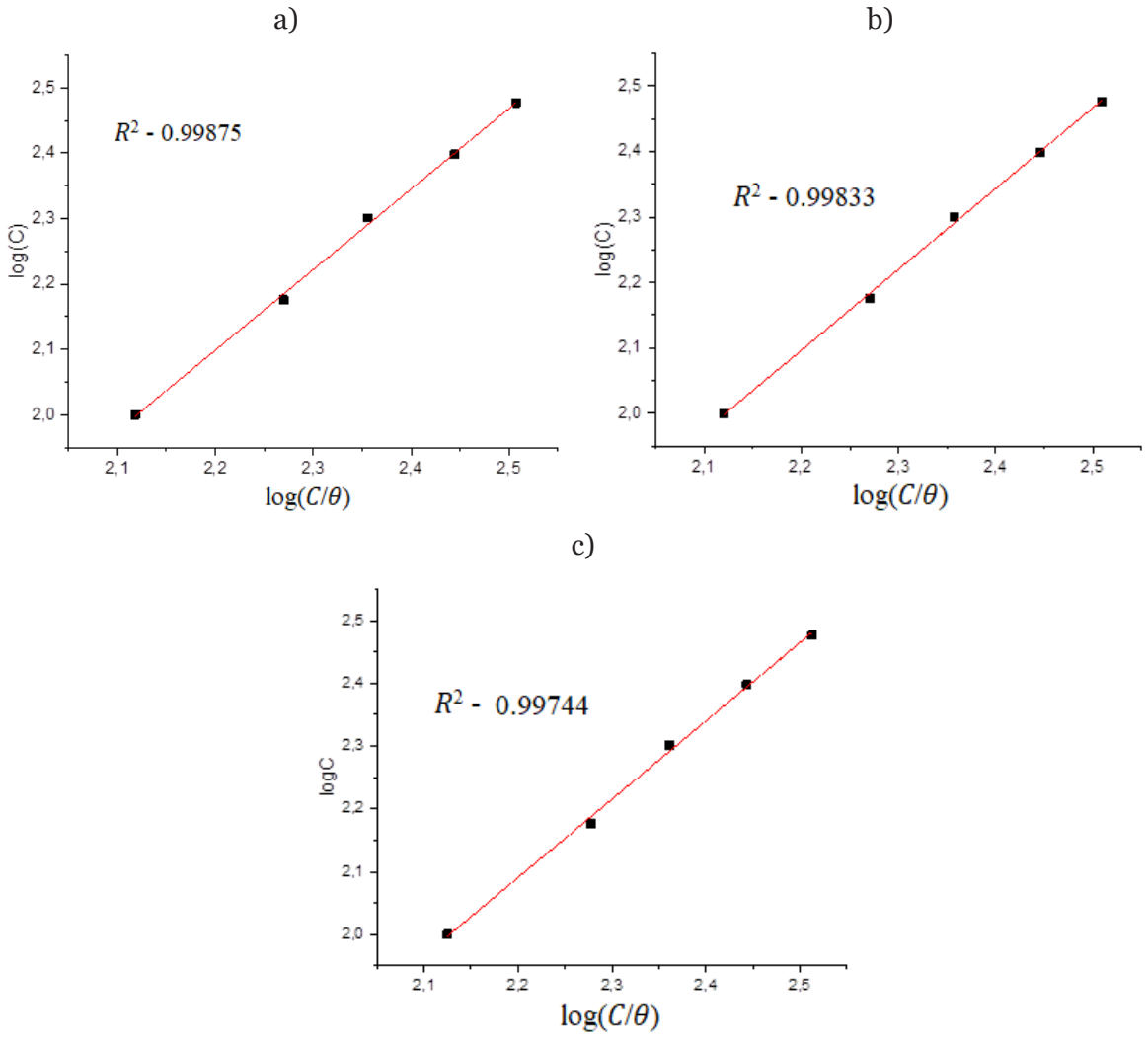

Based on the data obtained at these temperatures, the calculated R^2 values were 0.99875, 0.9833, and 0.99744, respectively. These results indicate a strong correlation with the Langmuir adsorption isotherm, confirming the applicability of the model to the adsorption behavior of GXMA on the steel surface. The high degree of fit suggests that the process follows a monomolecular physico-chemical adsorption mechanism, characterized by interactions between the donor atoms of the inhibitor molecules and the iron ions on the steel surface. This conclusion is supported by the assumptions of

the Langmuir equation, which describes monolayer adsorption without interaction between adsorbed species.

In the Temkin isotherm, the relationship between log C and θ was analyzed at three different temperatures. The calculated R^2 values were 0.9744 at 343 K, 0.9780 at 353 K, and 0.9692 at 363 K. These values indicate a reasonable correlation with the Temkin isotherm model, suggesting that the adsorption process is moderately consistent with the assumptions of this model at the investigated temperatures (Figure 2).

Figure 2. *Temkin adsorption isotherm plots of the GXMA inhibitor on the steel surface at: (a) 343 K, (b) 353 K, and (c) 363 K.*

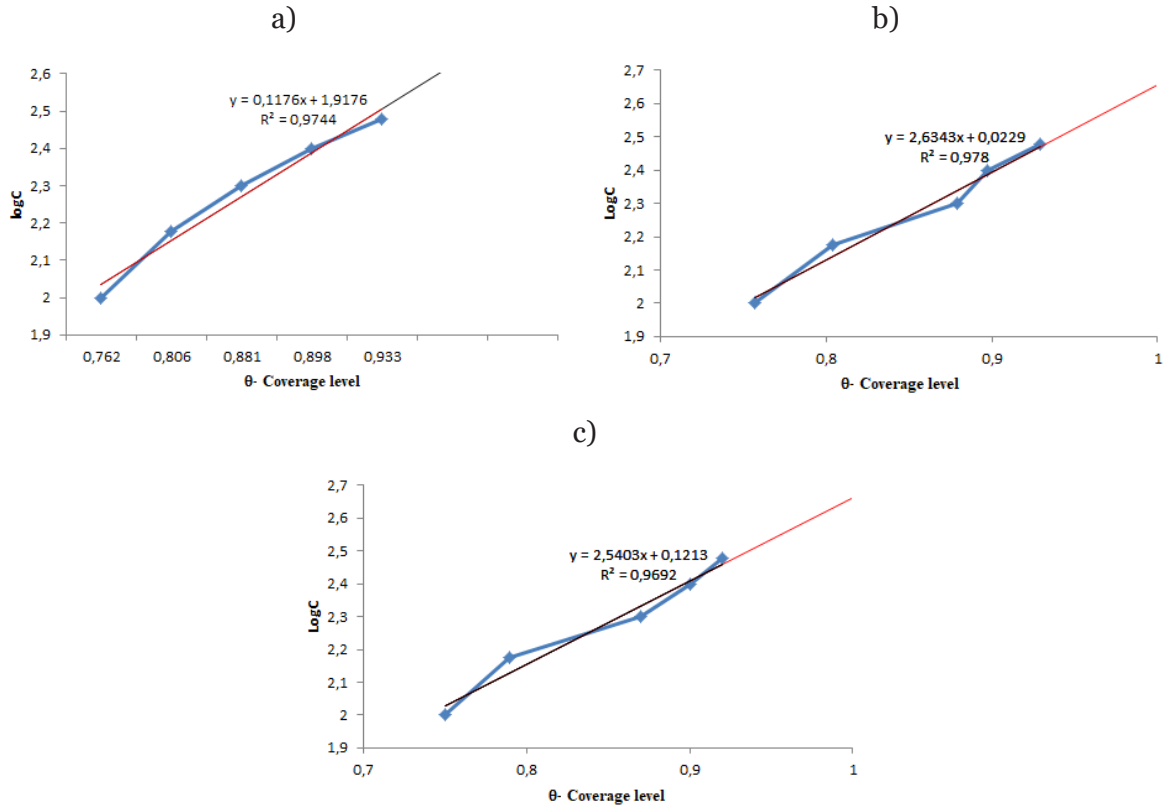

For the Frumkin isotherm, the relationship between log $[C\cdot(\theta/(1-\theta))]$ and θ was examined. The obtained R^2 values were 0.9891 at 343 K, 0.9892 at 353 K, and 0.9691 at 363 K. These values reflect a strong correlation with the Frumkin isotherm, indicating a good fit between the experimental data and the model. This suggests that intermolecular interactions between the adsorbed species may play a role in the adsorption mechanism of GXMA on the steel surface.

The adsorption process is characterized by the adsorption of inhibitor molecules onto the metal surface and the simultaneous desorption of water molecules. This can also be considered as an exchange process, in which the inhibitor molecules displace water molecules and adhere to the metal surface, forming a protective layer. The surface coverage (θ) increases proportionally with the inhibitor concentration, leading to enhanced inhibition efficiency. The parameter θ represents the percentage of the metal surface covered by the inhibitor and is expressed as a value from 0 to 1 (or 0% to 100%). The increase in θ indicates greater surface protection. The following graph illustrates the change in corrosion rate at various temperatures and inhibitor concentrations. The results obtained during the study show that at inhibitor concentrations of 250 mg/L and 300 mg/L, the calculated R^2 values were 0.9989 and 0.9976, respectively. These high values confirm the accuracy and reliability of the experimental procedures and the validity of the observed trends (Figure 4).

Figure 3. *Frumkin adsorption isotherm plots of the GXMA inhibitor on the steel surface at: (a) 343 K, (b) 353 K, and (c) 363 K.*

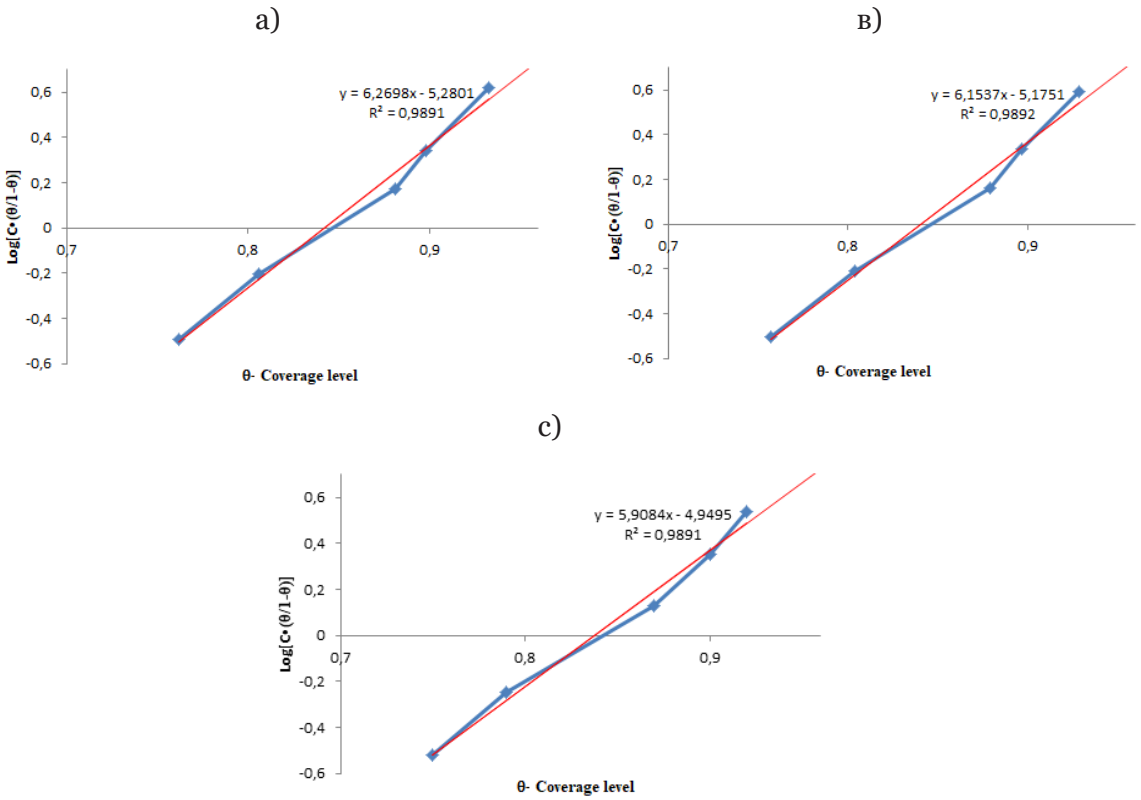

Figure 4. *Arrhenius plot for the activation energy of the GXMA corrosion inhibitor in an aggressive environment*

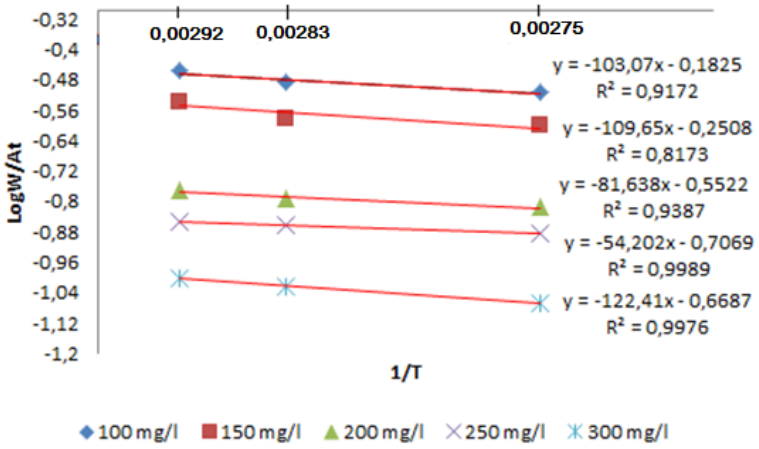

This analysis emphasizes the importance of thermodynamic and kinetic parameters in gaining a deeper understanding of the corrosion inhibition mechanisms. The conclusions derived from these calculations, along with the results obtained from the previously discussed adsorption isotherms, confirm that the adsorption of GXMA on the steel surface follows a monomolecular pattern and is of a physico-chemical nature.

4. Conclusion

In this study, the corrosion inhibition performance of guanidine chloride methylacrylate (GXMA), synthesized from locally available raw materials, was thoroughly investigated using the gravimetric method in a 15% HCl acidic environment on steel surfaces. At a concentration of 300 mg/L, GXMA provided up to 93.3% protection, which fully complies with the GOST standard (RH 39.0–

051:2007). After 300 hours of exposure in hydrochloric acid, a significant reduction in corrosion rate was observed based on mass loss measurements of the steel coupons.

The GXMA compound was found to form an effective monomolecular adsorption layer on the metal surface, acting as a strong physical barrier in an acidic medium. Detailed analysis of the adsorption process was carried out using Langmuir, Temkin, and Frumkin isotherms. The high correlation coefficients, particularly for the Langmuir model ($R^2 \approx 0.99$), confirmed that GXMA undergoes monomolecular adsorption on the metal surface. This suggests that each inhibitor molecule occupies a distinct active site on the metal, displacing water molecules in the process.

Thermodynamic evaluations, including calculations based on the Arrhenius equation, indicated an increase in activation energy (Ea) and a negative entropy change, both of which support a physico-chemical nature of adsorption. These results imply that the interaction between GXMA and the metal surface is not only superficial but also involves stable bonding at the ionic level.

It was also established that the optimal inhibitory efficiency of GXMA was achieved within the 250–300 mg/L concentration range, highlighting the compound's potential as an economically viable and highly effective corrosion inhibitor.

References

Narzullaev A. Kh., Beknazarov Kh. S., Dzhalilov A. T. Study of the efficiency of the corrosion inhibitor IKTsF-1 in 1M HCl // Universum: Chemistry and biology: electronic. scientific journal. 2019. – No. 2(56). URL: http://7universum.com/ru/nature/archive/item/6881/ (In Russian)

Beknazarov Kh. S., Dzhalilov A. T. Synthesis and study of the oligomeric corrosion inhibitor IKS-AEHG-1 // Collection of abstracts of reports of the V international conference of the school on chemistry and physical chemistry of oligomers. – Volgograd. 2015. –P. 35. (In Russian)

Yaro A. S., Abdul Masih N. Sh., Khadom A. A. The influence of temperature on corrosion inhibition of carbon steel in airsaturated 7N H3PO4 by potassium iodide, Iraqi J. Chem. Petrol. Eng. 1. 2000. – P. 83–87.

Oguzie E. E. "Adsorption and Corrosion Inhibitive Properties of Azadirachta Indica in Acid Solutions," Pigment & Resin Technology, – Vol. 35. – No. 6. 2006. – P. 334–340. Doi:10.1108/03699420610711335

Odiongenyi A. O., Odoemelam S. A. and Eddy N. O. "Corrosion Inhibition and Adsorption Properties of Ethanol Extract of Vernonia amygdalina for the Corrosion of Mild Steel in H2SO4". Portugalia Electrochimica Acta, – Vol. 27. – No. 1. 2009. – P. 33–45. Doi:10.4152/pea.200901033

Olimov B. B., Yoldosheva N. J. Gravimetric study of the mechanism of action of corrosion inhibitors used in the oil and gas industry // International scientific and educational electronic journal "Education and Science in the 21st century". Release. – No. 19.

Panoev E. R., Dustov H. B., Akhmedov V. N. Problems of corrosion in acidic component systems and methods for its reduction // Universum: technical sciences. 2021. – No. 12–5 (93). – P. 47–50. (In Russian)

Bobir O., Mashhura S., Islom B. Technology of obtaining effective corrosion inhibitors in the oil and gas industry // Universum: технические науки. 2022. – No. 1–3 (94). – C. 85–87.

submitted 21.03.2025;
accepted for publication 04.04.2025;
published 29.05.2025

Contact: chemistry2927@mail.ru

The Austrian Journal of Technical and Natural Sciences, No 3–4
ISSN 2310-5607

PREMIER Publishing
ppublishing.org

DOI:10.29013/AJT-25-3.4-28-31

IMPROVEMENT OF UREA-ASSISTED CLEANING OF RESINS AND COMPOUNDS IN DIESEL OR OIL

Khaidarov Bobomurod M. [1]***, Sodikov Usman Kh.*** [1]***, Rakhmanov Ortik K.*** [1]

[1] Fergana Polytechnic Institute

Cite: *Khaidarov B.M., Sodikov U.Kh. Rakhmanov O.K. (2025). Improvement of Urea-Assisted Cleaning of Resins and Compounds in Diesel or Oil. Austrian Journal of Technical and Natural Sciences 2025, No 3–4.* https://doi.org/10.29013/AJT-25-3.4-28-31

Abstract

Diesel fuel is one of the most popular petroleum products used in agricultural machinery. The composition, properties and quality of diesel fuels used in tractor and automobile engines largely determine the service life and reliability of fuel equipment and components and parts of the cylinder-piston group. The chemical stability of diesel fuel is its ability to resist oxidation processes that occur during storage. This problem arose with the deepening of oil refining by introducing middle distillate fractions of secondary oil processing, for example, gas oils obtained from catalytic cracking and coking, into the composition of commercial diesel fuel. The latter is enriched in unsaturated hydrocarbons, and also contains a large amount of sulfur and tar compounds. The presence of these compounds together with unsaturated hydrocarbons contributes to their oxidative polymerization, thereby affecting the formation of resins and deposits.

Keywords: *Diesel fuel, water, oil, coagulant*

Introduction

Currently, diesel engines are widely used in various areas of motor transport and are being developed as fuel for cars. Diesel engines are more economical than gasoline engines, have a lower risk of fire, are more reliable and have a longer service life, and are widely used due to their wide distribution. Diesel-fueled vehicles are 25–30% more fuel-efficient than gasoline-fueled vehicles. Diesel fuel has the property of operating more efficiently because it burns at a higher temperature than gasoline. The main reason for this is that diesel fuel has a higher cetane number (Mitusova T. N., Polina E. V., Kalinina M. V., 2002).

Diesel fuel has a standard of no more than 0.05% sulfur dioxide, other European and Eastern countries recommend that diesel fuel be produced according to the EN-590 standard (S < 0.005%) (Elvers B., 2012).

The production of diesel fuel with a low gold content of 0.035–0.001% is still it is also brewing at a low rate, but at a fast rate (Danilov A. M., 1998).

The composition, properties and quality of diesel fuels used in tractor and car engines largely determine the service life and reliability of the fuel equipment and components of the cylinder-piston group and the engine (Ostrikov V. V., Nagornov S. A. Gafurov I. D., 2006).

The ability to achieve a high compression ratio in diesel engines allows for a 25–30% reduction in specific fuel consumption compared to carburetor engines. The most important performance parameters of diesel fuel are the cetane number, fractional composition, low-temperature and lubricating properties, degree of purity, viscosity, presence of sulfur compounds, hydrocarbons and metals, as well as the flash point, which determines safety (Ostrikov V. V., Nagornov S. A. Gafurov I. D., 2006).

The cetane number determines the severity of the operating process, fuel consumption, and exhaust gas pollution. The higher the cetane number, the harder the engine will work. The higher the cetane number of diesel fuel, the faster the mixture will burn and the vehicle will start. However, as the cetane number increases, engine efficiency decreases and exhaust gas smog increases (Skarlykin A. N., 2003).

Research methods and objects G

As shown in Figure 1, the simulation of fuel cleaning processes to remove contaminants and water was carried out using a laboratory centrifuge.

The results were analyzed at centrifuge rotor operating or rotation speeds ranging from 2 to 10,000 rpm

Figure 1. *In the laboratory modeling centrifuge*

Cleaning for intended fuel from 20 to 30 °C was temperature between is heated. From this then 1% quartz powder to the fuel entered and harvest was mixed one trick to the state brought and later centrifuge with the help of again worked.

Experience from the beginning before, permanent dispersion provision for in fuel additional particles of the spread one variety microscopic in a way was evaluated.

Fuel cleaning process from 20 to 90 minutes changed standing time between to do increased.

Cleaning processes since it ended then, again worked in fuel exists of mechanical compounds The composition is regulated by GOST 6370–83 to the standard suitable was evaluated. The rest particle a pollutant substances microscopic analysis with the help of checked and described.

Results and Discussion

In addition to free water, which can be easily removed by physical treatment methods, diesel fuel also contains contaminants such as resins, asphaltenes, oxidation products, and sulfur compounds, which are almost impossible to completely remove.

The main difficulty in the removal process is the lack of effective fuel cleaning agents capable of removing additives in the dispersed phase smaller than 0.1 to 0.5 microns.

The presence of tars and sulfur in diesel fuel does not necessarily have a negative impact on its quality, since these substances can act as «lubricating agents» that help the combustion process to a certain extent. However, the accumulation of tars, sulfur, and heavy fractions in the fuel during combustion can lead to the formation of carbon deposits in the cylinder-piston complex. In addition, these components in diesel fuel can negatively affect engine efficiency and contribute to high levels of exhaust emissions, which worsens environmental pollution.

Dissolved components in fuel can only be removed by increasing the volume of dispersed particles using filters, centrifuges, and separators combined with physical and chemical cleaning methods.

The removal of fuel components can only be achieved by increasing the volume of dispersed particles using filters, centrifuges, and separators combined with physical and chemical cleaning methods.

Microscopic analysis with a magnification factor of Kuv = 110 shows that the tar content in the fuel is 60 mg/100 cm³, the mass fraction of sulfur is 0.5% or more, and no additives beyond this concentration were detected in the fuel.

Figure 2 shows the relationship between different concentrations of added acid and the resulting changes in fuel characteristics.

The use of sulfuric acid has been shown to help remove tars from diesel fuel (shown by curve 2 in Figure 2); however, this process simultaneously increases the sulfur concentration (S) and the acidity level (K) of the fuel, both of which are considered to be input effects.

Figure 2. *Dependence of changes in fuel properties on the concentration of introduced sulfuric acid*

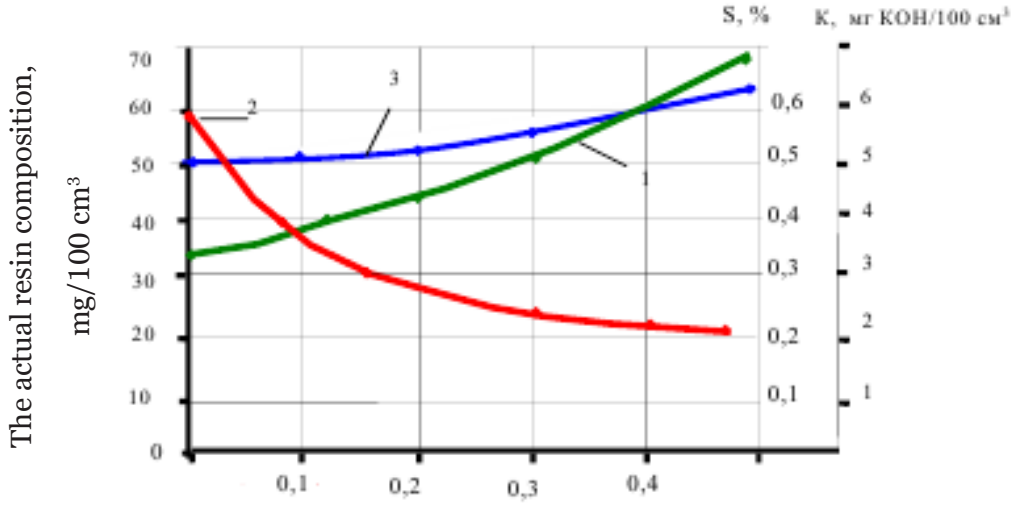

According to row 2 of Figure 2, the actual tar concentration in the fuel composition shows the most pronounced decrease in sulfuric acid concentration from 0.1% to 0.2%. Increasing the acid concentration to 0.5% does not lead to a significant additional decrease in tar content.

To evaluate the effectiveness of alkaline coagulants, a soda solution prepared with water was used. Various sodawater ratios - 5:1, 3:1 and 1:1 – were checked. 5:1 and 3:1 ratio yours truly complete to the end not achieved was determined. On the contrary, the ratio is 1:1 satisfactory solubility showed that more than 80% of soda dissolves As a result, next experimental processes 1:1 aqueous solution with the help of held, his in fuel concentration is kept at 1.5%.

Figure 3. *Water hydroxide solution since joining later diesel fuel samples photomicrographs*

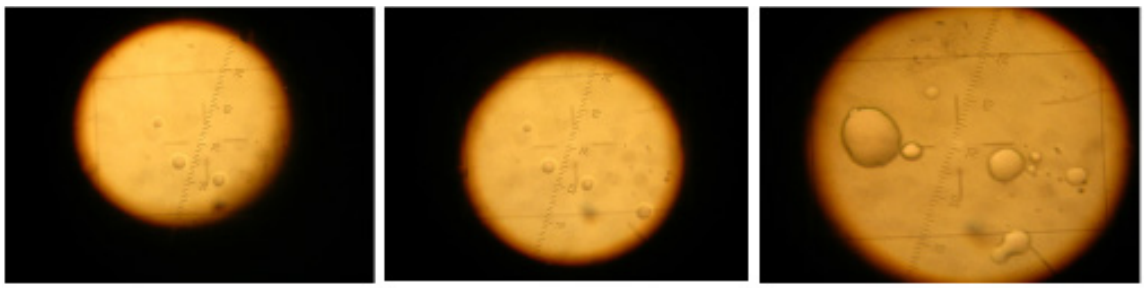

Aqueous hydroxide solution with mixed fuel up to 100 ° C heated , then permanent mixing from 0.5 to 1 hour under continue which permanent thermal impact under take will go the coagulation process efficiency microscopic in the method with the help of taken results analysis done.

Various in concentrations watery hydroxide solutions with processing given fuel samples photomicrographs are different in Fig. 3.

Is presented in Figure 3 experimental results analysis that shows that at concentrations of (a) 0.5%, (b) 1% and (c) 1.5% for fuel watery alkaline solution addition fuel in the composition melted to mixtures almost coagulant impact does not show.

If diesel fuel melted heavy hydrocarbon fractions, to sulfur based oil compounds and other substances included ultra-disperse system as if you look at it , its stability small in quantity electrolytes introduction noticeable to the extent impact to do can In lyophobic colloidal systems electrolytes the presence of the coagulation process noticeable to the extent accelerates . Coagulation installed theoretical principles and anointing in the oils disperse systems destabilization according to previous to research based on urea - wide widespread village farm mineral fertilizers fuel inside melted of mixtures coagulation in motion its potential effectiveness assessment for selected.

Given an optimized cleaning capacity of 100 liters per hour, the process operates in a continuous cycle, with 100 liters of diesel fuel being pumped from the primary storage tank over an hour, through a centrifugal separator, and back into the tank. This configuration allows for the simultaneous execution of key operations, including the addition of a coagulant, mixing, and homogenization of additives during a 60-minute cleaning period. From a mechanical perspective, the improvements in low-temperature fuel performance observed during this process can be attributed primarily to the uniform distribution of dissolved additive particles throughout the fuel matrix. This uniformity is facilitated by the hydrodynamic forces generated by the flow pressure as the fuel moves through the centrifuge rotor and then impacts the inner surface of the centrifuge housing, which also helps to remove residual water from the system.

Conclusion

Optimization studies using reactive centrifugation have shown that effective separation of resins and oxidation products can be achieved by collecting them. Optimal centrifugation performance was observed at a rotation speed of 7000 to 8000 rpm and a preheating temperature of 80 ° C. The required processing time, depending on the initial degree of contamination, was 45 to 60 minutes.

References

Mitusova T. N., Polina E. V., Kalinina M. V. Sovremennye dieselnye topliva i prisadki k nim. – M.: Technika, 2002. – 64 p.

Elvers B. Found. Production, application, properties. – Spb.: TsOP “Profession”, 2012. – 171 p.

Danilov A. M. // HTTM. – No. 5. 1998. – P. 14 – 16.

Mitusova T. N., Havkin V. A., Gulyaeva L. A., Kalinina M. V., Vinogradova N. Ya. // Mir nefteproduktov – No. 2. 2012. – P. 6–8.

Mitusova T. N. Sovremennoe sostoyanie proizvodstva diesel fuel. Trebovaniya k kachestvu // Mir nefteproduktov. 2009. – No. 9–10. – P. 6–9.

Ostrikov V. V., Nagornov S. A. Gafurov I. D. Toplivo i smazochnye materialy. Uchebnoe posobie. – Ufa: BGAU, 2006. – 292 p.

Skarlykin A. N. K voprosu obezvojivaniya dieselnyx topliv otstaivaniem // Sovershenstvovanie resur sosberegayushchih teknologii i teknicheskix sredstv proizvodstva selkhozproduktsii: Сб. mater, nauchn. – prakt. conf. “Problemy APK i puti ix solution”. – Penza: Penzenskaya GSXA, 2003. – P. 9–11.

submitted 17.04.2025;
accepted for publication 01.05.2025;
published 29.05.2025

Contact: eldor8501@gmail.com

The Austrian Journal of Technical and Natural Sciences, No 3–4
ISSN 2310-5607

PREMIER Publishing
ppublishing.org

DOI:10.29013/AJT-25-3.4-32-36

TECHNOLOGY FOR PROCESSING COAL AND CONVERTING IT INTO AN ENERGY SOURCE BY EXTRACTING GAS

Kucharov Azizbek [1,2]***, Yusupov Farkhod*** [1]***,***
Khalilov Sanjar [1]***, Yusupov Sukhrob*** [1]

[1] Institute of General and Inorganic Chemistry of the Academy of Sciences of Uzbekistan. Tashkent, Uzbekistan

[2] Pharmaceutical Education and Research Institute Yunusobod District, Tashkent, Uzbekistan

Cite: *Kucharov A., Yusupov F., Khalilov S., Yusupov S. (2025). Technology For Processing Coal and Converting it into an Energy Source by Extracting Gas. Austrian Journal of Technical and Natural Sciences 2025, No 3–4.* https://doi.org/10.29013/AJT-25-3.4-32-36

Abstract

This study explores the suitability of beneficiated Uzbek coal as a feedstock for gasification and pyrolysis processes. XRF analysis of the unprocessed coal indicated a high concentration of inert, ash-producing minerals, while SEM imaging showed a compact structure with minimal porosity. GC–MS analysis of the resulting fuel confirmed the presence of key hydrocarbon components. Overall, the results indicate that treated coal offers high efficiency and low residue, making it well-suited for modern fuel conversion applications.

Keywords: *coal beneficiation, gasification, pyrolysis, XRF analysis, SEM imaging, GC–MS, synthetic gas, energy efficiency, carbon content, Uzbekistan coal*

Introduction

Ensuring global energy security, reducing reliance on conventional fuels, and preserving environmental balance are among the most urgent scientific and practical challenges today (Li, F., & Fan, L. S., 2008). Coal gasification technology – used to convert coal into synthetic gas (CO, H_2, CH_4, and other components)—is becoming increasingly vital in the modern energy sector (Yusupov, F., & Khursandov, B., 2024). Leading countries by coal reserves include the United States (250 billion tons), China (143 billion tons), India (111 billion tons), Russia (160 billion tons), and South Africa (30 billion tons) (Miller, B. G., 2010). However, direct combustion of coal leads to substantial environmental pollution, especially through the emission of carbon dioxide (CO_2) (Miura, Kouichi, 2000), sulfur oxides (SO_x), and nitrogen oxides (NO_x), all of which significantly contribute to global warming and air quality deterioration (Kucharov, Azizbek, et al., 2025).

Consequently, scientific research is accelerating into coal conversion technologies such as pyrolysis and gasification, which aim to produce cleaner, high-efficiency synthetic gas. This gas not only improves fuel efficiency

but also expands its industrial applications–serving as a feedstock for heat and power generation, as well as the synthesis of methanol, ammonia, hydrogen, and other chemical products (Xursandov, Bobomurod, et al., 2024). While advanced solutions like Clean Coal Technology and Integrated Gasification Combined Cycle (IGCC) have been deployed worldwide, there remain key unresolved challenges regarding their energy efficiency and economic feasibility under varying conditions (Kucharov, Azizbek, et al., 2021).

In Uzbekistan, domestic coal resources – such as Angren (1.9 billion tons), Shargun (45 million tons), and Boysun (36 million tons)—remain largely underutilized. Implementing coal gasification technologies tailored to local conditions can enhance national energy security, reduce dependence on imported energy, and mitigate environmental risks (Qurbonov, Azizjon, Azizbek Kucharov, and Farxod Yusupov, 2024). Therefore, developing the scientific foundations for synthetic gas production from coal and applying these methods at industrial scale is a highly relevant and strategic scientific goal for the country.

Research method

Coal samples were collected from the [region] deposit. After drying at 105 °C and grinding below 100 μm, flotation was applied using an anionic surfactant to obtain an enriched coal fraction.

XRF analysis was performed to determine elemental composition using a Rh-anode XRF spectrometer under helium atmosphere. High levels of Si, Al, and Ca indicated inert, ash-forming compounds. Fe and S signaled the presence of pyrite, while trace Zn, Cu, Ag, Cd, Zr, and Rb reflected either geogenic or anthropogenic origins.

SEM imaging (500× magnification) was used to examine surface morphology before (Spectrum 29) and after enrichment (Spectrum 40). Untreated coal showed a dense, low-porosity structure with ~35% SiO_2 and 28% Al_2O_3. In contrast, enriched coal exhibited >25% porosity, reduced Si and Al (~10–12%), and increased carbon content (~65–70%).

GC–MS analysis of the synthesized fuel product was conducted using EI+ ionization and a 30 m capillary column. Major peaks at 4.79 min and 4–6 min confirmed volatile light fractions; heavier compounds appeared between 9–18 min, indicating a mixture of fuel-relevant and inert substances.

Result and discussion

According to the results of the XRF analysis, the coal sample contains high levels of silicon (Si), aluminum (Al), and calcium (Ca), indicating a significant presence of inert, ash-forming components. The detection of iron (Fe) and sulfur (S) suggests the presence of pyrite and other iron sulfides, which can lead to the release of hydrogen sulfide (H_2S) during the gasification process.

Additionally, trace amounts of heavy metals such as Zn, Cu, Ag, and Cd were recorded, which may be related to anthropogenic contamination or background signals specific to the equipment (Figure 1). The presence of rare elements such as zirconium (Zr) and rubidium (Rb) indicates that the coal deposit has a geologically unique and distinctive composition.

According to the morphological and elemental analysis, the untreated coal sample (Figure 2a) has a smooth and dense structure with low porosity (porosity density < 10%). This is clearly visible in the SEM image. The high content of SiO_2 and Al_2O_3—approximately 35% and 28%, respectively – indicates the presence of ash-forming inert compounds. The carbon (C) content is around 30–35%, suggesting a low proportion of combustible fractions. This implies that the coal may not be an efficient fuel source for pyrolysis or gasification processes.

On the other hand, the enriched coal sample (Figure 2b) shows an increased number of microcracks and micropores on its surface (porosity density > 25%), which significantly increases the total surface area and enhances contact with reactive gases. Elemental analysis shows a reduction in Al and Si content to around 10–12%, indicating lower ash formation. The carbon content is approximately 65–70%, which greatly improves its energy yield. Thus, the enriched coal stands out in pyrolysis or gasification processes with higher efficiency, a high calorific value (around 25–28 MJ/kg), and a low residue rate (~5–8%). According to the chromatogram results, a prominent peak detected at 4.79 minutes

in the analyzed organic substance indicates a high content of volatile, light fractions, suggesting good combustibility and energy release potential (**Figure 3**).

Figure 1. *XRF (X-ray fluorescence spectral analysis) image of the coal sample*

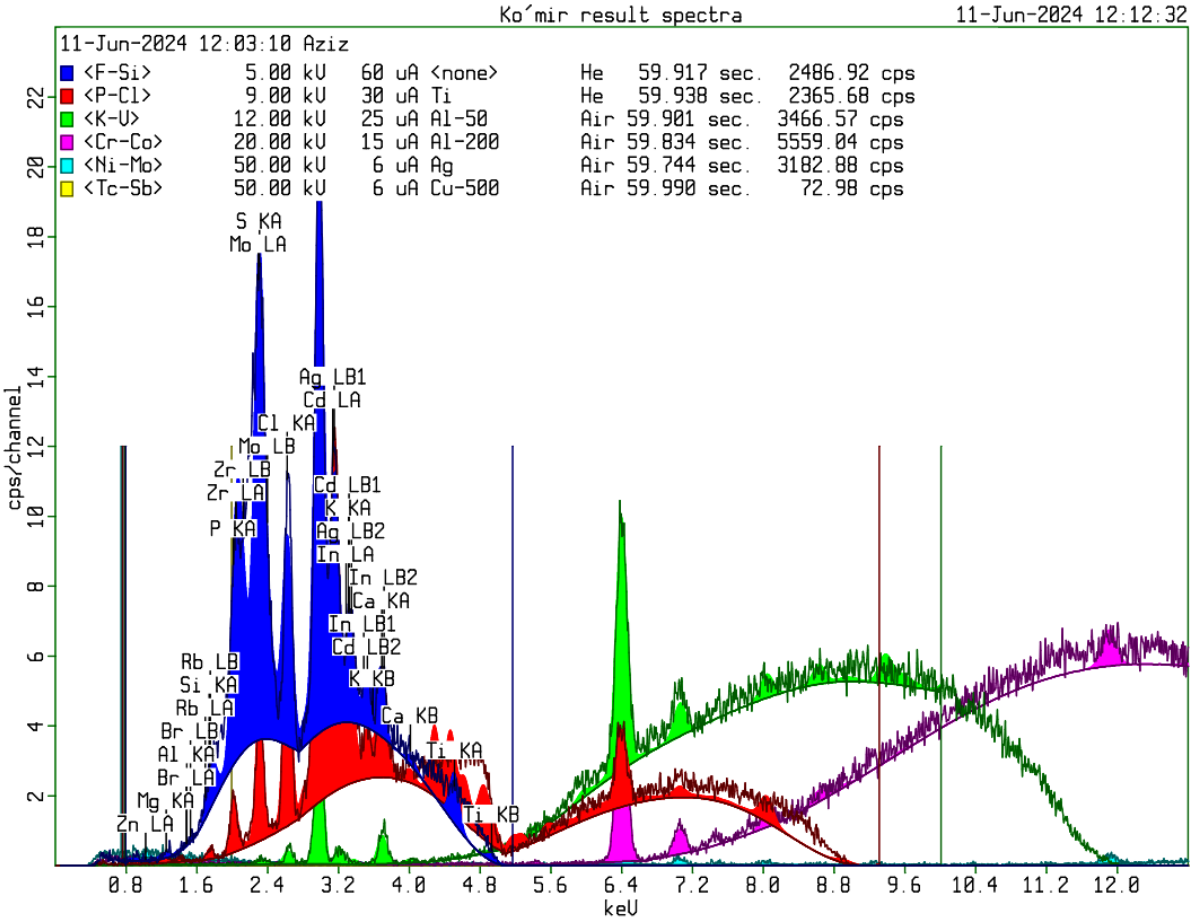

Figure 2. *SEM (Scanning Electron Microscope) images of the coal samples*

(a) before processing

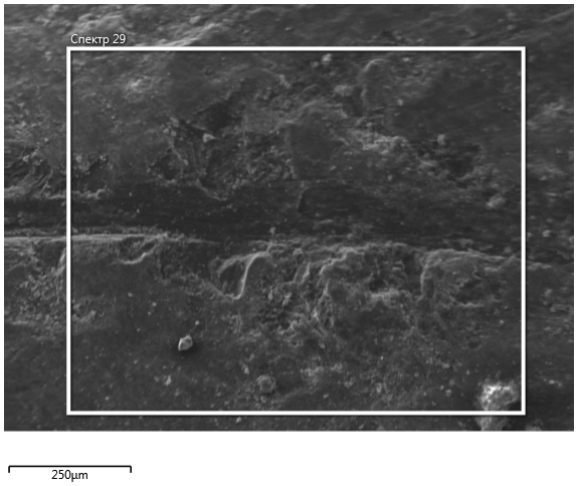

(b) after processing

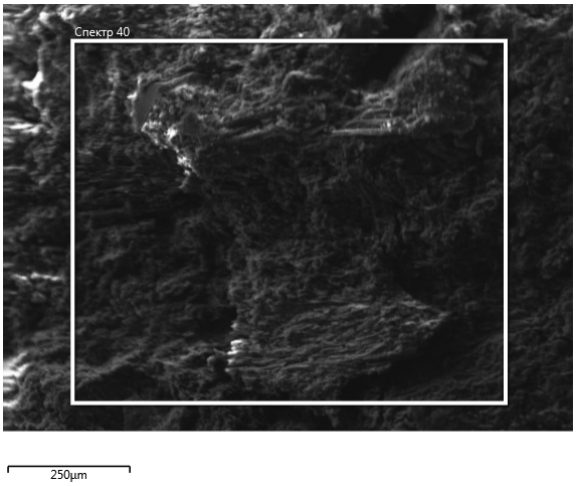

Figure 3. *"TIC (Total Ion Chromatogram) image of the synthesized fuel product obtained using GC–MS (Gas Chromatography–Mass Spectrometry)*

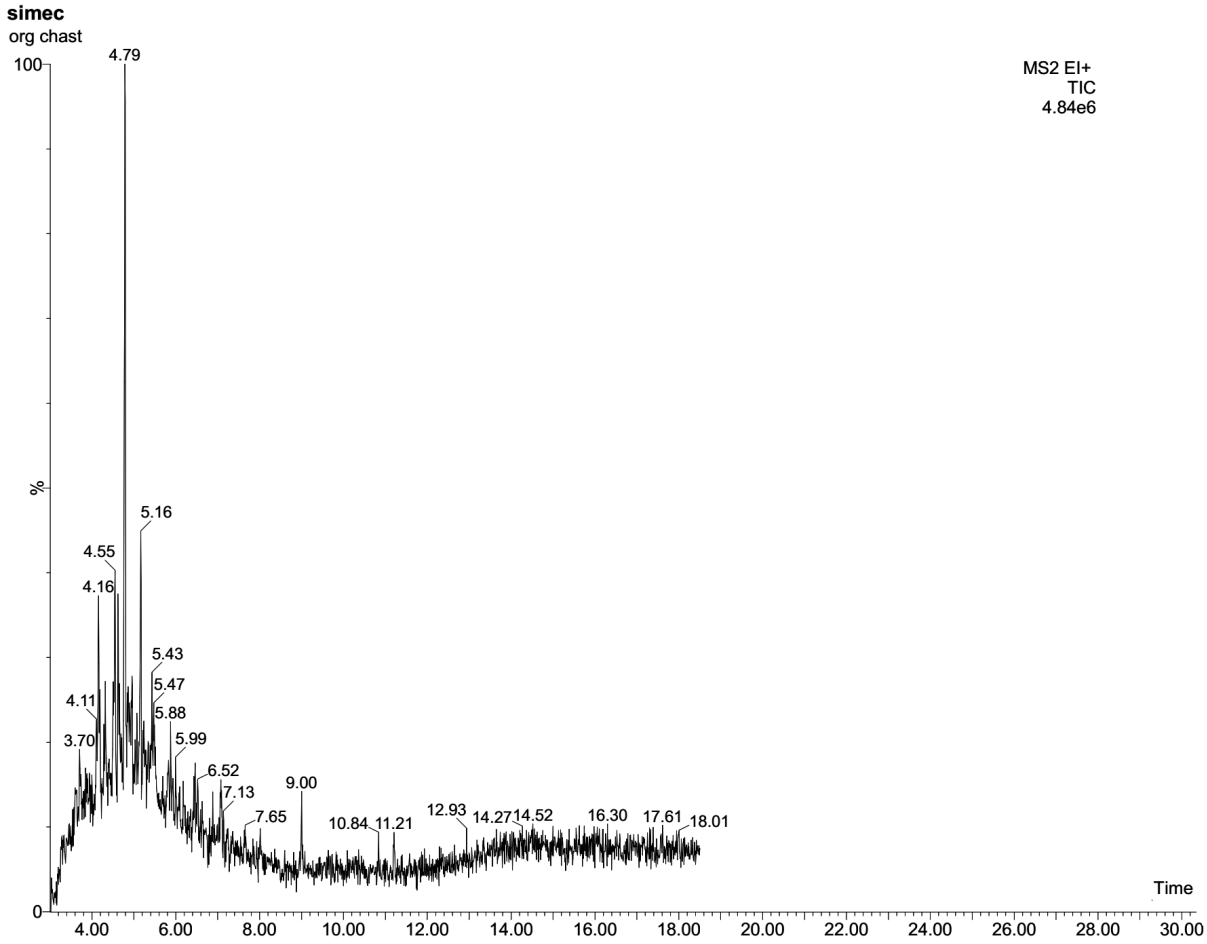

The strong peaks observed between 4–6 minutes point to components that could potentially be used as synthesis gas or light fuel. Between 9–18 minutes, heavier, higher molecular weight substances were identified; some of these are heat-resistant and may be useful as fuel, while others may require purification. After 18 minutes, the signal remains nearly constant, indicating the presence of inert residual substances.

Conclusion

The experimental findings demonstrate that coal beneficiation significantly enhances its effectiveness as a feedstock for synthetic gas and liquid fuel production. XRF analysis showed that raw coal contains high levels of ash-forming minerals – around 35% SiO_2 and 28% Al_2O_3—along with calcium, iron, and sulfur, indicating substantial inert and pyritic content. In contrast, the enriched coal exhibited a reduced presence of Si and Al (~10–12%) and a marked increase in carbon content (approximately 65–70%), reflecting a twofold rise in combustible material. SEM analysis confirmed a shift from the smooth, low-porosity (<10%) surface of raw coal to a porous microstructure (>25%) in the treated sample, enabling better gas-solid interaction during thermal processes. GC––MS analysis further supported these results, identifying strong peaks at 4.79 and between 4–6 minutes – indicating the presence of light, volatile hydrocarbons ideal for clean combustion and syngas production – alongside heavier fractions between 9–18 minutes and minimal inert residue beyond 18 minutes. Overall, the upgraded coal offers higher calorific value (25–28 MJ/kg), reduced ash content (5–8%), and improved reactivity, making it a strong candidate for advanced, cleaner fuel technologies like gasification and pyrolysis.

References

Li, F., & Fan, L. S. (2008). Clean coal conversion processes–progress and challenges. Energy & Environmental Science, – 1(2). – P. 248–267.

Yusupov, F., & Khursandov, B. (2024). Working Out the Optimal Conditions for Obtaining Import-Substituting Polymer Sulfur For the Oil And Gas and Rubber Industry. Science and innovation, – 3(A10). – P. 167–170.

Miller, B. G. (2010). Clean coal engineering technology. Elsevier.

Miura, Kouichi. "Mild conversion of coal for producing valuable chemicals". Fuel processing technology – 62.2–3 (2000): 119–135.

Kucharov, Azizbek, et al. "Scientific analysis of the development of new types of flotation reagents used in coal enrichment." EUREKA: Physics and Engineering – 2. 2025. – P. 32–39.

Xursandov, Bobomurod, et al. "Study of changes in the physical and mechanical properties of sulfur asphalt concrete mixture based on polymer sulfur". *AIP Conference Proceedings*. – Vol. 3045. – No. 1. AIP Publishing, 2024.

Kucharov, Azizbek, et al. "Development of technology for water concentration of brown coal without use and use of red waste in this process as a raw material for colored glass in the glass industry". *E3S Web of Conferences*. – Vol. 264. EDP Sciences, 2021.

Qurbonov, Azizjon, Azizbek Kucharov, and Farxod Yusupov. "Development of a technology for obtaining an anti-corrosion coating for gas pipelines". *AIP Conference Proceedings*. – Vol. 3102. – No. 1. AIP Publishing, 2024.

submitted 15.04.2025;
accepted for publication 29.04.2025;
published 29.05.2025

Contact: sciuzb@mail.ru

The Austrian Journal of Technical and Natural Sciences, No 3–4
ISSN 2310-5607

PREMIER Publishing
ppublishing.org

DOI:10.29013/AJT-25-3.4-37-42

POLYPRÉNOLS OF NEW VARIETIES OF COTTON

Mamatkulova Nodira Maxsumovna [1], ***Zokirova Umida Tolipovna*** [1], ***Mamarozikov Umidjon Baxtiyarovich*** [1], ***Khaxxarov Izatulla Tilovovich*** [2], ***Khidyrova Nazira Kudratovna*** [1]

[1] Institute of the Chemistry of Plant Substances, Academy of Sciences of the Republic of Uzbekistan, Tashkent, Uzbekistan

[2] Institute of Genetics and Experimental Plant Biology, Academy of Sciences of the Republic of Uzbekistan

Cite: *Mamatkulova N. M., Zokirova U. T., Mamarozikov U. B., Khaxxarov I. T., Khidyrova N. K. (2025). Polyprénols of New Varieties of Cotton. Austrian Journal of Technical and Natural Sciences 2025, No 3–4.* https://doi.org/10.29013/AJT-25-3.4-37-42

Abstract

This study presents the results of research conducted on the homologous composition of polyprenols found in the leaves of new cotton (Gossypium, Malvaceae) varieties. The analysis revealed that the leaves of early-maturing, salt- and drought-tolerant, as well as disease-resistant cotton varieties – Narpay, Kelajak, UzFA-703, and UzFA-705-can serve as promising sources of polyprenols. The extraction of polyprenols was carried out using standard chromatographic techniques. The study contributes to the identification of plant-based sources of biologically active compounds and supports the utilization of cotton plant by-products in biotechnology and pharmacology. These results suggest the potential for further development and application of polyprenol-containing preparations derived from cotton leaf biomass, particularly from stress-tolerant cultivars bred under the conditions of Uzbekistan.

Keywords: *leaves, Gossypium, Malvaceae, UzFA-703, UzFA-705, Kelajak, Narpay, extraction, HPTLC, polyprenols*

Introduction

Cotton is a versatile plant capable of meeting many human needs (Sadykov A. S., 1985). It belongs to the genus *Gossypium* of the family *Malvaceae*, with numerous regionally adapted varieties differing in earliness, wilt resistance, growth type (dwarf or tall), and fiber type (fine-fibered, medium-fibered, etc.) (Khidirova N. K., Mamatkulova N. M., Kikteev M. M., Shakhidoyatov Kh.M. 2000; Mamatkulova N. M., Eshmirzaeva N., Khidirova N. K., Shakhidoyatov Kh. M., 2001). All parts of the cotton plant are valuable raw materials for industry, and around 1,200 different products essential to human life can be obtained from them. For example, hydrolyzed alcohol and protein-rich fodder yeast can be derived from the stems; gossypol and medicinal preparations from the roots; citric and malic acids, the growth stimulant

Uchkun, and a poultry feed concentrate provisionally named *Gossipren* from the leaves (Khidirova N. K., Zakirova R. P., 2019; Oripov A. O., Khidirova N. K., Akhmedov B. N., Ismatova R. A., Sheralieva S. 2019; Khidyrova N. K., Asatova S., Mamatkulova N. M., Yuldashev S. U., Umarov A. A., Shakhidoyatov Kh.M., 2008; Zakirova R. P., Kurbanova E. R., Khidirova N. K., 2020).

The chemical composition of cotton leaves has been studied under the guidance of Academician A. S. Sadykov, later under Professors Ya. V. Rashkes and Kh. M. Shakhdoyatov. At the end of the last millennium, Abu Ali Ibn Sina (Avicenna) wrote that cotton seeds help with cough, chest, and stomach diseases, and that cotton leaf juice stops childhood diarrhea (Abdullaeva D. A., 2017).

In modern traditional medicine, cottonseed oil is used to treat skin diseases. Cotton ash is applied externally as a hemostatic agent (Sadykov A. S., Turulov A. V. 1967). In official medicine, the plant is still under investigation. It has been determined that the total flavonoids from cotton flowers have capillary-strengthening, hypotensive, anti-inflammatory, hepatoprotective, and gastroprotective properties. Gossypol exhibits antiviral, immunostatic, and antitumor properties (Rashkes A. M., Khidyrova N. K., Shakhidoyatov Kh. M., 1997; Ismailov A. I., Karimdzhanov A. K., Islambekov Sh. Yu., Rakhimkhanov Z. B. 1994; Khidyrova N. K., Shakhidoyatov Kh. M. 2002).

Based on this, the use of cotton leaves as a valuable and accessible raw material for producing agricultural and medicinal preparations can be considered.

Previously, we studied polyprenol concentrates isolated from the leaves of cotton varieties T-1, 108-F, S-6524, and others (Rashkes Ya.V., Rashkes A. M., Nadzhimov U. K., Khidyrova N. K., Shakhidoyatov Kh.M., Musaev Zh. A., 1989). There is great interest in polyprenols as potential agents for wound healing due to their high regenerative activity (Syrov V. N., Vais U. V., Egamova F. R., Khushbaktova Z. A., Mamatkulova N. M., Shakhidoyatov R.Kh., 2012). When applied to flat full-thickness skin wounds in rats, the polyprenol concentrate from cotton leaves had a pronounced effect on proliferative and synthetic processes, thereby accelerating wound healing. The effect of the investigated polyprenol concentrate was similar to that of sea buckthorn oil, but manifested to a greater extent (Vais E. V., Yusupova S. M., Zokirova U. T., Khushbaktova Z. A., Syrov V. N., 2019).

Polyprenol fractions were extracted from cotton leaves with high yields of 1–3.5% of the plant's air-dry mass (ADM). Their chemical structure and homologous composition were determined, and standardization was performed (Rashkes A. M., Khidyrova N. K., Rashkes Ya.V., Mirkhodjaev U. Z., Nadzhimov U. K., Shakhidoyatov Kh. M., 1995). It was established that polyprenols from cotton leaves exhibit gastroprotective activity in models of "stress-induced," acetylsalicylic acid-induced, and ethanol-induced ulcers, and also have therapeutic effects in a model of chronic ulcers caused by acetic acid (Vais E. V., Yusupova S. M., Zokirova U. T., Khushbaktova Z. A., Syrov V. N., 2019).

Materials and Methods

A study was conducted on the polyisoprenoids of cotton leaves from newly developed promising varieties: UzFA-703, UzFA-705, Kelajak, and Narpay, created by researchers from the Institute of Genetics and Experimental Plant Biology (Kakhkharov I. T., 2010).

The *Kelajak* variety was developed at the Institute of Genetics and Experimental Plant Biology of the Academy of Sciences of the Republic of Uzbekistan (Kakhkharov I. T., 2010). It was obtained by crossing the cotton species *Gossypium hirsutum* L. and *Gossypium barbadense* L., resulting in the L-6161 line. Through hybridization between L-6161 and the Bulgarian variety 146 (*Gossypium hirsutum* L.), the early-maturing *Kelajak* bush variety was created. The plant has a large bush type with a main stem height of 80–90 cm and 3–5-lobed leaves. Its average yield is 37.2 centners per hectare, and the vegetation period is 110–115 days. *Kelajak* differs from other varieties in fiber yield and quality, adaptability to different climatic conditions, early ripening, high yield, drought and salt tolerance, and its characteristic of self-pruning.

The *UzFA-703* variety was developed by hybridizing lines L-6161 and L-45. The main stem height is 100–120 cm, stems are pale green, and leaves are 3–5-lobed. The average

yield is 36.3–40.0 centners per hectare, with a vegetation period of 110–115 days. It differs from standard varieties by its earliness, high yield, and tolerance to drought and salinity.

The *UzFA-705* variety was created through multiple hybridizations between line L-6161 and line L-417. The main stem height is 90–100 cm, stems are green, and leaves are 3–5-lobed. Its average yield is 35.0–41.0 centners per hectare, with a vegetation period of 115 days.

The *Narpay* variety was developed from line L-470. It stands out for its fiber quality, early ripening, wilt resistance, drought and salt tolerance, and high yield under diverse climatic conditions. The main stem height is 100–120 cm, stems are pale green, and leaves are 3–5-lobed. The average yield is 37.0 centners per hectare, and the vegetation period is 115 days.

The *Namangan-77* industrial variety was developed by crossing variety 159-F with the semi-wild species *Gossypium punctatum*. Through subsequent selection from this cross, the industrial early-ripening *Namangan-77* variety was developed (authors: V. A. Avtanomov, M. Saidakhmedov). The plant has a large bush, the main stem height is 100–110 cm, and it is wilt-resistant. The average yield is 29–52 centners per hectare, with a vegetation period of 100–115 days.

Plant Material

Cotton leaves were collected from the lower tiers of plants grown on the same plot in September 2024.

The total extractive substances and neutral compounds were isolated according to described methods. A standard sample was obtained from the leaves of Rhus coriaria (Mamatkulova N. M., Khidirova N. K., Mamadrakimov A. A., Shakhidoyatov Kh. M., 2014).

Qualitative and quantitative analysis of polyprenols was performed using high-performance thin-layer chromatography (HPTLC) with a device from Camag (Switzerland) (Khidyrova N. K., Mamatkulova N. M., Mukarramov N. I., Shakhidoyatov Kh. M., 2012).

Isolation of Polyprenols (General Method)

Air-dried leaves of cotton varieties *Kelajak*, *Narpay*, *UzFA-703*, and *UzFA-705* (100 g each) were sequentially extracted with 3000 ml of 96% ethanol (1000 ml × 3), followed by 300 ml of benzene. To each extract, 90 ml of a 50% aqueous potassium hydroxide (KOH) solution was added, and the mixture was shaken at room temperature for one hour. The mixture was then diluted with water, and the benzene layer was separated, washed with water until neutral, and dried over anhydrous Na_2SO_4.

The organic layer was concentrated using a rotary evaporator to obtain the total extractives. Ten grams of the extractive mixture were weighed and subjected to column chromatography for fractionation. Silica gel of the KSK brand (100/250 mesh) was used as the adsorbent, with an adsorbent-to-substance ratio of 40:1. Elution was carried out first with hexane, then with a hexane–chloroform system, gradually increasing polarity.

As a result, polyprenol fractions were obtained with purity ranging from 94% to 98%, and yields of 2.82%, 2.72%, 2.49%, and 2.52% of the air-dry plant mass, respectively. The purity of polyprenols was monitored using thin-layer chromatography (TLC) on Silufol UV-254 plates in solvent systems: benzene–ethyl acetate (24:1) or hexane–chloroform (1:2). The detection reagent was a 1% solution of vanillin in concentrated sulfuric acid. The content of polyprenols in the fractions was determined using TLC and high-performance TLC (HPTLC) methods (Mamatkulova N. M., Eshmirzaeva N., Khidirova N. K., Shakhidoyatov Kh.M. 2001; Khidyrova N. K., Mamatkulova N. M., Mukarramov N. I., Shakhidoyatov Kh. M. 2012).

Discussion of Results

To determine the polyprenol content, the total amount of neutral compounds (NC) was isolated using the method described in (Mamatkulova N. M., Khidirova N. K., Mamadrakimov A. A., Shakhidoyatov Kh. M. 2014), and the content of polyprenols was determined by high-performance thin-layer chromatography (HPTLC) (Khidyrova N. K., Mamatkulova N. M., Mukarramov N. I., Shakhidoyatov Kh. M. 2012). The results are summarized in Table 1.

Table 1. *Yields of total extractives (TE), neutral compounds (NC), polyprenols (PP) in % of air-dry mass and polyprenol homologue content in % of sample weight*

№	Cotton Variety	TE, %	NC%	PP%	PP Homologue Content		
					n=10	n=11	n=12
1.	Namangan-77	11.6	5.2	2.53	Trace	23.10	8.5
2.	Kelajak	11.5	4.1	2.82	14.90	75.71	9.39
3.	Narpay	12.5	4.4	2.60	8.40	80.58	11.02
4.	UzFA-703	10.1	3.8	2.49	Trace.	85.27	14.72
5.	UzFA-705	11.1	4.0	2.57	Trace	82.6	17.29

** Standard polyprenols isolated from sumac (Rhus coriaria) leaves contained polyisoprenoid units ranging from C10 to C13, with the following composition: decaprenol (5.37%), undecaprenol (60.85%), dodecaprenol (20.47%), and tridecaprenol (13.31%)*

Discussion of Results

The data presented in Table 1 and HPTLC analysis of polyprenols indicate that the isolated compounds consist of three polymer homologues containing 10–12 isoprenoid units, with undecaprenol (n=11) being the dominant component.

Among the studied varieties, Kelajak showed the highest polyprenol content. This variety is characterized by self-topping, which is economically beneficial as it eliminates the need for mechanical topping. The quantitative composition of polyprenol homologues in Kelajak was as follows: decaprenol – 14.90%, undecaprenol – 75.71%, and dodecaprenol – 9.39% (Figure 1).

In other cotton varieties such as UzFA-703 and UzFA-705, the homologue profile is slightly different: decaprenol is present in trace amounts, while undecaprenol content reaches 85.27% and 82.6%, respectively.

For identification, polyprenols were isolated using column chromatography (CC) on silica gel with yields ranging from 2.49% to 2.82% of the air-dry plant material. Their structure was confirmed using IR spectroscopy, ^{1}H and ^{13}C NMR spectroscopy, and mass spectrometry.

IR spectral data of polyprenols included:

Absorption at 837 cm^{-1}: characteristic of C–H deformation in tri-substituted olefins (CH_2–C(CH_3)=CH–CH_2),1001 cm^{-1}: C–O stretching in allylic primary alcohols (CH=CH–CH_2OH), 1376 cm^{-1}: C–H deformation in CH_3 groups, 1448 cm^{-1}: CH_2 and CH_3 group vibrations, 1668 cm^{-1}: C=C stretching in the isoprenoid chain, 2856, 2927, 2962 cm^{-1}: C–H stretching of CH_2 and CH_3 groups, 3024 cm^{-1}: =CH group vibrations, 3561 cm^{-1}: free hydroxyl group, 3332 40 cm^{-1}: associated hydroxyl groups from polymer interactions.

Mass spectrometry revealed weak molecular ion peaks at: m/z 698 ($C_{50}H_{82}O$) – dodecaprenol, m/z 766 ($C_{55}H_{90}O$) – undecaprenol, m/z 834 ($C_{60}H_{98}O$) – tridecaprenol, along with fragment ions at m/z 680, 748, 816, and smaller fragments 153, 135; 85, 67; 69, consistent with known fragmentation patterns for polyprenols from other sources (Khidyrova N. K., Rakhmatova M. Zh., Kukina T. P., Shakhidoyatov Kh. M.).

^{1}H NMR spectrum showed: Singlets at δ 1.62 and 1.56 ppm – cis- and trans-methyl groups (CH_2–C(CH_3)–CH), Multiplet at δ 1.90–2.05 ppm (centered at 1.96 ppm) – methylene protons of the isoprenoid chain, Doublet at δ 3.97 ppm (J = 7.5 Hz) – methylene protons of the terminal –CH–CH_2OH group, Broad singlet at δ 5.05 ppm – olefinic protons in the middle of the chain, Triplet at δ 5.31 ppm (J = 7.5 Hz) – terminal olefinic proton.

^{13}C NMR spectrum showed: δ 32.21 ppm – methylene carbons in trans-cis (E-Z) arrangements, δ 32.41 ppm – cis-cis (Z-Z), δ 39.91–39.93 ppm – trans-trans (E-E) and terminal trans (ω-E) configurations. These chemical shift values confirm the structure of cotton-derived polyprenols.

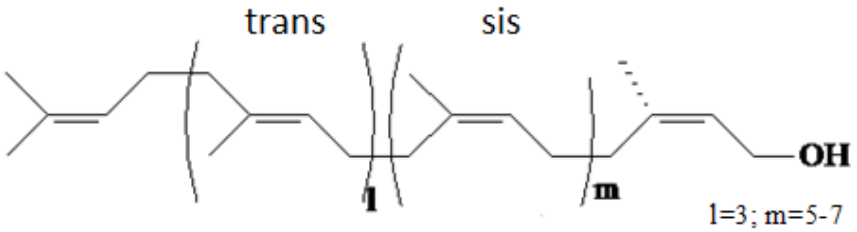

Conclusion

The conducted research demonstrated that the polyprenol content in the leaves of early-maturing, drought- and salt-tolerant cotton varieties – Kelajak, Narpay, UzFA-703, and UzFA-705-was 2.82%, 2.72%, 2.49%, and 2.52% of dry matter, respectively. Among these, the Kelajak variety showed the highest polyprenol yield. It is especially noteworthy for its self-topping trait, which is advantageous from an agricultural and economic standpoint, reducing the need for mechanical topping. These findings indicate that the Kelajak variety is a promising source of biologically active polyprenols and can be used for further biochemical and pharmacological studies in natural product research.

References

Sadykov A. S. Cotton – the Miracle Plant. – Moscow: Nauka, 1985. – 144 p.

Khidirova N. K., Mamatkulova N. M., Kikteev M. M., Shakhidoyatov Kh. M. Comparison of Some Secondary Metabolites in Cotton Leaves Differing in Genetic Traits. Chemistry of Natural Compounds, – Tashkent, 2000. – No. 6. – P. 478–480.

Mamatkulova N. M., Eshmirzaeva N., Khidirova N. K., Shakhidoyatov Kh. M. Isolation of Polyprenols from Cotton Leaves. Chemistry of Natural Compounds, Special Issue, – Tashkent, 2001. – P. 10–11.

Khidirova N. K., Zakirova R. P. "Uchkun" – an Environmentally Friendly Biostimulant. In: Prospects for the Development of Innovative Agrotechnologies in Horticulture, Viticulture and Winemaking. Republican Scientific-Technical Conference. Collection of Articles. – Tashkent, 2019. – P. 278–281.

Oripov A. O., Khidirova N. K., Akhmedov B. N., Ismatova R. A., Sheralieva S. Effect of Gossypol-Containing Feed Additive on Chick Viability and Hematological Parameters. Veterinary Medicine, – No. 3 (136). 2019. – P. 25–26.

Khidyrova N. K., Asatova S., Mamatkulova N. M., Yuldashev S. U., Umarov A. A., Shakhidoyatov Kh. M. Impact of Isoprenoids from Cotton Leaves on the Growth and Development of Wheat. Agrochemistry, 2008. – No. 2. – P. 33–36.

Zakirova R. P., Kurbanova E. R., Khidirova N. K. Effectiveness of the Biostimulator Composition "Uchkun Plus" on Cotton. Agrochemistry, 2020. – No. 5. – P. 26–30.

Abdullaeva D. A. Cotton – Perspectives of Use as a Medicinal Plant. Electronic Scientific Journal «Biology and Integrative Medicine», 2017. – No. 10 (November).

Sadykov A. S., Turulov A. V. Cotton Leaves – a Valuable Chemical Raw Material. – Tashkent: Uzbekistan, 1967. – 115 p.

Rashkes A. M., Khidyrova N. K., Shakhidoyatov Kh. M. Components of Cotton Leaves, Their Functional Role and Biological Activity. Chemistry of Natural Compounds, – Tashkent, 1997. – P. 773–788.

Ismailov A. I., Karimdzhanov A. K., Islambekov Sh.Yu., Rakhimkhanov Z. B. Flavonoids of Cotton and Related Plants. Chemistry of Natural Compounds, – Tashkent, 1994. – No. 1. – P. 3–19.

Khidyrova N. K., Shakhidoyatov Kh. M. Plant Polyprenols and Their Biological Activity. Chemistry of Natural Compounds. Tashkent. Translated from Russian. Springer, USA, 2002. – Vol. 38. – No. 2. – P. 107–120.

Rashkes Ya.V., Rashkes A. M., Nadzhimov U. K., Khidyrova N. K., Shakhidoyatov Kh.M., Musaev Zh. A. Comparative Analysis of the Chemical Composition of Leaves of Normal and Dwarf Cotton Mutants. Reports of the Academy of Sciences of the Uzbek SSR, – Tashkent, 1989. – No. 5. – P. 53–54.

Syrov V. N., Vais U. V., Egamova F. R., Khushbaktova Z. A., Mamatkulova N. M., Shakhidoyatov R. Kh. Antiulcer Activity of Polyprenols Isolated from Cotton Leaves. Pharmaceutical Chemistry Journal, Moscow, Russia, 2012. – Vol. 46. – No. 3. – P. 34–37.

Vais E. V., Yusupova S. M., Zokirova U. T., Khushbaktova Z. A., Syrov V. N. Experimental Evaluation of the Effectiveness of Polyprenols from Alcea nudiflora (Prenalon) and Vitis vinifera (Vitaprenol) Compared to Sea Buckthorn Oil and Methyluracil Ointment in Treating Trophic Ulcers of the Rabbit Footpad. Journal of Theoretical and Clinical Medicine, – Tashkent, 2019. – No. 6. – P. 6–8.

Rashkes A. M., Khidyrova N. K., Rashkes Ya.V., Mirkhodjaev U. Z., Nadzhimov U. K., Shakhidoyatov Kh. M. Method for Obtaining Polyprenols. Patent of the Republic of Uzbekistan – No. 1543, 19.12.1994. Bulletin of Inventions – No. 1. – 121. (1995).

Kakhkharov I. T. Institute of Genetics and Experimental Biology of Plants, Academy of Sciences of Uzbekistan. Description of Promising Cotton Varieties “UzFA-703”, “Kelajak”, “UzFA-705”, and “Narpay”. – Tashkent, 2010. – 36 p.

Mamatkulova N. M., Khidirova N. K., Mamadrakimov A. A., Shakhidoyatov Kh. M. Polyprenols from the Leaves of Rhus coriaria. Chemistry of Natural Compounds, 2014. – No. 5. – P. 723–726.

Khidyrova N. K., Mamatkulova N. M., Mukarramov N. I., Shakhidoyatov Kh. M. Polyisoprenoids from the Leaves of Morus alba and Morus nigra. Chemistry of Natural Compounds, 2012. – No. 1. – P. 98–99.

Khidyrova N. K., Rakhmatova M.Zh., Kukina T. P., Shakhidoyatov Kh. M. Polyprenols and Triterpenoids from Leaves of Alcea nudiflora. Chemistry of Natural Compounds.

submitted 01.05.2025;
accepted for publication 15.05.2025;
published 29.05.2025

Contact: nhidirova@yandex.ru

The Austrian Journal of Technical and Natural Sciences, No 3–4
ISSN 2310-5607

PREMIER Publishing
ppublishing.org

DOI:10.29013/AJT-25-3.4-43-46

OBTAINING POLYMER-BITUMEN COMPOSITES BASED ON THE MODIFICATION OF CATIONIC SURFACTANTS AND STUDYING THEIR PHYSICAL-MECHANICAL PROPERTIES

Muradov Javlonbek [1]***, Mavlonov Shokhrukh*** [1]***,***
Sapashov Ikramzhan [2]***, Khaydarov Akhtam*** [1]

[1] Bukhara Institute of Engineering and Technology

[2] Karakalpak State University named after Berdakh

Cite: *Muradov J., Mavlonov Sh., Sapashov I., Khaydarov A. (2025). Obtaining Polymer-Bitumen Composites Based on the Modification of Cationic Surfactants and Studying Their Physical-Mechanical Properties. Austrian Journal of Technical and Natural Sciences 2025, No 3–4.* https://doi.org/10.29013/AJT-25-3.4-43-46

Abstract

Cationic surfactants were synthesized for the production of polymer-bitumen emulsions, and the effects of temperature, reaction duration, and catalyst concentrations on their yield were studied. Based on the modification of the synthesized surfactants, the composition of polymer-bitumen emulsions and the impact of concentration variations on the physical-mechanical properties of the emulsions were determined.

Keywords: *Polymer-bitumen emulsion, cationic surfactant, stearic acid, N,N-dimethylethylenediamine, benzyl stearamide, viscosity*

Indroduction

Cationic surfactants (CSFM) used in bitumen emulsions primarily serve to improve the mixing properties of bitumen with water and enhance adhesion to the stone layer. These surfactants possess the necessary surface-active properties to emulsify bitumen in water, ensuring the stability of the emulsion. Additionally, cationic surfactants play a crucial role in increasing the stability of bitumen, improving dispersion, and facilitating better mixing of bitumen with water (Miljković, M. and Radenberg, M., 2014).

The primary goal of using bitumen in emulsion (liquid) form is to reduce its viscosity while ensuring the emulsion remains stable during storage and transportation. However, when applied to mineral fillers or road surfaces, it must break at a predetermined rate. The breaking rate mainly depends on the type of surfactant used and the grade of bitumen (Wang, Z., Wang, Q., and Ai, T., 2014).

Method and materials

For the preparation of polymer-bitumen emulsions under laboratory conditions, synthesized cationic surfactants were modified and used along with bitumen, water, an emulsifier, hydrochloric and phosphoric acids, adhesion polymers, and a colloid mill. In the

initial stage, 350 ml of water was heated to 50 °C, followed by the addition of 2.5 cm³ of the synthesized cationic emulsifier and 1 cm³ of phosphoric and hydrochloric acids until the pH reached 1.8–2.5. The bitumen was heated to 140°C and introduced into the colloid mill along with the prepared aqueous emulsifier solution. As a result, a polymer-bitumen emulsion was obtained, and its physicochemical and rheological properties were studied.

The physicochemical properties of synthesized cationic surfactants and the polymer-bitumen emulsions obtained through their modification were analyzed using the IRAffinity-1S Fourier Transform Infrared (FTIR) Spectrophotometer (Shimadzu). Methods were also employed to determine the viscosity of bitumen emulsions and to analyze the physicochemical properties of the residue left after water evaporation from the bitumen emulsion (Ludwig A.C., 1992).

Results

The synthesis of cationic surfactants consists of two stages, and in each stage, the effect of catalyst consumption and catalyst quantity on the reaction yield was determined. The reaction equation for the synthesis of cationic surfactants is presented in Figure 1.

Figure 1. *Stearamide cationic surfactant synthesis reaction*

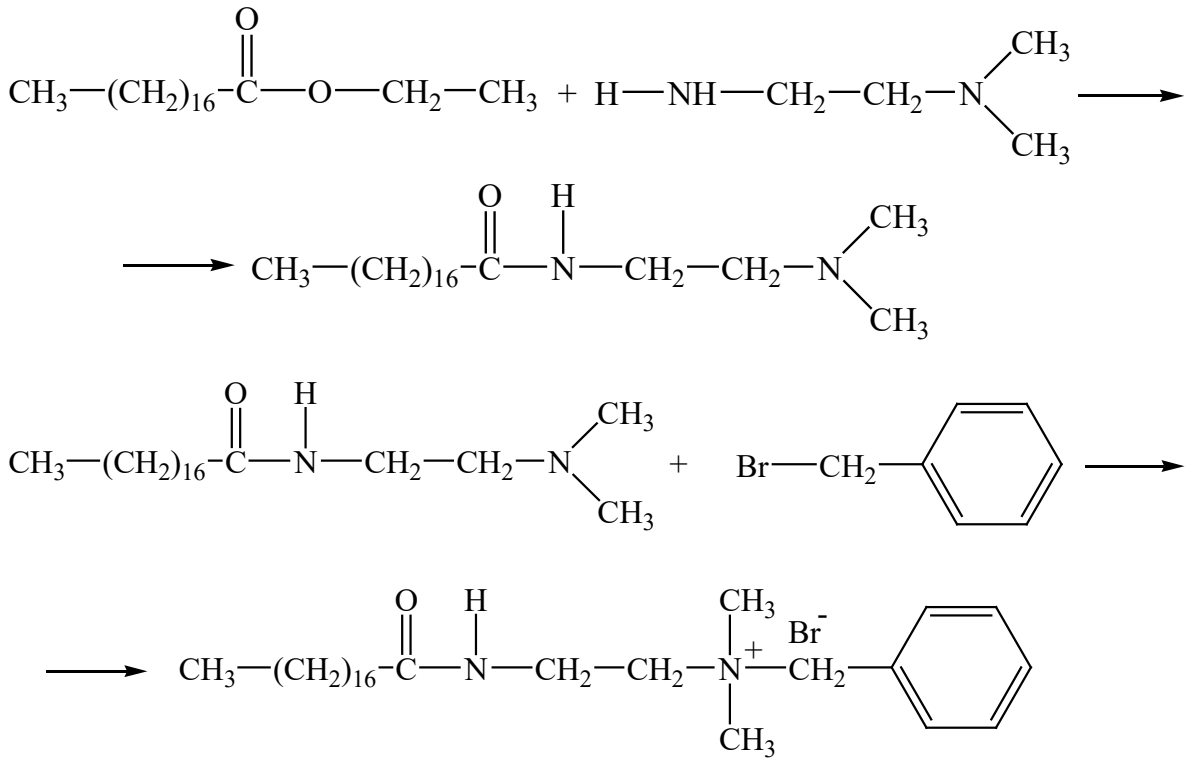

The graph in (Figure 2 a) illustrates the effect of temperature (80–120°C) and reaction time (6–9 hours) on reaction yield, ranging from 80% to 95%. It explains how higher temperatures and longer reaction times influence reaction efficiency, with the yield determined to be 89.7%. The factors affecting the reaction yield between N,N-dimethyl stearamide and benzyl bromide (temperature, catalyst, and time) are presented. The graph, with theoretical values, indicates that temperature and catalyst have the most significant impact, highlighting that optimizing these parameters is crucial for improving reaction efficiency.

The spectra in (Figure 2 b) show absorption regions corresponding to various functional groups. The absorption at 720.36–730.4 cm^{-1} is attributed to the CH_2 δ deformation of the sp^3-hybridized saturated alkyl group in stearic acid. The peaks at 806.25–846.75 cm^{-1} correspond to the benzene ring in the benzyl molecule, while the absorption at 1000.98 cm^{-1} is assigned to δ C-H in the

aromatic ring and hydrogen-bonded structures in long-chain compounds. The range of 1244.10–13751.23 cm^{-1} corresponds to weakly active CH_2 stretching vibrations. The peak at 1400.82 cm^{-1} is attributed to νC-N stretching of N,N-dimethylethylenediamine derivatives substituted with ethyl stearate. The absorptions at 1456.26 cm^{-1} (δC-H) and 1496.42 cm^{-1} (ν benzene ring) confirm the presence of aromatic structures.

Figure 2: *a) The effect of temperature, reaction duration, and catalyst on BSA-K reaction yield b) Infrared spectra absorption peaks*

a)

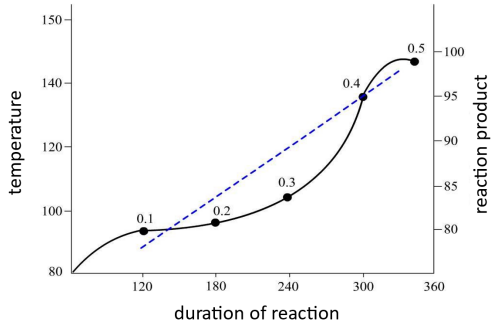

b)

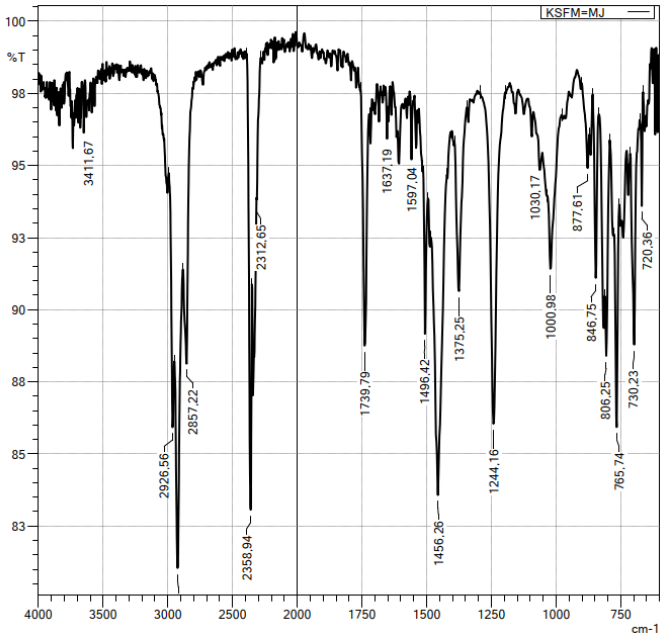

The peak at 1597.04 cm^{-1} corresponds to δN-H bending of the secondary amide group, while the range 1637.19-1739.79 cm^{-1} is assigned to νC=O stretching of the carbonyl group. Further, absorptions at 2857.52 cm^{-1} indicate νCH_3 stretching vibrations of the methyl group, and at 2926.56 cm^{-1}, the presence of a quaternary nitrogen group linked to the benzyl group and N,N-dimethylethylenediamine molecule is observed. The peak at 3411.67 cm^{-1} corresponds to the νN-H stretching of a secondary amide with moderate intensity.

For the preparation of high-quality bituminous emulsion, the synthesized benzyl stearamide was used in a concentration range of 0.5–1.5%, with the bitumen phase constituting 45–50%. The composition of the bitumen emulsions and their physical-mechanical properties are presented in (Tables 1 and 2).

Table 1. *The composition of modified bitumen emulsions with synthesized cationic surfactants*

PBE samples.	**The composition of modified polymer-bitumen emulsions**					
1 l (PBE)	**Bitumen BND 50/70 %**	**KSFM (BSA-K) %**	**Stabilizer ($CaCl_{2)}$ %**	**(HCl) %**	**Polymer (SBS) %**	**Kerosene %**
Sample 1	45	0,5	0,1	0,3	–	0,8
Sample 2		1,0	0,3	0,6	–	1,2
Sample 3		1,5	0,5	0,9	–	1,0
Sample 4		0,5	0,1	0,3	0,5	1,5
Sample 5		1,0	0,3	0,6	0,8	1,2
Sample 6		1,5	0,5	0,9	1,2	1,0
The rest is water (100%)						

Table 2. *Physico-mechanical properties of polymer-bitumen emulsions modified with cationic surfactants*

Composition of components 1 l (PBE)	Indicators of polymer-bitumen emulsions based on synthesized BSA-K modification				
	pH	Conditional viscosity at 40°C, c	Adhesion with mineral materials, %.	Homogeneity (%), according to sieve № 014	Storage stability % After 7 days
Sample 1	1,85	19,2	85,0	0,25	0,30
Sample 2	2,05	17,4	87,0	0,20	0,28
Sample 3	2,10	16,6	89,0	0,20	0,25
Sample 4	2,24	37,9	87,0	0,30	0,21
Sample 5	2,38	33,1	92,0	0,35	0,15
Sample 6	2,32	29,4	98,0	0,35	0,09

PBE containing 45% bitumen

Discussion

As seen in this table, the pH level of various samples of rapidly breaking polymer-bitumen emulsions ranged from 1.85 to 2.38, the conditional viscosity from 19.2 to 41.1, adhesion to mineral materials from 85% to 100%, and homogeneity (uniformity) from 0.2 to 0.35. To prevent bitumen particle coalescence, BSA-K was added to water before preparing polymer-bitumen emulsions. During the bitumen dispersion process, BSA-K was distributed over the surface of bitumen particles, preventing coagulation of the obtained bitumen emulsions during storage. In cationic BSA-K bitumen emulsions, positively charged ions were oriented on the surface of bitumen droplets, while negatively charged chloride ions were attracted to the positive charges, leading to the formation of an electric double layer within the emulsion. The stability of bitumen emulsions during storage is determined by the rate of stratification. Stratification occurs under the influence of gravitational force and the difference in density between the two phases. Research results showed that increasing the BSA-K content to 0.5–1.5% and the bitumen content in emulsions up to 45–50% prevented droplet coalescence and increased their mobility. Additionally, the inclusion of kerosene as a solvent and maintaining the pH level between 2.0 and 2.4 helped prevent phase separation.

References

Miljković, M. and Radenberg, M. Effect of compaction energy on physical and mechanical performance of bitumen emulsion mortar‖, Materials and Structures (article in press), 2014. – P. 5–11. DOI: 10.1617/s11527-014-0488-z.

Wang, Z., Wang, Q., and Ai, T. Comparative study on effects of binders and curing ages on properties of cement emulsified asphalt mixture using gray correlation entropy analysis‖, Construction and Building Materials, 2014. – 54. – P. 615–622.

Ludwig A. C. Emulsification of rock asphalt. U.S. Patent 5,089,052. (1992).

submitted 01.03.2025;
accepted for publication 14.03.2025;
published 29.05.2025

Contact: shoxrux-mavlonov@mail.ru

The Austrian Journal of Technical and Natural Sciences, No 3–4
ISSN 2310-5607

PREMIER Publishing
ppublishing.org

DOI:10.29013/AJT-25-3.4-47-53

ISOLATION OF METABOLITES FROM TRICHODERMA ASPERELLUM FUNGUS AND STUDY OF THEIR PROPERTIES

Nomozova Mohigul Zavqi qizi [1], Kamolov Luqmon Sirojiddinovich [1], Tojiyeva Sevara Namozovna [1] and Zokirov Asilbek Mirzokhid o'g'li [1]

[1] Karshi State University, Republic of Uzbekistan, Karshi

Cite: *Nomozova M.Z., Kamolov L.S., Tojiyeva S.N., Zokirov A.M. (2025). Isolation of Metabolites From Trichoderma Asperellum Fungus and Study of Their Properties. Austrian Journal of Technical and Natural Sciences 2025, No 3–4.* https://doi.org/10.29013/AJT-25-3.4-47-53

Abstract

Today, the issues of restoring human health, meeting the demand for food, or maintaining soil fertility in a moderate state are among the issues of a wide range of issues. Therefore, in order to solve these problems, today more and more natural resources are being eliminated. Therefore, we also aimed to isolate the secondary metabolites from the fungus Trichderma asperellum, which contains metabolites of different properties in itself, and to study their properties. During our treatment, the extract sum obtained from the fungus of Trichoderma asperellum was fractionated in different solvent systems (hexane, hexane chloroform, chloroform, chloroform methanol, methanol) and its secondary metabolites were extracted. In this study, we thought it necessary to introduce some chromatographic analyses of the fractionated secondary metabolites in the chloroform methanol 19:1 system and the properties of some of them.

Keywords: *Trichoderma asperellum, extract, secondary metabolites, chromatographic analyses*

Introduction

Identification of beneficial plants, organisms and microorganisms and the study of their beneficial properties is a wide network around the world. Our research team also carries out practical work on the identification of microorganisms, including micro- and macrofungi and the isolation and determination of metabolites they produce in order to study their beneficial and harmful properties. In this regard, in order to make our research more correct and complete, we have identified several sources on the isolation of metabolites of fungi of the constellation Trichoderma, the study of their biological properties. Volatile organic compounds produced by the trichoderma atrovirid fungus have been found to be related to plants, that is, these metabolites are associated with mycoparasitic interactions with host fungi. Three of them – described as agents of an antifungal nature – were highly secreted by the Δhda1 mutant, while 3-octanone was found in smaller amounts in the head cavity. The metabolites produced by T. atroviride were also significantly enhanced in the growth and development of B. cinerea

Δhda1 (Verena Speckbacher et al., 2024). In addition, 25 different MVOCs were found when Trichoderma atroviride was applied in biocontrol cultures (spectral compatibility factor of at least 90% and LTPRI ± 2% maximum relative deviation from the literature values). These metabolites were known to be VOCs of the classes of alkanes, alcohols, ketones, furans, pyrones (mainly bioactive 6-pentyl-alpha-pyrone), mono- and sesquiterpenes, while the production of 13 Trichoderma spp was not previously identified and 11 volatile substances were additionally validated using valid standards (Norbert Stoppacher et al., 2010). In another study, the effect of the herbicide 2,4-dichlorophenoxyacetic acid (2,4-D) synthesized by the T. harzianum IM 0961 strain on lipidome and selected extracellular substances was studied, and it was found that the herbicide 2,4-D affects the lipid moiety in the mycelium and that the herbicide has lipophilic properties (Julia Mironenka et al., 2020). Available data reveal the important importance of secondary metabolites of T. harzianum, which may reduce side effects in antioxidant and anti-inflammatory treatments. Therefore, T. harzianum has retained a potent antioxidant property and effectively clears ROS by lowering T-reg markers. (Alblihed et al., 2023). In order to study the peptidaibiotic substances synthesized by fungi of the constellation Trichoderma chromatographic and spectroscopic methods were used. All of these peptidaibiotic groups have been found to exhibit biological activity including antibacterial, antifungal, antiviral effects, as well as cytotoxic effects such as immunosuppressive and neuroleptic properties (Adigo Setargie et al., 2024). Ethyl acetate extract of TH-TIND02 Gas Chromatography – Mass spectrometry analyses revealed 21 major and small volatile organic compounds counted as a multiplicity component: acetamide, 2, 2, 2-trifluoro-N, N-bis trimethyl-Icylyl-C (94.74%), along with the isolation produced hydrolytic enzymes chitinase, cellulose, β-1, 3 glucanase and protease as a component (Abhay K et al., 2024). Trichoderma releases various volatile compounds, including alcohols, aldehydes, ketones, ethylene, hydrogen cyanide, and monoterpenes, as well as non-volatile compounds, including peptaibols, and diketopiperazine-like glycotoxins and gliovirin, which show antibiotic activity. (Amrita Saxena et al., 2025). In addition, when root samples of the plant were inoccated with Trichoderma asperellum, sometime after inoculation with Ganoderma. boninense, fungus-releasing metabolites were detected and detected in the GC–MS method (Muniroh Ms et al., 2025). Of the several isolates of another Trichoderma, the following most abundant substances were nabbed: 6-Pentil-2H-pyran-2-A, 2,3,5,5,8a-pentamyl-6,7,8,8a-tetrahydro-5H-chrome-8-ol Toluene, 2,4, Ditert-butyl phenol, 1,5, Dimethyl-6-methylene spiro (2,4) heptanes and 2,4, Ditert-butylphenol, 1,5, Dimethyl-1-methylenpyro (2,4) heptanes and N, N-dimethyl-1-(4-methylphenyl)ethanol, Benzenethanol, 1,5-dimethyl-6-methylenpyro(2.4) and 6-pentil-2H-pyran-2-one, Anethanol and 1-hydroxy-2,4-di.tert lequinyl Benzene vs Benzene (Srinivasa Nagappa Chowluru et al., 2017). In another study with T. hamatum, it was extracted in ethyl acetate and several secondary metabolites were obtained and purified and studied by HRESIMS, NMR, UV, IQ, circular dichroism, and Mosher deposition method. In this case, 1–7 structure compounds not previously known, 8 known are obtained. Metabolites 1, 2, and 9 are rare, compounds 3–8 are cyclonean sesquiterpenes, 6–5–4–7 are harzian diterpenes composed of tetracyclic carbon skeletons, and compound 5 is known to be cycloneranesesquiterpenes, which is the first to replace -OOH (Li Huang et al., 2024). Metabolites of Trichoderma strains found in the sea have also been studied. Molecular diversity of Trichoderma metabolites, especially the abundance of metabolites that conserve the skeletons of cycloneran, bisabolan, harzian, sorbitsillinoid, and peptaibol, has been identified. Among the metabolites, 235 members are known to have several bioactiveites such as microalgal, antifungal, cytotoxic, zooplankton-toxic, antibacterial, anti-inflammatory, anti-inflammatory (Yin-Ping Song et al., 2024). Ethyl acetate extraction sum of TRI07 isolate When GC–MS was examined, spathulenol, triacetin, and aspartame were checked to be the major substances, and were observed to be 28,90, 14,03, and 12,97%, respectively. The analysis of TRI07-VOC with the solid-phase microextraction technique

revealed that the most common compounds include ethanol, hydroperoxide, 1-methylhexyl, and 1-octen-3-one. When TRI07 interacts with Alt3, 34 compounds with key components including 1-octen-3-one, ethanol, and hexanedioic acid, bis(2-ethylhexyl) ester were identified. (Philip B et al., 2024). The filamentous fungus Trichoderma reesei is a multi-producer of plant cell wall-disrupting enzymes that are regulated in response to various environmental signals for optimal adaptation, but also produce a wide range of secondary metabolites (Schalamun M et al., 2023). To investigate the antiviral properties of secondary metabolite compounds derived from four Trichoderma spp. culture filtrates. GC–MS analysis. 24 substances with a relative amount of more than 10% of secondary metabolites have been reported (Rizk M. N. et al., 2024). In addition, identification of volatile metabolites isolated from Trichoderma strains and gas chromatography-mass spectrometry (GC–MS) assays revealed 98 volatile compounds with antifungal activity through GC–MS analysis: phenethyl alcohol, benzene derivatives, D-limonene, octadecanoic acid methyl ester, toluene, hexadecanoic acid, several phenolic isomers, and important volatile compounds with antifungal activity such as eicosamine and eicosamine (Abdenaceur R. et al., 2024). Our previous studies have provided information on the isolation of secondary metabolites from T. asperellum fungus and GC–MS analysis and their significance (Nomozova M. Z et al., 2023).

Method

Preparation of biomass

The strain of T. asperellum was primited for 2 weeks under mandible feed conditions, followed by isolation using filitation paper (Whatman #1.5). The collected biomass was dried at a temperature (+ 45 °C). In the next step, the biomass was ground until it became a powder. The resulting mass ethyl alcohol was mixed in a 1:2 state and put on a pendulum shaker at 155 µl/min for 20 h. The alcohol mixture was then subjected to filtration process and the obtained filtrate was driven in a rotary drive at 40 µL/min at 78.5 °C. This process was repeated 7–8 times. The total extract mass was collected and dried, so that the finished mass was 15gr.

Fractionation technology

For extraction of the extracted dry curd mass, colonical (columnar) chromatography was used to isolate the solids. The length of the glass column is 60 cm, and it is considered to have a diameter of 12 cm. Initially, the kalonka was washed in hexane substance, then 240 gr of 100/250 m size from silicagel L (Chemapol Prana-Czechoslovakia) was placed on this kalonka. The 15g biomass was thoroughly mixed with 14g silicagel and turned into paroshok and put into a column over the silicagel. Fractionation was applied sequentially according to the polarity of the solvents and each separated fraction was verified by TLCH analysis.

Figure 1. *Thin-layer and gaseous liquid chromatography of chloroform methanol 19:1 fraction*

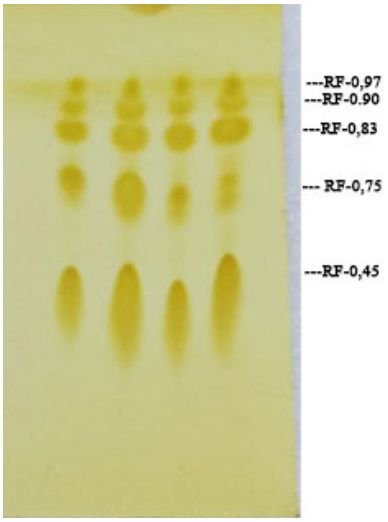

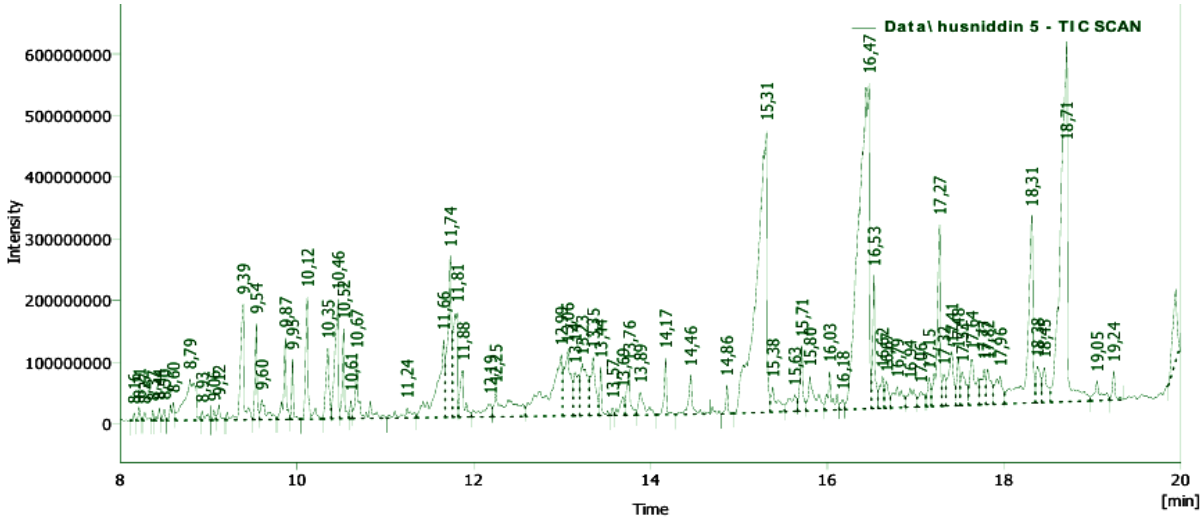

Results

In this study, we cited several analyses and some of the metabolites obtained when the fractionation process was conducted in a ratio of 19:1 to chloroform methanol. During this step of fractionation, the obtained fractions were treated with thin-layer (chloroform, methanol 9:1 solvent system was used) and gaseous liquid chromatographic analysis was performed (Fig. 1).

The volatile substances detected by the obtained chromatographic examinations were found to be the following compounds when compared with the data in the MS data library (Table 1).

Table 1. *Chloroform: methanol 19:1 in the fraction of metabolites decomposed*

№	Metabolit name	Molecular formula	Moleculyar mass g/mol	Time to absorption
1	Trans-2-undecenoic acid	C11H20O2	184.28	11,879
2	Cyclopropaneoctanoic acid, 2-octyl-, methyl ester	C20H38O2	310.5	12,990
3	9-Tetradecenal, (Z)	C14H26O	210.36	13,061
4	1,3-Benzenedicarboxylic acid, bis(2-ethylhexyl) ester	C24H38O4	390.55	13,226
5	1,4-Benzenedicarboxylic acid, bis(2-ethylhexyl) ester	C24H38O4	390.55	13,352
6	2-Butanone, 4-(2,6,6-trimethyl-1-cyclohexen-1-yl)	C13H22O	194.3132	13,438
7	9,12-Octadecadienoyl chloride, (Z, Z)-	C18H31ClO	298.9	13,688
8	Tetradecanoic acid	C14H28O2	228.37	13,760
9	Pentadecanoic acid	C15H30O2	242.40	14,455
10	Hexadecanoic acid, methyl ester	C17H34O2	270.4507	14,864
11	n-Hexadecanoic acid	C16H32O2	256.4241	15,312
12	11-Octadecenoic acid, methyl ester	C19H36O2	296.4879	16,028
13	Oleic Acid	C18H34O2	282.4614	16,473
14	Octadecanoic acid	C18H36O2	284.4772	16,530
15	Hexadecanoic acid, ethyl ester	C18H36O2	284.4772	17,272

№	Metabolit name	Molecular formula	Moleculyar mass g/mol	Time to absorption
16	7,10,13-Eicosatrienoic acid, methyl ester	C21H36O2	320.5093	17,318
17	Linoleic acid ethyl ester	C20H36O2	308.4986	17,956
18	9-Octadecenoic acid (Z)-, 2,3-dihydroxypropyl ester	C21H40O4	356.53	18,311
19	Diisooctyl phthalate	C24H38O4	390.6	18,709
20	Oxiraneoctanoic acid, 3-octyl-, cis-	C18H34O3	298.4608	19,053
21	Retinoic acid, methyl ester	C20H28O2	300.4351	19,243

Discussion

During this further fractionation, several undissociated metabolites were detected: 1,3-Benzenedicarboxylic acid, bis(2-ethylhexyl) ester, 1,4-Benzenedicarboxylic acid, bis(2-ethylhexyl) ester, 2-Butanone, 4-(2,6,6-trimethyl-1-cyclohexen-1-yl), retinoic acid, methyl ester. When the properties of retinoic acid were studied, it was found that vitamin A and its active metabolite all-trans-retinoic acid (ATRA) are a collection of substances that regulate several physiological functions in some organ systems, and normal immunity was considered important. Vitamin A derivatives are useful in the treatment of cancer, and ATRA is used in the differential treatment of acute promyelocytic leukemia (APL) (Łukasz Szymański et al., 2020). Vitamin A and retinoid derivatives are recognized as morphogens that govern body structure and skeletogenesis and, when excessive, cause profound defects (Alanna C. Green et al., 2016). At the same time, the decomposed linoleic acid (18:2ō6; cis, cis-9,12-octadecadienoic acid) was also known to be the most consumed PUFA in the human diet (Jay Whelan et al., 2013).

Conclusion

The results of the above study show that as a result of this stepwise fractionation, organic substances, unlike some other fractions, have decomposed and these substances are substances of specific biologically active properties.

References

Abdenaceur R., Farida, Bt. & Fatma, SH. Volatile organic compounds activities of Trichoderma species isolated from olive grove soil against the wilt pathogen, Verticillium dahliae. (2024). Eur J Plant Pathol (2024). – 170. – P. 789–803. URL: https://doi.org/10.1007/s10658-024-02839-8

Abhay K. Pandey Shivanand Yadav, Mahesh K. Samota, Harshit K. Sharma and Somnath Roy. (2024). Trichoderma harzianum TIND02 upregulates the expression of pathogenesis-related genes and enzymes and enhances gray blight resistance in tea. Pesticide Biochemistry and Physiology, – Vol. 205. November 2024. – 106115 p. URL: https://doi.org/10.1016/j.pestbp.2024.106115

Adigo Setargie, Chen Wang, Liwen Zhang and Yuquan Xu. (2024). Chromatographic and mass spectroscopic guided discovery of Trichoderma peptaibiotics and their bioactivity. Engineering Microbiology, – Vol. 4. – Issue 2. – June 2024. – 100135 p. URL: https://doi.org/10.1016/j.engmic.2023.100135

Amrita Saxena, Riddha Dey, Surya Prakash Dube and Richa Raghuwanshi. (2025). Advanced in Trichoderma biology for biocontrol applications, Chapter 5. Biodiversity, Bioengineering and Biotechnology of Fungi Developments in Applied Microbiology and Biotechnology 2025. – P. 77–104. URL: https://doi.org/10.1016/B978-0-443-13856-0.00017-8

Alblihed M. A. (2023). Metabolites of Trichoderma harzianum re-balance T-reg/Th-17 cytokine axis in epileptic rats. Beni-Suef Univ J Basic Appl Sci – 12, –113. (2023). URL: https://doi.org/10.1186/s43088-023-00425-1

Alanna C. Green, T. John Martin and Louise E. Purton. (2016). The role of vitamin A and retinoic acid receptor signaling in post-natal maintenance of bone. The Journal of Steroid Biochemistry and Molecular Biology., – Volume 155, Part A, – January, 2016. – P. 135–146. URL: https://doi.org/10.1016/j.jsbmb.2015.09.036

Jay Whelan and Kevin Fritsche. (2013). Linoleic Acid. Adv Nutr. 2013 yil 6-may;– 4(3): 311–312. Doi: 10.3945/an.113.003772

Julia Mironenka, Sylwia Różalska, Adrian Soboń and Przemysław Bernat. (2020). Lipids, proteins and extracellular metabolites of Trichoderma harzianum modifications caused by 2,4-dichlorophenoxyacetic acid as a plant growth stimulator. Ecotoxicology and Environmental Safety, – Vol. 194. – May, 2020. – 110383 p. URL: https://doi.org/10.1016/j.ecoenv.2020.110383

Li Huang, Qiang Bian, Mengdan Liu, Yiwen Hu, Lijuan Chen, Yucheng Gu, Qiwei Zu, Guangzhi Wang and Dale Guo. (2024). Structure and Fungicidal Activity of Secondary Metabolites Isolated from Trichoderma hamatum b. J. Fungi 2024. – 10(11). – 755 p. URL: https://doi.org/10.3390/jof10110755

Łukasz Szymański, Rafał Skopek, Małgorzata Palusińska, Tino Schenk, Sven Stengel, Sławomir Lewicki, Leszek Kraj, Paweł Kamiński and Arthur Zelent. (2020). Retinoic Acid and Its Derivatives in Skin. Cells., 2020 Dec – 11; 9(12): 2660. Doi: 10.3390/cells9122660

Muniroh Ms, Nusaibah Sa and Vadamalai G. (2025). Efficacy of Pseudomonas aeruginosa and Trichoderma asperellum in promoting plant growth and suppression of Ganoderma boninense disease infestations in oil palm. Physiological and Molecular Plant Pathology, – Vol. 138. July 2025. – 102662 p. URL: https://doi.org/10.1016/j.pmpp.2025.102662

Nomozova M. Z., Ruzieva Z. K., Shomurodova M. Z., Karimov X. X., Kamolov L. S. (2023). Vtorichnie metaboliti griba Trichoderma asperellum Uz-A4. Universum: ximiya i biologiya. – 6(108), iyun, 2023. – P. 61–67.

Norbert Stoppacher, Bernhard Kluger, Susanne Zeilinger, Rudolf Krska and Rainer Schuhmacher. (2010). Identification and profiling of volatile metabolites of the biocontrol fungus Trichoderma atroviride by HS-SPME-GC–MS. Journal of Microbiological Methods, – Vol. 81. – Issue 2. May 2010. – P. 187–193. URL: https://doi.org/10.1016/j.mimet.2010.03.011

Philip, B., Behiry, S.I., Salem, M.Z.M. (2024). Trichoderma afroharzianum TRI07 metabolites inhibit Alternaria alternata growth and induce tomato defense-related enzymes. Scientific Reports – 14. – 1874 p. URL: https://doi.org/10.1038/s41598-024-52301-2

Rizk M. N., Ketta, H.A. & Shabana, Y.M. (2024). Discovery of novel Trichoderma-based bioactive compounds for controlling potato virus Y based on molecular docking and molecular dynamics simulation techniques. Chem. Biol. Technol. Agric. 11, 110 (2024). https://doi.org/10.1186/s40538-024-00629-2

Srinivasa Nagappa Chowluru, Subbaraman Sriram, Chandu Singh and Shivashankar Kodthalu. (2017). Secondary Metabolites Approach to Study the Bio-Efficacy of Trichoderma asperellum Isolates in India. International Journal of Current Microbiology and Applied Sciences, – 6(5): 1105–1123. May, 2017. DOI:10.20546/ijcmas.2017.605.120

Schalamun M., Beier, S., Hinterdobler, W. et al. (2023). MAPkinases regulate secondary metabolism, sexual development and light dependent cellulase regulation in Trichoderma reesei. Scientific Reports, –13. – 1912 p. URL: https://doi.org/10.1038/s41598-023-28938-w

Verena Speckbacher, Daniel Flatschacher, Nora Martini-Lösch, Laura Ulbrich, Clara Baldin, Ingo Bauer, Veronika Ruzsanyi and Susanne Zeilinger (2024). The histone deacetylase Hda1 affects oxidative and osmotic stress response as well as mycoparasitic activity and secondary metabolite biosynthesis in Trichoderma atroviride. Microbiology Spectrum, – Vol. 12. – Issue 3, – 14. February, 2024. URL: https://doi.org/10.1128/spectrum.03097-23

Yin-Ping Song & Nai-Yun Ji. (2024). Chemistry and biology of marine-derived Trichoderma metabolites. Natural Products and Bioprospecting, – Vol. 14. article No. 14. URL: https://doi.org/10.1007/s13659-024-00433-3

submitted 15.04.2025;
accepted for publication 29.04.2025;
published 29.05.2025

Contact: mnomozova1992@gmail.com; kamolov.luqmon@mail.ru;
vivoafsgg1235@gmail.com;

The Austrian Journal of Technical and Natural Sciences, No 3–4
ISSN 2310-5607

PREMIER Publishing
ppublishing.org

DOI:10.29013/AJT-25-3.4-54-58

RATIONAL USE OF SPENT CATALYSTS AS A SOURCE OF MICRO- AND MACROELEMENTS FOR LIQUID FERTILIZERS

Obidzhonov Doniyorjon Orip ogli [1], ***Kucharov Bakhrom Xayriyevich*** [1], ***Erkaev Aktam Ulashevich*** [2], ***Zakirov Bakhtiyor Sabirjanoich*** [1], ***Yulbarsova Mashkhurakhon Vahobovna*** [1]

[1] Institute of General and Inorganic Chemistry of the Academy of Sciences of the Republic of Uzbekistan

[2] Tashkent Institute of Chemical Technology

Cite: *Obidzhonov D.O., Kucharov B.X., Erkaev A.U., Zakirov B.S., Yulbarsova M.V. (2025). Rational use of Spent Catalysts as a Source of Micro- and Macroelements for Liquid Fertilizers. Austrian Journal of Technical and Natural Sciences 2025, No 3–4.* https://doi.org/10.29013/AJT-25-3.4-54-58

Abstract

This article discusses the possibilities of obtaining water-soluble liquid fertilizers enriched with microelements by acid processing of spent catalysts of the SHIFT MAX 210 brand, widely used in the nitrogen industry. Studies have been conducted on the effect of nitric acid concentration (in the range of 20–50%) on the degree of extraction of macro- and microelements. Physicochemical and rheological properties of the obtained solutions have been determined. The results demonstrate the prospects for developing an energy-efficient technology for processing catalyst waste using local raw materials, which is relevant in the environmental conditions of the Republic of Uzbekistan.

Keywords: *microelements, system, catalyst, Shift max 210, liquid fertilizers, nitric acid, processing*

Introduction

At present, the problem of organizing the production of water-soluble complex fertilizers remains unresolved in Uzbekistan, since technologies for their production from local raw materials have not yet been developed in the conditions of the republic. In this regard, the creation of our own production of such fertilizers is a relevant and promising task.

One of the key objectives of the study is to determine the role of soil-forming processes, identify the deficiency or excess of microelements and develop recommendations for the effective use of micronutrients. Also, based on the data obtained, it will be possible to adjust micronutrient maps for planning fertilizers and conducting further research in agriculture.

Copper is found in all organs and all phases of cotton growing, when growing it on different soils. Copper microfertilizers for cotton are used with sufficient provision

of the optimal amount of basic fertilizers (N, P, K), in areas where the content of copper available to plants in the arable horizon is less than 0.6 mg / kg of soil (Chernavina I. A., 1970; Shkolnik M.Ya., Davydova V. N., 1962; Klimovitskaya Z. M., 1964).

The role of zinc in the ontogenesis of cotton in the conditions of irrigated agriculture in Central Asia has not been sufficiently elucidated (Rinkis G.Ya. 1972; Yakovleva V. V., Sobachkina L. N. 1972; Yakovleva V. V., Sobachkina L. N. 1972; Vinogradova H. T. 1952; Enileev H. H., Andrishchenko V. K. 1963; Pirahunov T. P. 1966). The forms and types of zinc bonds in a living organism are varied.

Manganese influences the course of oxidation-reduction reactions in plants: in ammonia, plants behave as an oxidizer, and in nitrate, as a reducing agent.

The physiological role of molybdenum in plants is associated with its participation in dense metabolism, primarily in enzymatic reduction to ammonia and in the synthesis of proteins and amino acids (Zhmai L. A., 20040.

In recent years, data have been obtained on the positive effect of molybdenum on phosphorus metabolism in plants (Zavalin A. A., Almetov N. S. 2006; Mineev V. G., 2006). The introduction of molybdenum not only sharply increases the amount of organic phosphorus, but also leads to a qualitative change in protein.

In order to provide a physicochemical justification for the process of obtaining microelements, the physicochemical characteristics of spent catalysts used in the nitrogen industry, the accumulation volumes of which reach hundreds of tons, were studied before the stage of decomposition with mineral acids. The energy dispersive spectra of these catalysts are shown in Figure 1. Before use, the catalysts were crushed to a particle size of less than 0.05 mm.

Methods and materials

To obtain liquid microelement-containing fertilizers, solutions were used that were obtained by nitric acid decomposition of spent catalysts formed during the production of the nitrogen industry.

The process of acid processing of catalysts was carried out as follows: in laboratory conditions, nitric acid solutions with concentrations of 20%, 30%, 40% and 50% were used to process 10 g of catalyst waste (SHIFT MAX 210 brand).

The process of decomposition of the crushed catalyst (to a particle size of 0.05 mm) was carried out on a laboratory setup consisting of a tubular glass reactor with a stirrer equipped with an electric wire and placed in a water thermostat. The temperature in the thermostat was maintained using a TK-300I thermometer and an RT-230U electronic relay and was constant, amounting to 45 °C. The rotation speed of the stirrer was regulated within 250–300 rpm.

The interaction process of the components lasted for 30 minutes. Upon completion of the decomposition, the reaction mass was separated into liquid and solid phases by filtration. The reactor contents were filtered through a Buchner funnel using a Bunsen flask, under a vacuum of 0.60 mm Hg and one layer of “white ribbon” filter paper. The filters were pre-weighed. The sediment remaining on the filter was washed with 10 g of water at a given temperature and dried with the filter at 100 °C until a constant weight was achieved.

Results and discussion

A comparative analysis of the results of energy-dispersive spectral research of spent catalysts showed that their elemental composition has a significant diversity. For example, in the catalyst of the SHIFT MAX 210 brand, the copper and zinc content is 2.52% and 2.47%, respectively (Table 1).

The results of mass spectrometric analysis (ICP-MS) presented in Table 3 also confirm that the spent catalysts contain a wide range of macro- and microelements that are necessary for the production of liquid complex fertilizers with microelements.

After decomposition with nitric acid, the liquid phase was analyzed for elemental composition, which is given in Table 2. As follows from Table 2, the liquid phase has in its composition and contains: P-242.0, K-478.0, Ca-1207, Mg-580 mcg/l macroelements and B-50.0, **Cu**-28000, **Zn**-19100, Co-68.0, Mn-214 and Fe-545605 mcg/l microelements, respectively.

Figure 1. *Energy dispersive spectrum of the spent initial catalyst of the SHIFT MAX 210 brand*

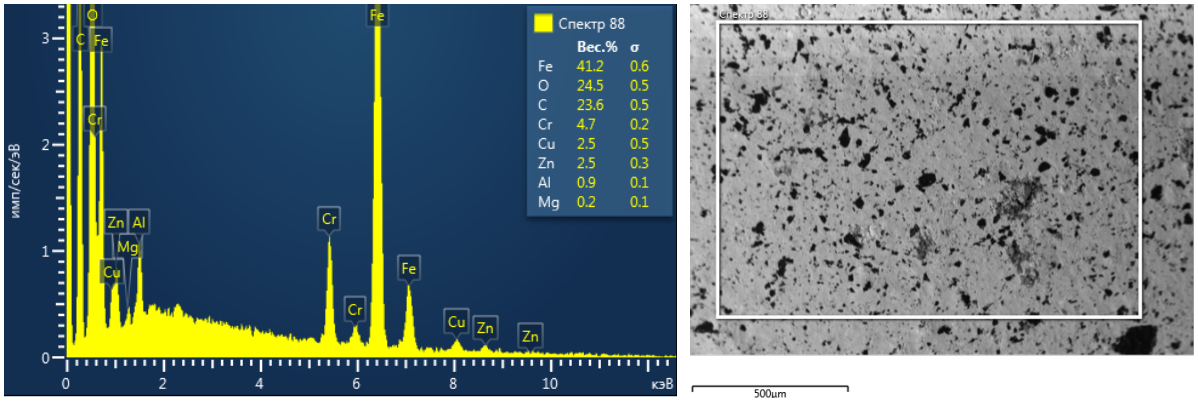

Table 1. *Elemental composition of the spent initial catalyst brand SHIFT MAX210*

Element	Weight.%	Sigma Weight%	Name of the standard
C	23.58	0.53	With Vit
O	24.47	0.46	SiO_2
Mg	0.25	0.08	MgO
Al	0.87	0.09	Al_2O_3
Cr	4.69	0.21	Cr
Fe	41.15	0.57	Fe
Cu	2.52	0.48	Cu
Zn	2.47	0.35	Zn
Sum:	100.00		

Table 2. *Mass spectrometric (ICP-MS) analysis of the initial spent catalysts*

Brand of catalysts	Macroelements, mcg/l				Microelements, mcg/l						
	P	K	Ca	Mg	Cu	Zn	B	Mn	Fe	Co	Mo
Shift max 210	242.0	478,0	1207	580	28000	19100	50.0	4300	545605	68.0	214

We then investigated the influence of process parameters on the process of nitric acid decomposition of catalyst waste (Table 3).

Table 3. *Study of the influence of technological parameters on the process of nitric acid decomposition of catalyst waste*

No.	Ratio Cat: HNO_3	Concentration HNO_3,%	Filtration rate, kg/m²* h		W: T ratio	Humidity, %
			main filtrate	wash filtrate		
Waste catalyst brand SHIFT MAX 210						
1	1:10	20	457.08	47.12	12.18:1.0	29.11
2	1:10	30	378.70	69,70	11.62:1.0	26.64
3	1:10	40	305.45	57.44	12.20:1.0	27.63
4	1:10	50	128.5	69.50	10.62:1.0	28.74

Table 4. *Mass spectrometric (ICP-MS) analysis liquid phase of SHIFT MAX 210 catalyst after decomposition with nitric acid*

acid concentration, %	Macroelements, mcg/l				Microelements, mcg/l						
	P	K	Ca	Mg	Cu	Zn	B	Mn	Fe	Co	Mo
20	1200	94000	320000	53000	2600	2100	56.0	55000	280000	4900	720
30	1300	60000	290000	54000	2900	2300	53.0	66000	350000	6300	530
40	1400	46000	260000	49000	2900	2300	43.0	69000	390000	4900	400
50	1400	58000	270000	49000	3100	2500	38.0	72000	400000	5500	420

The table presents the results of the analysis of the macro- and microelement composition of solutions obtained by decomposing nitrogen industry catalysts with nitric acid of different concentrations (20%, 30%, 40%, 50%). (Table 4)

Increasing the concentration of nitric acid contributes to:

- Increasing the content of phosphorus, iron, manganese and some other elements in the solution;
- At the same time, the solubility of potassium, calcium, boron and molybdenum deteriorates.

At a certain concentration of acid (approximately 40–50%), the process of release of many elements stabilizes, or their content changes insignificantly.

Table 5. *Rheological properties of the obtained solutions of Shift max 210 catalysts after ammonization before filtration at*

No.	Density before filtration, g/cm³				Viscosity before filtration, mm²/s				pH
	Temperature °C								
	10	20	30	45	10	20	30	45	
1	1.21596	1.21227	1.20545	1.19859	1.7167	1.4503	1.2727	1.2283	2.11
2	1.19318	1.18624	1.18182	1.17694	2.5455	2.2199	2.0127	1.8351	4.69
3	1.20563	1.20005	1.19563	1.18905	2.2791	2.0127	1.7759	1.6575	6.01
4	1.19800	1.19440	1.18699	1.18485	2.4271	2.3087	2.0719	1.9535	7.45

Studies have shown that with an increase in the temperature of the medium from 10 to 45 °C, the density and viscosity of the solution decrease in direct proportion, i.e. 1.19800–1.18485 g/cm³ and 2.4271–1.9535 mm²/s, respectively. (Table 5)

Conclusion

As a result of the conducted research, it was established that spent catalysts of the nitrogen industry of the SHIFT MAX 210 brand are a valuable source of macro- and microelements necessary for the production of liquid complex fertilizers.

The conducted studies have shown that the spent catalysts SHIFT MAX 210 contain a large number of useful elements (iron, copper, zinc, etc.), which can be used to obtain liquid fertilizers.

Decomposition of catalysts with nitric acid of different concentrations (20–50%) revealed that with increasing acid concentration, the content of phosphorus, iron and manganese in the solution increases, but the solubility of potassium, calcium, boron and molybdenum decreases; at an acid concentration of 40––50%, the composition of the solutions stabilizes. Rheological studies showed that with an increase in temperature from 10 to 45 °C, the density and viscosity of the solutions decrease, which improves the filtration conditions.

References

Chernavina I. A. Physiology and biochemistry of microelements. Moscow: Higher School, 1970. – 310 p.
Shkolnik M.Ya., Davydova V. N. On partial elimination of zinc deficiency in plants using vitamins B1 and B6 – "DAN SSSR", 1962. – No. 1.
Klimovitskaya Z. M. On the physiological significance of manganese for plant growth and development. Abstract of doctoral diss., – Kyiv, 1964.
Rinkis G. Ya. Molybdenum supply to plants depending on the amount of other elements in the nutrient substrate. In the book "Biological role of molybdenum", – Moscow, 1972.
Yakovleva V. V., Sobachkina L. N. Effect of molybdenum on phosphorus metabolism in plants. In: "Biological role of molybdenum" – Moscow, "Nauka" Publishing House, 1972.
Vinogradova H. T. Molybdenum and its biological role. In the collection "Microelements in the life of plants and animals". – Moscow, Publishing House of the USSR Academy of Sciences, 1952.
Enileev H. H., Andrishchenko V. K. On the influence of microelements on protein metabolism in germinating cotton seeds. "Uzb. biol. journal". 1963. – No. 4.
Pirahunov T. P. The Importance of Molybdenum in Increasing the Use of Soil Nitrogen and Fertilizers by Cotton. Abstracts of Reports at the All-Union Conference on Microelements, – Irkutsk, 1966.
Zhmai L. A. Ammonium nitrate in Russia and in the world // Scientific and technical news. – Moscow, 2004. Special issue. – No. 2. – P. 23–24.
Zavalin A. A., Almetov N. S. Effect of nitrogen fertilizer and biopreparations on the yield and grain quality of winter wheat on sod-weakly podzolic light loamy soil // Journal of Agrochemistry. – No. 6. 2006. – 38 p.
Mineev V. G., Journal of Agrochemistry, Science 2006. – 526 p.

submitted 16.04.2025;
accepted for publication 30.04.2025;
published 29.05.2025

Contact: doniyor_obidjonov94@mail.ru

The Austrian Journal of Technical and Natural Sciences, No 3–4
ISSN 2310-5607

PREMIER Publishing
ppublishing.org

DOI:10.29013/AJT-25-3.4-59-63

ANALYSIS OF THE SYNTHESIS PROCESS FOR LTA-TYPE ZEOLITE WITH ENHANCED SORPTIVE PROPERTIES DERIVED FROM METAKAOLIN

Pardayev Otabek To'khtamishovich [1,2,3], ***Abdurakhmonov Eldor Baratovich*** [3]

[1] Institute of General and Inorganic Chemistry, Academy of Sciences, Republic of Uzbekistan

[2] Termez branch of Tashkent Medical Academy

[3] Termez state pedagogical institute, st. Termez, Republic of Uzbekistan

Cite: *Pardayev O.T., Abdurakhmonov E.B. (2025). Analysis of the Synthesis Process For Lta-Type Zeolite With Enhanced Sorptive Properties Derived From Metakaolin. Austrian Journal of Technical and Natural Sciences 2025, No 3–4.* https://doi.org/10.29013/AJT-25-3.4-59-63

Absract

The synthesis of the materials in question is performed using two principal techniques. The first technique entails the production of granules composed of 65–85% mayonnaise, with an active zeolite base constituting 25–32% by weight, along with a binder material (natural clay for adsorbents and y-Al_2O_3 for catalysts). This method is primarily employed for obtaining the predominant portion of donor zeolites. The second technique involves the synthesis of donor zeolites without the use of binders. In this scenario, the granules are formed exclusively through the mutual growth of zeolite crystals, which leads to superior values in terms of adsorption capacity, concentration of catalytic active centers, and mechanical strength when compared to zeolite materials containing binders.

Keywords: *A and X zeolite, Na_2O/Al_2O_3, aluminum oxide, kaolin, aluminosilicate*

Introduction

The formation method, chemical composition, porous structure, shape, and size of amorphous aluminosilicate granules, which vary and impact the crystallization of A and X zeolites, have been thoroughly investigated in (Keltsev N. V., 1984; Pavlov M. L., 1984; Mirsky Ya. V. 1984; Hamilton K. E., 1993; Chandrasekhar S., 2008). In these investigations, the ratio of components that promote crystallization in the reaction mixtures was adjusted across a broad range to identify the optimal compositional conditions that ensure the consistent production of LTA and FAU-type zeolites with high adsorption and stability properties. In the preliminary experiments, the temperature conditions and crystallization time for each composition of the reaction mixture were selected, enabling the synthesis of zeolite granules with the highest crystalline phase content. It was observed that zeolite A formation occurred when the

Na_2O/Al_2O_3 ratio in the reaction mixture ranged from 1.0 to 2.63 and H_2O/Al_2O_3 = 50. However, it was not possible to produce granules with a high zeolite phase at Na_2O/Al_2O_3 = 1.0 (Imbert F. E., Moreno C., Montero A., Fontal B., Lujano J. 1994; Granizo M. L., Blanco-Varela M. T., Palomo A., 2000; Davies T. W. & Hooper R. M., 1985; Meinhold R. H., Atakul H., Davies T. W. & Slade R. C.T., 1992; Chandrasekhar S., 1996; Kovo A. S., 2008).

Objective: Kaolin is a crystalline natural aluminosilicate modification, with a ratio of silicon to aluminum atoms that is largely similar to zeolite A. Kaolin has a layered structure, consisting of repeating layers of silicon dioxide tetrahedra and aluminum oxide octahedra (Figure 1).

Figure 1. *Structure of kaolin*

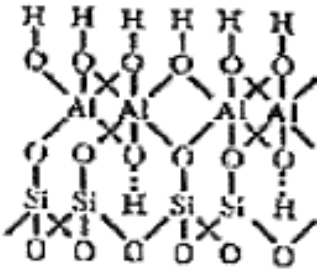

When heated in air, kaolins undergo several stages of transformation. At about 550 °C, an endothermic dehydration process occurs, leading to the formation of a disordered metakaolin phase (aluminum disilicate).

Subjects and Methods

Metakaolin underwent crystallization in aqueous sodium hydroxide solutions with Na_2O concentrations ranging from 132 to 558 g/l. Some of the experiments were conducted using a sodium aluminate solution with Na_2O = 132 g/l and Al_2O_3 = 26 g/l. The solution composition varied within the following ranges: Na_2O (2.0–12.0), Al_2O_3, SiO_2 (2.0–2.4), and H_2O (60.0–252.0). Essentially, the same compositions were utilized in the synthesis of high-dispersity zeolite A from sodium aluminate and silicate solutions.

Results and discussion. Zeolite A with high dispersion is generally synthesized from silica-alumino-hydrogel reaction mixtures, which are formed by the reaction of sodium aluminate and sodium silicate solutions. At the same time, there is a limited body of literature on the synthesis of high-dispersity zeolite A utilizing kaolin as a source of silicon and aluminum. Therefore, this section is dedicated to the development of a method for the synthesis and analysis of the mechanisms underlying the formation of high-dispersity NaA zeolite from $Al_2Si_2O_7$.

Previous studies have shown that a preliminary thermochemical treatment at low temperatures (~30 °C) is crucial for the formation of X-ray amorphous sodium aluminate in the granules during the production of granulated zeolite A from synthetic X-ray amorphous aluminosilicate granules. High phase purity and crystallinity of zeolite granules were achieved solely under these conditions during the subsequent crystallization process conducted at temperatures between 55 and 78 °C. This research further explores the influence of the duration of the initial exposure of highly dispersed metakaolin at 30 °C for periods of 1 to 6 hours. Crystallization was performed thereafter at temperatures between 60 and 80 °C for a period of 6 to 24 hours.

The results of the investigation, as shown in Table 1, examine the impact of the initial activation time of metakaolin in a sodium hydroxide solution at 30 °C on both the crystallization degree and the water adsorption capacity of the resulting crystallization products.

Table 1. *Examined the influence of the duration of pre-treatment at 30 °C on the properties of crystallization products formed in a hydroxide solution at 60 °C over a 20-hour period*

№	Duration, h	Zeolite A content according to X-ray phase analysis, %	AE_{water} sm^3/g
1	0	91.5	0,23
2	1	96.1	0,25
3	4	96.1	0,25
4	6	96.1	0,25

It is clear that a one-hour low-temperature treatment is adequate to yield zeolite A with a high degree of crystallinity during the subsequent crystallization. Prolonging the duration of this process does not influence either the crystallinity or the adsorption characteristics of the resulting product.

The presence of foreign chemical elements, constituting 2.0–3.0% by weight in the Al2Si2O7 composition, prevents the attainment of complete zeolite A formation.

Figure 2 illustrates the kinetic curves for the crystallization of metakaolin in sodium hydroxide and aluminate solutions at temperatures of 60 °C and 80 °C.

It is recognized that, during the crystallization of X-ray amorphous granules into zeolites of types A and X, the diffusion of crystallizing components from the solution to the surface and within the granules could represent the rate-limiting step.

Figure 2. *Depicts the crystallization kinetics of metakaolin: curve 1 represents the sodium hydroxide solution at 60 °C, curve 2 corresponds to the sodium hydroxide solution at 80 °C, and curve 3 shows the sodium aluminate solution at 60 °C*

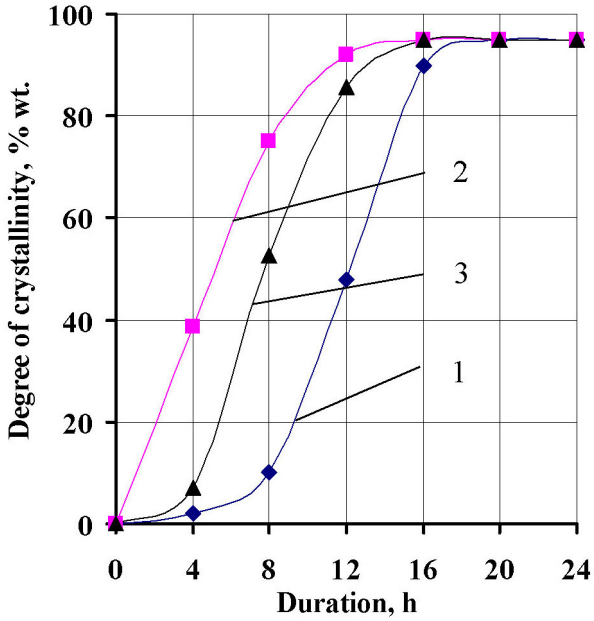

In our case, it appears that the diffusion stage is not limiting during the crystallization of zeolite A due to the high dispersion of the metakaolin powder particles, and therefore, the effect of low-temperature treatment is not significant (Figure 2., Curve 2).

Table 2. *Kinetics of crystallization of metakaolin at 60 °C in hydroxide* and aluminate** solutions.*

Name of indicators	Duration of crystallization							
	Aluminate solution				Alkaline solution			
	4h	8h	16h	24h	4h	8h	16h	24h
Zeolite A content according to XRD data, % wt.	3	48	92	96	2	8	88	96
Cation exchange capacity of the solid phase, mgCaO/g zeolite	31	82	137	138	8	15	131	138
AE_{water} sm^3/g	0,01	0,12	0.23	0.25	0.01	0.02	0.22	0.25

** PC: 2,4 Na_2O • Al_2O_3 • 2,4 SiO_2 • 60 H_2O; C(Na_2O) = 132,0 g/l*

*** PC: 2,4 Na_2O • Al_2O • 3–2,0 SiO_2 • 60 H_2O; C(Na_2O) = 132,0 g/l; C(Al_2O_3) = 26,0 г/л;*

It is apparent that with the rise in temperature from 60 °C to 80 °C, the crystallization time reduces from 20 to 16 hours, and the synthesis in the aluminate solution leads to a notable enhancement in the crystallization rate.

Table 2 provides information on the crystallization kinetics of Prosyanovskiy metakaolin in both alkaline and aluminate solutions.

It is clear that the crystallization of metakaolin in the aluminate solution takes 16 hours. The formation stages of X-ray amorphous sodium aluminosilicate and crystal nuclei proceed more quickly in the aluminate solution compared to the alkaline solution, with zeolite A achieving 48% of its weight after just 8 hours. This is further corroborated by data on the adsorption capacity of condensed water vapor and the cation-exchange properties of zeolites, particularly the substitution of Na^{+} cations with Ca^{+2}.

Table 3 provides details on the composition of the reaction mixture and the influence of sodium hydroxide concentration in the solution on the characteristics of the metakaolin crystallization products.

It is clear that zeolite A, exhibiting varying crystallinity levels, can be synthesized from the reaction mixtures of all the compositions analyzed. Additionally, a critical factor for achieving phase-pure zeolite is maintaining a Na_2O/H_2O ratio between 0.03 and 0.04. This corresponds to NaOH concentrations ranging from 135 to 160 g/l in the crystallization solution. During crystallization in an alkaline environment, the formation of zeolite A is accompanied by the partial formation of a hydrosodalite phase mixture.

Thus, the most favorable compositions of the reaction mixtures examined are as follows:

$$(2{,}0–2{,}4)\ Na_2O{*}Al_2O_3{*}2{,}0SiO_2(60{,}0–100{,}0)\ H_2O$$

Upon crystallization of these reaction mixtures, zeolite A demonstrates a high level of crystallinity and AEVOD. Additionally, both the NaOH consumption and the quantity of mother liquor requiring disposal are minimal.

Table 4 presents a comparison of the properties of crystallization products derived from metakaolins synthesized from clays under identical conditions. The data indicate that, in both instances, zeolite A is formed with a high degree of crystallinity.

Table 4. *Characteristics of crystallization products obtained from metakaolins derived from deposits in an alkaline solution*

№	Name of kaolins	Zeolite A content according to X-ray phase analysis, % by weight	AE_{water}, sm^3/g
1	Angren kaolin	95,5	0,24
2	Pakhtachi kaolin	95,5	0,24

** CR: 2,4 Na_2O • Al_2O_3 • 2,4 SiO_2 • 60 H_2O; C(Na_2O) = 132,0 g/l, 30 °C (1 h) (20 h)*

Conclusion

In our view, one of the contributing factors to the identified limitations is the relatively low reactivity of metakaolin in comparison to gels, leading to a slower crystallization process. Additionally, granules derived from kaolin, with a diameter of merely 2–4 mm, experience either excessive or inadequate conversion of hydroxide into the solution after calcination at temperatures between 5 and 65 °C. As a result, the crystallization of these granules occurs exclusively on the surface, leaving the internal layers unaffected.

References

Keltsev N. V. Fundamentals of adsorption technology / N. V. Keltsev – Moscow: Chemistry, 1984. – 592 p.

Pavlov M. L. Study of the crystallization region of NaA zeolite in the form of polycrystalline intergrowths/ M. L. Pavlov, Ya. V. Mirsky, V. V. Pirozhkov // ZhP H. 1984. – № 8. – P. 1857–1859. – 115 p.

Mirsky Ya. V. Kinetics of crystallization of aluminosilicate granules into polycrystalline intergrowths of type A zeolite/ Ya. V. Mirsky, V. V. Pirozhkov, M. L. Pavlov // Kinetics and catalysis. 1984. – Vol. 25. – Issue. 1. – P. 22–25.
Hamilton K. E. The effects of the silica source on the crystallization of zeolite NaX/ K. E. Hamilton, E. N. Coker, A. G. Dixon, R. W. Thomson // Zeolites – 1993. – Vol. 13. – P. 645–653.
Chandrasekhar S. Microwave assisted synthesis of zeolite A from metakaolin / S. Chandrasekhar, P. N. Pramada // Microporous and Mesoporous Materials. 2008. – Vol. 108. – P. 152–161.
Imbert F. E., Moreno C., Montero A., Fontal B., Lujano J. Venezuelan natural aluminosilicates as a feedstock in the synthesis of zeolite A // Zeolites- 1994. – Vol. 14. – P. 374–378.
Granizo M. L., Blanco-Varela M. T., Palomo A. Influence of the starting kaolin on alkali activated materials based on metakaolin. Study of the reaction parameters by isothermal conduction calorimetry // Journal of Materials Science, –2000. – Vol. 35. – P. 6309–6315.
Davies T. W. & Hooper R. M. Structural changes i Kaolinite caused by rapid dehy droxylation // Journal of Material science Letters, 1985. – Vol. 4. – P. 39–42.
Meinhold R. H., Atakul H., Davies T. W. & Slade R. C.T. Flash calcination of kaolinite studied by DSC, TG and MAS NMR // Journal of Thermal Analysis, – 1992. – Vol. 38. – P. 2053–2065.
Chandrasekhar S. Influence of metakaolinization temperature on the forma tion of zeolite 4A from kaolin // Clay Minerals, 1996. – Vol. 31. – P. 253–261.
Kovo A. S. Development of Zeolite X and Y from Ahoko Nigerian Kaolin // Chemical Engineering: First Year Ph.D Report Manchester The University of Man chester, 2008. – 119 p.

submitted 20.04.2025;
accepted for publication 04.05.2025;
published 29.05.2025

Contact: eldor8501@gmail.com

The Austrian Journal of Technical and Natural Sciences, No 3–4
ISSN 2310-5607

PREMIER Publishing
ppublishing.org

DOI:10.29013/AJT-25-3.4-64-68

STUDY OF COLLAGEN STRUCTURE AND TISSUE REACTION DURING IMPLANTATION

Radjabov Otabek Iskandarovich [1], ***Yariev Olimjon Oltinovich*** [2], ***Azimova Luiza Bakhtiyarovna*** [1], ***Filatova Albina Vasilievna*** [1]

[1] Academy of Sciences of the Republic of Uzbekistan, Institute of Bioorganic Chemistry

[2] Bukhara State University

Cite: *Radjabov O.I., Yariev O.O., Azimova L.B., Filatova A.V. (2025). Study of Collagen Structure and Tissue Reaction During Implantation. Austrian Journal of Technical and Natural Sciences 2025, No 3–4.* https://doi.org/10.29013/AJT-25-3.4-64-68

Abstract

This paper discusses the method of obtaining and studying collagen isolated from cattle skin using alkaline-salt hydrolysis. The physicochemical properties of collagen, its structure and biocompatibility were studied. The use of IR spectroscopy and SEM made it possible to confirm the preservation of the fibrillar structure of collagen after processing, which is important for its use in medicine. Morphological histological studies on male Wistar rats showed that collagen stimulates metabolic processes and promotes an increase in the number of fibroblasts and collagen fibers, indicating its active participation in tissue restoration. The results showed that collagen has high biocompatibility and is promising for use in medicine.

Keywords: *collagen, fibrils, IR spectroscopy, SEM, morphohistology, biocompatibility*

Introduction

The development of chemical science made it possible to develop a method for isolating a biopolymer, collagen, from collagen-containing tissues, which retains its basic biological properties. The absence of toxic and carcinogenic properties in collagen attracted the attention of specialists in various fields and stimulated the study of this natural material for its introduction into wide medical practice (Ivanova L. A., 1990; Radjabov O. I., Gulyamov T., Turaev A. S., 2011; Chaikovskaya E. A., Istranov A. P., 1990).

The role of collagen in people's lives has not diminished even today. And perhaps it is the continuous emergence of new synthetic polymers that will allow us to once again highly appreciate the properties of this natural polymer and admire it. Practically without giving up its positions in traditional areas of application – leather, clothing, food industry, collagen begins to penetrate into other areas of industrial production; its role as a polymer material in medicine in general, and in surgery in particular, is very great (Radjabov O. I., Turaev A. S., Gulmanov I. D., Otajanov A. Yu., Azimova L. B., 2022).

Collagen types are widely expressed, but have tissue-specific roles, many have specific functions. Collagen type I is mainly found in

the skin, tendons, blood vessels and cornea. It is highly expressive and its dermal microfibrillar network influences the rigidity and compactness of the substructures beneath the skin surface, which underlies the extensible biomechanical function of human skin. Therefore, its loss or damage can significantly reduce the strength of the skin and lead to failure of various skin functions (Shahrajabian M. H., Sun W., 2024).

Type I collagen is the most common and important. It is a raw material for a number of technical industrial sectors. Pharmaceutical felts occupy an important place and foams, surgical suture material, collagen membranes, filters, etc. (Radjabov, O.I., Otajonov, A.Y., Baratov, K.R., Azimova, L.B. 2023; Muydinov, N.T., Radjabov, O.I., Gulyamov, T., Turaev, A.S., Atajonov, A.Yu., Barotov, K.R. 2023; Radjabov, O.I., Turaev, A.S., Gulmanov, I.D., Otajanov, A.Yu., Azimova, L.B., 2022).

The purpose of the research work is to determine whether the natural structure of collagen extracted from cattle skin by alkaline-salt hydrolysis is preserved and its biological activity.

Materials and Methods

Objects of study: lyophilic collagen isolated from cattle skin by alkaline-salt hydrolysis.

IR spectroscopy. IR spectra of polysaccharides were recorded on a Perkin Elmer 2000 IR Fourier spectrometer in the frequency range of 400–4000 cm^{-1} in a tablet with KBr. To record the spectra, 10 mg of the studied samples were ground in a ball mill with 100 mg of potassium bromide for 1 min, then about 100 mg of KBr were added to the mixture and the mixture was ground again in the mill, after which the remaining potassium bromide was added (300 mg in total), ground for another ~30 sec and the tablets were pressed.

Molecular structure determination. The molecular structure of collagen was examined by scanning electron microscopy (SEM). For this purpose, the sample was coated with carbon in a Q 150 RES (QUORUM. USA) device at a vacuum voltage of 15 kV, and its morphological structures were studied in an EVOMA 10 (Zeis, Germany).

Implantation of biomaterial. The experiments were carried out on male Wistar rats weighing 150–200 g. Collagen was implanted under the skin in the area of the thigh and back of the rats in the operating unit of the Department of Anatomy and Clinical Anatomy of the Tashkent Medical Academy.

Morphohistological studies. Pieces of skin in the area of the implanted biomaterial were taken on the 5^{th}, 10^{th} and 15^{th} days after the introduction of the biomaterial. For this purpose, a marked area of skin measuring 0.5 × 0.5 cm was excised under ether anesthesia, after which the wound was sutured with interrupted sutures. The material was fixed in 10% neutral formalin and embedded in paraffin. Paraffin sections were stained with hematoxylin and eosin, picrofuchsin according to van Gieson.

Results and discussions

Infrared spectroscopy is one of the most informative methods for structural analysis of biopolymers such as collagen. The spectrum obtained from a lyophilized collagen sample shows a number of characteristic absorption lines indicating the presence of typical functional groups corresponding to its amino acid composition and polypeptide structure. The IR spectrum of lyophilized collagen is shown in Figure 1.

As can be seen from Figure 1, the most intense and wide absorption band is observed in the region of 3286 cm^{-1}, which indicates the presence of extended systems of hydrogen bonds caused by stretching vibrations of O-H and N-H groups. This region corresponds to vibrations of amino groups ($-NH_2$) and hydroxyl groups (–OH) located in the side chains in the collagen structure. The width and intensity of this band is due to the overlap of signals from intermolecular and intramolecular hydrogen bonds, which play a key role in the formation of a stable three-helix structure of the collagen molecule. In the region of 3000–2800 cm^{-1}, peaks are recorded at 3074 and 2941 cm^{-1}, corresponding to stretching vibrations of C-H bonds in CH_2^- and CH_3^- groups. These signals are associated with aliphatic hydrocarbon chains of amino acid residues such as proline and hydroxyproline, amino acids that play a key role in stabilizing the collagen helix.

Figure 1. *IR spectrum of collagen*

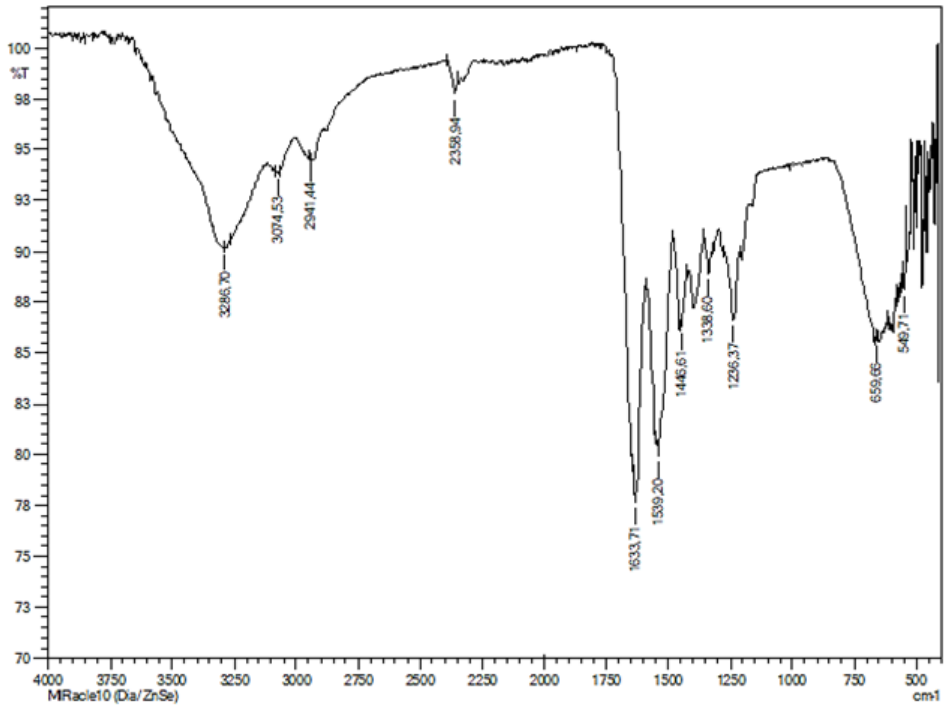

The most significant bands indicating the protein nature of the sample are found in the following ranges:

–1633 cm^{-1}: an intense Amide I band arising from the stretching vibrations of the carbonyl group (C = O) in the peptide bond. This band is especially sensitive to the type of secondary structure of the protein: for collagen it is characteristic of an organized triple helix;

–1539 cm^{-1}: the Amide II band caused by bending vibrations of the N-H and stretching of the C-N bond. Together, the Amide I and II bands serve as a reliable indicator of the preservation of the native collagen structure and the absence of deep denaturation;

–1338 cm^{-1}: the band corresponds to Amide III vibrations arising as a result of combined movements of the C-N and N-H bonds. This region provides an idea of the configuration of amino acid side chains and the spatial organization of the protein. Peaks in the low-frequency region, in particular 659 and 549 cm^{-1}, correspond to deformation vibrations of the molecule skeleton and reflect the stability of the spatial configuration of collagen. The absence of significant shifts and blurring of the amide bands indicates the preservation of the triple helical structure of the protein, which is especially important when assessing the functional suitability of collagen as a biomaterial.

Also in our research work, SEM images of lyophilized collagen were obtained to determine whether the fibrillar structure of collagen was preserved after hydrolysis.

Figure 2. *SEM of collagen*

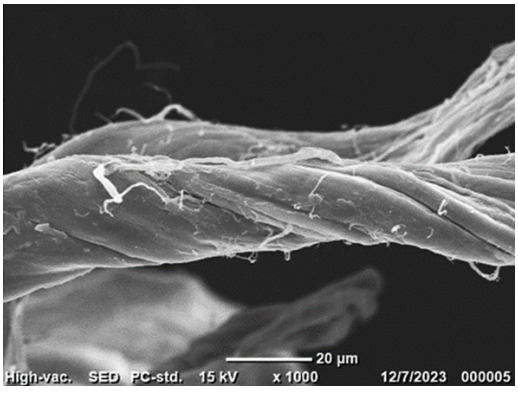

The presented SEM image demonstrates the microstructure of fibrillar collagen isolated by hydrolysis of cattle hide. The figure clearly shows the fibrous structure of collagen, where the fibrils have a characteristic helical organization. Such a structure is typical of native collagen, which confirms the preservation of its natural characteristics after hydrolysis. The surface of the collagen fibers has microroughness, possible ruptures and small fragments, which may indicate partial degradation of the fibrillar network due to the hydrolytic process. However, in general, the fibers retain their integrity, indicating a gentle hydrolysis mode. According to the scale (20 μm) of the figure, the fibril diameter varies in the range of 10–20 μm, which corresponds to natural fibrillar collagen. This parameter plays a key role in medical applications, since the fibril size affects the mechanical properties of the material, its biodegradation and cellular adhesion.

In the course of our research, experiments were conducted to determine the biological activity of collagen with a natural fibrillar structure isolated from cattle skin.

According to the results of the experiment, the general condition of the experimental animals is satisfactory. No pronounced allergic reactions were observed during the entire study period, either from the skin or from other organs and systems of the body. On the 5th day of the experiment, in the area of collagen injection, the epidermis is multilayered, flat, keratinized, consists of two to three layers of cells, with loose connective tissue under the epidermis. The dermis and hypodermis are represented by formed connective tissue, contain a large number of collagen fibers with pronounced edema and single cells of connective tissue. The preparation shows an area where the remains of the injected collagen have been preserved. Focal collagen fibers are tightly adjacent to each other in the form of parallel layers. Next to this zone, the dermis consists of young formed connective tissue. There are especially many cells under the epidermis. The closer to the intact zone in the dermis and hypodermis, a moderately pronounced stimulation of collagen fibers is noted. A large number of connective tissue fibers, small vessels with an expanded lumen are noted.

After 10 days, a macrophage reaction is observed in the hypodermis. The hypodermis contains many collagen fibers, loosely located with intense staining, as well as fibroblasts. The vessels are dilated and filled with blood. Next to this zone, young developing connective tissue with the presence of connective tissue cells is visible in the dermis and hypodermis.

On the 15 th day, the number of fibroblasts and collagen fibers increases in the collagen injection zone, which form a network between the mature collagen fibers of the dermis itself. In the hypodermis, there is formed connective tissue with single connective tissue cells, that is, there is development of collagen fibers and a large number of connective tissue cells (Fig. 3).

Figure 3. *Collagen implantation zone, day 15*

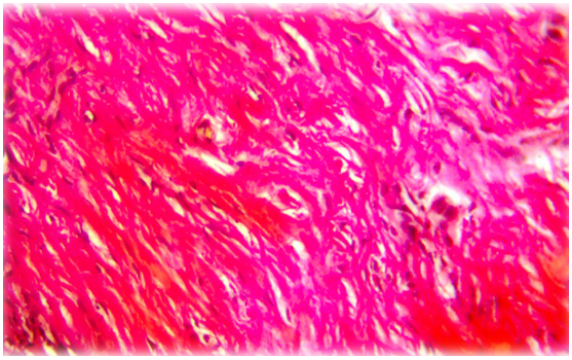

Conclusion

The conducted analysis of physical and chemical characteristics of powdered biomaterial based on collagen and polysaccharide demonstrates its high technological effectiveness and biocompatibility. Optimal indicators of humidity, pH and particle size ensure stability of the material, and a high degree of

grinding indicate its prospects for medical applications. According to SEM analysis, it was established that the obtained collagen from cattle skin retains its fibrillar structure. According to morphohistological studies, it was proven that collagen is included in metabolic reactions, stimulates metabolic processes, starting from the first day. Subsequently, on the 5th, 10th and 15th day, metabolic processes are enhanced, which is manifested by an increase in the number of fibroblasts and collagen fibers, which is confirmed by bright coloring according to van Gieson.

References

Ivanova L. A. Collagen and prospects for its use in the technology of dosage forms // Pharmacy. 1990. Vol. 1. – P. 81–82.

Radjabov O. I., Gulyamov T., Turaev A. S. Collagen medical, obtaining and research // Uzbek chemical journal. Special issue. – 2011. – P. 94–97.

Chaikovskaya E. A., Istranov A. P. Collagen in the technology of dosage forms and products for ophthalmology // Pharmacy. 1990. Vol. 4. – P. 82–83.

Radjabov O. I., Turaev A. S., Gulmanov I. D., Otajanov A. Yu., Azimova L. B. Obtaining Collagen and Morphological Studies of Injection Solution on Its Basis // International Journal of Materials and Chemistry. – 12(3). 2022. – P. 39–43. DOI: 10.5923/j.ijmc.20221203.01.

Shahrajabian M. H., Sun W. Mechanism of action of collagen and epidermal growth factor: A review on theory and research methods // Mini Reviews in Medicinal Chemistry. 2024. – Vol. 24(4). – P. 453–477.

Radjabov, O. I., Otajonov, A. Y., Baratov, K. R., Azimova, L. B. Local hemostatic biomaterial based on native collagen // E3S Web Conference., 2023. – 420 p. URL: https://doi.org/10.1051/e3sconf/202342009004.

Muydinov, N. T., Radjabov, O. I., Gulyamov, T., Turaev, A. S., Atajonov, A. Yu., Barotov, K. R. Developing composition and studying physico-chemical and antiadhesive properties of biopolymer films based on collagen and Na-CMC // Khimiya Rastitel'nogo Syr'ya. 2023. – Vol. 4. – P. 81–88.

Radjabov, O. I., Turaev, A. S., Gulmanov, I. D., Otajanov, A. Yu., Azimova, L. B. Obtaining Collagen and Morphological Studies of Injection Solution on Its Basis. International Journal of Materials and Chemistry. 2022. – Vol. 12(3). – P. 39–43.

submitted 26.03.2025;
accepted for publication 10.04.2025;
published 29.05.2025

Contact: ximik_07@mail.ru

The Austrian Journal of Technical and Natural Sciences, No 3–4
ISSN 2310-5607

PREMIER Publishing
ppublishing.org

DOI:10.29013/AJT-25-3.4-69-74

STUDY AND ANALYSIS OF THE IR SPECTRUM AND PHYSICO-CHEMICAL PROPERTIES OF CORROSION INHIBITORS THAT PREVENT THE DEPOSITION OF SALTS CONTAINING NITROGEN AND PHOSPHORUS USED IN INDUSTRIAL WATERS

Shamuradov Ulugbek Meilievich [1], Beknazarov Hasan Soibnazarovich [2], Jalilov Abdulakhat Turapovich [3], Togaev Eldar Makhmanazarovich [4]

[1] Tashkent Research Institute of Chemistry and Technology.

[2] Department of "General Medicine" of the Faculty of Medicine, Angren University

[3] Academician, "Tashkent Scientific Research Institute of Chemical Technology LLC"

[4] Department of Chemical Engineering and Biotechnology, Karshi State Technical University

Cite: *Shamuradov U.M., Beknazarov H.S., Jalilov A.T., Togaev E.M. (2025). Study and Analysis of the ir Spectrum and Physico-Chemical Properties of Corrosion Inhibitors That Prevent the Deposition of Salts Containing Nitrogen and Phosphorus Used in Industrial Waters. Austrian Journal of Technical and Natural Sciences 2025, No 3–4.* https://doi.org/10.29013/AJT-25-3.4-69-74

Abstract

The article discusses in detail the physico-chemical properties of the EDF-1 corrosion inhibitor containing nitrogen and phosphorus, which prevent the deposition of salt in the pipelines of heating boilers, as well as the occurrence of corrosion in water systems used in industry for heating and cooling. Which functional groups are present and formed in this inhibitor using an IR-Fourier device, Shimazu, were studied and, accordingly, the absorption peaks of the new substances obtained were determined. As a result of the synthesis, metal corrosion inhibitors were obtained and the degree of their corrosion protection was checked in accordance with the requirements of GOST 9.506–87 and conclusions were drawn.

Keywords: *Corrosion inhibitors, Nitrogen, organic compounds, inorganic compounds, industrial waters, furnace, GOST 9.506–87*

The formation of mineral deposits and corrosion of structural steels in technological processes related to industrial use as a heat carrier, heat carrier and hydraulic transport has been a serious problem for more than a hundred years and remains relevant today.

One of the most optimal ways to protect metals from corrosion is to use corrosion inhibitors. The use of inhibitors can only slow down corrosion, but not stop it completely (Shamuradov, Ulugbek Meylievich, Hasan Soyibnazarovich Beknazarov, and Abdulakhat Turapovich Dzhalilov. 2025;

Andreatta F., Fedrizzi L., 2016). Corrosion leads to huge economic losses for many industries. According to an international Nice study conducted in 2016, global corrosion costs amount to 2.5 trillion US dollars per year, which is equivalent to a significant portion of the global gross domestic product (GDP) (Amin H. M. A., Galal A., 2021). Various countries have conducted studies on the corrosion of national costs. According to this survey, the U.S. economy has shrunk by $70 billion due to corrosion, accounting for 4.2 percent of the gross national product. The government of India spends about 3.5% of the country's GDP per year on corrosion losses (Kamath, R., Venumuddala, V.R., 2023). Oil and gas storage tanks are made of aluminum and steel, which must be protected due to their tendency to corrosion, which directly or indirectly affects the economy. Steel and aluminum are important metals that are used in almost all parts of the Vegas oil industry prior to the distribution of final products (Kamath, R.; Venumuddala, V.R., 2023). Synthetic inhibitors are widely used in various industrial applications due to their effectiveness, but their potential environmental impact must be considered, and their choice and dosage must be carefully monitored (Fayomi O. S.I., Akande I. G., Odigie S., 2019).

Material and method

Synthesis of composite corrosion inhibitor EDF-1. Ethylenediamine was dissolved in 12 ml of distilled water, taking 2 grams and dissolving 0.59 grams of phosphoric acid in 3 grams of distilled water, and both prepared solutions were placed in a round-bottomed flask with a double bottom, the flask was lowered into an oil bath, into which a reversible inert gas cooler (nitrogen gas) was installed from one neck of the flask with two necks An ashtray was installed in the second neck of the chloride hose for adding acid and formalin and the technological part was prepared. Then the oil was placed in an oven with a bath, nitrogen gas was introduced to create an inert medium and added dropwise with a slow increase in temperature to 60–65 °C for 1.5–2 hours with a concentration of 37% hydrochloric acid of 1.92 g, after which formalin was removed from a 37% solution of 0.7 g until the temperature of the reaction mixture increased to 115–120 °C. taken off 24 hours drops are added during. The resulting reaction mixture is first cooled to room temperature, then neutralized with a 30% NaOH solution, while the precipitate is lowered to the bottom of the flask, and the resulting reaction mixture is dried in an oven until a dry mass is formed. The substance of the bright yellow shape of the tablets was used as a basis.

Infrared Spectroscopy (IR) – IR spectroscopy (Japanese-made Fury spectrometer. IR spectroscopic studies were performed using the powder method on a Shimazu infrared Fourier spectrometer (range 400–4000 cm^{-1}, resolution 4 cm^{-1}).

SEM analysis. The precorrosive, postcorrosive, and inhibited states of the steel surface were studied using a JEOL JSM-it200la multi-faceted tungsten filament scanning electron microscope with intuitive controls, including a touchscreen and a scanning electron microscope with SEM imaging and EDS analysis directly from the optical image.

The results obtained and their discussion

The EDF-1 corrosion inhibitor was tested by gravimetric method. This method is one of the widely used and effective methods for determining the rate of metal corrosion and the protective ability of corrosion inhibitors in the laboratory. The gravimetric method is based on calculation by measuring the mass difference before and after exposure to corrosion by placing controlled metal samples in inhibitory and inhibitory media. The disadvantage of using this method is that it describes the average rate of corrosion without taking into account irregularities on the metal surface.

Our test experience has been verified in accordance with GOST 9.506–87 "methods for determining the protective ability of metal corrosion inhibitors in a water-oil environment".

The analysis of the IR spectrum and the corrosion inhibitor EDF-1. EDF-1 was presented to study the composition and structure of the corrosion protection inhibitor (Fig. 1).

Figure 1. *IR spectrum of EDF-1 corrosion inhibitor*

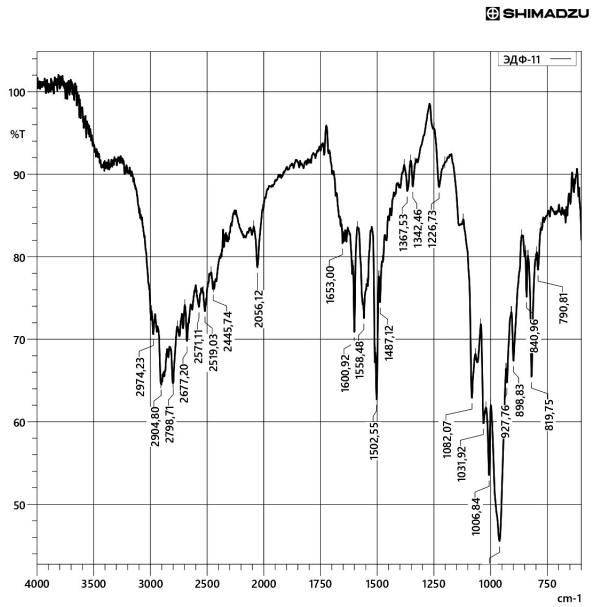

The composition and structure of the EDF-1 corrosion inhibitor were investigated using IR spectrometer technology (IQ-Fury, SHIMADZU, Japan) in the Dead range up to an area of 4000 cm^{-1}. The absorption line of IR spectroscopy is shown. 2677.20––2571.11 cm^{-1} intensity of weak –(PO)oh groups with valence vibrations in absorption regions, 2445.74 cm^{-1} –P–H groups with valence vibrations in absorption regions, 1653–1600.92 cm^{-1} type of vibrations in absorption regions valence, intense –C=N– group, 1487.12–1558.48 cm^{-1} absorption during asymmetric valence vibrations in fields of the C–N=O group, the type of vibrations in absorption fields is 1367.53 cm^{-1} Simm.The valence, intense –N–N=O group has lines corresponding to –P–O–C groups with a valence oscillation in the absorption region of 1226.73 cm^{-1}.

According to these analyzed results, our investigated corrosion inhibitor contains nitrogen and phosphorus, which indicates that it has anti-corrosion properties.

The results obtained using a scanning electron microscope, as well as their analysis.

A scanning electron microscope (SEM) is a device that uses directed beams of high-energy electrons on the surface of solid samples to generate various signals. SEM makes it possible to extract data such as surface structure (external morphology), chemical composition, orientation of components, as well as the crystal structure of the sample from the electronic interaction signals of the sample. The purpose of the SEM analysis is to determine the presence of an inhibitor on the steel surface.

Figure 2.1. *Initial photo of the steel sample*

Figure 2.2.*Photo of a steel sample in SEM*

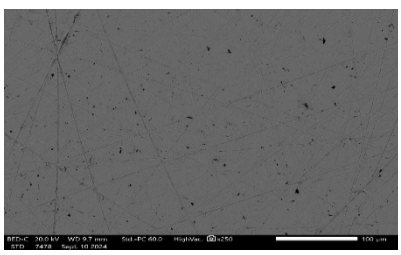

Figure 2.3. *Photo of a hardened steel sample in SEM*

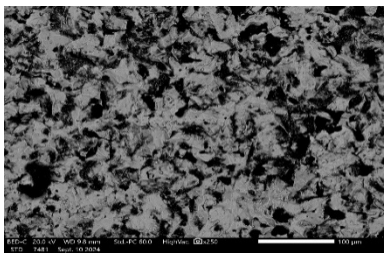

Typically, data is taken from the sample surface using a selected area (from 1 cm to 5 microns), represented as a 2D image. Magnification can range from 20× to 30000× with

a spatial resolution of 50 to 100 Nm. In addition, SEM analysis does not lead to a change in the composition of the sample. The reason is that the sample does not lead to a loss of sample volume during electronic interaction.

Morphologically, the surface surface of steel samples conducted with samples of the St 30 grade in various concentrations was studied using the Sem method.

It is known from the above figures that Figure 2.1 shows a preliminary photograph of a steel sample cleaned with sandpaper of different grades and washed in acetone. Micrographs of the initial steel sample made on an inhibitor-free surface were also obtained using a scanning electron microscope (Fig. 2.2) and inhibitory (Fig. 2.3) media.

Figure 3. *Microscopic image of the arrangement of elements on the surface of a trapped metal and a diagram of their presence using a scanning electron microscope*

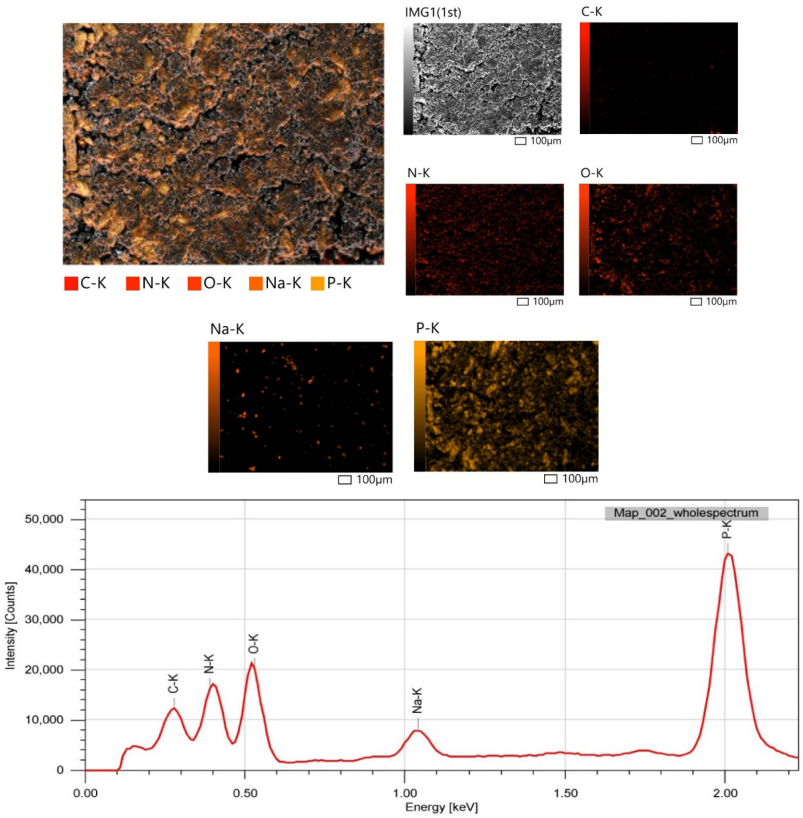

The analyses obtained using a scanning electron microscope show that our EDF-1 grade corrosion inhibitor provides excellent protection for metal surfaces, and we can see that it contains anti-corrosion elements, as well as how it settles on the metal surface. The properties of corrosion inhibitors that are highly soluble in water and retain nitrogen and phosphorus in their composition were tested according to GOST 9.506–87. The molecules of these corrosion inhibitors consist of one or more functional groups, which are organic substances containing a hydrocarbon radical.

3 different concentrations for 360 hours in the tester at atmospheric pressure. The test time is calculated from the moment the samples are placed in the environment. The duration of the tests was determined according to GOST 9.506–87. The tests were carried out on waters used in the oil and gas industry.

The concentration of EDF-1 grade corrosion inhibitor containing nitrogen and phosphorus is 1%, 3%, 5%; this was done in an acidic environment. The tests showed protection levels of 84.34, 96.3, and 99.98 percent, respectively. The graph below shows the degree of protection of our corrosion inhibitor at various temperatures.

Table 1 shows the corrosion rate and degree of protection for 360 hours in an environment without inhibitors and inhibitors.

Table 1. *Corrosion rate and degree of protection 360 hours in an environment without inhibitors and inhibitors*

	Sample Surface; S, m^2	Sample weight before testing; M, g	Mass of the sample after the test; M, g	Sample mass loss; M1 – M2, g	Degree of corrosion in an environment without inhibitors, $g/m^2 * s$	Degree of corrosion in an inhibitory environment; $g/m^2 * s$	Protection level; (Z)%
Without inhibitors	0,11053	14,20894	13,26007	0,94887	0,02384		
1	0,11053	14,10306	14,09591	0.00715		0,000179	84,34
2	0,11053	14,63365	14,63027	0.00338		0,000085	96,3
3	0,11053	14,85650	14,85374	0.00276		0,00073	99,98

Table 2. *The values of corrosion rate, protection levels and surface treatment coefficient are EDF-1 corrosion inhibitors in various molar mass ratios*

Ethylenediamine: phosphic acid	Corrosion rate	Protection level	θ	Temperature, °C
1:3	0,074	73,3	0,733	20
1:2	0,068	81,7	0,817	50
1:1	0,053	92,6	0,926	70
2:1	0,061	85,5	0,855	80
3:1	0,079	69,7	0,697	90

Table 2 shows the values of the corrosion rate, protection levels, and surface treatment coefficient of the EDF-1 corrosion inhibitor in various molar mass ratios. The results showed that the rate of metal inhibition was also higher when the starting products obtained in different proportions during the reaction, namely ethylenediamine and phosphitic acid, were obtained in a 1:1 ratio.

Figure 3. *Dependence of EDF-1 corrosion inhibitor on molar ratios and degree of protection, scheme*

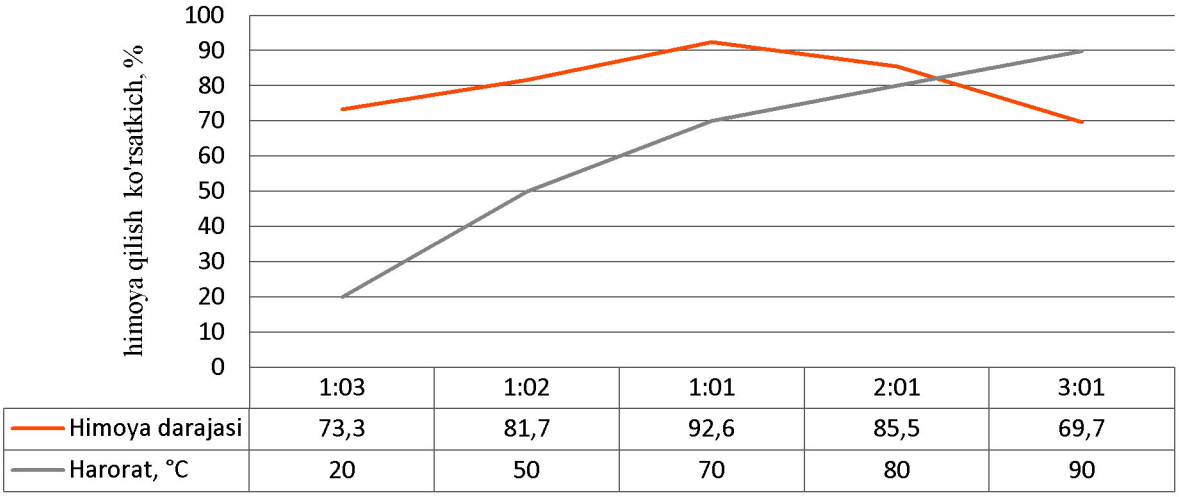

Figure 3 shows a graph of the dependence of the molar ratios of the synthesized corrosion inhibitor on the degree of protection. The results show that the optimal conditions for the synthesis of an EDF-1 inhibitor are 70°C, and the concentration of the starting substance is 1:1, and the reaction yield is 92.6%, as can be seen from the data presented.

As a result of trial studies, we can see using Table 1 and Table 2 that the best mass ratio of amino compounds and phosphitic acid is 1:1, and its protection level is 92.6%.

Conclusion

The physicochemical properties of the EDF-1 corrosion inhibitor synthesized by us and the analysis of the IR spectrum of the synthesized product, SEM (scanning electron microscope), were obtained. From the analysis results, it can be concluded that the corrosion inhibitor contains nitrogen and phosphorus, these elements have maximum inhibitory properties at a temperature of 70 °C. Exposure to metals in testing processes has shown that inhibitors slow down the corrosion process and also protect the metal surface from corrosion. These compounds have proven to be the most effective against corrosion.

References

Shamuradov, Ulugbek Meylievich, Hasan Soyibnazarovich Beknazarov, and Abdulakhat Turapovich Dzhalilov. “Differential thermal analysis of corrosion inhibitor edf-1 used to prevent salt deposition in heating and cooling systems. Study and characteristics”. Universum: technical sciences. 2025. – 7.2 (131). – P. 23–27.

Andreatta F., Fedrizzi L. Corrosion ingibitors // Springer Ser. Mater. Sci. Springer Verlag, 2016. – Vol. 233. – P. 59–84.

Amin H. M. A., Galal A. (ed.). Corrosion protection of metals and alloys using graphene and biopolymer based nanocomposites. – CRC Press is, 2021.

Kamath, R., Venumuddala, V. R. Emerging Technologies and the Indian IT Sector; CRC Press: Boca Raton, FL, USA, 2023. ISBN 9781000853759. [Google Scholar]

Fayomi O. S.I., Akande I. G., Odigie S. Economic Impact and Prevention of Corrosion in Oilfields: An Overview // Journal of Physics: Conference Series. – IOP Publishing, 2019. – T. 1378. – No. 2. – P. 022037.

Olajire A. A. Recent Advances in Oil and Gas Production Water Treatment Technology for Sustainable Energy Industry – Mechanistic Aspects and Process Chemistry Perspectives // Journal of Chemical Engineering Advances. 2020. – T. 4. – 100049 p.

Shomuradov, Ulugbek, Hasan Beknazarov, and Abdulahat Djalilov. “Investigation of the Physico-Chemical Properties of Inhibitors Based on Ethylene Diamine and Hydrochloric Acid”. Science and innovation 2024. – 3.A2. – P. 128–131.

submitted 03.04.2025;
accepted for publication 17.04.2025;
published 29.05.2025

Contact: ulugbekshomurodov94@gmail.com

The Austrian Journal of Technical and Natural Sciences, No 3–4
ISSN 2310-5607

PREMIER Publishing
ppublishing.org

DOI:10.29013/AJT-25-3.4-75-81

SCIENTIFIC STUDY OF THE PHYSICOCHEMICAL PROPERTIES AND THERMAL TRANSFORMATIONS OF USED ZEOLITES

Sultonov Sadulla [1], ***Kucharov Azizbek*** [1,2], ***Yusupov Farkhod*** [1], ***Dusmatova Anzirat*** [2], ***Toshboboyeva Ra'no*** [2]

[1] Institute of General and Inorganic Chemistry of the Academy of Sciences of Uzbekistan. Tashkent Uzbekistan

[2] Pharmaceutical Education and Research Institute. Yunusobod District, Tashkent, Uzbekistan

Cite: *Sultonov S., Kucharov A., Yusupov F., Dusmatova A., Toshboboyeva R. (2025). Scientific Study of the Physicochemical Properties and Thermal Transformations of Used Zeolites. Austrian Journal of Technical and Natural Sciences 2025, No 3–4.* https://doi.org/10.29013/AJT-25-3.4-75-81

Abstract

This study investigates the properties of granules prepared using various binding solutions and explores the effect of adding combustible materials and metal oxides to catalysts. Electrolyte solutions significantly increased the specific surface area and total pore volume of the granules, while combustible materials like cellulose decreased density and mechanical strength. A specific amount of calcium oxide improved the specific surface area; however, exceeding the optimal content reduced strength. The addition of calcium hydroxide suspension yielded better results. The optimal composition was identified in catalysts containing calcium oxide and magnesium oxide. Thermal analysis confirmed phase transformations occurring at different temperatures, contributing valuable insights into the material behavior and catalytic properties.

Keywords: *Zeolite, processing, physicochemical properties, thermal analysis, metal oxides, catalyst, surface area, porosity, active components, thermal transformations*

Introduction

Zeolites, with a density range of 2––2.3 g/cm³ (Derouane, Eric G., et al., 1981), play vital roles in adsorption, catalysis, and ion exchange due to their physicochemical properties. Thermal transformations, crucial for stability and activity, significantly impact their performance (Cruciani, Giuseppe. 2006). Current research emphasizes improving the structure, surface area, and pore volume of zeolites to optimize functionality under diverse conditions (Yusupov, F., & Khursandov, B., 2024). For example, clinoptilolite demonstrates a surface area of 300––400 m²/g (Temirov G. et al., 2023), showcasing its adsorption potential. Studies show that modifying zeolites, such as adding calcium oxide, further enhances specific surface area and catalytic efficiency (Khursandov, B. Sh., Kucharov, A. A. U., & Yusupov, F. M., 2022).

This study aims to investigate the physicochemical properties and thermal behavior of zeolites, focusing on phase transformations and heat resistance (Yusupov, F.M., Mamanazarov, M.M.U., Kucharov, A.A.U., & Saidobbozov, S.Sh., 2020). Enhancements in catalytic and adsorption activities ensure extended application in petrochemistry, environmental protection, and chemical synthesis (Yusupov Farkhod, Azizjon Qurbonov, Kucharov Azizbek, Yodgorov Normahmad, 2025). Results contribute to increasing zeolite efficiency and service life, offering economic benefits alongside ecological impact (Yusupov, F., Kucharov, A., Baymatova, G., Shukurullayev, B., & Yuldashev, R., 2023). Improvements in surface area and pore volume through structural optimization highlight the significance of zeolites in advanced scientific applications (Kucharov, Azizbek, et al., 2025).

Research method

The physicochemical properties of the produced granules can vary widely depending on several factors (Xursandov, Bobomurod, et al., 2024). For instance, the chemical composition, moisture content, particle size distribution, and physicochemical properties of the raw material significantly influence the granules' characteristics (Piccione, Patrick M., et al., 2000). Other factors such as the quantity and ratio of powder and binding solution used in the granulation process, the nature of the binding solution, as well as the granulator's angle of inclination and rotational speed, also play a crucial role (Kucharov, Azizbek, et al., 2021).

For the preparation of catalyst samples, aluminum oxide waste, previously utilized as an adsorbent, was used as the primary raw material (Ozin, Geoffrey A., Alex Kuperman, and Andreas Stein. 1989). Additionally, active components such as CaO, MgO, TiO_2, and V_2O_5 were employed. These oxides were incorporated in the initial stage as powders (e.g., CaO, MgO, TiO_2) or introduced in solution form (e.g., $Ca(OH)_2$, $Mg(OH)_2$, NH_4VO_4) either during the granulation step with the binding solution or by impregnating the final granules with their respective solutions (Qurbonov, Azizjon, Azizbek Kucharov, and Farxod Yusupov, 2024).

Figure 1. *Technological Process Scheme for Producing Zeolite of Sb-14 Brand*

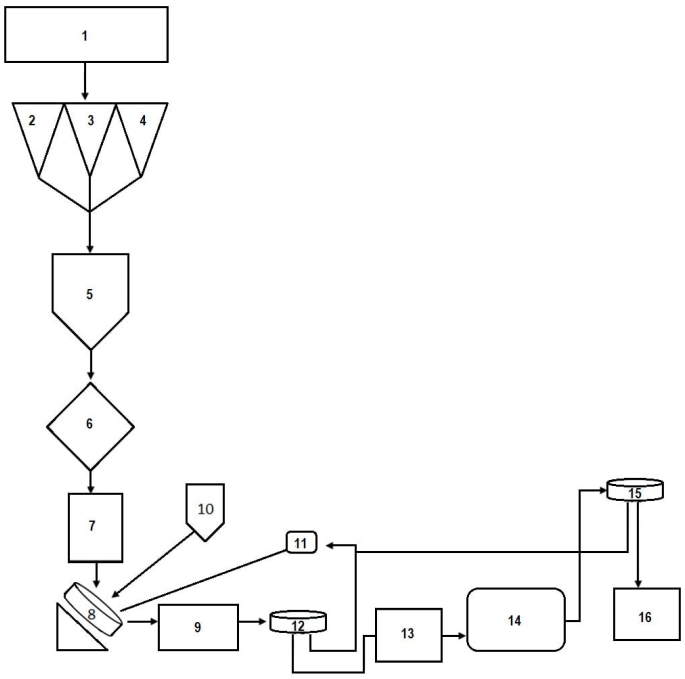

1–2,3,4 – Collecting hoppers; 5 – Dispenser; 6 – Disintegrator; 7 – Collecting dispenser; 8 – Pan granulator; 9 – Reactor for physicochemical treatment; 10 – Reactor for binding solution; 11 – Mill; 12, 15 – Sieves; 13 – Container for active component impregnation; 14 – Furnace; 16 – Storage

Initially, raw materials were crushed to 100 μm. More than 50% of the crushed sample consisted of fractions under 70 μm. The crushed raw materials and binding solution were fed into a rotating pan granulator at a speed of 15–20 rpm, with the granulator's angle of inclination set between 40–60°. Granulation time varied from 15 to 45 minutes. The binding solution was added at 30% of the initial raw material powder weight. The raw material powder was supplied at a rate of 160–180 g/min, while the binding solution was added at 60–80 ml/min. Water, catalyst active component solutions, and NaOH solutions were used as binding agents. Spherical granules with 25–30% moisture content were obtained from the granulator and subjected to physicochemical processing.

The granules were treated with water vapor at 80–90 °C for 2 hours, then sieved and dried at 110–120 °C for 15–20 hours. Active components were impregnated into the dried granules, followed by thermal treatment at 420–550 °C. Heating was conducted at a rate of 70 °C/hour until the desired temperature was reached, and thermal processing continued for 4 hours at that temperature.

Result and discussion

Properties of granules prepared using different binding solutions are summarized in Table 1. The use of electrolyte solutions as binders significantly increased both the specific surface area and total pore volume of the granules. When NaOH and H_3BO_3 were employed as binding agents, the mechanical strength of the granules improved, whereas the use of ethanol led to a slight decrease in strength. Electrolyte-based binders were found to have a notable effect on pore structure. Specifically, the addition of NaOH resulted in an increased number of macropores, while ethanol promoted the formation of micropores and reduced the presence of macropores. In contrast, the inclusion of boric acid had minimal impact on overall pore volume.

Table 1. *The effect of adding electrolytes to the binder solution on the properties of granules*

Binder Solution	H_2O	10% NaOH	10% C_2H_5OH	10% H_3BO_3
Micropores, cm^3/g	0.05	0.18	0.28	0.08
Macropores, cm^3/g	0.26	0.31	0.16	0.28
Total pore volume, cm^3/g	0.31	0.49	0.44	0.39
Density, g/cm^3	0.694	0.722	0.697	0.719
Mechanical strength, MPa	4.5	6.2	4.1	5.2

It was found that the addition of various combustible materials to the raw material had different effects on the properties of the granules. The addition of combustible materials significantly decreased the mechanical strength and density of the granules. The inclusion of combustible materials increased the total pore volume, mainly due to an increase in the number of macro- and mesopores. It was also found that the amount and particle size of the combustible materials affected the properties of the granules (Table 2).

Table 2. *Physical and mechanical properties of granules prepared with combustible materials*

Binder Solution	Without additives	Cellulose 8%	Coal 8%	Wood shavings 8%
Micropores, cm^3/g	0.05	0.06	0.10	0.07
Macropores, cm^3/g	0.27	0.27	0.28	0.35
Total pore volume, cm^3/g	0.32	0.38	0.40	0.41
Specific surface area, m^2/g	290	240	265	285
Density, g/cm^3	0.712	0.676	0.655	0.633
Mechanical strength, MPa	5.7	4.2	3.9	3.3

During granule preparation, pure aluminum oxide was also used together with SHKM (adsorbent) waste. Aluminum oxide and SHKM waste were mixed in different ratios to prepare the granules. The physical and mechanical properties of the samples were studied. The results shown in Table 3 demonstrate that the addition of pure aluminum oxide to the composition improved the properties of the granules.

Table 3. *Physical and mechanical properties of granules prepared from different ratios of pure aluminum oxide and adsorbent waste*

Ratio	10/90	20/80	30/70	40/60
Density, g/cm³	0.694	0.705	0.689	0.704
Mechanical strength, MPa	4.4	4.9	5.8	6.1
Specific surface area, m²/g	280	290	310	315
Total pore volume, cm³/g	0.31	0.35	0.41	0.42

The TG, DTG, and DSC curves of the obtained sample are shown in Figure 2. According to the literature (Yusupov, F., & Khursandov, B., 2024), the endothermic effect observed at low temperatures indicates the release of adsorbed water from the sample. The second endothermic effect observed at 250–300 °C indicates the formation of boehmite and the low-temperature aluminum oxide phase – η-Al_2O_3. The endothermic effect at 500–700 °C is associated with the release of water from boehmite-structured aluminum hydroxide and the formation of γ-Al_2O_3.

Figure 2. *Thermal analysis of a sample obtained from SHKM (adsorbent) waste*

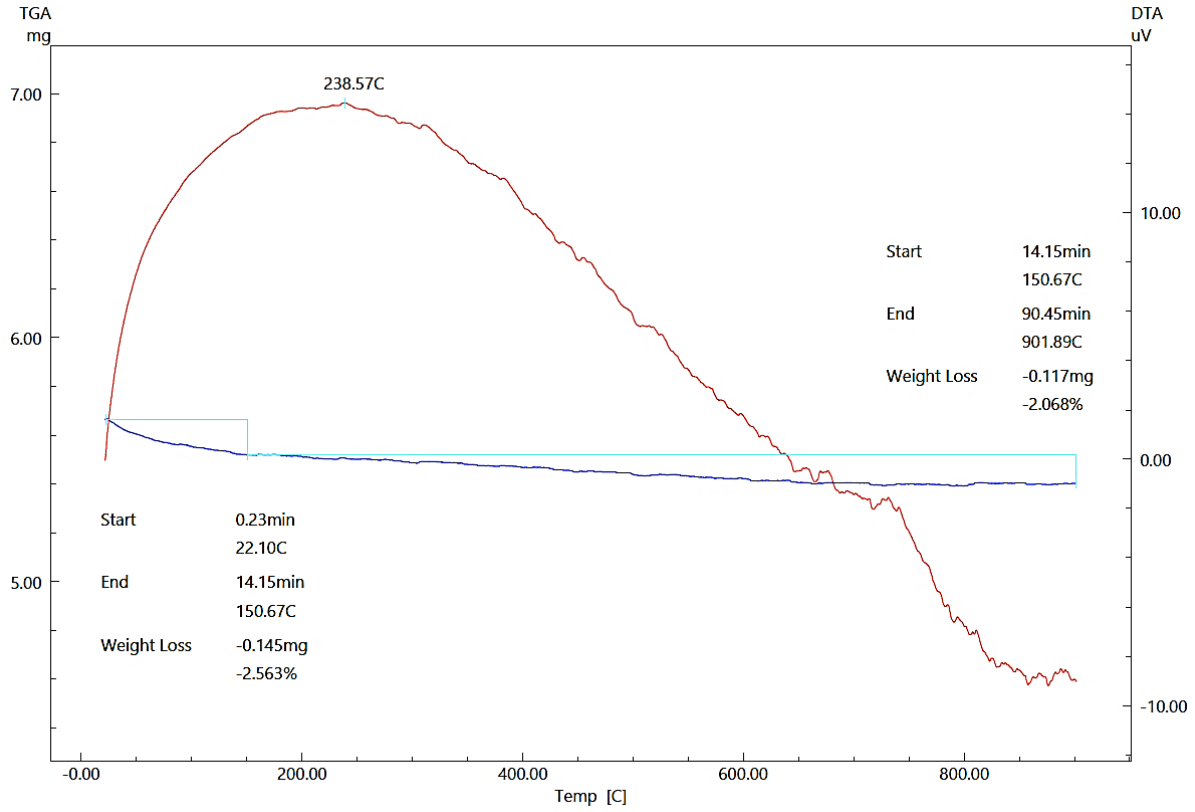

In addition to adding various electrolytes and combustible materials to the catalyst composition, it is also possible to modify the catalyst properties by incorporating oxides of various metals (as active components). Various sources report that the oxides of *d*-metals and alkaline earth metals have a positive effect on catalyst properties. These metal ox-

ides can be added to the catalyst by different methods and at different stages of the preparation process.

Calcium and magnesium oxides can be added in dry form, while their hydroxides can be introduced in suspension form (during the granulation process) as binder solutions. Calcium compounds, in particular, are considered relatively inexpensive.

To study the effect of CaO (as a promoter) on the catalyst properties, five different samples were prepared with varying compositions, and their physical and mechanical properties were analyzed.

Table 4. *Main physical-chemical properties of catalysts obtained with different amounts of active component (CaO)*

Cao content (%)	Mechanical strength (mpa)	Total pore volume (cm^3/g)	Specific surface area (m^2/g)	Density (g/cm^3)
0	6.4	0.50	260	0.79
0.5	6.1	0.48	265	0.74
1.1	5.3	0.50	285	0.70
3.1	4.5	0.49	270	0.64
4.8	3.9	0.51	265	0.62

Analysis results showed that as the CaO content increased, the specific surface area increased while the density decreased (Table 4). It was also observed that with increasing CaO content, the mechanical strength of the granules decreased.

The temperature dependence of the carbon disulfide (CS_2) hydrolysis in the obtained catalyst samples was studied. The results showed that when the CaO content is 1%, the CS_2 hydrolysis reaction becomes temperature-independent. In contrast, when the CaO content is less than 1%, the reaction efficiency is dependent on temperature and decreases with temperature reduction.

Figure 3. *Temperature dependence of the hydrolysis degree of the reaction carried out on clean and actively component-loaded catalyst samples*

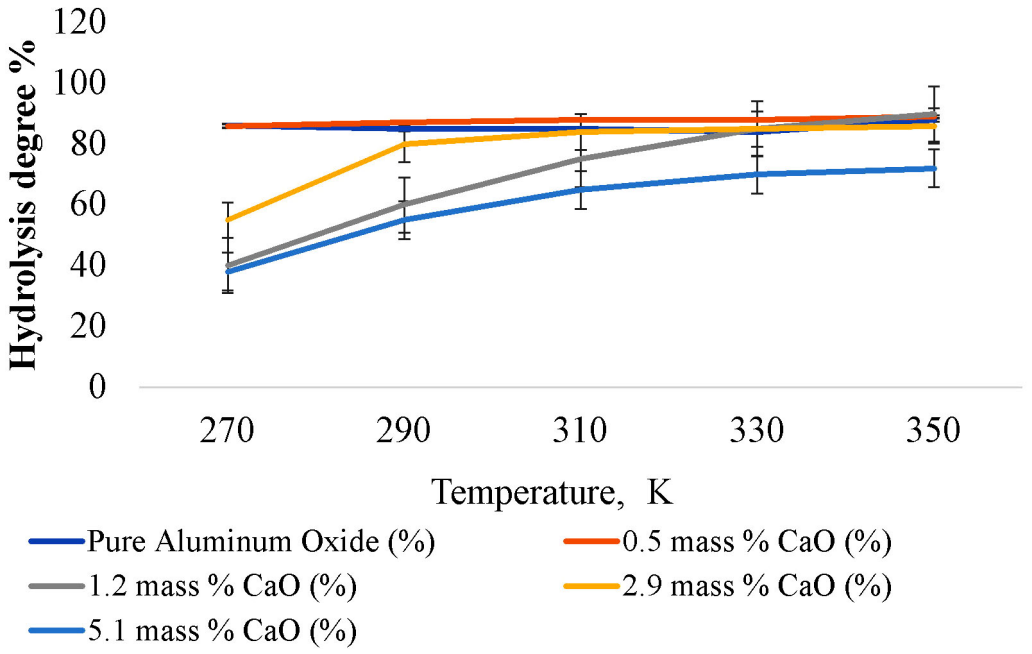

It was determined that the properties of the catalyst depend not only on its composition but also on its preparation method. it is evident that samples prepared by adding

a $Ca(OH)_2$ suspension have a higher surface area and a lower density compared to samples prepared by other methods. The temperature dependence of the hydrolysis degree of carbon disulfide was studied on catalyst samples prepared by different methods. The results showed that the samples prepared by adding a $Ca(OH)_2$ suspension exhibited a higher hydrolysis degree. This can be explained by the better mixing of raw materials when using the active component suspension.

Figure 4. *Temperature dependence of the hydrolysis degree of the reaction carried out on catalyst samples prepared by different methods*

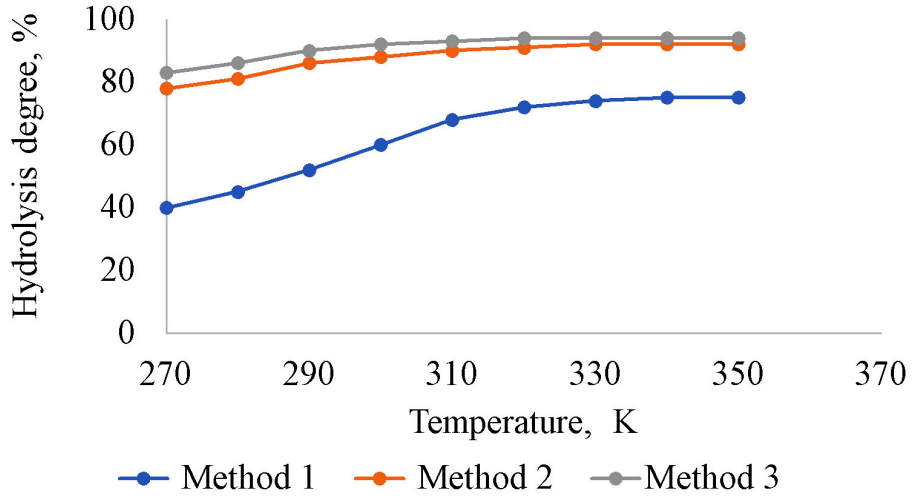

The addition of CaO to the catalyst composition resulted in an improvement in its properties. Specifically, the addition of CaO increased the catalyst's specific surface area and reduced its density. The overall hydrolysis reaction of CS_2 also improved. Based on the above analysis, it was determined that the optimal amount of the active component is 1%, because when the promoter amount exceeds 1%, the mechanical strength of the granules decreases, and other properties do not improve. Additionally, it was concluded that adding the active component to the catalyst in the form of a $Ca(OH)_2$ suspension is the most effective method.

Since a decrease in strength was observed when the CaO content exceeded 1%, it is considered appropriate to further study ways to enhance the strength of zeolite granules, especially under conditions with high amounts of active components, and to explore various metal oxides and their optimal quantities.

Conclusion

This study demonstrated that 10% NaOH increased microporosity from 0.05 to 0.18 cm^3/g and macroporosity from 0.26 to 0.31 cm^3/g; 8% cellulose reduced density from 0.712 g/cm^3 to 0.676 g/cm^3 and mechanical strength from 5.7 MPa to 4.2 MPa. An increase in CaO content from 0 to 4.8% enhanced specific surface area from 260 m^2/g to 265 m^2/g while decreasing density from 0.79 g/cm^3 to 0.62 g/cm^3. Adding $Ca(OH)_2$ suspension raised surface area to 295 m^2/g and density to 0.69 g/cm^3. The optimal composition was identified in catalysts containing 1% CaO (pore volume 0.37 cm^3/g) and 1% MgO (pore volume 0.41 cm^3/g). Thermal analysis confirmed boehmite formation at 250–300 °C and γ-Al_2O_3 formation at 500–700 °C.

References

Derouane, Eric G., et al. "Synthesis and characterization of ZSM-5 type zeolites I. physico-chemical properties of precursors and intermediates." Applied catalysis 1981. – 1.3–4. – P. 201–224.

Cruciani, Giuseppe. "Zeolites upon heating: Factors governing their thermal stability and structural changes". Journal of Physics and Chemistry of Solids. 2006. – 67.9–10. – P. 1973–1994.

Yusupov, F., & Khursandov, B. (2024). Working Out the Optimal Conditions For Obtaining Import-Substituting Polymer Sulfur For The Oil and Gas And Rubber Industry. Science and innovation, – 3(A10). – P. 167–170.

Temirov G. et al. Study of phosphogypsum conversion from Kyzylkum phosphorites with soda ash solution. 2023. IOP Conf. Ser. Earth Environ. Sci. 1142 012066. DOI: 10.1088/1755-1315/1142/1/012066

Khursandov, B. Sh., Kucharov, A. A. U., & Yusupov, F. M. (2022). Study of the properties of sulfur bitumen obtained on the basis of modified polymer sulfur. Universum: technical sciences, – (12–6 (105)). – P. 21–25.

Yusupov, F. M., Mamanazarov, M. M. U., Kucharov, A.A.U., & Saidobbozov, S. Sh. (2020). Properties of spherical granules based on aluminum oxide. Universum: chemistry and biology, – 3–1 (69). – P. 59–63.

Yusupov Farkhod, Azizjon Qurbonov, Kucharov Azizbek, Yodgorov Normahmad Results of Physicochemical Analysis of Composite Bitumen Mastications Developed For Protection of Gas Pipes From Corrosion // European Journal of Technical and Natural Sciences. 2025. – № 2. URL: https://ppublishing.org/archive/publication/1432-results-of-physicochemical-analysis-of-compos

Yusupov, F., Kucharov, A., Baymatova, G., Shukurullayev, B., & Yuldashev, R. (2023, August). Development and study of adsorption properties of a new sulfur polyvinyl chloride cation exchanger for water treatment. In *IOP Conference Series: Earth and Environmental Science,* – Vol. 1231. – No. 1. – P. 012027. IOP Publishing.

Kucharov, Azizbek, et al. "Scientific analysis of the development of new types of flotation reagents used in coal enrichment". EUREKA: Physics and Engineering 2025. – 2. –P. 32–39.

Xursandov, Bobomurod, et al. "Study of changes in the physical and mechanical properties of sulfur asphalt concrete mixture based on polymer sulfur." *AIP Conference Proceedings*. – Vol. 3045. – No. 1. AIP Publishing, 2024.

Piccione, Patrick M., et al. "Thermochemistry of pure-silica zeolites". The Journal of Physical Chemistry B 104.43. (2000). – P. 10001–10011.

Kucharov, Azizbek, et al. "Development of technology for water concentration of brown coal without use and use of red waste in this process as a raw material for colored glass in the glass industry". *E3S Web of Conferences*. – Vol. 264. EDP Sciences, 2021.

Ozin, Geoffrey A., Alex Kuperman, and Andreas Stein. "Advanced zeolite, materials science". Angewandte Chemie International Edition in English, 1989. – 28.3. – P. 359–376.

Qurbonov, Azizjon, Azizbek Kucharov, and Farxod Yusupov. "Development of a technology for obtaining an anti-corrosion coating for gas pipelines". *AIP Conference Proceedings*. – Vol. 3102. – No. 1. AIP Publishing, 2024.

submitted 09.04.2025;
accepted for publication 23.04.2025;
published 29.05.2025

Contact: sciuzb@mail.ru

The Austrian Journal of Technical and Natural Sciences, No 3–4
ISSN 2310-5607

PREMIER Publishing
ppublishing.org

DOI:10.29013/AJT-25-3.4-82-86

CLEANING OF THE HEAT EXCHANGER FROM NaX ZEOLITE

Jalolidinov Zukhridin [1], ***Yusupov Farkhod*** [1],
Rayimjonov Burhonjon [1], ***Yusupov Shaxzod*** [1]

[1] Institute of General and Inorganic Chemistry of the Academy of Sciences of Uzbekistan. Tashkent, Uzbekistan

Cite: *Jalolidinov Z., Yusupov F., Rayimjonov B., Yusupov Sh. (2025). Cleaning of the Heat Exchanger From Nax Zeolite. Austrian Journal of Technical and Natural Sciences 2025, No 3–4*. https://doi.org/10.29013/AJT-25-3.4-82-86

Abstract

In this study, the dissolution of NaX-type zeolite deposits from the surface of a heat exchanger was investigated using nitric acid solutions of varying concentrations. The main objective was to remove the zeolite layer without damaging the aluminum-based structure of the exchanger. Experimental results showed that a 42% nitric acid solution achieved complete dissolution of the zeolite within 30 minutes, without causing corrosion or damage to the metallic surface. In contrast, concentrations above 50% led to significant degradation of the aluminum surface. Post-dissolution analysis by Inductively Coupled Plasma Optical Emission Spectroscopy (ICPE-OES) confirmed the presence of aluminum (95.72%), sodium (2.44%), magnesium (1.17%), and calcium (0.67%) in the residual material, indicating effective removal of the zeolite phase and preservation of the heat exchanger material. These findings demonstrate that a controlled 42% nitric acid treatment provides an effective and safe method for restoring the operational capacity of aluminum-based heat exchangers fouled with NaX zeolite deposits.

Keywords: *Heat exchanger, NaX zeolite, nitric acid dissolution, ICPE-OES analysis, optimal acid concentration*

Introduction

Heat exchangers are an integral technological element of the oil and gas industry, enhancing the overall efficiency of production processes by effectively transferring energy from one medium to another. In particular, aluminum-based heat exchangers are widely used due to their lightweight nature, high thermal conductivity, and resistance to corrosion. However, the chemical sensitivity of aluminum—specifically its vulnerability to certain chemical reagents and mechanical impacts—requires careful handling during operation and maintenance.

Practical observations have shown that, over time, chemical residues accumulate on the surface of aluminum heat exchangers. This leads to a decrease in heat transfer efficiency, the formation of blockages that hinder the full circulation of gas flows, and, consequently, a significant reduction in the operational efficiency of the entire technological line.

Observations at the Muborak Gas Processing Plant have revealed that during the

gas drying process, NaX-type zeolites degrade into fine powder and mix with the gas flow. In the subsequent stages, this powder accumulates on the internal surfaces of aluminum heat exchangers, negatively impacting their performance. The primary cause of the accumulation of solid particles in the heat exchangers is associated with the low chemical stability of NaX zeolites and the aggressive effects of acids, aldehydes, and ketones present in the gas on the zeolites.

Zeolites are natural and synthetic mineral compounds characterized by a high degree of porosity and a crystalline structure. They are widely used in the chemical and gas industries as adsorbents, catalysts, and ion-exchange materials. Their primary structure consists of $[SiO_4]^{4-}$ and $[AlO_4]^{5-}$ tetrahedra, which are interconnected through oxygen atoms to form a complex aluminosilicate framework. Within this framework, pores and channels are designed for ion exchange and molecular adsorption. The internal stability of zeolites is maintained by cations such as Na^+, K^+, Ca^{2+}, and water molecules.

The raw gas supplied to the Muborak Gas Processing Plant primarily consists of methane (92.312%), along with additional components such as ethane, propane, butane, pentane, and other heavier hydrocarbons, as well as inert components (nitrogen, carbon dioxide) and reactive compounds (water, aldehydes, acids, ketones).

These components, particularly acids and carbonyl compounds, weaken the chemical structure of zeolites by degrading their molecular framework, leading to the loss of hardness in the NaX zeolite. As a result, the degraded zeolite particles move in powder form through the heat exchangers and accumulate on aluminum surfaces, causing blockages.

This article scientifically analyzes the causes of NaX zeolite degradation, the mechanism of clogging in aluminum heat exchanger equipment, and technological approaches to prevent or mitigate these problems.

Material and methods

In this study, a SHIMADZU ICPE-9800 model Inductively Coupled Plasma Optical Emission Spectroscopy (ICP-OES) instrument was used to determine the inorganic elements in the samples. This method allows the simultaneous and highly accurate detection of multiple elements within a material. ICP technology operates based on argon gas: a high-frequency radiofrequency (RF) field ionizes the argon, creating a high-temperature plasma reaching approximately 10,000 K.

The sample is introduced into the plasma in solution form using a specialized nebulizer. At such high temperatures, atoms and ions within the sample become excited and, upon returning to their ground state, emit light at characteristic wavelengths. Since each element has a unique emission spectrum, the qualitative and quantitative composition of the elements in the sample can be determined by measuring the intensity of the emitted radiation.

This method is particularly sensitive for detecting the concentrations of aluminum, sodium, silicon, calcium, iron, and other metal ions. Additionally, the ICP-OES technique is distinguished by its speed, accuracy, wide dynamic range, and low background noise.

X-ray Diffraction (XRD) Analysis

To assess the crystallinity, phase composition, and morphological changes of the zeolite powders, X-ray Diffraction (XRD) analysis was employed. This method is a universal physical-analytical technique used to determine the internal crystalline structure of materials. X-rays are a part of the electromagnetic spectrum with short wavelengths (0.01–10 nm) and high energy, and they are diffracted by the atomic arrangements in crystalline materials.

The diffraction patterns are interpreted according to Bragg's Law ($n\lambda = 2d \sin\theta$), where λ is the X-ray wavelength, d is the interplanar spacing, θ is the diffraction angle, and n is an integer. Each phase has distinct diffraction peaks, which can be identified on the XRD pattern (plotted against the 2θ angle). The intensity and position of these peaks allow for the determination of the phase composition, degree of crystallinity, and disorder within the zeolite sample.

Through XRD analysis, valuable information was obtained regarding the extent of degradation of NaX zeolite powders, the transition from crystalline to amorphous states, and the transformation into other phases (such as amorphous aluminosilicates or weakened skeletal structures).

Result and discussion

Initially, a sample was taken from the heat exchanger, and XRD analysis was performed. The results are presented in Table 1.

Table 1. *XDR peak data table*

Peak no.	2 Theta (°)	d-spacing (Å)	Relative Intensity (I/I1 %)	FWHM (°)	Intensity (counts)	Integrated Intensity
1	17.8684	4.96007	5.0	0.7142	99.0	2445.0
2	20.7108	4.28531	3.0	1.6222	57.0	1649.0
3	21.1097	4.20523	5.0	0.0	91.0	0.0
4	21.9077	4.05382	5.0	0.0	102.0	0.0
5	23.0051	3.86287	4.0	2.1834	79.0	4360.0
6	38.1852	2.35497	8.0	0.7876	150.0	3041.0
7	39.2644	2.29269	99.0	0.5441	1889.0	21349.0
8	42.3197	2.13397	15.0	0.5431	289.0	3539.0
9	78.5834	1.21639	56.0	0.4755	1069.0	11122.0
10	45.4323	1.99474	100.0	0.5608	1913.0	23080.0

According to table 1, Based on the XRD analysis results, peaks numbered 10, 7, and 29 were identified as having the highest diffraction intensities. Peak 10, located at 2θ = = 45.4323°, exhibited maximum intensity (100%) with a d-spacing of 1.99474 Å; this peak corresponds to the (111) plane of metallic aluminum. Peak 7 was detected at 2θ = = 39.2644°, showing 99% intensity and a d-spacing of 2.29269 Å, corresponding to the NaX-type zeolite phase accumulated in the heat exchanger. Peak 29 appeared at 2θ = = 78.5834°, recorded with 56% intensity and a d-spacing of 1.21639 Å; this peak corresponds to the higher-order crystallographic planes of the high-angle aluminum phase. Thus, the XRD results confirmed the presence of metallic aluminum and NaX zeolite as the main phases in the heat exchanger.

In the next stage of the study, to dissolve the zeolites accumulated in the heat exchanger, different concentrations of nitric acid ranging from 10% to 50% were used, and the results are presented in Figure 1.

Figure 1. *The Relationship Between Nitric Acid Concentration and the Dissolution Efficiency of NaX Zeolite*

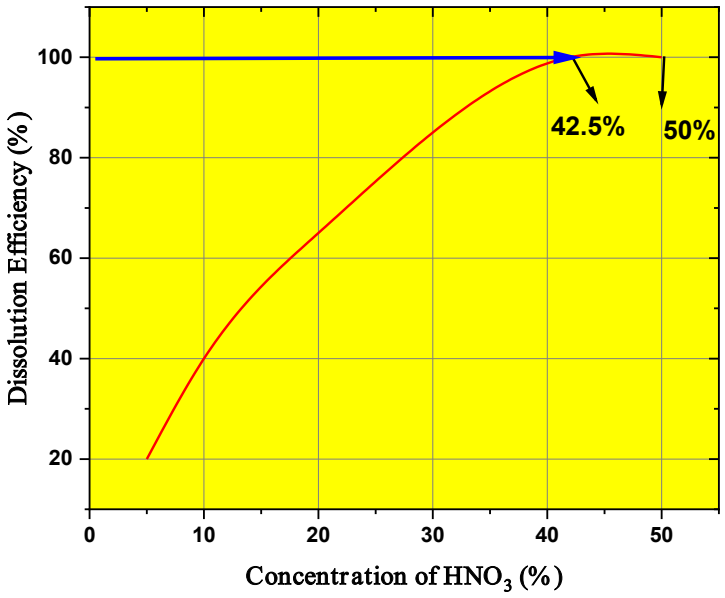

According to Figure 1, when analyzing the graph showing the relationship between nitric acid concentration and dissolution efficiency, it was observed that the dissolution efficiency increased steadily with the rise in acid concentration. At a concentration of 42.5%, the dissolution efficiency reached its maximum level (100%), enabling the complete dissolution of the zeolite layer without causing any damage to the metallic surface of the equipment.

However, although the dissolution efficiency remained at 50% concentration, damage to the metallic surface was detected as indicated by the decline in the blue line on the graph. Based on this observation, it can be concluded that the optimal nitric acid concentration for the effective and safe cleaning of the heat exchanger is around 42–43%. Higher concentrations may negatively affect the metallic components of the equipment.

After determining the optimal concentrations of the nitric acid solution, ICPE analysis of the heat exchanger was performed. The results are presented in Table 2.

Table 2. *ICPE-OES Analysis Results of Heat Exchanger Surface after NaX Zeolite Dissolution*

Element	Wavelength (nm)	Concentration (%)	Comment
Na	589.592	2.44	Main ion from NaX seolite
Mg	285.213	1.17	Detected after dissolution
Ca	422.673	0.67	Minor contamination
Al	396.153	95.72	Main component of heat exchanger

The ICPE analysis results obtained from the NaX zeolite solution showed that the primary element detected from the heat exchanger was aluminum (Al), with a concentration of 95.72%, confirming that aluminum is the dominant material of the equipment. Sodium (Na) was found at a concentration of 2.44%, resulting from the dissolution of NaX zeolite in nitric acid. Magnesium (Mg) and calcium (Ca) were detected at concentrations of 1.17% and 0.67%, respectively, likely originating either from the zeolite structure or from minor impurities introduced during the dissolution process. Overall, the analysis results indicate that after the dissolution process, the material primarily consists of aluminum, while the main ions from the NaX zeolite have been transferred into the solution.

Conclusion

In this study, different concentrations of nitric acid were tested to dissolve the NaX-type zeolite layer hardened inside the heat exchanger without causing damage to the equipment. The dissolution experiments revealed that a 42% nitric acid solution provides optimal conditions for completely dissolving the zeolite layer while preserving the metallic surface of the heat exchanger. The dissolution efficiency and the extent of impact on the metal surface were evaluated based on concentration and time parameters. At concentrations higher than 50%, signs of corrosion were observed on the aluminum surface.

After the dissolution process, samples taken from the device surface were analyzed using ICPE-OES. According to the analysis results, aluminum (95.72%), sodium (2.44%), magnesium (1.17%), and calcium (0.67%) were identified, confirming that the primary metallic material—aluminum—was largely preserved, while the structural ions of the zeolite had migrated into the solution. The XRD and ICPE results, along with the evaluation of the dissolution conditions, enabled the determination of an optimal dissolution technology.

Overall, the study recommends the use of a 42% nitric acid solution to dissolve NaX zeolite layers without damaging the heat exchanger. This technological approach plays an important role in extending the operational life and reducing the need for maintenance of such equipment.

References

Baerlocher, C., Mc Cusker, L. B., & Olson, D. H. (2007). *Atlas of Zeolite Framework Types* (6th ed.). Elsevier. URL: https://doi.org/10.1016/B978-044453064-6/50001-1

Geankoplis, C. J. (2003). *Transport Processes and Separation Process Principles* (4th ed.). Prentice Hall.

Henley, E. J., & Seader, J. D. (1981). *Equilibrium-Stage Separation Operations in Chemical Engineering*. John Wiley & Sons.

Skoog, D. A., Holler, F. J., & Crouch, S. R. (2017). *Principles of Instrumental Analysis* (7th ed.). Cengage Learning.

Wang, S., & Peng, Y. (2010). Natural zeolites as effective adsorbents in water and wastewater treatment. *Chemical Engineering Journal*, – 156(1). – P. 11–24. URL: https://doi.org/10.1016/j.cej.2009.10.029

Figueiredo, F. M., & Labrincha, J. A. (2001). Zeolites and their applications: A brief review. *Materials Research*, – 4(1). – P. 35–42. URL: https://doi.org/10.1590/S1516-14392001000100007

Eslamian, M. (2017). Chemical cleaning of heat exchangers. In M. Eslamian (Ed.), *Handbook of Cleaning for Semiconductor Manufacturing,* – P. 187–205. CRC Press.

submitted 15.04.2025;
accepted for publication 29.04.2025;
published 29.05.2025

Contact: sciuzb@mail.ru

The Austrian Journal of Technical and Natural Sciences, No 3–4
ISSN 2310-5607

PREMIER Publishing
ppublishing.org

DOI:10.29013/AJT-25-3.4-87-90

OXIDATION OF POLYPRENOLS IN VITIS VINIFERA L. LEAVES

Zokirova Umida Tolipovna [1], Mamatkulova Nodira Maxsumovna [1], Khidyrova Nazira Kudratovna [1], Saitkulov Foziljon Ergashevich [2]

[1] Institute of the Chemistry of Plant Substances, Academy of Sciences of the Republic of Uzbekistan, Tashkent, Uzbekistan

[2] Tashkent state agrarian university, Tashkent, Uzbekistan

Cite: *Zokirova U.T., Mamatkulova N.M., Khidyrova N.K., Saitkulov F.E. (2025). Oxidation of Polyprenols in Vitis Vinifera L. Leaves. Austrian Journal of Technical and Natural Sciences 2025, No 3–4.* https://doi.org/10.29013/AJT-25-3.4-87-90

Abstract

The study presents data on the oxidation reaction of polyprenols (PP) in grape leaves (*Vitis vinifera* L.) containing isoprene units with n = 10–12 in the following ratio: n = 10 (8.3%), n = = 11 (42.4%), and n = 12 (49.3%). The oxidation process was carried out under conventional conditions using a solvent and under microwave irradiation (MWI) in the absence of a solvent. The influence of MWI on the oxidation efficiency and selectivity of the process was analyzed. The obtained results demonstrate the potential of MWI as an effective and environmentally friendly method for the oxidation of polyprenols in grape leaves.

Keywords: *Vitis vinifera L., leaves, polyprenols, oxidation, microwave irradiation, isoprene units, solvent-free, selective oxidation, environmentally friendly, reaction efficiency, green chemistry, oxidative process, molecular transformation, natural compounds, alternative methods, bioactive substances, structural modification, sustainable synthesis*

Introduction

It is known that polyprenols in plants occur as polyprenyl homologs (Kukina T. P., Bayandina I. I., Pokrovsky A. N., 2007). Unlike most plants, the polyprenols in *Vitis vinifera* L. leaves contain a lower number of polyprenyl homologs (3–4), with the content of prenols with n = 13 being minimal. Column chromatography primarily isolates polyprenol fractions with n = 10–12, yielding more than 2.0% of the air-dried mass, making them suitable for modification. Additionally, Uzbekistan has sufficient raw material reserves of *Vitis vinifera* L. (Temurov Shukur. 2005). Therefore, studying the modification of grape leaf polyprenols is of great interest.

The chemical transformations of polyprenols are of interest due to their biological role in living organisms. Polyprenols are natural low-molecular-weight bioregulators that facilitate the transport of hydrophilic particles across cell membranes during the biosynthesis of polysaccharides, glycoproteins, and other carbohydrate-containing polymers (Lamani, E. et. al. 2006). The presence of an isoprenoid substituent in some aromatic

molecules enhances their biological activity (Chukicheva I.Yu., Fedorova I. V., Koroleva A. A., Kuchin A. V., 2018).

Plant-derived polyprenols, as promising synthons for pharmaceutical development, improve interactions with cell membranes, allowing for the design of targeted drugs (Koroleva A. A., Karmanova L. P., Belykh D. V., Kuchin A. V., 2006). The chemical properties of polyprenols must be considered when studying their transformations. As partially saturated alkyl terpenoid alcohols ($R_2C=CH-CH_2-X$, where X is a functional group), polyprenols have C–X bond dissociation energies 50–105 kJ/mol lower than their saturated analogs, making them highly chemically reactive.

For modification, we used polyprenols from *Vitis vinifera* L. leaves cultivated in the Surkhandarya region, containing isoprene units with n = 10–12 and a purity of 95–97% based on HPLC data, in the following ratios: n = 10 (8.3%), n = 11 (42.4%), n = 12 (49.3%) (Zokirova U. T., Khidyrova N. K., Khodjaniyazov H. U., Shakhidoyatov Kh. M., 2013).

Microwave irradiation (MWI) has been used to accelerate chemical reactions since 1986 (Gedye R., Smith F., Westaway K., Ali H., Baldisera L., Laberge L., & Rousell, J., 1986; Berdonosov S. S., 2001). Over time, its application in organic synthesis has expanded significantly (Berdonosov S. S., Berdonosova D. G., Znamenskaya I. V. 2000; Romanova N. N., Kudan P. V., Gravis A. G., Bundel Yu. G., 2000). Therefore, in this study, oxidation reactions of grape leaf polyprenols were conducted under conventional conditions with a solvent and under MWI without a solvent to compare their efficiency and selectivity.

Materials and Methods

Polyprenols (1) were extracted from the leaves of *Vitis vinifera* L. growing in the Surkhandarya region using a previously described method (Zokirova U. T., Khidyrova N. K., Khodjaniyazov H. U., Shakhidoyatov Kh. M., 2013).

Determination of the Homologous Composition of Polyprenols. The fraction analysis was performed using an Agilent Technologies-1100 chromatograph on a 0.46 × × 150 mm Eclipse XDB-C-18 column. The elution phase was gradient: 0–20 min 0–75% B; 20–25 min 75–100% B; 25–30 min 100–0% B, with a flow rate of 0.75 mL/min, and total analysis time of 30 min. System A – a mixture of methanol-water 9:1 (v/v), B – methanol-hexane-isopropanol 2:1:1. The chromatographic profile was recorded at 210 nm. The quantity of prenols was determined relative to the chromatogram of a standard sample by comparing peak areas using Agilent Chemstation software. Polyprenols from *Rhus coraria* leaves were used as the standard reference.

Oxidation of Polyprenols was carried out using a freshly prepared solution of manganese dioxide in hexane, resulting in the formation of a nucleophilic reaction center at the carbonyl carbon. The reaction was initially conducted at room temperature with stirring for 0.5 hours, but no oxidation occurred. The reaction was then performed under reflux, with the reaction progress monitored hourly using TLC. The obtained data are presented in Figure 1. As a result of the reaction, polyprenal (2) was formed.

Figure 1. *Effect of Time on the Progress of Polyprenol Oxidation*

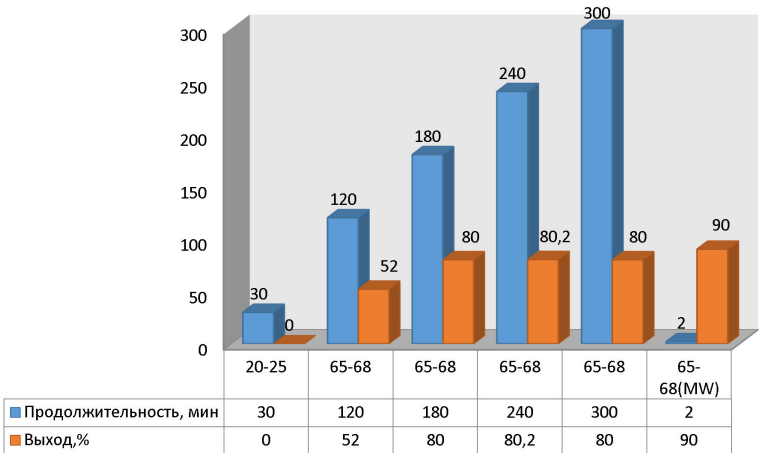

Maximum yield of polyprenal under normal conditions was 80.0%. Increasing the duration to 5 hours did not yield positive results. To accelerate the oxidation process and increase the product yield, the reaction was conducted under microwave irradiation conditions. Polyprenol oxidation under microwave irradiation occurs within 2 minutes, increasing the polyprenal yield to 90%. Thus, the use of microwave irradiation accelerates the oxidation process by 180 times and increases the polyprenal yield by 9% (Scheme 1):

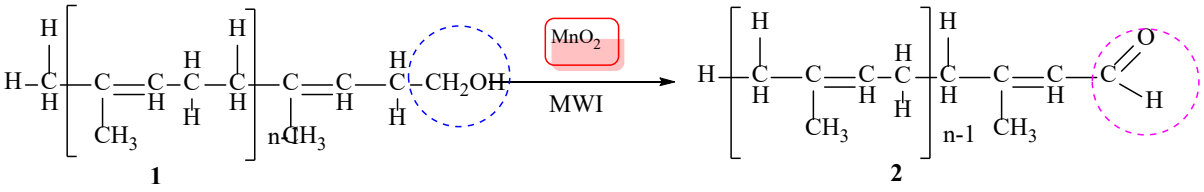

Scheme 1. Polyprenol Oxidation Reaction

The structure of polyprenal (2) was confirmed using spectral analysis methods. The appearance of an absorption band at 1643 cm^{-1} in the IR spectrum, corresponding to the stretching vibrations of the C=O bond in the aldehyde group, and the disappearance of the hydroxyl group absorption band at 3300 cm^{-1} confirm the formation of polyprenal aldehyde.

In the ^1H NMR spectrum, signals at 1.63, 1.70, 1.98 ppm (s, CH_3), 2.05 ppm (m, CH_2), a broad signal at 5.14 ppm (s, C=CH), 6.04 ppm (s, H-2), and 9.80 ppm (s, CHO) further confirm the formation of polyprenal.

For the synthesis of polyprenyl acid (3), polyprenyl aldehyde (PPA) was oxidized using silver oxide (molar ratio PPA: $AgNO_3$ = =1:2, 1:3, and 1:4). The reaction was conducted by heating at 150 °C for 1 hour, yielding polyprenyl acid at 50–52% (Scheme 2):

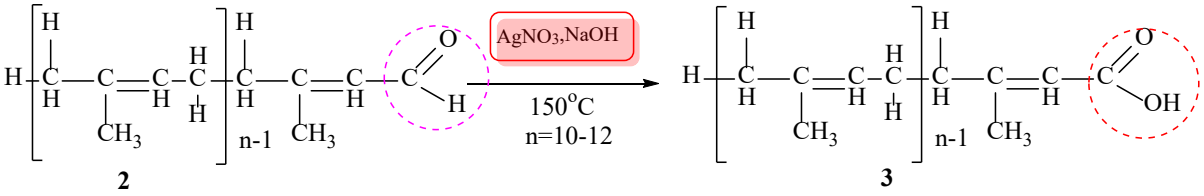

Scheme 2. Synthesis of Polyprenyl Acid

The appearance of an absorption band at 1665 cm^{-1} in the IR spectrum, corresponding to the stretching vibrations of the C=O bond, and a band at 3327 cm^{-1} for the hydroxyl group confirm the formation of polyprenyl acid (PPA).

Experimental Part

Synthesis of Polyprenal under Normal Conditions (2). Polyprenol 1 (0.40 g, 0.522 mmol) was dissolved in 10 mL of hexane, and 1.2 g of active manganese dioxide (MnO_2) was added. The reaction mixture was stirred on a magnetic stirrer for 3 hours at a temperature of 75–78 °C, then cooled to room temperature, filtered, and the precipitate was washed three times with hexane and dried over anhydrous sodium sulfate. The solvent was then removed using a rotary evaporator. PPA was purified on a 60 × 1.8 cm silica gel column (100/160 mesh). A mobile phase of hexane/diethyl ether in the ratios 100:1, 100:2, and 100:5 was used. For TLC, the systems hexane/diethyl ether = 3/1 (Rf = 0.65) and benzene–EtOAc 24:1 (R_f = 0.67) were used. Polyprenal 2 was obtained as a light yellow oil (0.32 g, 80% yield).

Synthesis of Polyprenal (2) under Microwave Irradiation (MWI). To a solution of polyprenol 1 (0.10 g) in 1 ml of hexane, 0.25 g of active MnO_2 was added. The mixture was stirred for 2 minutes at 450 W in MWI. Further processing was carried out according to the general procedure. As a result, 0.089 g of yellow oil was obtained, with a polyprenal yield of 89%.

IR Spectrum of Polyprenal (KBr, νmax, cm^{-1}): 2738–3040, 1680 (C=O), 1633, 1450, 1390, 1100, 1041, 853.

^{1}H NMR (300 MHz, $CDCl_3$, δ, ppm, J/Hz): 1.63, 1.70, 1.98 (s, CH_3), 2.05 (m, CH_2), 5.14 (br s, C=CH), 6.04 (s, H-2), and 9.80 (s, CHO).

Synthesis of Polyprenyl Acid (3). To a solution of polyprenylaldehyde (PPA) (0.25 g, 0.326 mmol) in 2.5 mL of methanol, 0.12 g of silver nitrate (0.706 mmol) in 1 ml of water and 0.1 g of sodium hydroxide dissolved in 2 mL of water were added at molar ratios PPA: $AgNO_3$ = 1:2, 1:3, and 1:4. The reaction was conducted at 150 °C for 1 hour. The yield of polyprenyl acid was 0.123 g (50%). R_f = = 0.52 (PE-DE 3:1 system). **IR Spectrum of Polyprenyl Acid** (KBr, ν_{max}, cm^{-1}): 3327–3600 (broad, OH), 1665 (C=O), 1448, 1376, 1086, 999, 837.

Conclusion

Thus, the study of the oxidation reaction of polyprenols (PP) from grape leaves (*Vitis vinifera* L.) under conventional conditions using a solvent and under microwave irradiation (MWI) without a solvent demonstrated that oxidation under MWI significantly accelerates the process by 180 times and increases the yield of polyprenal by 9%. This method provides a more efficient and rapid approach to obtaining polyprenal, making it a promising alternative for industrial and laboratory applications. The use of MWI enhances reaction efficiency, reducing processing time and improving overall yield.

References

Kukina T. P., Bayandina I. I., Pokrovsky A. N. Non-polar components of St. John's wort extracts // Chemistry of plant raw materials. – Barnaul, Russia. 2007. No. 3. – P. 39–45. (In Russian)

Temurov Shukur. Uzumchilik. Darslik. – T.: Ozbekiston Milliy encyclopediasi davlat ilmiy nashriyoti 2005. – 249 b. (In Russian)

Lamani, E. etal. (2006). Structural studies and mechanism of Saccharomyces cerevisiae dolichyl-phosphate-mannose synthase: insights into the initial step of synthesis of dolichylphosphate-linked oligosaccharide chains in membranes of endoplasmic reticulum // Glycobiology. Oxford, Great Britain. 2006. – V. 16. –P. 666–678.

Chukicheva I. Yu., Fedorova I. V., Koroleva A. A., Kuchin A. V. Алкилирование фенола и гидрохинона пренолом в присутствии органо-алюминовых катализаторов // Chem. Nat. Compd. Springer, USA. 2018. – V. 54. – 1 p.

Koroleva A. A., Karmanova L. P., Belykh D. V., Kuchin A. V. Synthesis of prenylated derivatives of chlorin e6 // News of Universities. Chemistry and Chemical Technology. Ivanovo, Russia. 2006. – Vol. 49. – Issue 6. – P. 73–76. (In Russian)

Zokirova U. T., Khidyrova N. K., Khodjaniyazov H. U., Shakhidoyatov Kh. M. Acylation of Grape leaves Polyprenols. American Chemical Science Journal, New York, USA. 2013. – V. 3(2). – P. 124–136.

Gedye R., Smith F., Westaway K., Ali H., Baldisera L., Laberge L., & Rousell, J. The use of microwave ovens for rapid organic synthesis // Tetrahedron Letters. Tetrah. Lett. Elsevier BV, Niderlands. 1986. – V. 27. – P. 279–282.

Berdonosov S. S. Microwave Chemistry // Soros Educational Journal. – Moscow, Russia. 2001. – V. 7. – No. 1. – P. 31–36. (In Russian)

Berdonosov S. S., Berdonosova D. G., Znamenskaya I. V. Microwave Radiation in Chemical Practice // Chem. Technology. Ivanovo. Russia. 2000. – No. 3. – P. 2–8. (In Russian)

Romanova N. N., Kudan P. V., Gravis A. G., Bundel Yu. G. Application of Microwave Activation in the Chemistry of Heterocyclic Compounds // Chemistry of Heterocyclic Compounds. Riga, Latvia. 2000. – No. 10. – P. 1308–1320. (review). (In Russian)

submitted 04.03.2025;
accepted for publication 20.03.2025;
published 29.05.2025

Contact: saitkulovfoziljon@gmail.com

The Austrian Journal of Technical and Natural Sciences, No 3–4
ISSN 2310-5607

PREMIER Publishing
ppublishing.org

DOI:10.29013/AJT-25-3.4-91-94

REACTION OF 6-AMINO-2-METHYLBENZOPYRIMIDIN-4-ONE WITH ARYL SULFACHLORIDES

Zulpanov Fazliddin Abduxakimovich [1], Elmuradov Burkhon Juraevich [1], Kholikov Akbar Oybek ugli [2], Akhmedova Malika Alijon kizi [2], Arzanov Ravshan Xurramovich [3]

[1] Akad. S. Yu. Yunusov Institute of the Chemistry of Plant Substances, Academy of the Republic of Uzbekistan, Tashkent, Uzbekistan

[2] Branch of Russian Mendeleev University of Chemical Technology in Tashkent Faculty of Chemical Technology

[3] School № 3, Samarkand District, Uzbekistan

Cite: *Zulpanov F.A., Elmuradov B.J., Kholikov A.O., Akhmedova M.A., Arzanov R.X. (2025). Reaction of 6-Amino-2-Methylbenzopyrimidin-4-One With Aryl Sulfachlorides. Austrian Journal of Technical and Natural Sciences 2025, No 3–4.* https://doi.org/10.29013/AJT-25-3.4-91-94

Abstract

As a result of studying the synthesis and biological activity of condensed heterocyclic compounds, new drugs have been developed, including derivatives of 6-aminobenzopyrimidin-4-one, and their bioactive derivatives have been identified. The development of new drugs based on them is relevant.

Keywords: *o-aminobenzoic acid, thyoacetamide, cyclization, nitration, reducation, 2-alkhylbenzopyrimidin-4-one, 6-amino-2-alkhylbenzopyrimidin-4-one, IR, ^{1}H and ^{13}C NMR*

Introduction

In recent years, most representatives of drugs created in various fields of agriculture and modern medicine are derivatives of compounds containing a condensed pyrimidine ring. In recent years, as a result of the study of synthesis and biological activity of condensed heterocyclic compounds, new drugs have been developed (Pawan K. Pawan K., Premnath D., Muhammad T., Mazlee S., Yaman M., Nurul S., Muhammad S. et al., 2019). Among them we can point out the majority of quinazoline derivatives in the second and third states of the condensed pyrimidine ring. Compounds based on benzopyrimidin are widely used against viruses, microbes, fungi, colds and cancer (Xiaoqing Wu, Mingdong Li, Yang Qu, Wenhua Tang, Youguang Zheng, Jiqin Lian, Min Ji, Liang Xu., 2010), and as stimulants for plants (Raffaella Sordella, Daphne W. Bell, Daniel A. Haber, Jeffrey Settleman. 2004). Anticancer drugs prepared from compounds of the benzopyrimidin family have shown a very low level of toxicity (Muhammad T., Mazlee S., Yaman M., Nurul S., Muhammad S. et al., 2019). In this

regard, especially the N-6 state electrophilic substitution reactions (Zulpanov F. A., Elmuradov B.J, Saitkulov F. E., Arzanov R. X., 2024), i.e. synthesis of new types of derivatives with various halogen compounds of alkyl halides, and with the change of their functional group, it is possible to find new types of fundamental systematic laws and among them, bioactive compounds. Avast number-of quinazoline derivatives have been synthesized to provide synthetic drugs and to design more effective medicines. There are a number of reviews and monographs on quinazoline and quinazoline alkaloids. Recently, we have documented a formal collection of significant developments (2013) on the synthetic methods through which these heterocycles (quinazolines and quinazolinones) could be accessed, along with diverse biological profile which they possess. Some other groups also published independently the synthesis of quinazolinones and bioactive quinazolines, respectively. There has been no dicussion on the mechanistic aspects of key transformations. So, incorollary of these fascinating findings as well as part of a programme aimed at discovering heterocyclic structures with various pharmacological properties, in general, and in continuation of our previous work on these skeletons, we report here the very recent developments (2014) in the environmentally benign, green, and efficient synthetic protocols (in most cases) to access quinazoline and quinazolinone derivatives from cheap and readily available commercial feedstocks. Quinazolinone and their derivatives are also building block for approximately 150 naturally occurring alkaloids isolated from a numberoffamilies of theplant kingdom, frommicroorganisms and animals. Some of the compounds incorporating quinazolinone motif like raltitrexed and thymitaq possess antitumor activities (Zulpanov F. A., Elmuradov B.J, Saitkulov F. E., Arzanov R. X. 2024; Sordella R., Bell D. W., Haber D. A. and Settleman J. 2004; Deng X. Q., Zheng Y., Yuan Y. P., Quan Z. S., Guan L. P.; 2012; Petrov K. G., Zhang Y. M., Carter M., Cockerill G. S., Dickerson S., Gauthier C. A., Guo Y., Mook R. A. Jr, Rusnak D. W., Walker A. L., Wood E. R., Lackey K. E., 2006; Imtiaz Khana, Aliya Ibrar, Waqas Ahmed, Aamer Saeed. 2014). Therefore bicyclic benzopyrimidin-4-ones are of great practical and theoretical interest.

Methods and results

Results and discussion

An efficient and convenient method for the synthesis of 2- methylbenzopyrimidine-4-one in high yields was developed by the reaction of o-aminobenzoic acid with thioacetamide.

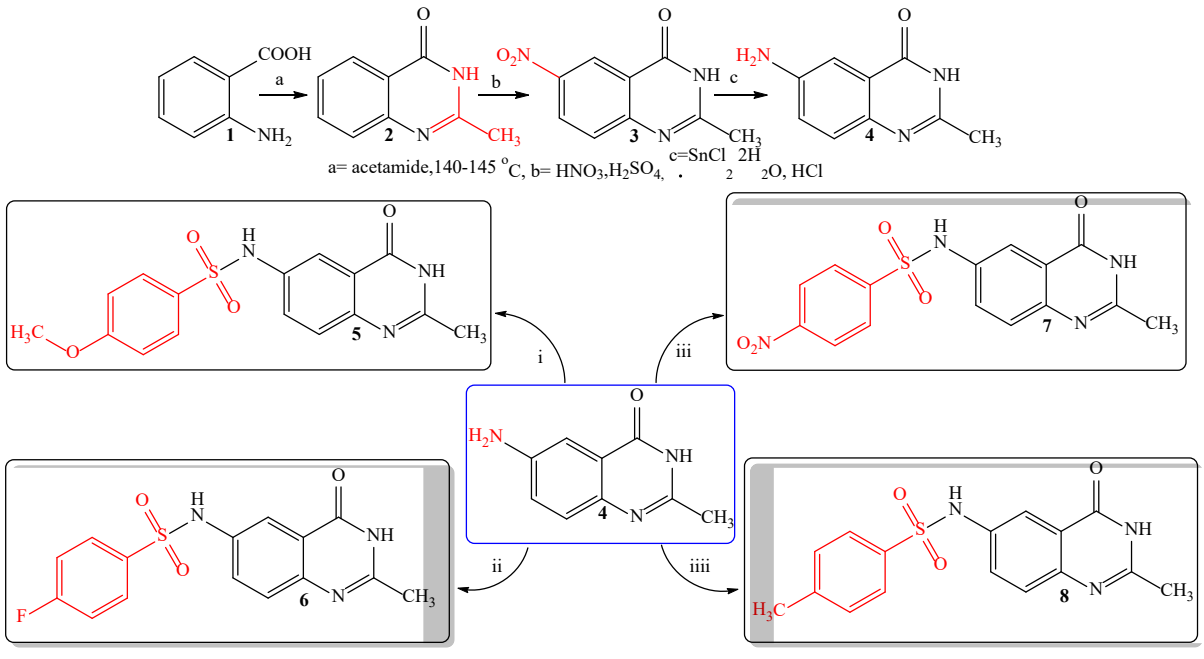

Under the influence of a nitrating mixture of the synthesized substance, 2-methyl-6-nitrobenzopyrimidine-4-one was synthesized in a nitrolab with a yield of 95%. The resulting nitroblock was reduced with tin (II) chloride dihydrate ($SnCl_2 \cdot 2H_2O$) and HCl to obtain the corresponding 6-amino-2- methylbenzopyrimidine-4-one (1) with a yield of 65%. Then, 6-amino-2-methyl quinazolin-4-one (1) was synthesized in the presence of aryl sulfochlorides in the presence of DMF solvent and K_2CO_3. The structure of the obtained substances was studied using physical research methods: IR, 1H and 13C NMR spectra, and their in-depth analysis fully proved that they correspond to the proposed structure.

Experimental part

Synthesis of 2-methylbenzopyrimidin-4-one (1). 1.37 g (0.01 mole) of o-aminobenzoic acid and 1.52 g (0.02 mole) of thioacetamide were added to a 100-ml round bottom flask and heated for 2-3 hours in an oil bath connected with a reflux condenser at 140-145°C, first it boils and then a solid is formed. The obtained solid is thoroughly rubbed in a mortar, 40 ml of 5% aqueous NaOH solution is added, completely dissolved and brought to neutral (pH-7) medium by a weak solution of HCl. The precipitate is filtered and washed with distilled water. The substance is recrystallized from ethyl alcohol (C_2H_5OH) and as a yield 1.56 g (98%) of substance (**1**), melting point 238–140 °C, R_f = 0.73 (system: chloroform:methanol - 10:1) is obtained. IR spectrum (ν, cm^{-1}): :3171 cm^{-1} (C-N), 2979 cm^{-1} (C-H), 2990 cm^{-1} (C-H_2), 1669 cm^{-1} (C=O), 1609 cm^{-1} (C=N). ^{1}H NMR (400 MHz, DMSO-d6+CCl_4, ppm, δ, J/Hz): 8.06 (1H, ddd, J=7.9, 1.6, 0.6, H-5), 7.65 (1H, m, H-7), 7.49 (1H, m, H-8), 7.34 (1H, m, H-6), 5.72 (1H, broad s, NH), 2.36 (3H, s, H-9). ^{13}C NMR spectrum (100 MHz, DMSO-d6+CCl_4, ppm, δ): 154.24 (C-2), 162.24 (C-4), 120.74 (C-4a), 126.24 (C-5), 124.80 (C-6), 133.10 (C-7), 125.52 (C-8), 149.12 (C-8a), 21.45 (C-9).

Synthesis of 4-methoxy-N-(2-methyl-4-oxo-3,4-dihydrobenzopyrimidine-6-yl)benzenesulfonamide (4). Heteroaromatic compounds (4) (1.752 g, 0.01 mole) were dissolved in anhydrous acetone (5 ml) with dry pyridine (1.5 ml) and 4-methoxybenzenesulfonyl chloride (2.273 g, 0.011 mole) was added at room temperature. The reaction was heated to 50 °C for 24 hours. 4-methoxy-N-(2-methyl-4-oxo-3,4-dihydrobenzopyrimidine-6-yl)benzenesulfonamide **(4)** precipitated as a crystalline solid after suction filtration. The crude product was recrystallized from dimethylformamide (DMFA). The substance was synthesized with a high yield of 86%. R_f = 0.73.

Synthesis of 4-fluoro-N-(2-methyl-4-oxo-3,4-dihydrobenzopyrimidine-6-yl)benzenesulfonamide). Heteroaromatic compounds (4) (1.752 g, 0.01 mole) were dissolved in anhydrous acetone (5 ml) with dry pyridine (1.5 ml) and 4-methoxybenzenesulfonyl chloride (2.273 g, 0.011 mole) was added at room temperature. The reaction was heated to 50 °C for 24 hours. 4-methoxy -N-(2-methyl-4-oxo-3,4-dihydrobenzopyrimidine-6-yl)benzenesulfonamide **(4)** precipitated as a crystalline solid after suction filtration. The crude product was recrystallized from dimethylformamide (DMFA). The substance was synthesized with a high yield of 86%. R_f = 0.73.

Synthesis of N-(2-methyl-4-oxo-3, 4-dihydrobenzopyrimidine-6-yl)-4-nitrobenzenesulfonamide). Heteroaromatic compounds (4) (1.752 g, 0.01 mole) were dissolved in anhydrous acetone (5 ml) with dry pyridine (1.5 ml) and 4-methoxybenzenesulfonyl chloride (2.273 g, 0.011 mole) was added at room temperature. The reaction was heated to 50 °C for 24 hours. 4-methoxy-N-(2-methyl-4-oxo-3,4-dihydrobenzopyrimidine-6-yl)benzenesulfonamide **(4)** precipitated as a crystalline solid after suction filtration. The crude product was recrystallized from dimethylformamide (DMFA). The substance was synthesized with a high yield of 86%. R_f = = 0.73.

Synthesis of 4-methyl-N-(2-methyl-4-oxo-3,4-dihydrobenzopyrimidine-6-yl)benzenesulfonamide). Heteroaromatic compounds (4) (1.752 g, 0.01 mole) were dissolved in anhydrous acetone (5 ml) with dry pyridine (1.5 ml) and 4-methoxybenzenesulfonyl chloride (2.273 g, 0.011 mole) was added at room temperature. The reaction was heated to 50 °C for 24 hours.

4-methoxy-N-(2-methyl-4-oxo-3,4-dihydrobenzopyrimidine-6-yl) benzenesulfonamide **(4)** precipitated as a crystalline solid after suction filtration. The crude product was recrystallized from dimethylformamide (DMFA). The substance was synthesized with a high yield of 86%. R_f = 0.73.

Conclusion

An improved method for the quantitative synthesis of benzopyrimidin-4-one by heterocyclization in the presence of thioacetamide and o-aminobenzoic acid was developed. As a result of nitration reactions in the presence of a nitrating agent, the resulting substance was synthesized as 2-methyl-6-nitrobenzopyrimidin-4-ones. The reduction reaction was carried out in the presence of nitrobramic tin chloride digidate. The obtained substances were synthesized as important synthons for further modifications of sulfonamides in the presence of aryl sulfochloridates. The structure of the obtained substances was analyzed and confirmed using modern physical research methods

References

Pawan K. Pawan K., Premnath D., Muhammad T., Mazlee S., Yaman M., Nurul S., Muhammad S. et al. *Afatinib Dimaleate*. February 2019. – 4. – P. 5-105–106. DOI:10.25082/CR.2019.01.001

Xiaoqing Wu, Mingdong Li, Yang Qu, Wenhua Tang, Youguang Zheng, Jiqin Lian, Min Ji, Liang Xu. *Bioorg Med Chem*. 2010. Apr, 21. – 18(11). – P. 3812–3822. Doi: 10.1016/j.bmc.2010.04.046

Raffaella Sordella, Daphne W. Bell, Daniel A. Haber, Jeffrey Settleman. *Europe PMC*. 20 Aug., 2004. – Vol 305. – Issue 5687. – P. 1163–1167. DOI: 10.1126/science.1101637

Muhammad T., Mazlee S., Yaman M., Nurul S., Muhammad S. et al. A controlled, efficient and robust process for the synthesis of an epidermal growth factor receptor inhibitor: *Afatinib Dimaleate*. February, 2019. – 4. – P. 5–105–106. DOI:10.25082/CR.2019.01.001

Zulpanov F. A., Elmuradov B. J., Saitkulov F. E., Arzanov R. X. Study of benzylation reactions of quinazolin-4-one in the presence of various solvents. The Austrian Journal of Technical and Natural Sciences, – No 11, 12. DOI:10.29013/AJT-24-11.12-52-56

Sordella R., Bell D. W., Haber D. A. and Settleman J. *Science*. 2004. – Vol. 305. – P. 1163–1167.

Deng X. Q., Zheng Y., Yuan Y. P., Quan Z. S., Guan L. P. *European journal of medicinal chemistry*. 2012. – 56. – P. 39–144 p.

Petrov K. G., Zhang Y. M., Carter M., Cockerill G. S., Dickerson S., Gauthier C. A., Guo Y., Mook R. A. Jr, Rusnak D. W., Walker A. L., Wood E. R., Lackey K. E. *Bioorg Med Chem Lett*; 2006. – 16. – P. 4686–4691.

Imtiaz Khana, Aliya Ibrar, Waqas Ahmed, Aamer Saeed. Synthetic approaches, functionalization and therapeutic potential of quinazoline and quinazolinone skeletons. European Journal of Medicinal Chemistry. URL: https://doi.org/10.1016/j.ejmech.2014.10.084

submitted 01.05.2025;
accepted for publication 15.05.2025;
published 29.05.2025

Contact: zulpanovf@g.mail.com

The Austrian Journal of Technical and Natural Sciences, No 3–4
ISSN 2310-5607

PREMIER Publishing
ppublishing.org

Section 3. Food processing industry

DOI:10.29013/AJT-25-3.4-95-98

COLOURING PIGMENTS FROM CRUDE FORPRESS OILS FROM COTTON SEEDS

Niyazov Mamurjon Bobonazarovich [1], ***Akhmedov Azimjon Normuminovich*** [1], ***Ishankulova Gavkhar Norkulovna*** [1]

[1] Karshi State Technical University, PhD student, Karshi, Uzbekistan

Cite: *Niyazov M.B., Akhmedov A.N., Ishankulova G.N. (2025). Colouring Pigments From Crude Forpress Oils From Cotton Seeds. Austrian Journal of Technical and Natural Sciences 2025, No 3–4.* https://doi.org/10.29013/AJT-25-3.4-95-98

Abstract

Vegetable oils contain accompanying substances and impurities of various compositions and properties that affect the quality of the finished product and further processing processes. To remove these substances, a refining process is carried out, in particular adsorption refining using activated carbon, silica gel, zeolite, etc.

This scientific article presents the results of a study on the bleaching processes of cottonseed oils and the fact that the amount of coloring substances in cottonseed oil, namely carotenoids and gossypol, is higher in oils obtained from grades III–IV. It was also found that the mass fractions of chlorophyll and bound gossypol in the oil obtained from a mixture of grades III–IV were higher than in the cottonseed oil obtained from a mixture of grades I and II.

Keywords: *refining, chigiti buttermilk, moya buttermilk, okartirish, caratinoid, gossypol, chlorophyll*

Introduction

Currently, the process of liberalization is being carried out consistently in all sectors and branches of the economy of our country, and economic reforms are being deepened. The absence of adsorbent residues in the oil composition during the bleaching process using adsorbents indicates that the bleaching process has been perfected (Kopeikovsky V. M., Danilguk S. I., Garbuzova G. I., et al., 1982).

The adsorption process is carried out by the absorption of molecules from a liquid or gas onto the surface of a solid substance (adsorbent). The most effective adsorbents for vegetable oils are materials such as activated carbon and silica gel.

Development of new adsorbents: The purity and quality of the oil can be improved by using nanomaterials and bioadsorbents.

Process optimization: Process efficiency can be improved by properly adjusting

parameters such as temperature, pressure, and time.

Oil purification technologies: New technologies can be used to purify oil and separate foreign substances from oil during the adsorption process.

The republic processes approximately 1 million tons of cotton seeds annually, from which up to 30% of oil is extracted (of the total production of vegetable oils in the country) and about 1.5 million tons of valuable protein feed meal is produced. Complex processing of cottonseed oil ensures the production of high-quality products – salad oil and palmitin, which can replace sunflower, olive and coconut oils in the country. Salad oil is close in quality and fatty acid composition to refined and deodorized sunflower oil. Palmitin is used in the production of margarine products and toilet soap instead of coconut oil (Korostelev V. M., Maznyak I. E., 1986; Holapek M., Jandera P., Zderadika P., Hruba L., 2003; Khodjaev A. A., Ataullaev A. Kh., 1986).

The color of cottonseed oils obtained from seeds of grades III–IV is also significantly influenced by the protoplasmic pigment localized in plastids – chlorophyll, which, when saponified with alkali, produces reaction products colored brown or yellow (Akhmedov A. N., Abdurakhimov S. A., Azimov Yu. Kh.).

A distinctive feature of cottonseed oils from other vegetable fats is the presence of coloring pigments: gossypol and its derivatives, which are localized in the seed kernel in gossypol glands impregnated with pectin, hemicellulose and other unidentified substances (Akhmedov A. N., Erkaeva N. Ch., 2021).

In order to save expensive highly active bleaching earths for adsorption refining of cottonseed oil containing gossypol, as well as for oils containing significant amounts of chlorophyll, activated carbon is added to the bleaching earth (Tyutyunnikov B. N., Naumenko P. V., Tovbin I. M., Faniev G. G., 1970).

Currently, oil extraction plants use expensive imported adsorbents. Replacing them with local raw materials is a pressing issue.

Thus, cottonseed oils contain a significant amount of free fatty acids, phospholipids and pigments: derivatives and modified forms of gossypol, chlorophylls and coloring agents, unsaponifiable lipids, which worsen the consumer properties of oils during alkaline treatment. The quantity and composition of these accompanying substances depends on the quality of cotton seeds, methods of extracting oils from them, duration and methods of their storage. In oils obtained from low-grade seeds, their quantity is somewhat higher.

The variety of accompanying substances and foreign impurities, the heterogeneity of their chemical composition and properties determines the variety of methods for their removal.

Materials and methods

Qquantitative determination of gossypol was carried out by HPLC (Karishma R., Lakshmi Sahithya U., Suneetha P., et al. 2016); – the content of free gossypol (Abou–Donia S.A., Laches J. M., Abou–Donia M.B., 1981) was determined by high-performance liquid chromatography. A liquid chromatograph Agilent Technologies 1200 series (USA) with a DAD detector was used. Column Ultropac Columen Lihroprep RP18, 5 μn, 2.6 × 100mm. Gossypol was injected in 1.0–1.5 μn acetonitrile and eluted from the column isocratically with a solution consisting of acetonitrile – 0.1% phosphoric acid in water (80: 20) at room temperature. Detection was performed at 254 nm.

Also, in some studies, the mass fraction of free gossypol in oil was determined using the method certified by Certificate No. 188 of the State Standard (Technical Requirements 88.06–27: 2011).

This method for measuring the mass fraction of free gossypol applies to unrefined cottonseed oil and unrefined high-sypol cottonseed oil in the range from 0.50% to 1.5% and uses the aniline method.

The method is based on the reaction of gossypol with aniline and the formation of dianiline-gossypol, which is insoluble in oil and in some organic solvents.

Conducting measurements. A sample of filtered unrefined high-sypol cottonseed oil (10 g) was placed in a conical flask with a capacity of 200–250 cm^3, with a gossypol content in the oil of 0.5–1.5%, and 20–30 g with a gossypol content below 0.5%.

A double amount of petroleum ether, 2 cm^3 of aniline and 2.0–2.5 cm^3 of pyridine were added to the flask. The contents of the

flask were shaken, covered with a small funnel and left in a thermostat at a temperature of 40–60 °C for 1 hour.

After this, the flask was closed with a stopper and left in the dark until the dianilingossypol precipitate fell out. Two days after the precipitate fell out, it was separated from the mother liquor by filtration through a crucible with a porous plate No. 3 or No. 4, previously dried at 100–105 °C.

The sediment and the flask were washed with small portions of a mixture of 96% ethyl alcohol and petroleum ether in a ratio of 1: 2.

The crucible was dried in a drying cabinet at a temperature of 100–105 °C to a constant weight and weighed.

The first weighing was carried out after 1 hour, the subsequent weighings after 30 minutes.

Processing of measurement results. The mass fraction of free gossypol in percent (X) was calculated using the formula:

$$X = \frac{P_1 \times 0{,}775 \times 100}{P}; \quad (1)$$

where: P_1 – mass of dianilingossypol sediment in g;

0.775 – coefficient characterizing the ratio between gossypol and dianilingossypol.

P – weight of unrefined high-sypol cottonseed oil in g.

Results

It is known that the color of dark-colored cottonseed oils, along with the presence of gossypol and its derivatives, is also determined by the content of carotenoids and chlorophylls (Kopeikovsky V. M., Danilguk S. I., Garbuzova G. I. et al. 1982). Moreover, carotenoids appear in the red colors of the resulting cottonseed oil, and chlorophylls – in blue units of oil color.

Taking this into account, we conducted analyses to determine the content of carotenoids and chlorophylls in the composition of raw forepress oils obtained from mixtures of cotton seeds of grades I–II and III–IV. The results of the analyses are presented in Table 1.

Table 1. *Indicators of coloring pigments of raw forepress oils obtained from mixtures of cotton seeds of I–II and III–IV varieties*

Name of oil coloring pigments	Unit of measurement	Cottonseed Oil:	
		I and II grades	III and IV grades
mass fraction of carotenoids	$\times 10^{-4}$,%	4,8–5,0	6,0–7,2
mass fraction of chlorophylls	$\times 10^{-4}$,%	0,5–0,7	0,8–1,3
mass fraction of total gossypol	%	0,38–0,51	0,25–0,35
mass fraction of bound gossypol	%	0,11–0,15	0,21–0,28

Discussion and Conclusion

It is evident from Table 1 that the content of mass fractions of carotenoids and free gossypol in oil obtained from a mixture of cotton seeds is higher than from a mixture of grades III and IV. And vice versa, the mass fractions of chlorophyll and bound gossypol in oil obtained from a mixture of grades III–IV are higher than from a mixture of grades I and II. This is also confirmed by the high color of oil obtained from a mixture of cotton seeds of grades III–IV (Table 1).

Данные результаты были получены при соблюдении в опытно-производственных условиях соотношения сортов семян хлопчатника в смеси равным 50: 50 (%).

These results were obtained under experimental production conditions when the ratio of cotton seed varieties in the mixture was 50:50 (%).

Analysis of the annual receipts of cotton seeds to the oil and fat enterprises of the Republic shows that approximately 2/3 of the seeds are grades I and II, and 1/3 are grades III and IV. The trend over the last 5 years shows an increase in the supply of grades III and IV cotton seeds to the country's oil and fat enterprises, which reduces the yield of

the oils obtained and their quality. Refining of crude oils obtained from low-grade and non-standard cotton seeds requires improvement of the existing technology.

References

Technology of production of vegetable oils / (V. M. Kopeikovsky, S. I. Danilguk, G. I. Garbuzova et al.): edited by V. M. Kopeikovsky – M.: Light and food industry, 1982. – 416 p.

Korostelev V. M., Maznyak I. E. Results of the oil and fat industry for 1985 // Oil and fat industry. – Moscow, 1986. – No. 6. – P. 16–22.

Holapek M., Jandera P., Zderadika P., Hruba L.: Characterization of triacylglycerol and diacylglycerol composition of plant oils using high-performance liquid chromatography-atmospheric pressure chemical ionization mass spectrometry. Journal of Chromatography A, 1010, – 2. 2003. – P. 195–215.

Khodjaev A. A., Ataullaev A. Kh. Improving the quality and reducing losses of cotton seeds // Oil and fat industry. – Moscow, 1986. – No. 12. – P. 12–13.

Akhmedov A. N., Abdurakhimov S. A., Azimov Yu. Kh. Bentonite adsorbents modified with urea solution. Universum: technical sciences, – P. 59–62.

Akhmedov A. N., Erkaeva N. Ch. Improving the process of primary purification of vegetable oils. Journal of innovative technologies. – Karshi, – Special issue. 2021. – P. 35–39.

Akhmedov A. N. Study of the indicators of cottonseed oil obtained by the method of forpressing from low-grade cotton seeds. Universum: Technical sciences. Issue: – 4 (61) April, 2019. – Moscow, – P. 23–26.

Tyutyunnikov B. N., Naumenko P. V., Tovbin I. M., Faniev G. G. Technology of fat processing. – Moscow: Food industry, 1970. – 652 p.

Karishma R., Lakshmi Sahithya U., Suneetha P., et al. Determination of Total Gossypol and Free Gossypol Content in different varieties of Bt and Non Bt Cotton seed extracts by High- Performance Liquid Chromatography (HPLC) // Research journal of biotechnology. 2016. – Vol. 11. – No. 2. – P. 70–74.

Abou-Donia S. A., Laches J. M., Abou-Donia M. B. High performance liquid chromatography analysis of gossypolum. J. Chromatography. 1981. – 206 (3). – P. 606–610.

Technical Requirements 88.06–27: 2011. Unrefined high-gossypol cottonseed oil. Appendix “B”. Method for determining the proportion of free gossypol. – Tashkent. Gosstandart. 2011. – 9 p.

submitted 15.04.2025;
accepted for publication 29.04.2025;
published 29.05.2025

Contact: a.ahmedov80@mail.ru

The Austrian Journal of Technical and Natural Sciences, No 3–4
ISSN 2310-5607

PREMIER Publishing
ppublishing.org

Section 4. Technical science in general

DOI:10.29013/AJT-25-3.4-99-107

CHROMATOGRAPHIC ANALYSIS OF POMEGRANATE PEEL EXTRACTS OBTAINED WITH VARIOUS SOLVENTS

Niyozov Khasan Niyoz ugli [1], ***Odinayev Mirzamat Isaevich*** [2], ***Nazarov Golib Abdishukur ugli*** [3], ***Aripov Mirolim Mirazim ugli*** [3]

[1] M. Mirzayev Research Institute of Horticulture, Viticulture and Winemaking

[2] Tashkent State Agrarian University

[3] Tashkent University of Chemical Technology

Cite: *Niyozov Kh.N., Odinayev M.I., Nazarov G.A., Aripov M.M. (2025). Chromatographic Analysis of Pomegranate Peel Extracts Obtained With Various Solvents. Austrian Journal of Technical and Natural Sciences 2025, No 3–4.* https://doi.org/10.29013/AJT-25-3.4-99-107

Abstract

This study involved the extraction of pomegranate peel from four local varieties – Qoradon qizil, Achchiqdona, Qozoqi, and Qayum – using various organic solvents. The composition of the resulting extracts was analyzed using high-performance liquid chromatography (HPLC), and the antioxidant activity of the compounds extracted from the pomegranate peels was compared. Water, ethyl acetate, and ethanol were used as solvents, and the analysis was conducted at a wavelength of 254.4 nm.

Keywords: *Karadon kyzyl, Achchikdona, Kazoki, Kayum, antioxidant, gallic acid, ellagic acid*

Introduction

As a solution to the shortage of food and other consumer goods observed in the world today, rapid development of the agricultural sector is shown as a solution to current problems. Along with the horticulture industry, the processing of products obtained from them and the efficient use of secondary products retain their importance. Among the research carried out by scientists of the world, there are many developments that are scientifically based and put into production, which make it possible to organize measures to find a solution to such problems.

Within the framework of measures for the development of the Republic of Uzbekistan until 2030, tasks have been clearly defined regarding the development of effective methods of growing horticulture, viticulture and many other agricultural products. Numerous experimental works are being carried out on the productivity of pomegranate varieties grown in our country and their adaptation to soil and climatic conditions.

By studying and analyzing pomegranate varieties that can be grown in the regions, it is possible to make a significant contribution to the future results of these plans. At this point, taking into account the plans of the Fergana Valley, Kashkadarya and Surkhandarya regions, as well as the existing pomegranate orchards in other regions of the country, it is aimed to increase the indicator of pomegranate cultivation and productivity in the republic's agriculture in the next decade, and increase the production volume to 600,000 tons per year.

Literature Review

Currently, the value of biologically active compounds, which are necessary for the human body, have healing properties, is of particular importance. Examples of biologically active substances are proteins, carbohydrates, lipids, enzymes, vitamins, hormones, macro-micro elements and many other primary and secondary metabolites. Among these main biologically active compounds, the role of secondary biologically active substances that stimulate metabolism in the body and have a high effect is also important, one of such substances is gallic acid and ellagic acid formed as its residues, and other tannins, as well as nitrogen-containing and acid-based vital compounds, each of them plays an irreplaceable and very important role in the life activity of the human body (Braga, L.C., Shupp, J.W., Cummings, C., Jett, M., Takahashi, J.A., Carmo, L.S., Nascimento, A.M.A., 2005; Menezes, S.M.S., Cordeiro, L.N., & Viana, G.S.B., 2006).

Pomegranate is distinguished from other fruits by its medicinal properties. The fruit contains on average 25–32% sugar, 0.2––2.5% organic acids, 10% tannin, up to 3.4% proteins, 2–6% pectin, as well as iron, cobalt, iodine, C, PP, A vitamins. The amount of vitamin C in fruits is 250–1300 mg. This causes an increase in interest in its consumption (Hosseini, B., Saedisomeolia, A., Wood, L.G., Yaseri, M., & Tavasoli, S., 2016).

These natural antioxidants play a role in preventing free radical oxidation, aging process and the development of many diseases in the human body. Ellagic acid is a polyphenolic compound with strong antioxidant properties. It combines with various biomacromolecules, for example, proteins and collagen, and has the property of improving the immunity in the body. Ellagic acid has been found to have high effectiveness against cancer, this substance slows down the development of tumors due to its high effect (Li, Y., Guo, C., Yang, J., Wei, J., Xu, J., & Cheng, S., 2006).

Pomegranate peel is rich in ellagic acid, in addition, pomegranate fruit peel forms complex compounds, which further increases the effect of the substance. Another positive effect of ellagic acid is due to its skin-tightening properties. For medical purposes, ellagic acids isolated from pomegranate peel are effectively used in various biochemical methods. Ellagic acid has many effects, including important effects such as narrowing the pores of the organ system in the body, reducing sebum secretion, and improving the formation of tissues that improve skin lubrication (Bell, C., & Hawthorne, S., 2008).

Figure 1. *Pomegranate peel and its dried and crushed sample*

Extraction of ellagic acid from this raw material is recognized as a technology with high efficiency due to the fact that the production technology is somewhat simple and high productivity (Usta, C., Ozdemir, S., Schiariti, M., & Puddu, P.E., 2013).

The purpose of the work is to carry out quantitative analyzes of gallic and ellagic ac-

ids, which have antioxidant properties, in the local pomegranate skin.

Methods

In the extraction stages, 3 samples of dried and ground biomass of pomegranate peel of 4 different varieties, 50 g each, corresponding to 3 types of solvents, are measured. each of the measured samples was placed in separate containers (500 ml flat-bottomed flasks) into which equal amounts of all solvents (water, ethyl acetate, and ethyl alcohol) were poured (250 ml per sample) and extracted in a magnetic stirrer for 30 minutes, after which the samples were left at room temperature for 48 hours. At the end of the specified time during the process, the liquid part of each sample is poured separately, and the remaining part is poured with the same amount of solvent as the initial volume, and it is kept in the unit of time specified in the initial stage. In this way, the extraction is carried out three times, and all the extractants (the liquid part of the sample of the extraction process obtained from the three steps of the pomegranate peel using solutions) are collected in one container depending on the pomegranate variety. Extract concentration process, rotor evaporation was carried out using RE100-Pro equipment. In this case, the process methodology, the rotation speed of the rotor is 60 rpm, the temperature is 38–40 °C and the pressure is 0.9 Pa. The duration of the process is on average 60–90 minutes when evaporating the extract obtained through organic solvents (ethyl acetate and ethyl alcohol) to a residual amount of 10% of the solution content. When evaporating aqueous extracts, the temperature of the water bath rises to 70–75 °C, the duration of the process is 90–120 minutes, compared to 25–30% residual content. Each concentrated sample is collected in separate containers, and at the next stage, their qualitative and quantitative analysis is carried out.

In the second stage of the research, modern chromatographic methods were used to analyze the amounts of gallic and ellagic acids in the extracts extracted from the peel of different varieties of pomegranate. Gallic and ellagic acids from polyphenols contained in the sample were determined using liquid chromatography to organize the work process.

5–10 g of the sample is taken on an analytical balance and placed in a 300 ml flat flask. Add 50 ml of 70% ethanol solution. The mixture was heated at 70–80 °C with vigorous stirring for 1 hour, equipped with a magnetic stirrer, reflux condenser, and then stirred at room temperature for 2 hours. The mixture is cooled and filtered. 25 ml of 70% ethanol is added to the remaining part and it is re-extracted for the 2nd time. The filtrates were combined and filled to the mark with 70% ethanol in a 100 mL volumetric flask. The resulting solution is spun in a centrifuge at a speed of 6000–8000 rpm for 20–30 minutes. The resulting solution is taken from the upper part for analysis.

First, working standard solutions and then prepared working solutions were introduced into the chromatograph. High-performance liquid chromatography is used in the analysis. The experimental conditions of the chromatographic environment adapted for the analysis include the following: Chromatograph Agilent-1200 (equipped with an autodoser), Column Exlipse XDB C 18 (obraschenno-faznyy), 5 μm, 4.6 × 250mm, Diode matrix detector (DAD), 254 nm, 272 nm identified. Flow rate 0.8 ml/min, eluent phosphate buffer: acetonitrile: 0–5 min 95:5, 6–12 min 70:30, 12–13 min 50:50, 13––15 min 95:5, thermostat temperature 30 °C, the amount of sample included in the process is 10 μl (vcol). Studies are conducted on 3 solvent-extracted solutions of each sample, so that a total of 12 extracts were tested in each step (4 × 3).

Results and discussion

During the research, 250 ml of the 4 types of pomegranate varieties selected for the extraction process in different solvents (water, ethyl alcohol, ethyl acetate) make a total volume of 750 ml of solvent in three stages. One-stage extraction takes 48 hours, with all three stages totaling 144 hours. Pomegranate skin taken in solution is shaken up to 3 times a day using a shaker (Shaker GFL-3017) to increase the solubility of substances in extraction.

Table 1. *Amount of reagent used for the extraction of pomegranate peel and extraction period*

№	Varieties of pomegranate 50 gr	Water ml	Ethanol ml 144 soat	Ethyl acetate ml
1.	Karadon kyzyl	250	250	250
		250	250	250
		250	250	250
2.	Achchikdona	250	250	250
		250	250	250
		250	250	250
3.	Kazoki	250	250	250
		250	250	250
		250	250	250
4.	Kayum	250	250	250
		250	250	250
		250	250	250

Note: the solvent volumes given in the table are selected for a 50 g sample, increasing the sample volume may result in a decrease or increase in the amount of solvents

Based on the results of the analysis, different ratios of solvents and extraction periods were carried out based on several experiments, and the optimal amounts as well as time units were selected as the results given in Table 1. As the samples age, the mixture becomes a brown mass (see Figure 2). After the fractionation and filtration process, the liquid contents have a dark red, bright appearance (see Figure).

Figure 2. *Extracted samples*

Figure 3. *The separated extract fluids*

Since the residual moisture content of the samples during drying is 3–6%, it is well absorbed by the crushed bark during the extraction stages. The liquid part of the substances dissolved in three different solvents is poured into separate containers according to the type of pomegranate and the type of solvent. The amount of extract obtained is different, the reason for this can be said that the rate of absorption and retention of the solvents in the plant source is different, therefore the amounts show a difference, but not much from each other (see Table 2).

Table 2. *Amounts of extract from pomegranate varieties*

№	Varieties of pomegranate	Water ml	Ethanol ml	Ethyl acetate ml
1.	Karadon kyzyl	375	550	345
2.	Achchikdona	345	530	340
3.	Kazoki	180	540	360
4.	Kayum	370	530	340

A total of 750 ml of solvents were included in the three-stage extraction process, and the amount of extracts obtained from them is different for several reasons, for example, the amount of extract obtained from the peel of black red pomegranate is 375 ml, the amount of ethyl alcohol extract is 550 ml, and the amount of ethyl acetate is 345 ml. The amount of solvents used in the extraction of pomegranate peels of other varieties almost repeats these volumes. With the exception of the skin of the Kazoki pomegranate variety in the aqueous solution, the reason is that the amount of this solution decreases in a sharply different volume compared to the others. From this, it can be concluded that, due to the preservation of solvents in the source and their evaporation over time, among them, the alcohol extract dominates in terms of quantity. In addition, it is observed that some of the samples retain a large amount of aqueous solution in their cells.

Figure 4. *Chromatograms of the analysis of ellagic and gallic acids in the peel of a pomegranate variety (studied in a-ethyl acetate, b-ethyl alcohol and c-aqueous solutions)*

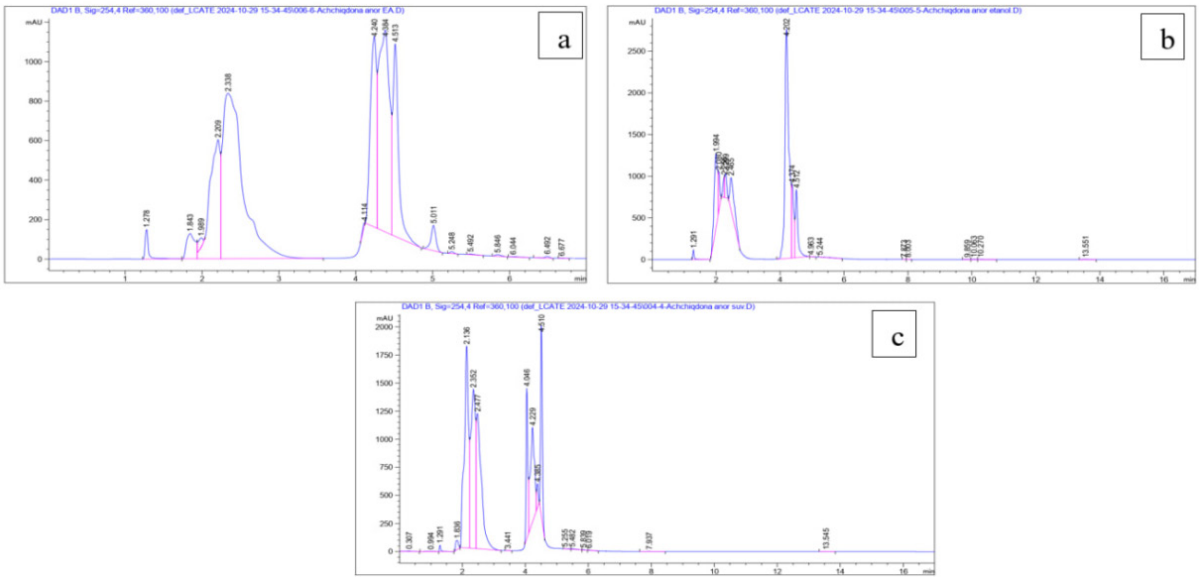

Figure 5. *Chromatograms of the analysis of ellagic and gallic acids in the peel of Kayum pomegranate variety (studied in α-ethyl acetate, β-ethyl alcohol and c-aqueous)*

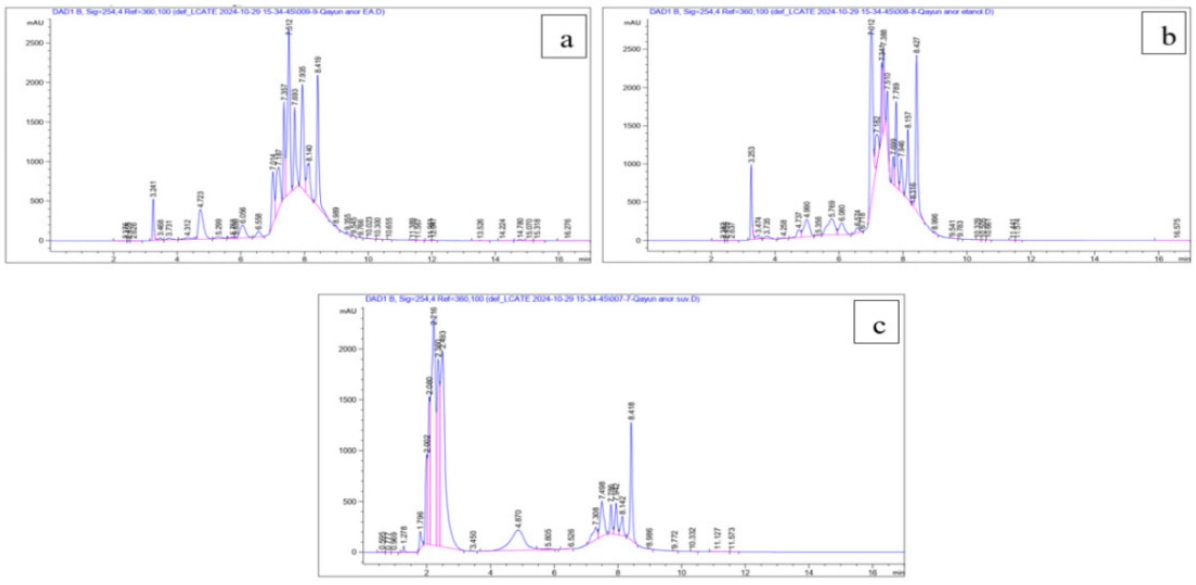

High performance liquid chromatography (HPLC) analysis results. This method is a high-precision, reliable analysis method for the analysis of the quantity and quality of biologically active substances. According to the analysis of polyphenol substances in pomegranate peel, the number of intense peaks visible in the obtained chromatogram, as well as their intensity indicators, led to accurate information about the quality and quantity of the substances.

Intense peaks in these chromatograms indicate the presence of both polyphenols. According to it, it was found out that the substance coming out of the column in the first 2–4 minutes is ellagic acid in accordance with the standard.

Also, according to the standard chromatogram, the retention period of gallic acid in the column corresponds to an average interval of 4–6 minutes, the chromatogram of the analyzed solution showed intensive peaks related to gallic acid during these minutes. It can be seen that the periodicity of substances leaving the column has not changed in all three solution samples isolated from bitter pomegranate peel.

The compositional chromatograms of Kayum pomegranate peel have a slightly different appearance compared to other pomegranate varieties, including the fact that the content of ellagic and gallic acids in the extracts obtained through all three types of solvents is relatively low, besides, it can be seen that the content of other polyphenol substances in the content of three different solvents is present in large quantities.

Figure 6. *Chromatograms of the analysis of ellagic and gallic acids in the peel of Karadon kyzyl pomegranate variety (studied in α-ethyl acetate, β-ethyl alcohol and c-aqueous solutions)*

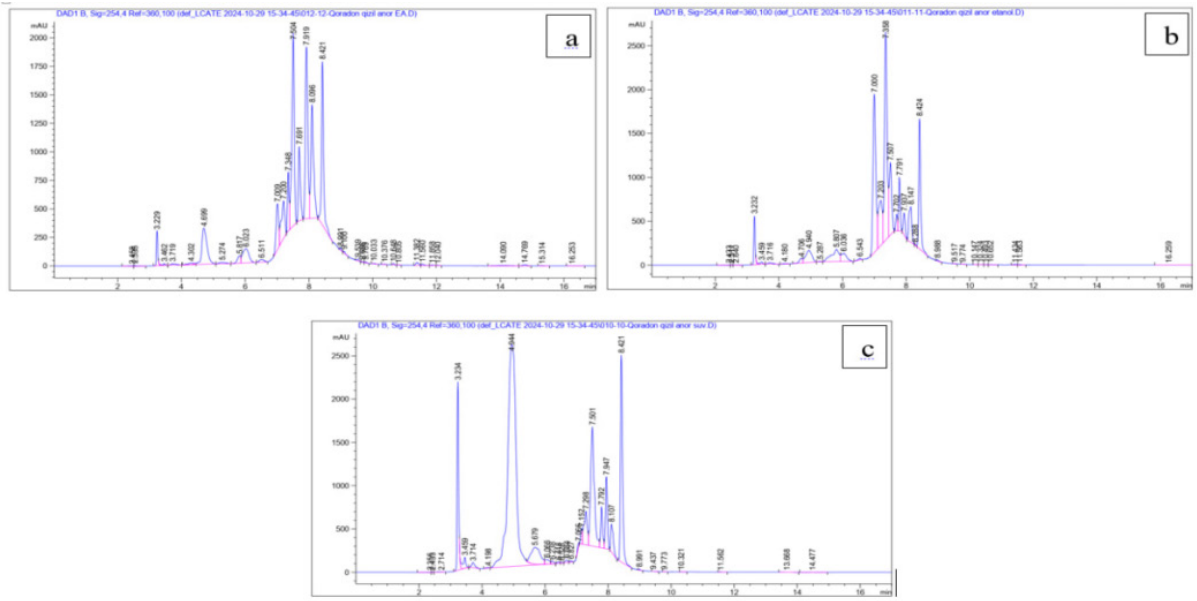

If we pay attention to the chromatograms of the extracts isolated from the Karadon kyzyl pomegranate variety (given in Figure 6), the intense peaks corresponding to the amounts of ellagic acid show that the extracts dissolved in all solvents contain the amount of ellagic acid, but the amount of gallic acid is significantly less in the ethyl alcohol solution. In all three of these chromatograms, it was found that there are polyphenol-based substances with a relatively long retention period in the column.

According to the quantitative analysis of gallic and ellagic acids, which contain polyphenols in Kazoki pomegranate peel, the peaks in the obtained chromatogram prove that the solutions mainly consist of two types of polyphenolic bases, i.e., ellagic and gallic acids. As a result of the results of the chromatograms, it can be said that the amount of polyphenol-based substances in the peel of all the selected pomegranate varieties is high enough. Among such substances, ellagic and gallic acids, which are studied in this

work and have important therapeutic functions for the human body, can be mentioned as an example.

Figure 7. *Chromatograms of the analysis of ellagic and gallic acids in the skin of the Kazoki pomegranate variety (studied in a-ethyl acetate, b-ethyl alcohol and c-aqueous solutions)*

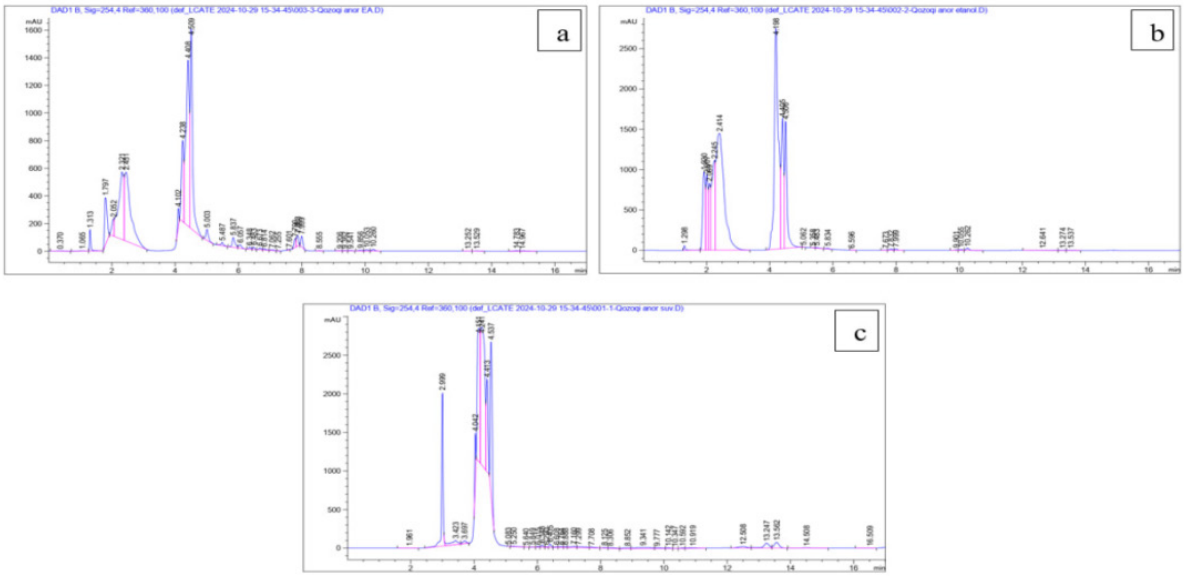

By calculating the amount of substances appearing in the chromatograms, it was possible to know their exact size. According to it, the exact amount of two types of polyphenols dissolved in each solvent is quite different from each other. Table 3 below shows the results of chromatographic quantitative analysis of the amount of gallic and ellagic acid in the peel of pomegranate varieties.

Table 3. *Results of chromatographic analysis of the contents of gallic and ellagic acids in the samples*

Polyphenol name	Achchikdona variety (ethyl acetate)	Achchikdona variety (ethanol)	Achchikdona variety (water)	Kayyum variety (ethyl acetate)	Kayum pomegranate (ethanol)	Kayyum pomegranate (water)
			Concentration mg/g			
Gallic acid	0.058986	0.171384	0.07421	0.312362	0.00424	0.009564
Ellagic acid	0.225619	0.11314	0.16023	0.050285	0.060209	0.035067
Polyphenol name	Karadon kyzyl variety (ethyl acetate)	Karadon kyzyl variety (ethanol)	Karadon kyzyl variety (water)	Kazoki variety (ethyl acetate)	Kazoki variety (ethanol)	Kazoki variety (water)
Gallic acid	0.110716	0.056253	0.075428	0.038633	0.003345	0.047914
Ellagic acid	0.112478	0.097261	0.066825	0.052269	0.022138	0.060870

The results of chromatographic studies show that the content of substances in different solvents is different. For example, in the extracts obtained from the peel of the Achchikdona pomegranate variety, using ethyl acetate solution, it can be seen that the content of ellagic acid (0.225619 mg/gr) is higher than that of gallic acid (0.058986 mg/gr). On the contrary, in the ethyl alcohol extract of the same variety, it can be seen that the content of gallic acid (0.171384 mg/gr) is significantly higher than that of ellagic

acid (0.11314 mg/gr). In the aqueous extract of the Achchikdona pomegranate peel, the content of ellagic acid (0.16023 mg/gr) is also recorded in a larger amount than that of gallic acid (0.07421 mg/gr). The solubility of polyphenols from the peel of this pomegranate variety was recorded at the highest rate in ethyl acetate. The lowest solvent content among the samples was observed in the aqueous solution.

It can be seen that the extracts obtained from the peel of the Kayum pomegranate variety using ethyl acetate solution contain a high amount of gallic acid (0.312362 mg/gr) compared to ellagic acid (0.050285 mg/gr). It was found that the ethyl alcohol extract of this variety contains a low amount of gallic acid (0.00424 mg/gr) compared to ellagic acid (0.060209 mg/gr). The aqueous extract of the Kayum pomegranate peel also contains a low amount of ellagic acid (0.009564 mg/gr) compared to gallic acid (0.035067 mg/gr). The solubility of both substances in solvents from the peel of the Kayum pomegranate variety, according to the results, is high in ethyl acetate solution and highest in ethyl acetate. In this case, the aqueous solution also contains a low amount of gallic and ellagic acid.

Extracts obtained from the peel of the Karadon kyzyl pomegranate variety using ethyl acetate solution contain a low amount of gallic acid (0.110716 mg/gr), compared to ellagic acid (0.112478 mg/gr). It can be seen that the content of gallic acid (0.056253 mg/gr) in the ethyl alcohol extract of the same variety has a low amount of ellagic acid (0.097261 mg/gr). The content of ellagic acid (0.038633 mg/gr) in the aqueous extract of the Karadon kyzyl pomegranate peel is also noted, which is low in comparison to gallic acid (0.066825 mg/gr). The ethyl acetate solution also showed the best results in the Karadon kyzyl peel, and it can be said that the content of gallic and ellagic acid in this solvent is almost equal.

Extracts from the peel of the Kazoki variety, obtained using ethyl acetate solution, contain a lower amount of gallic acid (0.038633 mg/gr), compared to ellagic acid (0.522694 mg/gr). It can be seen that the content of gallic acid (0.003345 mg/gr) in the ethyl alcohol extract of the same variety is lower than that of ellagic acid (0.221384 mg/gr). The content of ellagic acid (0.047914 mg/gr) in the aqueous extract of the Kazoki pomegranate peel was also shown to be lower than that of gallic acid (0.608707 mg/gr). Compared to extracts from the peel of other pomegranate varieties, the amounts of the Kazoki pomegranate variety in all solvents were recorded at similar levels.

Conclusion

The fruit peels of four types of pomegranate varieties selected for the study were first dried and ground. The samples were extracted in three different solvents, and the amount of extract in them was measured separately. This revealed the ability of the crushed fruit peels to sorb three different solutions.

The composition of the extracts dissolved in three types of solvents from each sample was analyzed using high-performance liquid chromatography (HPLC). When the amounts of ellagic and gallic acid in the extracted extracts were studied, it was determined that each solvent contained these polyphenol-based substances, and their retention time on the chromatographic column was in accordance with the standard, which was ellagic and gallic acid. The resulting chromatograms were analyzed and the amount of substances was determined.

Based on the results of the chromatographic analysis, the amounts of polyphenol-based ellagic and gallic acids in each solvent were compared to each other and an optimal solvent analysis was performed, according to which it was determined that ethyl acetate had the highest efficiency among all solvents.

References

Braga, L. C., Shupp, J. W., Cummings, C., Jett, M., Takahashi, J. A., Carmo, L. S., Nascimento, A. M. A. (2005). Pomegranate extract inhibits Staphylococcus aureus growth and subsequent enterotoxin production. Journal of Ethnopharmacology, – 96(1–2). – P. 335–339. Doi:10.1016/j.jep.2004.08.034

Menezes, S. M. S., Cordeiro, L. N., & Viana, G. S. B. (2006). Punica granatum (Pomegranate) Extract Is Active Against Dental Plaque. Journal of Herbal Pharmacotherapy, – 6(2), 79–92. Doi:10.1080/j157v06n02_07

Hosseini, B., Saedisomeolia, A., Wood, L. G., Yaseri, M., & Tavasoli, S. (2016). Effects of pomegranate extract supplementation on inflammation in overweight and obese individuals: A randomized controlled clinical trial. Complementary Therapies in Clinical Practice, – 22. – P. 44–50. Doi:10.1016/j.ctcp.2015.12.003

Li, Y., Guo, C., Yang, J., Wei, J., Xu, J., & Cheng, S. (2006). Evaluation of antioxidant properties of pomegranate peel extract in comparison with pomegranate pulp extract. Food Chemistry, – 96 (2). – P. 254–260. Doi:10.1016/j.foodchem.2005.02.033

Bell, C., & Hawthorne, S. (2008). Ellagic acid, pomegranate and prostate cancer – a mini review. Journal of Pharmacy and Pharmacology, – 60(2). – P. 139–144. Doi:10.1211/jpp.60.2.0001

Usta, C., Ozdemir, S., Schiariti, M., & Puddu, P. E. (2013). The pharmacological use of ellagic acid-rich pomegranate fruit. International Journal of Food Sciences and Nutrition, – 64 (7). – P. 907–913. Doi:10.3109/09637486.2013.798268

submitted 14.04.2025;
accepted for publication 29.04.2025;
published 29.05.2025

Contact: niyozovxasan8@gmail.com; nazarovgolib05@gmail.com

The Austrian Journal of Technical and Natural Sciences, No 3–4
ISSN 2310-5607

PREMIER Publishing
ppublishing.org

DOI:10.29013/AJT-25-3.4-108-118

MODEL OF DIAGNOSTICS INFORMATION SYSTEM PANCREAS CANCER

Hajiyeva Tarana Adil [1], ***Ahmadov Shamil Azer*** [1]

[1] Azerbaijan State Oil Industry University

Cite: *Hajiyeva T.A., Ahmadov Sh.A. (2025). Model of Diagnostics Information System Pancreas Cancer. Austrian Journal of Technical and Natural Sciences 2025, No 3–4.* https://doi.org/10.29013/AJT-25-3.4-108-118

Abstract

The article analyzes the development of a medical decision support system based on fuzzy logic. In an era of increased healthcare demands and complex analytical situations, the role of information technology is indispensable. The ambiguous behavior of cancer in the early stages can lead to late detection and sometimes to erroneous treatment. The proposed method is intended to help doctors make optimal decisions. The use of fuzzy logic techniques in oncology can increase efficiency in diagnosing and predicting cancer.

Keywords: *Oncological diseases, Pancreatic cancer, Decision support system*

Introduction

A huge problem today is the increase in the number of cancer patients, and all sciences, not just oncology, must fight it. Pancreatic cancer, unlike other oncological diseases, behaves more aggressively and has a very high mortality rate. The pancreas is an abdominal organ that plays a significant role in the digestive and endocrine systems. Pancreatic cancer occurs as a result of a mutation of the body's own cells, which multiply randomly and spread to other organs. The development of the disease is based on damage to the DNA structure and disruption of tissue growth regulation. The reason for this behavior of cells remains a mystery. However, its development is most often associated with some possible prerequisites for its appearance, such as: age; use of hormonal drugs; diabetes; chronic pancreatitis; poor nutrition, history of cancer; exposure to radiation; excess weight; smoking; alcohol abuse. In the early stages, the disease is difficult to identify, as it does not produce any obvious symptoms. They can be confused with pancreatitis, inflammatory processes and other various diseases that have similar patterns of symptoms. Discomfort occurs at later stages and this complicates treatment (Cherenkov V. G., 2010). Symptoms of an uncertain nature become a major problem on the way to making an accurate diagnosis and can lead to incorrect treatment. Late detection is one of the main reasons for high mortality. There are various methods for diagnosing pancreatic cancer, such as laboratory tests, tumor markers, magnetic resonance imaging, computed tomography, ultrasound, endoscopic scanning, biopsy, and so on. Saving a human life depends on timely diagnosis. To elimi-

nate medical errors and help doctors make decisions, it is extremely important to create advanced self-learning information and analytical systems based on expert knowledge, patient data, laboratory test results, diagnostic methods, treatment, rehabilitation, and so on. These include a decision support system based on fuzzy logic, which uses intelligent analysis and data processing technologies that effectively influence the processes of diagnosis, disease development prediction, treatment plan and rehabilitation program. The system evaluates and provides accurate results by providing a set of methods designed to improve patient diagnosis. At present, there is no longer any doubt that the use of fuzzy logic models in various areas of human activity allows for a complete transition to a higher quality level of solving the assigned task (Litvin A. A., Litvin V. A., 2018). Fuzzy logic is a suitable and applicable basis for developing decision support systems in medicine. It is especially necessary in oncology, to detect cancer in the early stages, because the incidence rate is growing, but survival is not increasing. The purpose of creating and developing fuzzy approaches is to adapt mathematical models to real life, the ability to organically combine the potential of computational methods with the characteristics of human thinking (Aliyev R. A., Aliyev R. R., 2001).

Main goal. Diagnostics plays a decisive role in the treatment of cancer pathologies. To grow, tumors use substances necessary for the human body and release toxic compounds, thereby causing changes in the composition of the blood. Therefore, it can be argued that blood test results are an important tool for making a preliminary diagnosis of cancer (Congress 2021). In connection with the above, the material for the research work was taken from the blood test results, since deviations from the norm can be signs of pancreatic cancer in the early stages. The work involved seven input variables (Leukocytes, ESR, Hemoglobin, C 19–9, CA 242, CEA, Glucose) and one output variable.

– Leukocytes, or white blood cells, perform a protective function in the body. They cleanse the blood of dead cells and fight viruses and infections. Most often, leukocytes decrease in the following cases: viral diseases that disrupt the functioning of the red bone marrow; long-term infections, as a result of which their consumption exceeds the production of new ones; autoimmune diseases, and malnutrition;

– ESR – erythrocyte sedimentation rate. Deviation of the indicators from the norm indicates an inflammatory process and general intoxication of the body, and also exceeding this indicator indicates the breakdown of tissues in the body and, as a consequence, the presence of a malignant neoplasm;

– Hemoglobin is a chemical compound of protein and iron that carries oxygen from the respiratory system to the tissues. A sharp decrease in hemoglobin, as well as a sharp increase, can occur with various oncological diseases;

– C 19–9 and CA-242 are tumor markers used in the diagnosis of pancreatic cancer. High levels of C 19–9 CA-242 are found mainly in patients with tumors and metastases;

– CEA is a cancer embryonic antigen that is used as a tissue marker for cancer. Reasons for an increase: malignant neoplasms, metastases, relapse of the oncological process, pancreatitis, autoimmune diseases, and reasons for a decrease: surgical removal of a malignant tumor and remission of a benign tumor;

– Glucose is an indicator of carbohydrate metabolism, the sugar content in the blood. Increased – diabetes, endocrine disorders, pancreatitis, pancreatic tumor, chronic liver and kidney damage. Decreased – liver and pancreas damage, hypothyroidism, stomach or adrenal cancer, drug poisoning, alcohol intoxication (Lugovskaya S. A., Pochtar M. E., 2018).

Based on expert consultations and medical literature, a database has been compiled consisting of 211 rules that determine the degrees of risk (high, medium and low) based on the assessment of the input variables mentioned above. The output variable takes values from 1 to 3 (Healthy, Non-oncology, Below, respectively). The mechanism for finding the output variable is developed in the MATLAB application, as a tool for fuzzy logic.

x_1 – Leukocytes; x_2 – ESR; x_3 – Hemoglobin; x_4 – C 19–9; x_5 CA-242; x_6 – CEA; x_7 – Glucose.

If x_1 = “Norm” and x_2 = “Norm” and x_3 = “Norm” and x_4 = “Norm” and x_5 =

= “Norm” and x_6 = “Norm” and x_7 = “Norm”, then y = “Healthy”;

If x_1 = “Norm” and x_2 = “Above normal” and x_3 = “Below normal” and x_4 = = “Norm” and x_5 = “Norm” and x_6 = “Norm” and x_7 = “Above normal”, then y = “Non-oncology”;

If x_1 = “Above normal” and x_2 = “Above normal” and x_3 = “Norm” and x_4 = Above normal” and x_5 = “Above normal” and x_6 = = “Norm” and x_7 = “Below normal”, then y = = “Oncology”;

Table 1. *Test values*

Leuko-cytes	ESR	Hemoglobin	C 19–9	CA-242	CEA	Glucose	Risk
6	9	142	0	1	0	102	1
5	11	155	4	2	5	367	2
7	58	140	89	37	16	103	3

Conclusion

The use of the proposed technology helps to systematize and solve many problems that can prevent medical errors in the future. To make reliable decisions in many complex problems and under conditions of uncertainty, an excellent tool in the field of intelligent systems is the use of fuzzy logic. Fuzzy logic was created by Zadeh in 1965. It has not lost its relevance to this day and continues to benefit the entire world.

Problem statement with using MATLAB application.

```
[System]
Name='Tarana'
Type='sugeno'
Version=2.0
NumInputs=7
NumOutputs=1
NumRules=28
AndMethod='prod'
OrMethod='probor'
ImpMethod='min'
AggMethod='max'
DefuzzMethod='wtaver'

[Input1]
Name='in1'
Range=[1 79]
NumMFs=28
MF1='in1mf1':'gaussmf',[13.784199951097 2.99794236926917]
MF2='in1mf2':'gaussmf',[13.7885209176873 1.99997155591377]
MF3='in1mf3':'gaussmf',[13.7862190439433 2.99928881913682]
MF4='in1mf4':'gaussmf',[13.7885665060583 5.99999595562293]
MF5='in1mf5':'gaussmf',[13.7887735212013 5.00024707891369]
MF6='in1mf6':'gaussmf',[13.7885880931532 5.00000252367064]
MF7='in1mf7':'gaussmf',[13.7885808546855 4.99999942034524]
MF8='in1mf8':'gaussmf',[13.7885943021989 20.0000827821728]
MF9='in1mf9':'gaussmf',[13.7885757556728 4.99999549138783]
MF10='in1mf10':'gaussmf',[13.7885589387925 8.00001180288298]
MF11='in1mf11':'gaussmf',[13.790062931338 8.0007889982706]
MF12='in1mf12':'gaussmf',[13.7886076275242 7.99987548522249]
```

```
MF13='in1mf13':'gaussmf',[13.7887788710529 63.9998929807899]
MF14='in1mf14':'gaussmf',[13.7885823103998 6.99999885466846]
MF15='in1mf15':'gaussmf',[13.7885822322937 79.0000000003147]
MF16='in1mf16':'gaussmf',[13.7885822258102 5.99999989932597]
MF17='in1mf17':'gaussmf',[13.7885824084647 6.99999935445724]
MF18='in1mf18':'gaussmf',[13.7885821930246 5.99999949307296]
MF19='in1mf19':'gaussmf',[13.7885727118994 17.0000145552124]
MF20='in1mf20':'gaussmf',[13.7889519607068 41.9999730287192]
MF21='in1mf21':'gaussmf',[13.7885688670492 21.0000260327451]
MF22='in1mf22':'gaussmf',[13.7885840677044 7.00000157391282]
MF23='in1mf23':'gaussmf',[13.788582244227 7.99999962928076]
MF24='in1mf24':'gaussmf',[13.7885996715349 49.9999918381779]
MF25='in1mf25':'gaussmf',[13.7885819374963 7.99999867745641]
MF26='in1mf26':'gaussmf',[13.7885793762749 5.99998342324126]
MF27='in1mf27':'gaussmf',[13.7886443532014 5.00028553402236]
MF28='in1mf28':'gaussmf',[13.7885826247576 7.99999725649094]

[Input2]
Name='in2'
Range=[1 79]
NumMFs=28
MF1='in2mf1':'gaussmf',[13.7874712937645 7.99892147819958]
MF2='in2mf2':'gaussmf',[13.7885452415155 4.99996837191323]
MF3='in2mf3':'gaussmf',[13.788767359398 6.00025645393153]
MF4='in2mf4':'gaussmf',[13.788335090615 11.9998303927488]
MF5='in2mf5':'gaussmf',[13.7896650529975 9.00088123628266]
MF6='in2mf6':'gaussmf',[13.7885799229285 10.000011806689]
MF7='in2mf7':'gaussmf',[13.788585490763 25.9999987289876]
MF8='in2mf8':'gaussmf',[13.7885474213368 10.9999851443871]
MF9='in2mf9':'gaussmf',[13.7885798189959 1.99999859281522]
MF10='in2mf10':'gaussmf',[13.7875955998786 47.0004567406339]
MF11='in2mf11':'gaussmf',[13.788436742188 10.9999623049682]
MF12='in2mf12':'gaussmf',[13.7886510026341 21.0002035639603]
MF13='in2mf13':'gaussmf',[13.7885906812275 13.0000049872946]
MF14='in2mf14':'gaussmf',[13.7885778817618 73.0000087942471]
MF15='in2mf15':'gaussmf',[13.7885822328049 9.99999999978021]
MF16='in2mf16':'gaussmf',[13.7885809949686 79.0000010864767]
MF17='in2mf17':'gaussmf',[13.7885786568309 39.0000002746357]
MF18='in2mf18':'gaussmf',[13.7885698470766 53.9999924226066]
MF19='in2mf19':'gaussmf',[13.788572853402 12.9999865630233]
MF20='in2mf20':'gaussmf',[13.7904872224745 35.9988544965694]
MF21='in2mf21':'gaussmf',[13.7885840402734 13.9999943630411]
MF22='in2mf22':'gaussmf',[13.7887598486209 58.0001371292173]
MF23='in2mf23':'gaussmf',[13.788555486147 7.99998591315297]
MF24='in2mf24':'gaussmf',[13.7885823410876 10.999998887538]
MF25='in2mf25':'gaussmf',[13.7885440319096 41.9999842029195]
MF26='in2mf26':'gaussmf',[13.7886038138004 9.99999787796662]
MF27='in2mf27':'gaussmf',[13.7887194538361 25.9994795970838]
MF28='in2mf28':'gaussmf',[13.7885979582048 33.9999975841266]

[Input3]
Name='in3'
Range=[34 302]
```

```
NumMFs=28
MF1='in3mf1':'gaussmf',[47.3756709862444148.999649375775]
MF2='in3mf2':'gaussmf',[47.3761415029086141.999996350736]
MF3='in3mf3':'gaussmf',[47.3762207631041138.00008642151]
MF4='in3mf4':'gaussmf',[47.3761512687661142.000012675253]
MF5='in3mf5':'gaussmf',[47.3765421650898152.000339052881]
MF6='in3mf6':'gaussmf',[47.3761525668339154.999995253584]
MF7='in3mf7':'gaussmf',[47.3761535101057131.999999925717]
MF8='in3mf8':'gaussmf',[47.3761430191315149.999984849764]
MF9='in3mf9':'gaussmf',[47.3761473012466 33.9999984580962]
MF10='in3mf10':'gaussmf',[47.37613622589381 73.0000044025 53]
MF11='in3mf11':'gaussmf',[47.3760909511838137.999926121256]
MF12='in3mf12':'gaussmf',[47.3765583161983139.000256860743]
MF13='in3mf13':'gaussmf',[47.3761564694532128.000005917858]
MF14='in3mf14':'gaussmf',[47.3761511209684169.000005321015]
MF15='in3mf15':'gaussmf',[47.3761543394974135.000000000006]
MF16='in3mf16':'gaussmf',[47.376154269367150.999999816916]
MF17='in3mf17':'gaussmf',[47.3761431099014300.000002420124]
MF18='in3mf18':'gaussmf',[47.3761533892352169.99999969458]
MF19='in3mf19':'gaussmf',[47.3761478292513184.000005530509]
MF20='in3mf20':'gaussmf',[47.3761729044144131.0000524631]
MF21='in3mf21':'gaussmf',[47.3761508444103302.000004449734]
MF22='in3mf22':'gaussmf',[47.3761735351144140.000028389578]
MF23='in3mf23':'gaussmf',[47.3761544478268143.00000104424]
MF24='in3mf24':'gaussmf',[47.3761529397446145.999997079112]
MF25='in3mf25':'gaussmf',[47.3761463978576193.000008460845]
MF26='in3mf26':'gaussmf',[47.3761560612092140.999998554479]
MF27='in3mf27':'gaussmf',[47.377121738472213.999378483707]
MF28='in3mf28':'gaussmf',[47.3761619286253129.000006186691]

[Input4]
Name='in4'
Range=[0 63]
NumMFs=28
MF1='in4mf1':'gaussmf',[11.1355497061568 12.0017092092006]
MF2='in4mf2':'gaussmf',[11.1368803647054 17.9999623621159]
MF3='in4mf3':'gaussmf',[11.1406251530404 37.0017725758196]
MF4='in4mf4':'gaussmf',[11.137090582141 16.999982840282]
MF5='in4mf5':'gaussmf',[11.1372679384935 0.000855195956750406]
MF6='in4mf6':'gaussmf',[11.1369304369495 4.00000918960865]
MF7='in4mf7':'gaussmf',[11.1369241482671 21.0000082890013]
MF8='in4mf8':'gaussmf',[11.1368896308532 38.9999273439181]
MF9='in4mf9':'gaussmf',[11.1369303855826 14.0000147838788]
MF10='in4mf10':'gaussmf',[11.1368873022127-9.35336410255384e-005]
MF11='in4mf11':'gaussmf',[11.1369811359785 57.999784553431]
MF12='in4mf12':'gaussmf',[11.1372864883825 62.999503712504]
MF13='in4mf13':'gaussmf',[11.1369768658443 5.60707925878016e-005]
MF14='in4mf14':'gaussmf',[11.1370322300606 41.9999645979043]
MF15='in4mf15':'gaussmf',[11.1369318038628 18.0000000002693]
MF16='in4mf16':'gaussmf',[11.1369079280597 0.999993260298189]
MF17='in4mf17':'gaussmf',[11.1369164462713 50.9999997942781]
MF18='in4mf18':'gaussmf',[11.1368805719129 14.9999796667079]
MF19='in4mf19':'gaussmf',[11.1369285579536 59.9999939403885]
```

```
MF20='in4mf20':'gaussmf',[11.1373096517696 1.00051533842489]
MF21='in4mf21':'gaussmf',[11.1369169354488 21.9999194508064]
MF22='in4mf22':'gaussmf',[11.1369501042309 39.0000519573287]
MF23='in4mf23':'gaussmf',[11.1369178574018 46.000011071821]
MF24='in4mf24':'gaussmf',[11.137041451765 20.0000849594401]
MF25='in4mf25':'gaussmf',[11.1368950137178 46.0000253989682]
MF26='in4mf26':'gaussmf',[11.1369969885842 15.0000150038764]
MF27='in4mf27':'gaussmf',[11.1377736876357 55.0012195556629]
MF28='in4mf28':'gaussmf',[11.1369574280233 25.9999843046497]

[Input5]
Name='in5'
Range=[0 43]
NumMFs=28
MF1='in5mf1':'gaussmf',[7.59926459188048 8.0020715093402]
MF2='in5mf2':'gaussmf',[7.60132213765624 25.0002609302061]
MF3='in5mf3':'gaussmf',[7.60157934042515 13.0004553061719]
MF4='in5mf4':'gaussmf',[7.60186916330255 15.0002868204589]
MF5='in5mf5':'gaussmf',[7.60269984716425 0.00145875652658039]
MF6='in5mf6':'gaussmf',[7.60139833992624 2.00000888225644]
MF7='in5mf7':'gaussmf',[7.60146242257518 42.9999627012554]
MF8='in5mf8':'gaussmf',[7.60134964842517 27.999907675912]
MF9='in5mf9':'gaussmf',[7.60139870135319 5.00001238355857]
MF10='in5mf10':'gaussmf',[7.60113968596479-0.00027271516952573]
MF11='in5mf11':'gaussmf',[7.60136888108471 16.0000032202041]
MF12='in5mf12':'gaussmf',[7.6017941277505 37.0006899373548]
MF13='in5mf13':'gaussmf',[7.60148329449408 1.00009211073052]
MF14='in5mf14':'gaussmf',[7.60152633665644 11.0000310920049]
MF15='in5mf15':'gaussmf',[7.60139789752608 11.000000000101]
MF16='in5mf16':'gaussmf',[7.60138610119228-5.36643470984109e-006]
MF17='in5mf17':'gaussmf',[7.60140100996985 38.0000053289007]
MF18='in5mf18':'gaussmf',[7.60133481884519 29.0000250455709]
MF19='in5mf19':'gaussmf',[7.60109358910675 15.9998894778132]
MF20='in5mf20':'gaussmf',[7.60259869276335 0.00116235805383418]
MF21='in5mf21':'gaussmf',[7.60146514615021 12.9999374611743]
MF22='in5mf22':'gaussmf',[7.60162482294568 16.9998418148056]
MF23='in5mf23':'gaussmf',[7.60140387421992 10.999996561519]
MF24='in5mf24':'gaussmf',[7.60122605143318 29.000038661513]
MF25='in5mf25':'gaussmf',[7.60131437805835 31.0000811517335]
MF26='in5mf26':'gaussmf',[7.60132096492219 35.0001558782512]
MF27='in5mf27':'gaussmf',[7.60235155037974 41.9984692050973]
MF28='in5mf28':'gaussmf',[7.60148198759842 16.000057753279]

[Input6]
Name='in6'
Range=[0 44]
NumMFs=28
MF1='in6mf1':'gaussmf',[7.77777681213287 5.00107226347141]
MF2='in6mf2':'gaussmf',[7.77818466999869 6.00001115672066]
MF3='in6mf3':'gaussmf',[7.77849007414464 4.00098522961423]
MF4='in6mf4':'gaussmf',[7.77796007418371 25.9999145020677]
MF5='in6mf5':'gaussmf',[7.77864315757405 0.00119808129188027]
MF6='in6mf6':'gaussmf',[7.77817523664121 4.99998816199959]
```

```
MF7='in6mf7':'gaussmf',[7.77814839821338 0.999984732712118]
MF8='in6mf8':'gaussmf',[7.77831904565211 15.0000042178203]
MF9='in6mf9':'gaussmf',[7.77817571970581 1.00000639081919]
MF10='in6mf10':'gaussmf',[7.77813754727103-0.000116187909116826]
MF11='in6mf11':'gaussmf',[7.77841028409561 6.99952402153888]
MF12='in6mf12':'gaussmf',[7.77840383809685 10.9994677611237]
MF13='in6mf13':'gaussmf',[7.77818193833618 3.00002338568721]
MF14='in6mf14':'gaussmf',[7.77811853329801 14.000084095572]
MF15='in6mf15':'gaussmf',[7.77817458726864 44.0000000010939]
MF16='in6mf16':'gaussmf',[7.77816637248174 1.99999517328402]
MF17='in6mf17':'gaussmf',[7.77818814812492 24.9999977992609]
MF18='in6mf18':'gaussmf',[7.77816705696754 20.0000077417621]
MF19='in6mf19':'gaussmf',[7.77801302461623 27.0000792169191]
MF20='in6mf20':'gaussmf',[7.77862977248134 0.0007371677387927 42]
MF21='in6mf21':'gaussmf',[7.7781786309481 5.99998100382059]
MF22='in6mf22':'gaussmf',[7.7786147254641 5.00033157747811]
MF23='in6mf23':'gaussmf',[7.7781910780137 37.9999904630284]
MF24='in6mf24':'gaussmf',[7.77817158149271 2.99998436753166]
MF25='in6mf25':'gaussmf',[7.77806225381182 23.0000419033875]
MF26='in6mf26':'gaussmf',[7.77809879032444 28.9999109166023]
MF27='in6mf27':'gaussmf',[7.77854022911812 7.00110008737918]
MF28='in6mf28':'gaussmf',[7.77835141796003 37.9998976175329]

[Input7]
Name='in7'
Range=[21 487]
NumMFs=28
MF1='in7mf1':'gaussmf',[82.3778645561421 50.9997891370676]
MF2='in7mf2':'gaussmf',[82.3779423732722113.000004768913]
MF3='in7mf3':'gaussmf',[82.3779444236336103.999999015086]
MF4='in7mf4':'gaussmf',[82.3779614226838116.000023395654]
MF5='in7mf5':'gaussmf',[82.3781957992333102.000061003014]
MF6='in7mf6':'gaussmf',[82.37794827213573 67.00000117177]
MF7='in7mf7':'gaussmf',[82.3779375579068 87.9999973505523]
MF8='in7mf8':'gaussmf',[82.37794687359021 58.999999003701]
MF9='in7mf9':'gaussmf',[82.3779500839988110.000003389708]
MF10='in7mf10':'gaussmf',[82.3779452947135 97.0000041911469]
MF11='in7mf11':'gaussmf',[82.3779378597246105.000000966963]
MF12='in7mf12':'gaussmf',[82.3781801589073398.999848538774]
MF13='in7mf13':'gaussmf',[82.3779917024653285.999977553512]
MF14='in7mf14':'gaussmf',[82.3778994493483 45.000016306329]
MF15='in7mf15':'gaussmf',[82.3779400081906 99.9999999999845]
MF16='in7mf16':'gaussmf',[82.3779396016493452.000000325067]
MF17='in7mf17':'gaussmf',[82.3779437382521486.999999097207]
MF18='in7mf18':'gaussmf',[82.377938669964 11.000000901985]
MF19='in7mf19':'gaussmf',[82.3779373054853465.000002997372]
MF20='in7mf20':'gaussmf',[82.3780397189137 79.0000607318225]
MF21='in7mf21':'gaussmf',[82.377939250243108.99999984321]
MF22='in7mf22':'gaussmf',[82.3781408551459103.000068496496]
MF23='in7mf23':'gaussmf',[82.3779397980624102.000000228715]
MF24='in7mf24':'gaussmf',[82.3779401086157 94.0000004931807]
MF25='in7mf25':'gaussmf',[82.3779356283345114.000000147445]
MF26='in7mf26':'gaussmf',[82.3779196170231112.999980771133]
```

```
MF27='in7mf27':'gaussmf',[82.3784916658578267.000361833462]
MF28='in7mf28':'gaussmf',[82.3779409527934 96.0000015023281]

[Output1]
Name='out1'
Range=[1 3]
NumMFs=28
MF1='out1mf1':'linear',[0.158846382660904 0.0587524383286939
0.0104779451703429-0.0370191946309623-0.0876483038777152
0.010253761724145 0.0140654173728168 0.00464357845222863]
MF2='out1mf2':'linear',[0.056183456285464 4-0.0153538376101239
0.00351808780979215-0.0140714419182644 0.0663210539572894
0.0875780159085567 0.00614975520482215 0.00188076681864329]
MF3='out1mf3':'linear',[0.0771575118801949 0.00602401730324073
0.00573641943181894 0.0612813618447968 0.0205588224957719-
0.00696519655375428-0.00119084360816463 0.00510760016191922]
MF4='out1mf4':'linear',[-0.025549563984591-0.00856225774008171
0.010575242130827 0.0242685569659812 0.0277813718744204-
0.0822692984282304 0.0264873429395337 0.0011574345174786]
MF5='out1mf5':'lin-
ear',[0.00695797394114312-0.127189981062661-0.00204236276384948
0.0293665535841354 0.120492276604518 0.106687603509042
0.0159323790945404 0.01108662376174]
MF6='out1mf6':'linear',[-0.000416324454824522-0.00151757080354308
0.00361230326976529-0.00133084838485524 0.000203045717135199
0.00141352351047578 0.00391956578751069 4.12688331443791e-005]
MF7='out1mf7':'linear',[-0.00419845760335789 0.0226446647083472
0.00256968656337916-0.0107546464199351 0.0500800564999357-
0.0014217766944071 0.00182917280404271 0.00013449845027435]
MF8='out1mf8':'linear',[0.0116583687024116-0.0126741278595615
0.00512502020543052 0.0202400892028078 0.0344207887479192
0.0185838174334332 0.000453005093695126 0.000564346728511731]
MF9='out1mf9':'linear',[-0.0127816846574794-0.0209673073280881
0.00969213601412203 0.0129725886787988-0.00551790752328125
0.0129331927113231 0.014632544602351-0.00039174383645203]
MF10='out1mf10':'linear',[0.00359898906580869-0.0485411108960952
0.0207346430307942 0.011980358698493 0.0403400019994528
0.00980035383201311 0.00792287700255176 0.000845836281415888]
MF11='out1mf11':'linear',[-0.0283134574554906 0.00332062683414345-
0.0214546139618103 0.0931928969603685 0.0141216627902833
0.0123279923002054 0.00156165279495802 0.000680869200657812]
MF12='out1mf12':'linear',[0.000101166093010777 0.000403507680235701
0.00109928818396514 0.00101735137783403 0.000668690221527047
4.71696511125267e-005 0.00683352697063924 1.28815709764724e-005]
MF13='out1mf13':'lin
ear',[-0.000114367356941918-0.000758903843047438-0.0119427989199992-
0.00160690380427125-0.00132885533423678-0.000585425533694486
0.0124671775265036-6.9607241413189e-005]
MF14='out1mf14':'linear',[0.000136549603645853 0.00142100694334504
0.00328543512002408 0.00081802427513195 0.000216667993194162
0.000269958329777766 0.00664903056064466 1.95107510170207e-005]
MF15='out1mf15':'linear',[0.00641451006328544 0.000811959297538643
0.0109612834116412 0.00146149834039186 0.000893146340533295
```

0.0035726198812947 0.00811953704924713 8.11958546806982e-005]
MF16='out1mf16':'linear',[5.12886474046489e-005 0.000676538585548326
0.00129129993822092 8.61047157629884e-006 1.32638361333705e-008
1.7162599349221e-005 0.00387430673238141 8.55504908837456e-006]
MF17='out1mf17':'linear',[6.24850939918067e-005 0.000352068233390456
0.00269330873407931 0.000457107679845885 0.000341713843445802
0.000224290314510362 0.00438520432215799 8.94729883452548e-006]
MF18='out1mf18':'linear',[8.75680326374059e-005 0.000807171530695437
0.00249906228322489 0.000217361779250552 0.000427787404873433
0.00029149640301829 0.00610454869020792 1.46937920108882e-005]
MF19='out1mf19':'linear',[0.000221113022605768 0.000106454301108803
0.00111589245942067 0.000600296087796417 3.28973817280287e-005
0.000305185445350886 0.00590207883245058 7.33698158494062e-006]
MF20='out1mf20':'linear',[0.0066840433251709 0.0610534050657449
0.0109372213148057-0.0179998483230184-0.0151730396443169-
0.0107024610472769-0.0236470423788051 0.000276965249035705]
MF21='out1mf21':'linear',[0.00901465034762551-0.000999453279116807
0.016184986728107-0.00618808081049198 0.0010621464323299-
0.000717224989598662-0.0269962670071518-0.000241701267939011]
MF22='out1mf22':'linear',[0.00055474984387186 0.0086069407791468
0.00951125561311244 0.0038317206573539 0.0015686491021937
0.000399332238451362 0.00964852106772644 9.80641012661468e-005]
MF23='out1mf23':'linear',[0.000797425700368113 0.00096186270877293
0.0121195676344536 0.00557469327267542 0.000985904375379471
0.00425215003845595 0.00810863388541316 9.63589561592896e-005]
MF24='out1mf24':'linear',[0.0140310455236635-0.0012777709194829
0.016021620133379-0.00239745327958035 0.0107637323450148
0.000258682356176569-0.00313102519244721 8.01329554874265e-005]
MF25='out1mf25':'linear',[0.00114292289269646 0.00679771003613147
0.0136098160326833 0.00433507533328529 0.00402201620172893
0.00281520882315064-0.0027342223715192 9.00247202419326e-005]
MF26='out1mf26':'linear',[5.01342475587267e-005 0.000261215854896123
0.0374245739060928 0.00391059752847331 0.0178064251250527
0.00334905780515485-0.0272206701833488 0.000310550975448819]
MF27='out1mf27':'linear',[7.88255983582174e-006 0.00137121849601779
0.00470065744816945 0.00181184076259553 0.00214164927808507-
0.000498257054942344 0.00676079022483021 2.43537423742934e-005]
MF28='out1mf28':'linear',[0.00149221357802887 0.0126900386297353
0.0146145949980682 0.00789759690870224 0.00261798008022367
0.0093755718578698 0.00177123959808159 0.000179511639465914]

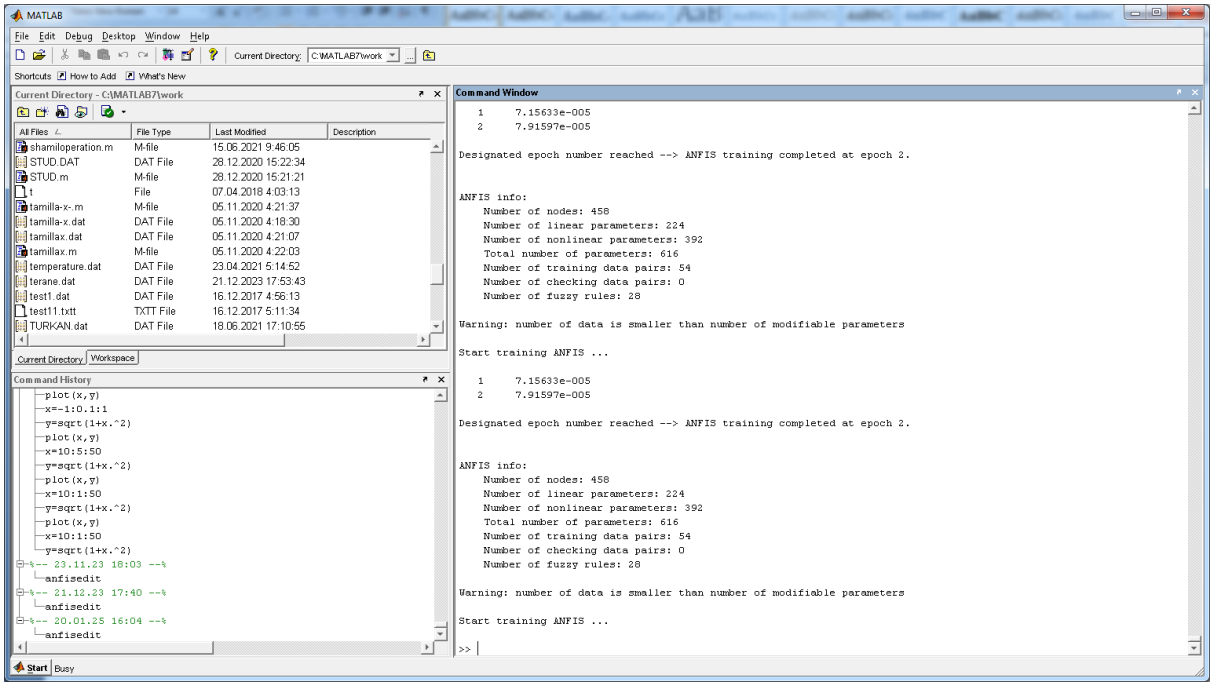
MATLAB
File Edit Debug Desktop Window Help
Current Directory: C:\MATLAB7\work
Shortcuts How to Add What's New
Current Directory - C:\MATLAB7\work
All Files File Type Last Modified Description
shamiloperation.m M-file 15.06.2021 9:46:05
STUD.DAT DAT File 28.12.2020 15:22:34
STUD.m M-file 28.12.2020 15:21:21
t File 07.04.2018 4:03:13
tamilla-x-.m M-file 05.11.2020 4:21:37
tamilla-x.dat DAT File 05.11.2020 4:18:30
tamillax.dat DAT File 05.11.2020 4:21:07
tamillax.m M-file 05.11.2020 4:22:03
temperature.dat DAT File 23.04.2021 5:14:52
terane.dat DAT File 21.12.2023 17:53:43
test1.dat DAT File 16.12.2017 4:56:13
test11.txtt TXTT File 16.12.2017 5:11:34
TURKAN.dat DAT File 18.06.2021 17:10:55
Current Directory Workspace
Command History
plot(x,y)
x=-1:0.1:1
y=sqrt(1+x.^2)
plot(x,y)
x=10:5:50
y=sqrt(1+x.^2)
plot(x,y)
x=10:1:50
y=sqrt(1+x.^2)
plot(x,y)
x=10:1:50
y=sqrt(1+x.^2)
%-- 23.11.23 18:03 --%
anfisedit
%-- 21.12.23 17:40 --%
anfisedit
%-- 20.01.25 16:04 --%
anfisedit
Command Window
1 7.15633e-005
2 7.91597e-005
Designated epoch number reached --> ANFIS training completed at epoch 2.
ANFIS info:
Number of nodes: 458
Number of linear parameters: 224
Number of nonlinear parameters: 392
Total number of parameters: 616
Number of training data pairs: 54
Number of checking data pairs: 0
Number of fuzzy rules: 28
Warning: number of data is smaller than number of modifiable parameters
Start training ANFIS ...
1 7.15633e-005
2 7.91597e-005
Designated epoch number reached --> ANFIS training completed at epoch 2.
ANFIS info:
Number of nodes: 458
Number of linear parameters: 224
Number of nonlinear parameters: 392
Total number of parameters: 616
Number of training data pairs: 54
Number of checking data pairs: 0
Number of fuzzy rules: 28
Warning: number of data is smaller than number of modifiable parameters
Start training ANFIS ...
>>
Start Busy

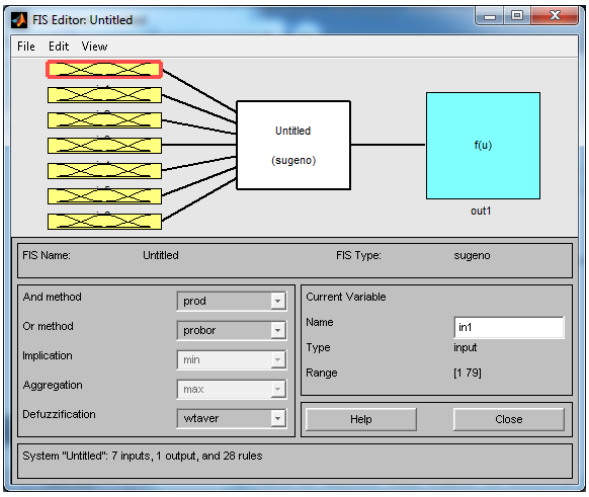
FIS Editor: Untitled
File Edit View
Untitled
(sugeno)
f(u)
out1
FIS Name: Untitled
FIS Type: sugeno
And method prod
Or method probor
Implication min
Aggregation max
Defuzzification wtaver
Current Variable
Name in1
Type input
Range [1 79]
Help
Close
System "Untitled": 7 inputs, 1 output, and 28 rules

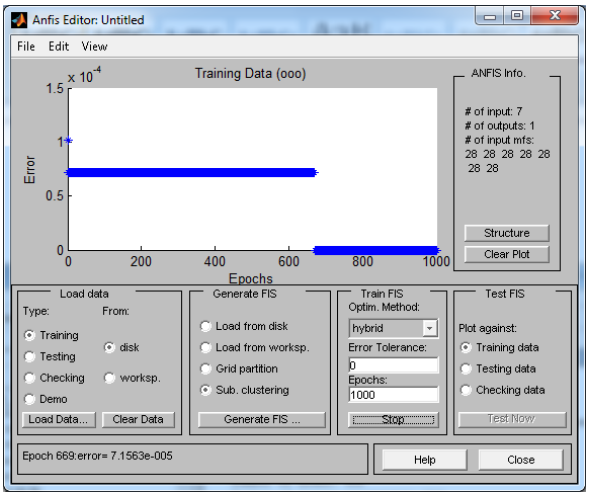
Anfis Editor: Untitled
File Edit View
Training Data (ooo)
x 10^-4
Error
Epochs
ANFIS Info.
# of input: 7
# of outputs: 1
# of input mfs:
28 28 28 28 28 28 28
Structure
Clear Plot
Load data
Type: From:
Training
Testing
Checking
Demo
disk
worksp.
Generate FIS
Load from disk
Load from worksp.
Grid partition
Sub. clustering
Load Data...
Clear Data
Generate FIS ...
Train FIS
Optim. Method: hybrid
Error Tolerance: 0
Epochs: 1000
Stop
Test FIS
Plot against:
Training data
Testing data
Checking data
Test Now
Epoch 669:error= 7.1563e-005
Help
Close

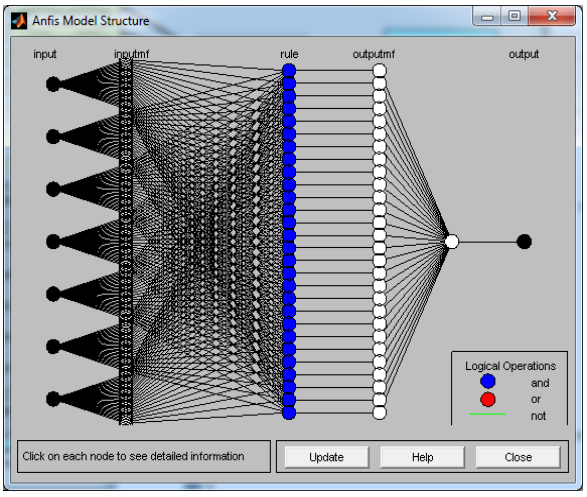
Anfis Model Structure
input
inputmf
rule
outputmf
output
Logical Operations
and
or
not
Click on each node to see detailed information
Update
Help
Close

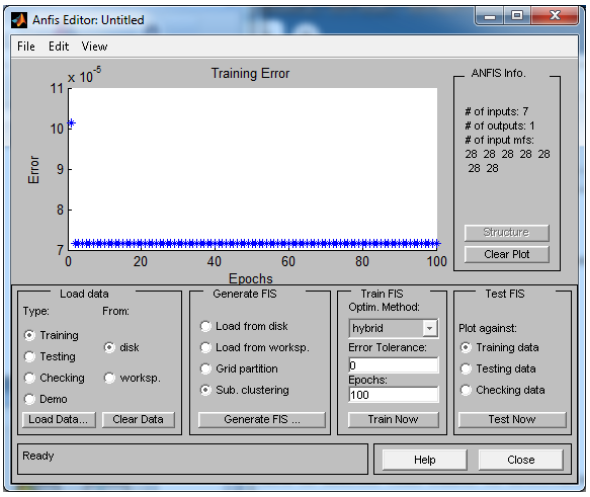
Anfis Editor: Untitled
File Edit View
Training Error
x 10^-5
Error
Epochs
ANFIS Info.
# of inputs: 7
# of outputs: 1
# of input mfs:
28 28 28 28 28 28 28
Structure
Clear Plot
Load data
Type: From:
Training
Testing
Checking
Demo
disk
worksp.
Generate FIS
Load from disk
Load from worksp.
Grid partition
Sub. clustering
Load Data...
Clear Data
Generate FIS ...
Train FIS
Optim. Method: hybrid
Error Tolerance: 0
Epochs: 100
Train Now
Test FIS
Plot against:
Training data
Testing data
Checking data
Test Now
Ready
Help
Close

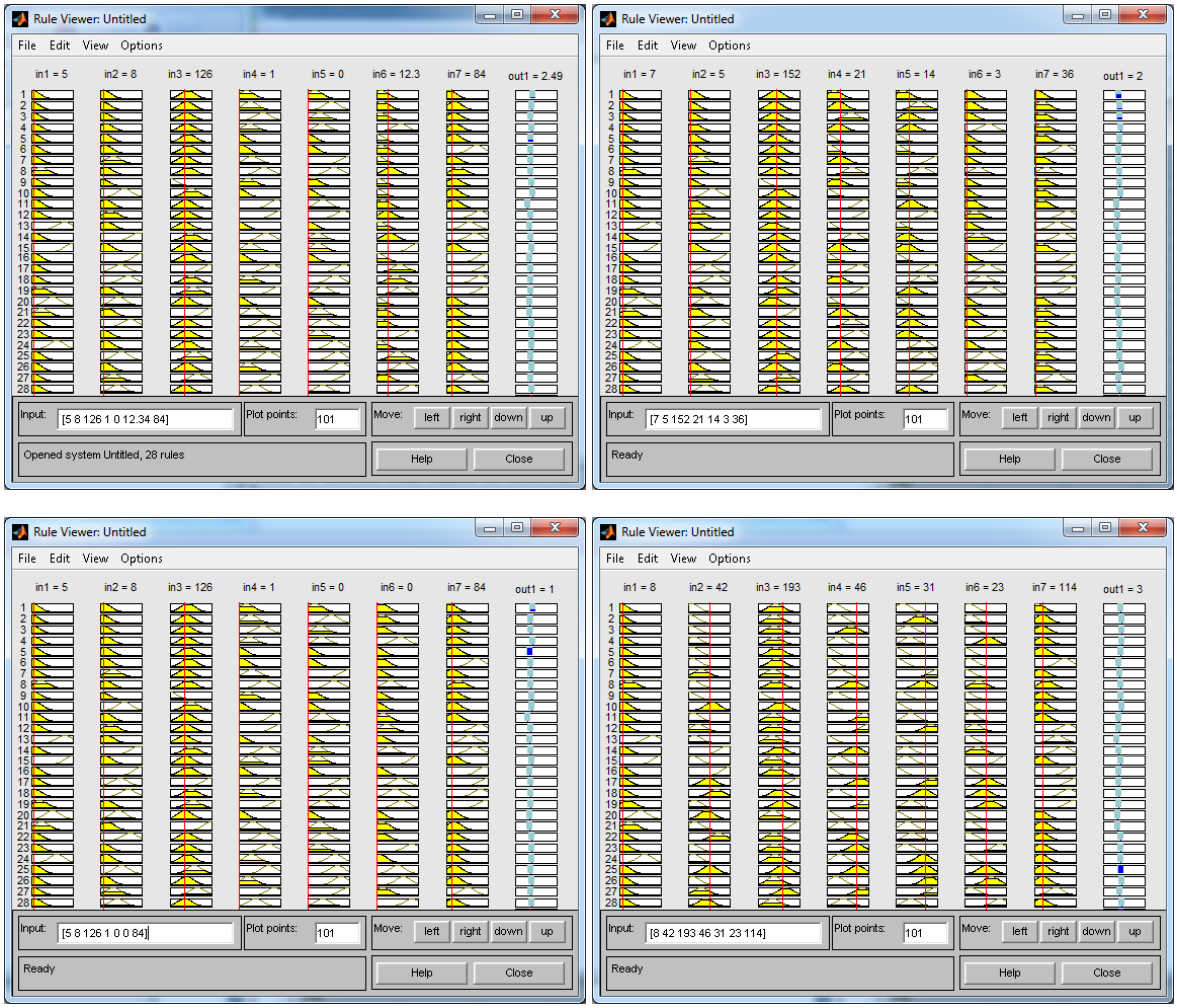

References

Cherenkov V. G. // Clinical oncology // – Moscow, Russia, 2010.
Litvin A. A., Litvin V. A. //Decision support systems in surgery // – Minsk, Belarus. 2018.
Aliyev R. A., Aliyev R. R. // Theory of Intelligent Systems // – Baku, Azerbaijan, 2001.
Congress // Information technologies in medicine // Tech LAB platform, – Moscow, 2021.
Lugovskaya S. A., Pochtar M. E. // Hematological Atlas // – Moscow, 2018.

submitted 17.03.2025;
accepted for publication 21.03.2025;
published 29.05.2025

Contact: taranahaciyeva@yandex.com

The Austrian Journal of Technical and Natural Sciences, No 3–4
ISSN 2310-5607

PREMIER Publishing
ppublishing.org

DOI:10.29013/AJT-25-3.4-119-123

STUDY OF THE INTERACTION OF COMPONENTS IN THE $NiSO_4$ – $(NH_4)_2SO_4$ – H_2O SYSTEM

Hakimova Xurshida Nosirjanovna [1], Maxkamova Dilnoza Ne'matjon qizi [1], Latifov Muhammadbobur Zokirjon o'g'li [1], Turayev Zokirjon [1]

[1] Namangan State Technical University, Republic of Uzbekistan, Namangan

Cite: *Hakimova X.N., Maxkamova D.N., Latifov M.Z., Turayev Z. (2025). Study of the Interaction of Components in the* $NiSO_4$ – $(NH_4)_2SO_4$ – H_2O *System. Austrian Journal of Technical and Natural Sciences 2025, No 3–4.* https://doi.org/10.29013/AJT-25-3.4-119-123

Abstract

To study the interaction of components in the $NiSO_4$ – $(NH_4)_2SO_4$ – H_2O system, the inflection point associated with the formation of a new phase was studied using the isomolar series method. Through this method, the interaction of nickel sulfate and ammonium sulfate in different ratios was theoretically substantiated.

Keywords: *nickel sulfate, ammonium sulfate, isomolar sequence method, pH value, density, viscosity, refractive index, crystallization temperature*

Introduction

In recent years, much research has been conducted to improve the yield and quality of agricultural crops. Proper and balanced plant nutrition with micronutrients is one of the necessary conditions for maximizing the potential yield of agricultural crops (Kulikova A. Kh., Cherkasov E. A., 2014, p. 9–25).

Microelements are not only involved in all processes of plant development and growth and are the main components of many enzymes, but are also active catalysts that accelerate a number of biochemical reactions (Kulikova A. Kh., Cherkasov E. A., 2014, p. 45–50). At the same time, micronutrients build plant immunity against bacterial and fungal diseases and increase their resistance to adverse environmental conditions, such as heat, drought, and rapid climate change (Ageev V. V., Podkolzin A. I., 2001).

The microelement nickel is one of the 17 essential elements that are important for plant development and growth (Liu G. D. 2001, p. 101–103). When nickel microelement deficiency is observed, it can directly affect symbiotic N2 fixation, which is associated with a decrease in the activity of the symbiotic hydrogenase enzyme of the bacterium Rhizobium leguminosarum (Zobiole, L. H. S., Oliveira Jr, R. S., Kremer, R. J., Constantin, J., Yamada, T., Castro, C., & Oliveira Jr. A., 2010, p. 176–180).

Nickel is a microelement that is a component of metalloenzymes essential for life, such as carbon monoxide dehydrogenase (EC 1.2.99.2), acetyl coenzyme-A synthase (EC 2.3.1.169), acireductone dioxygenase (EC 1.13.11.54), Ni superoxide dismutase (EC 1.15.1.1.), glyoxylase (EC 4.4.1.5), urease (EC 3.5.1.5), and hydrogenase

(EC 1.12.1.2.) (Harasim P., Filipek T., 2015).

In plants, nickel is mainly absorbed through the roots, a process that occurs through passive diffusion or active transport mechanisms that require energy. Passive diffusion refers to the spontaneous movement of nickel depending on the concentration difference, while active transport occurs with the help of special proteins and with the expenditure of metabolic energy, maintaining the amount of nickel necessary for plant life (Seregin I. V., Kozhevnikova A. D., 2006, p. 257–277).

The microelement nickel plays an important role in all physiological processes in plants, from seed germination to fruiting. Without this element, plants cannot complete the full stages of ontogenesis. At the same time, high levels of nickel disrupt water metabolism, mineral nutrition, and chlorophyll structure, reducing the efficiency of photosynthesis and plant productivity (Patra A., Pradhan S. N., Dutta A., Mohopatra K. K., 2020, p. 35–37).

One of the most effective ways to obtain agricultural products of high consumer quality is to adjust the conditions for plant nutrition, that is, to establish the correct ratios between micro- and macroelements and to determine optimal doses (Pisarev B. A. 1972; Karimova V. B., Nazmieva R. R., Safiullina G. F., Zamalieva F. F., 2005, p. 171–178; Kulanovskaya T. N., 1990; Dilnoza M., Zokirjon T., Dilshoda R., 2023, p. 17–20; Xurshida H., Dilnoza M., Malika M., Zokirjon T., 2025, p. 50–53; Ne'matjon qizi Makhkamova D., Turayev Z., 2024, p. 137–144).

Microelements applied in the right amount to fertilizers improve all vital processes of the plant, including photosynthesis and mineral nutrition, and contribute to their rapid and healthy development. Therefore, the isomolar sequence method (Namangan State University. 2024, p. 145–146) was used to determine their quantity and norms when applying microelements to fertilizers.

To study the interaction of components in the $NiSO_4 – (NH_4)_2SO_4 – H_2O$ system, the inflection point associated with the formation of a new phase was studied using the isomolar series method. Through this method, the interaction of nickel sulfate and ammonium sulfate in different ratios was theoretically substantiated. During the study, isomolar solutions of components with the same molar concentration were mixed in certain ratios based on the isomolar series method, and experimental analyses were carried out while maintaining a constant sum of the initial volumes. Based on the results obtained, the complex formation process of nickel sulfate and ammonium sulfate was explained using graphical analysis.

Materials and Methods

To theoretically substantiate the interaction of nickel sulfate and ammonium sulfate, the physicochemical properties of diluted solutions were analyzed using the isomolar series method by measuring the pH, density, refractive index, and viscosity values of the 0.01 M solution mixture based on the ratio of components in the ($NiSO_4$ (0.01 M)) : (($(NH_4)_2SO_4$ (0.01 M)) system.

For the study, 0.01 M nickel sulfate and 0.01 M ammonium sulfate solutions were initially prepared. Then, a gradually increasing amount of ammonium sulfate solution was added to the nickel sulfate solution. The pH value, refractive index, viscosity, and density of the resulting mixtures were determined. All measurements were carried out in a water thermostat at a temperature of 20 ± 0.1 °C.

The kinematic viscosity of the solution was measured with an accuracy of $\pm 0.0001 \cdot 10^{-1}$ mm²/s using a 0.82 mm diameter VPJ-4 capillary viscometer. The relative density was determined using a pycnometric analysis method (Zdanovsky A. B., Hallurgy, 1972). The pH of the solution was measured using a FiveGo™ F2 Mettler-Toledo pH apparatus.

The results of the dependence of the change in the physicochemical properties of solutions on the ratio of components in the $NiSO_4$ and $(NH_4)_2SO_4$ system are shown in Table 1and Figure 1.

Results and discussion

Analysis of the "pH - composition" diagram in the system ($NiSO_4$ (0.01M)): :(($(NH_4)_2SO_4$ (0.01 M)) shows that with an increase in the amount of 0,01 M ammonium sulfate solution from 3 ml to 30 ml, the pH values of the solutions decrease from 6,85 to 6,77, and with a ratio of

($NiSO_4$ (0,01 M)):((NH_4)$_2SO_4$ (0,01M))=5:5, a break is observed at a pH value of 6,68. This characteristic of the pH value change indicates the formation of a new compound resulting from the chemical reaction between ($NiSO_4$ (0,01 M)) and ((NH_4)$_2SO_4$ (0,01 M)).

Figure 1. *Changes in the physicochemical properties of solutions depending on the ratio of components in the system ($NiSO_4$ (0.01 M) + (NH_4)$_2SO_4$ (0.01 M))*

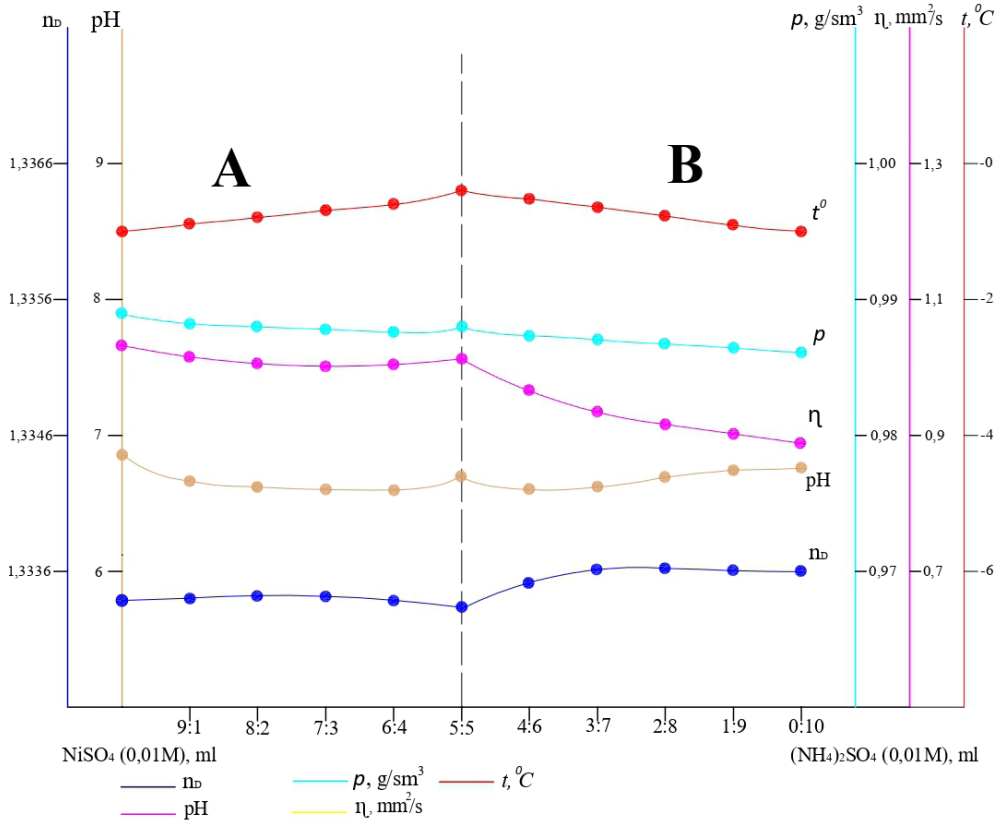

In the "Composition – Density" diagrams, with an increase in the amount of ammonium sulfate and a decrease in the amount of nickel sulfate, the density of the solutions gradually decreases from 0.9889 g/cm^3 to 0.9648 g/cm^3, and a change in the density value to 0.9883 g/cm^3 is observed with a composition ratio of ($NiSO_4$ (0.01 M)):((NH_4)$_2SO_4$ (0.01 M))= = 5:5. This change may be due to the interaction between the ions of the ammonium sulfate and nickel sulfate solutions and the formation of a new compound.

Table 1. *Changes in the physicochemical properties of solutions depending on the ratio of components in the system ($NiSO_4$ (0.01 M) + (NH_4)$_2SO_4$ (0.01 M))*

№	Composition of components		pH	Density, g/cm^3	Viscosity, mm^2/c	Refractive index	Crystallization temprature, °C
	$NiSO_4$, ml	(NH_4)$_2SO_4$, ml					
1	30	0	6,85	0,9889	1,0341	1,33340	-1,0
2	27	3	6,67	0,9883	1,0140	1,33350	–0,9
3	24	6	6,61	0,9879	1,0041	1,33350	–0,8
4	21	9	6,59	0,9878	1,0021	1,33350	–0,7
5	18	12	6,60	0,9876	1,0012	1,33350	–0,6
6	15	15	6,68	0,9883	1,0051	1,33345	–0,4

№	Composition of components		pH	Density, g/cm³	Viscosity, mm²/c	Refractive index	Crystallization temperature, °C
	$NiSO_4$, ml	$(NH_4)_2SO_4$, ml					
7	12	18	6,61	0,9878	0,9651	1,33360	–0,5
8	9	21	6,62	0,9871	0,9361	1,33370	–0,6
9	6	24	6,72	0,9865	0,9142	1,33370	–0,8
10	3	27	6,75	0,9855	0,8960	1,33370	–0,9
11	0	30	6,77	0,9648	0,8810	1,33370	–1,0

Analysis of the data of the "Composition – refractive index" diagram shows that the refractive indices in the system gradually decreased from 1,33340 to 1,33345 up to the ratio ($NiSO_4$ (0.01 M)):($(NH_4)_2SO_4$ (0.01 M))= = 5 : 5, and it can be noted that there was a significant break in the diagram. With increasing ammonium sulfate content in the mixture, the refractive index value continued to decrease to 1,33370.

The viscosity values of the solution of the studied system decrease from 1.0341 mm²/s to 0.8810 mm²/s with a decrease in the amount of 0.01 M nickel sulfate and an increase in the amount of 0.01 M ammonium sulfate, which is also explained by the presence of a breaking point of 1.0051 mm²/s at a ratio of 5:5.

In the "Composition-Crystallization Temperature" diagram, as the amount of 0.01M ammonium sulfate solution increases from 3 ml to 30 ml and the amount of nickel sulfate decreases from 30 ml to 0 ml, the crystallization temperature of the solutions rises from –1 °C to –0.4 °C, with a breaking point observed. Additionally, as the amount of ammonium sulfate in the solution increases, the temperature drops to –1 °C.

Conclusion

In summary, to study the interaction of micronutrient salts with mineral fertilizer components, using 0.01 M solutions of ammonium sulfate and nickel sulfate, an isomolar series method was investigated, and the hydrogen index of the mixtures, density, viscosity, crystallization temperature, and refractive index characteristics were studied.

References

Kulikova A. Kh., Cherkasov E. A. Microelements in soils of the Ulyanovsk region and the efficiency of microelement-containing fertilizers in the cultivation of winter wheat // Bulletin of the Ulyanovsk State Agricultural Academy. 2014. – No. 4 (28). – P. 19–25. (In Russian)

Isakov V. Yu., Isakov M. Yu., Mukimzhonova U. V. K. Microbiogenic elements in the "rock-soil-plant" system on meadow-oasis soils of western Fergana // Universum: chemistry and biology. 2022. – No. 9–1 (99). – P. 45–50.

Ageev V. V., Podkolzin A. I. Fertilizer systems in crop rotations of the South of Russia // VV Ageev, VI Podkolzin/textbook for universities of agronomic specialties – Stavropol: State Educational Institution Stavropol State Agricultural Academy. 2001.

Liu G. D. A new essential mineral element–Nickel //Plant Nutrition and Fertilizer Science. 2001. – T. 7. – No. 1. – P. 101–103.

Zobiole, L. H. S., Oliveira Jr, R. S., Kremer, R. J., Constantin, J., Yamada, T., Castro, C., & Oliveira Jr, A. Effect of glyphosate on symbiotic N2 fixation and nickel concentration in glyphosate-resistant soybeans // Applied Soil Ecology. 2010. – T. 44. – No. 2. – P. 176–180. URL: https://doi.org/10.1016/j.apsoil.2009.12.003Get rights and content

Harasim P., Filipek T. Nickel in the environment // Journal of Elementology. 2015. – T. 20. – № . 2. DOI 10.5601/jelem.2014.19.3.651

Seregin I. V., Kozhevnikova A. D. Physiological role of nickel and its toxic effects on higher plants //Russian journal of plant Physiology. 2006. – T. 53. – P. 257–277. URL: https://doi.org/10.1134/S1021443706020178

Patra A., Pradhan S. N., Dutta A., Mohopatra K. K. Nickel the ultra-micronutrient: Significant for plant growth and metabolism // Food Chem Toxicol. 2020. – T. 1. – P. 35–37.

Pisarev B. A. Methods of increasing potato yields // – Moscow: Mosk. rabochy. – 1972. (In Russian)

Karimova V. B., Nazmieva R. R., Safiullina G. F., Zamalieva F. F. Influence of water-soluble fertilizer “Akvarin” on productivity, yield and structure of potato crop // Scientific works of young scientists of the State Scientific Institution Tatar Research Institute of Agriculture. 2005. – P. 171–178.

Kulanovskaya T. N. Optimization of the agrochemical system of soil nutrition of plants. Moscow: VO Agrokhimizdat, 1990. – 218 p. (In Russian)

Dilnoza M., Zokirjon T., Dilshoda R. The Interaction of salts of Microelements with Components of Mineral Fertilizers //Universum: технические науки. 2023. – No. 5–8 (110). – P. 17–20. DOI – 10.32743/UniTech.2023.110.5.15506

Xurshida H., Dilnoza M., Malika M., Zokirjon T. Study of The Interaction of Components in the Niso4–Kno3–H2o System // Universum: технические науки. 2025. – T. 7. – No. 3 (132). – P. 50–53. DOI – 10.32743/UniTech.2025.132.3.19625

Ne’matjon qizi Makhkamova D., Turayev Z. Studying the Solubility of the System $ZnSO_4$-KNO_3-H_2O // Journal of Chemical Technology and Metallurgy. 2024. – T. 59. – № . 1. – P. 137–144. DOI: https://doi.org/10.59957/jctm.v59.i1.2024.16

Namangan State University. Analytical, physical and colloidal chemistry. – Namangan: NamDU Publishing House, 2024. – 256 p. – P. 145–146. (In Uzbek)

Zdanovsky A. B., Hallurgy. – Leningrad, Chemistry, 1972. (In Russian)

submitted 20.04.2025;
accepted for publication 01.05.2025;
published 29.05.2025

Contact: dilnozamaxkamova_7007@mail.ru

The Austrian Journal of Technical and Natural Sciences, No 3–4
ISSN 2310-5607

PREMIER Publishing
ppublishing.org

DOI:10.29013/AJT-25-3.4-124-129

TECHNOLOGICAL SCHEME AND MATERIAL BALANCE OF THE PRODUCTION OF NITROGEN-CALCIUM FERTILIZERS FROM SODA PLANT SLUDGE WASTE

Ergashev Mansur [1], ***Saidova Durdonakhon*** [1], ***Rajabov Shohrukh*** [1], ***Mirzakulov Kholtura*** [1]

[1] Department of Chemical Technology of Inorganic Substances, Tashkent Institute of Chemical Technology

Cite: *Ergashev M., Saidova D., Rajabov S., Mirzakulov Kh. (2025). Technological Scheme and Material Balance of the Production of Nitrogen-Calcium Fertilizers From Soda Plant Sludge Waste. Austrian Journal of Technical and Natural Sciences 2025, No 3–4.* https://doi.org/10.29013/AJT-25-3.4-124-129

Abstract

Today, the utilization of waste from soda production enterprises and the production of high-quality and profitable products based on them is an urgent problem. Because by utilizing these wastes, a very large environmental problem can be eliminated. In addition, it can be learned from our ongoing research that these wastes are actually raw materials. In particular, this article presents a technological scheme and material flow calculations for obtaining liquid fertilizers containing nutrients such as nitrogen and calcium from sludge waste generated during soda production.

Keywords: *Liquid nitrogen-calcium fertilizers, ammonization, crystallization, filtration, ammonia, nitric acid slurry, calcium nitrate*

Introduction

In recent years, the European Union (EU) and other developed countries have been increasingly interested in renewable energy sources, waste-free technologies, and resource-efficient production methods. In order to ensure economic and environmental efficiency, it is important to optimize the consumption of raw materials, determine the profitability of semi-finished and finished products, analyze them, and manage their material balance of technological processes (European Commission. 2020; ISO 14051:2011).

In the soda ash production industry, large volumes of sludge waste are generated during many technological stages. These wastes mainly contain calcium carbonate ($CaCO_3$), calcium hydroxide ($Ca(OH)_2$), sodium salts, and other useful components, which can be recycled as secondary raw materials (Yunusov A. S., et al., 2019; Yunusov A. S., et al., 2021). However, in practice, these sludges are often dumped into the environment, occupying land resources and increasing environmental hazards (Mamatqulov B., Karimova D., 2020).

At the same time, one of the important factors of sustainable industrial development is the saving of resources through waste recycling and their return to the economy (UNEP. 2019). In this context, the development of a technology for the production of nitrogen-calcium fertilizers from soda ash sludge is scientifically and practically relevant. Such fertilizers contain nitrogen and calcium, which are important in increasing soil fertility, especially in neutralizing acidic soils (Xodjayev B., 2022; Kolesnikov A. A., 2018).

The proposed technological approach allows simultaneously reducing waste, ensuring environmental safety and achieving economic efficiency. At the same time, the material balance compiled for the stages of the process allows for a scientific assessment of production efficiency (Khusanov D. R., 2023). This article reviews the technological scheme for the production of fertilizer from soda ash sludge, its main stages and material balances, and analyzes their efficiency.

The ongoing research work is devoted to the processing of sludge waste generated during the brine washing process at the JV "Kungroat Soda Plant" LLC and the production of liquid nitrogen-calcium fertilizers based on it. In this regard, all technological parameters from raw materials to the process of obtaining finished products have been determined and the results have been presented in the articles (Ergashev M. T., Rajabov Sh.Sh., Mirzakulov X.Ch., 2024; Ergashev M. T., Rajabov Sh.Sh., Mirzakulov X.Ch., 2025).

Research methodology and methods

The main goal of this scientific research work is to develop a technology for producing nitrogen-calcium fertilizer using soda ash sludge waste and determine the material balance of the process. The research was conducted based on the following stages and methods:

1. Experiments with reagents for obtaining nitrogen-calcium fertilizer: The main components of the sludge and their ability to react with other nitrogen compounds were tested. Conditions – factors such as pH level, temperature and mixing speed were determined experimentally.

2. Material balance calculations: The mass of incoming and outgoing substances according to the technological process was calculated. The amount of fertilizer produced was compared with the amount of sludge, ammonium nitrate and other reagents. This created a material balance scheme for production and ensured maximum recycling of waste.

3. Product quality assessment: The physicochemical properties of the obtained nitrogen-calcium fertilizer samples (solubility, crystal size, nitrogen and calcium content) were analyzed in the laboratory in accordance with GOST standards.

Main part: When nitric acid slurry is evaporated to 85% of its initial mass, the content of soluble substances in the composition is as follows: $Mg(NO_3)$-2–9.5%; $Ca(NO_3)$2–56.1%; $Al(NO_3)_3$–0.4%; Fe_2O_3––0.1%; NH_4NO_3–6.1%. The resulting solution can be used as a liquid nitrogen-calcium fertilizer (LNCF-A) containing magnesium.

The resulting solution can be crystallized to obtain calcium nitrate, and the resulting crystals can be filtered and used as a liquid nitrogen-calcium fertilizer (LNCF-B) containing magnesium.

The results of the research work provided the basis for developing a technology for producing liquid nitrogen-calcium and nitrogen-calcium-magnesium fertilizers using sludge waste from a soda plant. The figure below shows the basic technological scheme for the production of liquid nitrogen-calcium fertilizers with and without the separation of calcium nitrate.

The description of this technological scheme is as follows: From the nitric acid tank (1), unconcentrated nitric acid is supplied to the reactor (4) through a pump (2) through a flow meter (3). Sludge waste from the soda plant is supplied from special tanks (5) for sludge collection via a weigher (6). The nitric acid standard is supplied at 100–105% to convert all cations in the sludge into nitrates. Filter washing water is also supplied there. Due to the exothermic nature of the process, the temperature in the reactor (4) is maintained at 45–55 °C. The residence time of the reaction mixture in the reactor is 15–30 minutes.

Then the reaction pulp is sent by gravity to the ammonizer (7), where the excess acid is neutralized with gaseous ammonia. Neutralization is carried out to pH = 5.5–7. In the ammonizer, the conversion of iron and aluminum nitrates into hydroxides, i.e. their transition to

insoluble compounds, also occurs. Then the neutralized pulp is transferred by gravity to a continuously operating centrifuge (8). In the centrifuge, the pulp is separated into liquid and solid phases. The liquid phase is transferred by gravity to a collection tank (9) for the neutralized extract. The insoluble residue of the slurry is sent to the solid phase waste collection. The neutralized extract collected from the collection tank (9) is sent to the consumer as a liquid nitrogen-calcium fertilizer (LNCF-A) or for further processing.

Figure 1. *Basic technological scheme for processing filter press sludge into nitrogen-calcium fertilizers*

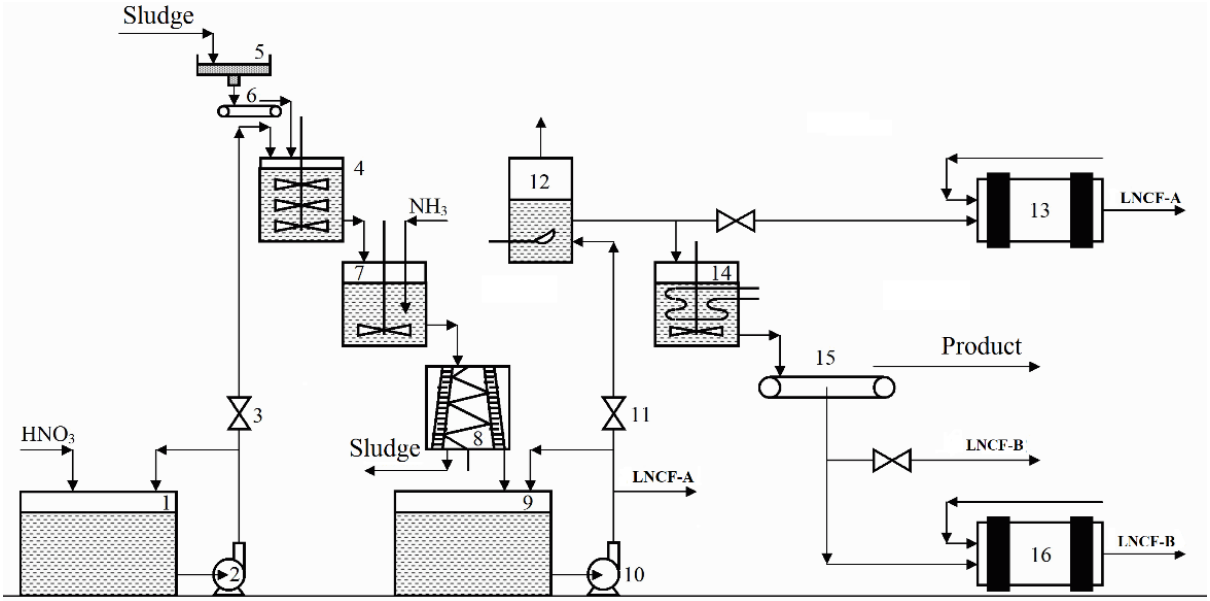

Further processing of LNCF-A involves evaporation to remove part of the calcium nitrate or to obtain a granular product.

Evaporation of LNCF-A occurs in a foam evaporation unit (FEU) (12), where LNCF-A is directed by a pump (10). If it is necessary to reduce the amount of calcium nitrate in the product, LNCF-A, after evaporation in FEU (12), is sent to the crystallizer (14) for cooling. In the crystallizer (14), calcium nitrate crystals are formed, which are separated from the solution on a belt vacuum filter (15). After separating the crystals, the liquid phase is sent to the consumer as liquid nitrogen-calcium fertilizer LNCF-B or sent for further processing.

Thus, the presented technological scheme allows obtaining three types of fertilizers differing in the ratio and composition of nutrients.

In the ongoing research work, a material balance was developed to determine the consumption of raw materials, the profitability of semi-finished products and finished products. Also, as mentioned above, samples of two types of fertilizers (LNCF-A and LNCF-B) were presented in the research work.

In particular, Table 1 shows the material balances for the production of LNCF-A and calcium nitrate (for 1000 kg of finished product).

Table 1. *Material balance of LNCF-A production (per 1000 kg of finished product)*

Sludge	326,19	–	–	–	–	–	–	–
HNO_3	–	478,16	–	57,38	–	–	–	–
H_2O	–	353,43	–	433,14	–	415,75	409,06	6,69

CO_2	–	–	90,16	–	–	–	–	–
E.Q.	–	–	–	49,03	–	49,03	0,00	49,03
$Mg(NO_3)_2$	–	–	–	22,18	–	22,18	21,82	0,36
$NaNO_3$	–	–	–	29,92	–	29,92	29,43	0,49
$Ca(NO_3)_2$	–	–	–	433,06	–	433,06	426,12	6,95
$Fe(NO_3)_3$	–	–	–	16,63	–	0,42	0,42	0,00
$Al(NO_3)_3$	–	–	–	26,28	–	1,31	1,28	0,03
NH_3	–	–	–	–	14,09	–	–	–
NH_4NO_3	–	–	–	–	–	113,71	111,88	1,83
$Fe(OH)_3$	–	–	–	–	–	7,18	–	7,18
$Al(OH)_3$	–	–	–	–	–	9,17	–	9,17
∑	326,19	831,59	90,16	1067,62	14,09	1081,71	1000,00	81,71

As can be seen from the table above, to produce 1000 kg of LNCF-A, we need 326.19 kg of dry sludge waste. To decompose sludge waste at an acceptable acid concentration and rate, 478.16 kg of acid is required. Since the acid concentration is 57.5%, 353.43 kg of water is added to the acid and enters the process. During the decomposition process, 90.16 kg of CO_2 is released in the gaseous state. In the next stage, i.e., the ammonization process, 14.09 kg of ammonia is added and the mixture is sent to the filtration process. During the filtration process, mainly insoluble residue is removed with a certain amount of moisture. In addition, it was found that the insoluble residue contains small amounts of $Ca(NO_3)_2$, $Fe(OH)_3$ and $Al(OH)_3$. The composition of the resulting 1000 kg of LNCF-A fertilizer was as follows. $Mg(NO_3)_2$–21.82 kg; $NaNO_3$–29.43 kg; $Ca(NO_3)_2$–426.12 kg; $Fe(NO_3)_3$–0.42 kg; $Al(NO_3)_3$–1.28 kg; NH4NO3–111.88 kg and 409.06 kg of water.

The material balance of the proposed technology for obtaining LNCF-B fertilizer proceeds in the following stages (Table 2).

As can be seen from Table 2, to produce 1000 kg of LNCF-B, we need 748.22 kg of dry sludge waste. To decompose sludge waste at an acceptable acid level and concentration, 1096.82 kg of nitric acid is required. Since the acid concentration is 57.5%, 810.70 kg of water in it is added to the acid and enters the process. During the decomposition process, 206.81 kg of CO_2 is released in the gaseous state. As a result, 2448.93 kg of suspension is formed. In the next stage, i.e., the ammonization process, 32.32 kg of ammonia is added. As a result of the addition of ammonia, NH_4NO_3 is also formed in the suspension and the total volume of the suspension increases to 2481.26 kg. After that, the mixture is sent to the filtration process. During the filtration process, 112.45 kg of insoluble residue is removed with a certain amount of moisture. This leads to a partial loss of soluble substances present in the solution. As a result, a total mass loss of 187.43 kg is observed at this stage. In the next stage, a crystallization process was carried out to separate $Ca(NO_3)_2 \cdot 4H_2O$ in a crystalline state. As a result, 573.44 kg of water was evaporated and 720.39 kg of $Ca(NO_3)_2 \cdot 4H_2O$ crystals were filtered and separated. The composition of the remaining solution, i.e. 1000 kg of LNCF-B fertilizer, was as follows: $Mg(NO_3)_2$–46.98 kg; $NaNO_3$–63.35 kg; $Ca(NO_3)_2$–490.25 kg; $Fe(NO_3)_3$–0.90 kg; $Al(NO_3)_3$–2.76 kg; NH_4NO_3–240.87 kg and 154.90 kg of water.

In conclusion, in the current research work, a material balance was established to determine the cost of raw materials, the profitability of semi-finished products and finished products. In particular, to obtain 1 ton of LNCF-A fertilizer, a dry sample of 326.19 sludge waste can be obtained by decomposing it with 478.16 kg of 57.5% nitric acid. In addition, it was determined that 654.90 kg of

Table 2. *Material balance of calcium nitrate and LNCF-B production (per 1000 kg of finished product)*

Name	Stream number according to the scheme												
	1	**2**	**3**	**4**	**5**	**6**	**7**	**8**	**9**	**10**	**11**	**12**	**13**
Sludge	748,22	–	–	–	–	–	–	–	–	–	–	–	–
HNO_3	–	1096,82	–	131,61	–	–	–	–	–	–	–	–	–
H_2O	–	810,70	–	993,56	–	953,67	938,32	15,35	364,88	573,44	165,06	154,90	10,16
CO_2	–	–	206,81	–	–	–	–	–	–	–	–	–	–
H.o.	–	–	–	112,45	–	112,45	–	112,45	–	–	–	–	–
$Mg(NO_3)_2$	–	–	–	50,87	–	50,87	50,05	0,82	50,05	–	50,05	46,98	3,08
$NaNO_3$	–	–	–	68,62	–	68,62	67,50	1,12	67,50	–	67,50	63,35	4,15
$Ca(NO_3)_2$	–	–	–	993,37	–	993,37	977,43	15,94	977,43	–	522,35	490,25	32,10
$Fe(NO_3)_3$	–	–	–	38,15	–	0,95	0,95	0,00	0,95	–	0,95	0,90	0,06
$Al(NO_3)_3$	–	–	–	60,29	–	3,01	2,94	0,07	2,94	–	2,94	2,76	0,18
NH_3	–	–	–	–	32,32	–	–	–	–	–	–	–	–
NH_4NO_3	–	–	–	–	–	260,83	256,64	4,19	256,64	–	256,64	240,87	15,77
$Fe(OH)_3$	–	–	–	–	–	16,46	0,00	16,46	–	–	–	–	–
$Al(OH)_3$	–	–	–	–	–	21,03	0,00	21,03	–	–	–	–	–
$Ca(NO_3)_2 \cdot \cdot 4H_2O$	–	–	–	–	–	–	–	–	–	–	654,90	–	654,90
$\sum$	748,22	1907,52	206,81	2448,93	32,32	2481,26	2293,83	187,43	1720,39	573,44	1720,39	1000,00	720,39

$Ca(NO_3)2 \cdot 4H_2O$ can be obtained by obtaining 1 ton of LNCF-B fertilizer.

References:

European Commission. Circular Economy Action Plan for a Cleaner and More Competitive Europe. Brussels, 2020.
ISO 14051:2011. Environmental management – Material flow cost accounting – General framework.
Yunusov A. S., et al. Soda ishlab chiqarish chiqindilarini utilizatsiya qilish usullari. Kimyo va texnologiya jurnali, 2019. – No. 3. – P. 45–49.
Mirzayev O. T. Kimyoviy sanoat chiqindilarini qayta ishlash texnologiyalari. Toshkent: Fan nashriyoti. (2021).
Mamatqulov B., Karimova D. Sanoat chiqindilarining ekologik xavfliligi va ularni kamaytirish yo‘llari. Ekologiya va atrof-muhit jurnali, 2020. – № 1. – P. 12–18.
UNEP. Waste Management Outlook for Asia and the Pacific. (2019).
Xodjayev B. va boshq. Azotli va kalsiyli o‘g‘itlarning agronomik xossalari. Agroilmlar, 2022. – № 2. – P. 33–38.
Kolesnikov A. A. Secondary utilization of chemical waste in agriculture. Journal of Environmental Engineering, 2018. – Vol. 14(2). – P. 67–72.
Khusanov D. R. Moddiy balans asosida texnologik jarayonlarning optimallashuvi. Texnika va ishlab chiqarish, 2023. – № 4. – P. 21–26.
Ergashev M. T., Rajabov Sh.Sh., Mirzakulov X. Ch. Nitric Acid Decomposition Process of Sludge Waste of the Soda Plant. International Journal of Advanced Research in Science, Engineering and Technology – Vol. 11. – Issue 7, July, 2024. – P. 22040–22046. ISSN: 2350–0328.
Ergashev M. T., Rajabov Sh. Sh., Mirzakulov X. Ch. “Study of the separation process of insoluble residues in the nitric acid processing of sludge waste from a soda plant”. International Conference on Developments in Education Hosted from Amsterdam, Netherlands URL: https: econferencezone.org/ 22 nd January, 2025. – P. 76–78.

submitted 17.04.2025;
accepted for publication 01.05.2025;
published 29.05.2025

Contact: ncsms@mail.ru; shohrux.rajabov@bk.ru; khchmirzakulov@mail.ru

The Austrian Journal of Technical and Natural Sciences, No 3–4
ISSN 2310-5607

PREMIER Publishing
ppublishing.org

DOI:10.29013/AJT-25-3.4-130-135

POTENTIAL OF CLEANING SPENT TURBINE OILS USING LOCAL BENTONITE SORBENTS

Bekhruz Salomatov [1], ***Nodir Panoev*** [1], ***Jasur Safarov*** [1],

[1] Bukhara State Technical University

Cite: *Salomatov B., Panoev N., Safarov J. (2025). Potential of Cleaning Spent Turbine Oils Using Local Bentonite Sorbents. Austrian Journal of Technical and Natural Sciences 2025, No 3–4.* https://doi.org/10.29013/AJT-25-3.4-130-135

Abstract

The article covers the potential of regenerating spent turbine oils and renewal of their physical and chemical properties. Samples of spent Shell Turbo S4 GX46 turbine oil were selected as the object of research. Natural and activated bentonite sorbents were used in their purification process. During the research, the samples were analyzed using the gas chromatography-mass spectrometer (GC–MS) method, and the main components in the oil were qualitatively and quantitatively determined. The analysis results showed that the purification process using activated bentonite was the most effective, as a result of which the amount of useful hydrocarbon components increased and pollutants decreased.

Keywords: *Turbine oil, regeneration, bentonite, activated sorbent, gas chromatography-mass spectrum, adsorption, physical and chemical analysis, ecological safety, industrial waste hydrocarbon components*

Introduction

The persistent and efficient operation of modern industry depends on many complex technological systems. One of these systems is turbines, which play an important role in energy production. The reliable and stable operation of turbines is unthinkable without turbine oils, which are one of their important components. The turbine performs such functions as reducing friction, cooling and protecting turbine parts from corrosion, and extending the service life of mechanisms. In particular, the correct selection and use of these oils in power plants, thermal and hydropower systems directly determines production efficiency.

In addition to that, turbine oils, like any oil product, are contaminated from various sources over time. These contaminants not only worsen the physicochemical properties of the oil, but also increase the risk of equipment failure. The causes of contamination of used turbine oils are associated with dust and moisture entering from the external environment, metal fragments released from the internal system, combustion products, and compounds formed as a result of chemical reactions. This problem poses a serious environmental and technological threat to industrial enterprises, further increasing the need to monitor the quality and service life of the oil.

Assessment of the quality of oil, identification of the contaminating components in it is important for the safe operation of equipment and the prevention of environmental hazards. In this regard, the chromatography method, especially gas and liquid chromatography, is one of the most effective analytical tools for analyzing used turbine oils. This method allows determining the oxidation products, additional chemical compounds, the degree of suitability of additives and contaminants in the oil. Chromatographic analysis not only shows how much oil has been used, but also allows making optimal decisions on oil replacement and cleaning. Therefore, this method is of great scientific and technical importance in working with waste oils in industry.

Materials and methods

A sample of the Shell Turbo S4 GX46 type used turbine oil was taken as the research object. In order to carry out the research, modern physicochemical (gas chromatography-mass spectroscopy) analysis methods, as well as methods for analyzing oil and oil products in accordance with state (GOST) and world standards were used.

The adsorption of used turbine oil was studied in the laboratory using bentonite from the Navbahor mine. Bentonite is a natural aluminosilicate with high sorption activity, and its main active component is the montmorillonite mineral. Due to its porous structure and high surface area, it has the property of effectively absorbing organic and inorganic contaminants contained in the oil.

In the course of the experiment, the used turbine oil was cleaned of mechanical impurities using filter paper and 10 g of bentonite, previously dried, crushed and sieved to a particle size of 0.01 mm, was placed in a burette and 50 ml of used turbine oil was taken and filtered. The filtration process was carried out at a temperature of 30 °C, under normal atmospheric conditions. After passing through the bentonite, the color of the oil changed. In the next stage, bentonite was activated using a muffle furnace at a temperature of 500 °C for 1 hour and the experiment was repeated. During the activation of bentonite at high temperatures, the adsorption level is increased by removing volatile organic compounds and excess bound and unbound water from its content. The oil passed through the activated bentonite was observed to be discolored. One of the modern research methods, gas chromatography-mass spectrometry, was used to separately study the structural components of the obtained samples. The qualitative and quantitative composition of the purified turbine oil was analyzed using Agilent 5975C inert MSD/7890A GC (Agilent Technologies) gas chromatography-mass spectrometer (Tilloyev L. I., Dustov H. B., Murodov M. N., Yuldashev N.Kh., 2022).

Results and discussions

In order to determine the hydrocarbon content of laboratory results obtained from used turbine oils, gas chromatograph-mass spectrometers with an accuracy of 80% or higher were selected. The gas chromatograph-mass spectrum of a sample taken from spent Shell Turbo S4 GX46 turbine oil is shown in (Fig. 2).

The qualitative and quantitative composition of a sample of spent Shell Turbo S4 GX46 turbine oil is presented in Table 1.

The percentages of the four main components in a sample of Turbo S4 GX46 oil are shown. As can be seen, hexatriacontane has the largest share, followed by 17-pentatriacontane and the other two components in much smaller amounts. 1-Naphthalenecarboxamide usually increases the high-temperature resistance of the oil and provides stability. It is added as an acidity reducer and antioxidant.

17-Pentatriacontane is an unsaturated hydrocarbon that controls the viscosity level of the oil and provides high lubricating properties. The main component hexatriacontane is a saturated hydrocarbon and forms the main lubricating part of the oil. It provides high thermal stability, low evaporation rate and good lubricating properties.

According to the analysis results, Shell Turbo S4 GX46 oil has a high content of hexatriacontane, which makes it resistant to high temperatures, stable and effective for long-term use. Other components play an important role in improving the overall quality of the oil by performing additional functions.

The qualitative and quantitative composition of the sample of Shell Turbo S4 GX46 spent turbine oil purified using bentonite is presented in Table 2.

Figure 2. *Gas chromatographic mass spectrum of a sample of spent Shell Turbo S4 GX46 turbine oil*

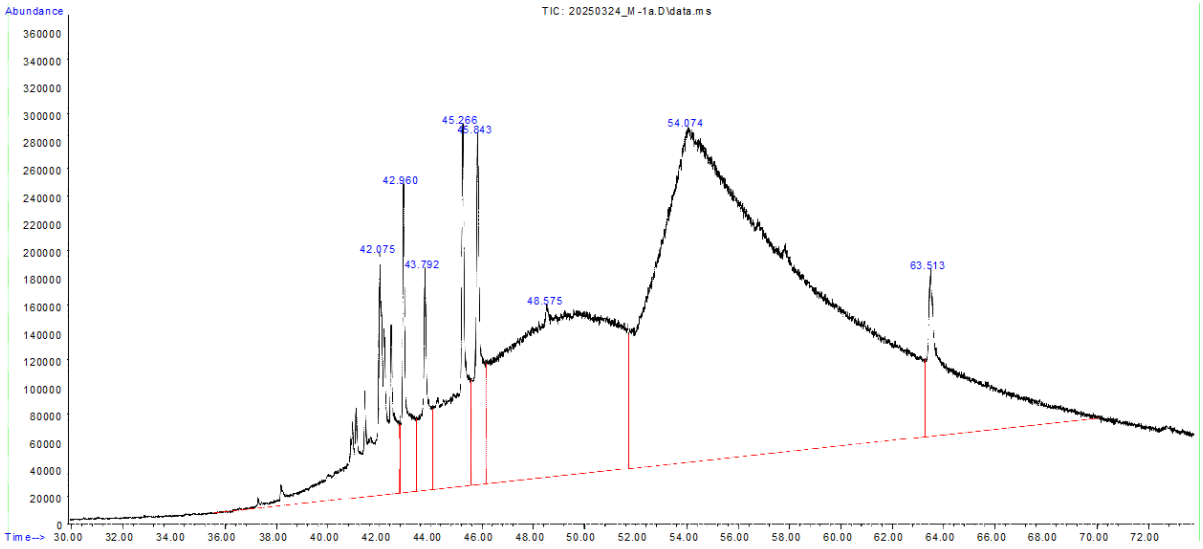

Table 1. *Qualitative and quantitative composition of a sample of spent Shell Turbo S4 GX46 turbine oil*

No.	Components	Rf, min	Content, %
1.	1-naphthalenecarboxamide	45.264	4.75
2.	17-pentatriaconten	48.576	23.94
3.	Hexathriacontane	54.074	63.75
4.	4,4-diamine-p-terphenyl	63.512	7.56

Figure 3. *Gas chromatographic mass spectrum of a sample of Shell Turbo S4 GX46 spent turbine oil purified using bentonite*

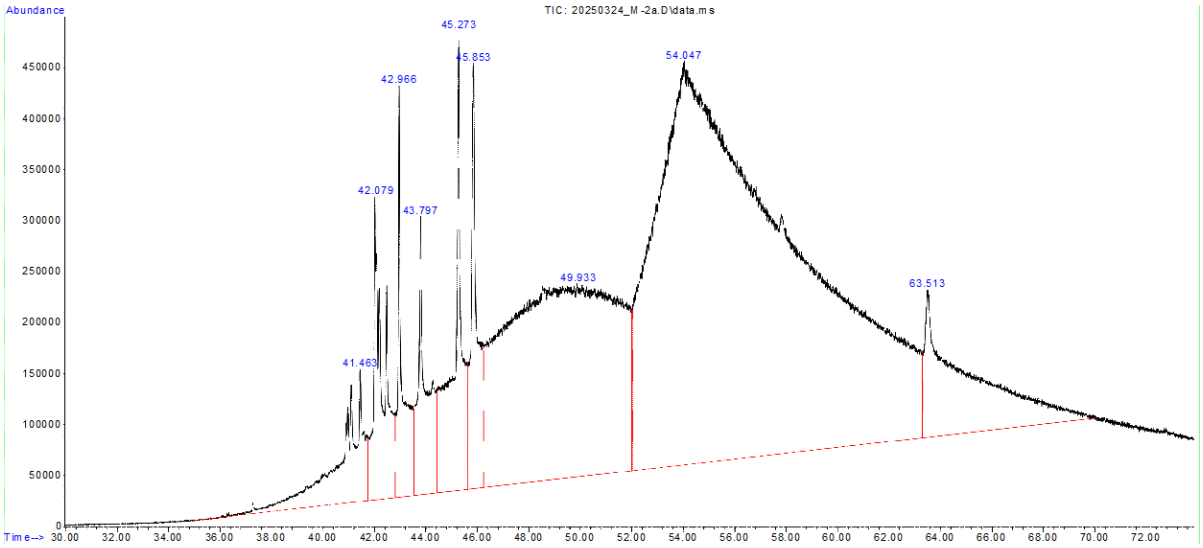

4,4-Diamine-p-terphenyl is added as an antioxidant or stabilizer and also serves to increase thermal stability

Table 2. *The qualitative and quantitative composition of the sample of Shell Turbo S4 GX46 spent turbine oil purified using bentonite*

No.	Components	Rf, min	Content, %
1.	Tricosane	49.934	26.70
2.	Hexatriacontane	54.048	65.95
3.	Benzo[a]anthracene	63.512	7.35

The percentages of the three main components in the sample after purification of Turbo S4 GX46 spent oil with bentonite can be seen to have changed, with hexatriacontane having the largest share, and after purification with bentonite, the composition changed, with the remaining components, tricosane and benzo[a]anthracene, increasing in content.

Figure 4. *Gas chromatographic mass spectrum of a sample of spent Shell Turbo S4 GX46 turbine oil purified using activated bentonite*

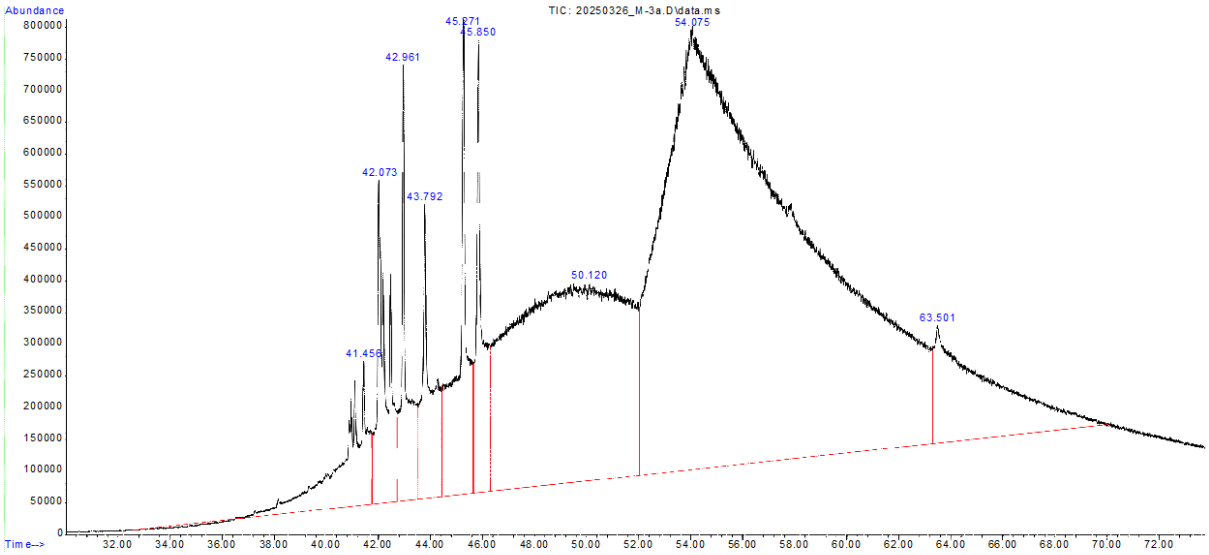

Tricosane is a medium-chain alkane that improves cold-weather performance, provides fluidity, and balances viscosity. Benzo[a]anthracene is an aromatic compound that provides stability at high temperatures and, although in small amounts, helps to provide dispersant and detergent properties.

The gas chromatographic-mass-spectrum image of a sample of Shell Turbo S4 GX46 spent turbine oil purified with activated bentonite is shown in (Fig. 4).

The qualitative and quantitative composition of the sample of spent Shell Turbo S4 GX46 turbine oil purified using activated bentonite is presented in (Table 3).

Table 3. *The qualitative and quantitative composition of the sample of spent Shell Turbo S4 GX46 turbine oil purified using activated bentonite*

No.	Components	Rf, min	Content, %
1.	4-methyl-2-mercaptopyridine-1-oxide	43.789	2.91
2.	Tetratriacontane	50.122	26.53
3.	Hexatriacontane	54.074	70.56

After purification of Turbo S4 GX46 oil with activated bentonite, the percentages of the three main components in the sample were observed to change. In this case, after

purification with activated bentonite, which has the largest share of hexatriacontane, a change in the composition occurred, and an increase in the amount of Tetratriacontane and 4-methyl-2-mercaptopyridine-1-oxide in the oil was observed.

Tetratriacontane is a high-molecular saturated alkane, which increases the viscosity of the oil and provides anti-friction properties. It also provides thermal and oxidative stability of the oil.

1,4-methyl-2-mercaptopyridine-1-oxide is a pyridine derivative, which contains a mercaptan (–SH) and an N-oxide group. The mercaptan group (–SH) binds well to metal surfaces, therefore this substance is used as an anti-corrosion additive. Due to the N-oxide group, it captures free radicals, therefore protecting oils from oxidation.

The samples of used turbine oils were classified into groups based on the composition of the components determined by gas chromatographic-mass-spectral analysis. The volumetric content of the components determined in the samples according to the hydrocarbon groups is given in Table 4.

Table 4. *Classification of samples of spent turbine oils by hydrocarbon groups*

No.	Unpurified turbine oil (%)	Bentonite-purified turbine oil (%)	Activated bentonite- purified turbine oil (%)
1-naphthalenecarboxamide	4.75	–	–
17-pentatriaconten	23.94	–	–
Hexatriacontane	63.75	65.95	70.56
4,4-diamine-p-terphenyl	7.56	–	–
Tricosane	–	26.70	–
Benzo[a]anthracene	–	7.35	–
4-methyl-2-mercapto-pyridine-1-oxide	–	–	2.91
Tetratriacontane	–	–	26.53

The table above shows the percentage of components in Shell Turbo S4 GX46 turbine oil in unpurified, bentonite-purified and activated bentonite-purified cases. Hexatriacontane is present in all three cases. This indicates that the percentage of this substance increases further with purification.

Conclusion

In conclusion, we can say that according to the research results, each purification stage led to an increase in the amount of the main hydrocarbon components in the oil. The increase in the amount of hexatriacontane ($C_{36}H_{74}$) in the samples purified with activated bentonite to 70.56% indicates a high efficiency of purification. This confirms the possibility of making spent turbine oils technologically reusable by their regeneration.

Scientific research conducted have shown that the use of natural and activated bentonite sorbents in the regeneration of spent turbine oils is an effective technological solution. In particular, the results of gas chromatographic-mass spectrometric analysis proved that stepwise purification processes using sorbents have a significant impact on physicochemical and structural changes.

In the course of the experiments, it was observed that the high adsorption activity of activated bentonite resulted in an increase in the concentration of heavy hydrocarbon components in the oil, while the content of polluting compounds decreased. In particular, a sharp increase in the amount of hexatriacontane indicates the preservation of useful fractions in the oil and the efficiency of processing. This creates an opportunity to repurpose used turbine oils, not just as waste, but as valuable secondary raw materials.

References

Safarov J. A., Khayitov R. R. Scientific and technical journal "Development of science and technologies". – No. 3/2021. – Bukhara, – P. 63–70.
Safarov J. A., Khaitov R. R. Research of physicochemical properties and chemical composition of spent motor oils // Universum: technical sciences, 2021. – No. (6–4 (87)). – P. 14–19.
Safarov, J. A., Khaitov, R. R., Murodov, M. N., Jumaeva, M. T. (2019). Complex processing of spent motor oils in order to obtain valuable products. *Theory and practice of modern science*, 2019. – No. 4. – P. 201–206.
Safarov J. A., Rustamovich, H. L., Temirov A. H. (2021, January). Restoring the quality of used engine oils. In *Euro-Asia Conferences* (Vol. 1. – No. 1. – P. 29–33).
Safarov J. A. Choice of refining method and complex processing of used oils to obtain valuable products. *EPRA International Journal of Multidisciplinary Research (IJMR)*, – 75 p.
Tilloyev L. I., Dustov H. B., Murodov M. N., Yuldashev N. Kh. Research of the composition of the oily fraction obtained from the waste "yellow oil". Scientific and technical journal "Oil and gas of Uzbekistan" – No. 2/2022. – Tashkent, – P. 30–34.

submitted 14.04.2025;
accepted for publication 28.04.2025;
published 29.05.2025

Contact: salomatovbehruz@gmail.com; nodirpanoyev@89mail.ru;
jasur.safarov1993@mail.*ru*

Contents

Section 3. Food processing industry

Section 4. Technical science in general